This is to certify that the
dissertation entitled

TISSUE- AND ORGAN-SPECIFIC PHYTOCHROME-MEDIATED RESPONSES IN *ARABIDOPSIS THALIANA*

presented by

SANKALPI NADEEKA WARNASOORIYA

has been accepted towards fulfillment
of the requirements for the

Doctoral degree in Genetics

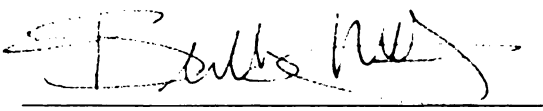

Major Professor's Signature

12/02/10

Date

MSU is an Affirmative Action/Equal Opportunity Employer

TISSUE- AND ORGAN-SPECIFIC PHYTOCHROME-MEDIATED RESPONSES IN *ARABIDOPSIS THALIANA*

By

Sankalpi Nadeeka Warnasooriya

A DISSERTATION

Submitted to
Michigan State University
in partial fulfillment of the requirements
for the degree of

DOCTOR OF PHILOSOPHY

Genetics

2010

ABSTRACT

TISSUE- AND ORGAN-SPECIFIC PHYTOCHROME-MEDIATED RESPONSES IN *ARABIDOPSIS THALIANA*

By

Sankalpi Nadeeka Warnasooriya

The red/far-red light-absorbing phytochrome photoreceptor family regulates numerous responses throughout the life cycle of *Arabidopsis thaliana*. Despite the discovery of individual and redundant phytochrome functions through mutational analyses, conclusive reports on distinct sites of photoperception, and the mechanisms by which localized pools of phytochromes act at the molecular level in mediating tissue- and organ-specific responses are limited. The objectives of this thesis research are to identify sites of phytochrome photoperception in Arabidopsis, correlate them with the regulation of tissue- and organ-specific responses and recognize candidate downstream target genes that define the molecular bases of such responses. To address these objectives, a mammalian gene encoding an enzyme capable of reduction of functional phytochromes was expressed in a tissue-specific manner in transgenic Arabidopsis plants. Transgenic lines were probed for perturbed phytochrome-mediated responses under blue, red and far-red illumination and comparative phenotypic and photobiological analyses of transgenic lines with constitutive, mesophyll- and meristem-specific phytochrome inactivation revealed distinct functions of localized pools of phytochromes. Mesophyll-localized phyA was found to exert a dominant role on hypocotyl inhibition, whereas hypocotyl-localized phyA was implicated in regulation of hypocotyl elongation in the absence of the inhibitory action of mesophyll-localized phyA under far-red light. Through comparative microarray-based gene expression profiling of transgenic Arabidopsis lines with

constitutive and mesophyll-specific phytochrome inactivation and subsequent phenotypic characterization of mutants, this study also identified two proteins, a GNAT family protein and a caldesmon-related protein, as putative signaling intermediates in regulating phyA-mediated hypocotyl development under far-red light. Furthermore, phytochrome-dependent sucrose-stimulated anthocyanin accumulation was distinctively altered in transgenic lines with mesophyll-specific phytochrome inactivation. The analysis of anthocyanin pigmentation responses confirmed a functional role for mesophyll-localized phyA in regulating anthocyanin accumulation in far-red light and its contribution in blue light. Individual phytochrome isoforms were recognized to have divergent roles in anthocyanin accumulation under red light; phyA through phyD exhibit inductive roles and phyE functions as a novel suppressor of anthocyanin accumulation. Additionally, metabolic inactivation of the phytochrome chromophore in roots suggested that root-localized phytochrome and/or the phytochrome chromophore is vital for the photoregulation of root development and confers sensitivity to jasmonic acid. Thus, conclusive evidence from this study indicates that the analyses of spatially isolated pools of phytochromes is an effective tool for providing novel insight into the complex signaling pathways controlled by phytochromes.

DEDICATION

To my mother, for her support from pre-school through graduate school

ACKNOWLEDGMENTS

I would like to acknowledge the people that have shared their knowledge, advice, experience and time with me during my graduate school years. I am grateful to my advisor, Dr. Beronda Montgomery, for her support, for investing time in discussions and for providing a stimulating work environment.

Each member of my guidance committee, Dr. Jianping Hu, Dr. Robert Larkin, Dr. Gregg Howe and Dr. Daniel Jones, has given me thoughtful advice and constructive criticism which has been of great help. Dr. Barb Sears, the members of the Genetics Program and the Plant Research Laboratory have been supportive and encouraging throughout my graduate work at Michigan State University.

A big thank you goes to past and present members of the Montgomery lab, especially to Melissa Whitaker, Bagmi Pattanaik, Sookyung Oh, Julie Bordowitz, and Stephanie Costigan whose help and support enabled me to complete this work.

Lastly, I would like to express my sincere appreciation to my mother, Mrs. Padma Warnasooriya, my brother, Aminda Warnasooriya, and my husband, Ravin Kodikara, for the support and encouragement given during the years of my education.

TABLE OF CONTENTS

LIST OF TABLES

LIST OF FIGURES

"Images in this dissertation are presented in color."

KEY TO ABBREVIATIONS

avg - average

B - blue

Bc - continuous blue

bHLH - basic helix-loop-helix

BphPs - bacteriophytochromes

BR - bilirubin

BV - biliverdin

BVR - biliverdin reductase

BVR - gene encoding biliverdin reductase

CAB3 - promoter of gene encoding chlorophyll a/b binding protein

CaMV - Cauliflower Mosaic Virus promoter

chl - chlorophyll

CLSM - confocal laser scanning microscopy

Cphs – Cyanobacterial phytochromes

cry2 - cryptochrome 2

D - dark

DEG -differentially expressed genes

FACS - fluorescence-assisted cell sorting

FP - forward primer

Fphs – fungal phytochromes

FR - far-red light

FRc - continuous far-red light

FR-HIR - Far-red high irradiance responses

GFP - green fluorescent protein

GNAT - GCN5-related N-acetyltransferase

HCl - hydrochloric acid

HIR - high irradiance responses

HRP - horseradish peroxidase

Ile - isoleucine

JA - jasmonic acid

JA-Ile - jasmonoyl-L-isoleucine

KOH - potassium hydroxide

LC-MS - liquid chromatography-mass spectrometry

LFR - low fluence responses

MeJA - methyl jasmonate

MES - 2-(N-morpholino) ethanesulfonic acid

NDPK2 - nucleoside diphosphate kinase 2

NIH - National Institute of Health

NTE - plant-specific amino-terminal extension

PAS - Per–Arnt–Sim

PBS - phycobilisome

PCB - phycocyanobilin

PCR - polymerase chain reaction

PΦB - phytochromobilin

PΦR - phytochromorubin

qRT-PCR - quantitative reverse transcription polymerase chain reaction

QTL - quantitative trait locus

R - red

Rc - continuous red

R-HIR - red high irradiance responses

RP - reverse primer

rpm - revolutions per minute

RT-PCR - reverse transcription polymerase chain reaction

SD - standard deviation

SDS - sodium dodecyl sulfate

SDS-PAGE - sodium dodecyl sulfate –polyacrylamide gel electrophoresis

suc -sucrose

TAIR - The Arabidopsis Information Resource

T-DNA - transfer-DNA

UAS - upstream activating sequence

UBC21 – gene encoding ubiquitin-conjugating enzyme 21

VLFR - very low fluence responses

W - white

Wc - continuous white

WT - wild-type

YEP – yeast extract-peptone

Chapter 1 Introduction

Some of the information included in chapter 1 was published in a book chapter: **Warnasooriya SN** and Montgomery BL, Using Transgenic Modulation of Protein Accumulation to Probe Protein Signaling Networks in *Arabidopsis thaliana,* Plant Biotechnology and Transgenic Research, Bentham Science Publishers, Oak Park, IL (in press).

1.1 Overview

Perception of changes in the environment is important to any living organism. To monitor environmental variations, plants are equipped with multiple sensory systems. Among the environmental factors that determine plant survival and reproduction, light is the most variable and dominating factor. In addition to being the source of energy for photosynthesis, it mediates a myriad of growth, developmental and adaptive processes throughout the life cycle of plants (Chory et al., 1996; Franklin and Quail, 2010; Franklin and Whitelam, 2004; Neff, Fankhauser, and Chory, 2000; Schepens, Duek, and Fankhauser, 2004). Proper onset and fine-tuning of developmental transitions and adaptive processes not only require detection of the presence or absence of light but also spectral quality, quantity, directionality and periodicity. To perceive fluctuations in the temporal and spatial patterns of light, photoreceptors function at the interface between the organism and the environment. The regulation of plant growth and development by light signals, otherwise known as photomorphogenesis, involves three main classes of photoreceptors, blue (B)/UV-A-absorbing cryptochromes and phototropins and red (R)/far-red (FR)-absorbing phytochromes (Chen, Chory, and Fankhauser, 2004; Ulm and Nagy, 2005). The most studied and best-characterized group among plant photoreceptors is the R/FR light-absorbing phytochromes (Franklin and Quail, 2010; Neff, Fankhauser, and Chory, 2000; Schepens, Duek, and Fankhauser, 2004; Smith, 2000).

Phylogenetic and genomic analyses have revealed that phytochromes and/or phytochrome-like chromoproteins are present not only in plants but also in cyanobacteria (Kehoe and Grossman, 1996; Rockwell and Lagarias, 2010; Yeh et al., 1997), bacteria (Davis, Vener, and Vierstra, 1999; Hughes, 2010; Jiang et al., 1999) and fungi

(Blumenstein et al., 2005; Hughes, 2010; Idnurm and Heitman, 2005). Existing evidence supports that photosynthetic organelles, chloroplasts, in plant cells evolved from a bilin sensor protein in the bacterial progenitor which in turn gave rise to phytochromes (Montgomery and Lagarias, 2002). Thus, the evolutionary origins of higher plant phytochromes are represented by prokaryotic genes (Jiang et al., 1999). Bacteriophytochromes (BphPs), cyanobacterial phytochromes (Cphs) and fungal phytochromes (Fphs) fall into distinct functional clades (Karniol et al., 2005) and phytochrome-like proteins, e.g., regulator of chromatic adaptation E (RcaE) and phytochrome-like protein A (PlpA), are present in some cyanobacterial systems allowing the organisms to respond to predominant light conditions in the environment (Kehoe and Gutu, 2006; Montgomery, 2007).

In Arabidopsis, phytochromes regulate a range of developmental and adaptive responses, such as seed germination, de-etiolation, gravitropic orientation, stomatal development, shade avoidance, entrainment of the circadian clock and flowering (Chen, Chory, and Fankhauser, 2004; Franklin and Quail, 2010; Mathews, 2006). Multiple BphPs could be present in bacteria, allowing them to regulate capacity of photosynthesis, movement towards or away from light and pigmentation process (Vierstra and Davis, 2000). FphA in *Aspergillus nidulans* regulates asexual sporulation in R light (Blumenstein et al., 2005) and is potentially a phytochrome with many functional roles in regulating morphological and physiological differentiations, as well as tuning of asexual and sexual reproduction in response to light (Brandt et al., 2008; Purschwitz et al., 2008). A histidine kinase protein, Cph1 in the cyanobacterium *Synechocystis* sp. strain PCC 6803, allows the organism to adapt to light-dark transitions (Garcia-Dominguez et al.,

2000). Photoreceptor RcaE in the cyanobacterium, *Fremyella diplosiphon*, regulates the green-red photoreversibility of complementary chromatic adaptation and enables the organism to adapt to changes in ambient light in freshwater (Kehoe and Gutu, 2006). In *Synechocystis* sp. strain PCC 6803, PlpA regulates growth (Vierstra and Davis, 2000) and potentially has a role for regulating growth in B light (Wilde et al., 1997). Despite the apparent diversity observed in photosensory and functional roles among the members of the phytochrome-class photosensors, all members appear to share a common photochemical mechanism for light sensing (Rockwell and Lagarias, 2010). Numerous responses/adaptations to light in organisms across kingdoms suggest that, from eubacteria to higher plants, informational light cues are utilized to maintain their growth, metabolism and developmental transitions in accordance with the environment.

1.2 Substructure and Biosynthesis of Phytochromes

Phytochromes are soluble chromoproteins and consist of an apoprotein and a chromophore (Montgomery, 2009; Terry, Wahleithner, and Lagarias, 1993). A nuclear gene family encodes the apoprotein and the chromophore biosynthesis is localized in the plastid (Emborg et al., 2006; Kohchi et al., 2001). Thus, the synthesis of a holophytochrome involves coordination of two physically separated subcellular biosynthetic pathways (Montgomery, 2008). Multiple phytochrome species are present in plants and three distinct apoprotein encoding genes (*PHYA-PHYC*) are conserved within angiosperms (Mathews, Lavin, and Sharrock, 1995). The phytochrome family contains only three members (*PHYA–PHYC*) in monocotyledonous plants (Takano et al., 2005), whereas in dicotyledonous plants, additional apophytochrome-encoding genes have

arisen due to recent gene duplication events (Mathews, Lavin, and Sharrock, 1995; Mathews and Sharrock, 1997). In the model plant *Arabidopsis thaliana*, a family of five nuclear genes, *PHYA-PHYE* encodes the apoproteins (Fankhauser and Staiger, 2002; Quail, 1994). The canonical photosensory core of phytochromes consists of an N-terminal sensory module of 3 distinct domains (Figure 1.1); Period/ARNT/Sim (Garcia-Dominguez et al., 2000), cGMP phosphodiesterase/adenylate cyclase/FhlA (GAF) and phytochrome-specific (PHY; Hughes, 2010; Rockwell and Lagarias, 2010). Recent data suggest that phytochromes can dimerize to form homodimers and heterodimers (Clack et al., 2009; Sharrock and Clack, 2004) and site-directed mutagenesis has revealed that the Per–Arnt–Sim 2 (PAS2) domain is required for dimerization (Figure 1.1; Kim et al., 2006). The C-terminal transmitter module consists of a dimerization/phosphoacceptor domain and an ATPase catalytic domain (Figure 1.1; Hughes, 2010). The bilin linear tetrapyrrole chromophore is covalently attached to the GAF domain (Figure 1.1; (Hughes, 2010; Rockwell and Lagarias, 2010) and the chromophore can either be phycocyanobilin (PCB), phytochromobilin (PΦB), or biliverdin IXα (BV) depending on the organism (Rockwell and Lagarias, 2010). All higher plant phytochromes utilize phytochromobilin as the chromophore, which is essential for phytochrome photoperception (Lagarias and Rapoport, 1980; Terry, Wahleithner, and Lagarias, 1993).

The first committed step of plastid-localized chromophore biosynthesis is the oxidative cleavage of heme by multiple heme oxygenases to form biliverdin IXα (Figure 1.2; Emborg et al., 2006). A ferredoxin-dependent phytochromobilin synthase further reduces biliverdin to (3Z)-phytochromobilin (Figure 1.2; Kohchi et al., 2001). Phytochromobilin attaches to a conserved Cys residue in the GAF domain in each

monomer via a thio-ether linkage (Figure 1.1; Franklin et al., 2003; Karniol et al., 2005) through intrinsic autocatalytic activity of the apophytochrome molecule (Karniol et al., 2005). The phytochromes are R/FR reversible between two forms, the R-absorbing Pr (λ max~660 nm) and the FR-absorbing Pfr (λ max~730 nm). The biologically inactive form of phytochrome, Pr, is synthesized in the dark, and through photoconversion Pfr, the biologically active form is generated (Franklin and Quail, 2010). Photointerconvertibility between Pr and Pfr forms results in a dynamic photoequilibrium in natural light conditions (Franklin and Quail, 2010). The analysis of the three-dimensional structure of the ~ 20 kDa GAF domain fragment of SyB-Cph1 phytochrome from *Synechococcus* OSB' suggests that light-induced rotation of the A pyrrole ring determines photoconversion (Ulijasz et al., 2010). However, a wealth of data still suggest that isomerization of the D ring is likely correct for other phytochromes (Fodor, Lagarias, and Mathies, 1990; Kneip et al., 1999; Rudiger et al., 1983).

1.3 Phytochrome Activity at the Molecular Level

The elucidation of phytochrome function at the molecular level has been the focus of plant photobiology for many years. Studies with PHYA-GFP and PHYB-GFP fusion proteins confirmed that upon conversion to the Pfr form, phytochromes display light-dependent nuclear translocation (Chen, Chory, and Fankhauser, 2004; Kircher et al., 1999; Nagatani, 2004; Yamaguchi et al., 1999). However, for nuclear translocation of phyA, involvement of additional proteins, FHL and FHY, has been implicated recently (Hiltbrunner et al., 2006). The best-studied mechanism of phytochrome signalling is the physical interaction of a nuclear-translocated photoreceptor with a class of bHLH

transcription factors called PHYTOCHROME INTERACTING FACTORS (PIFs; Bauer et al., 2004; Kim et al., 2003; Monte et al., 2007; Shen et al., 2007). Recent studies suggest that nuclear translocated phyB directly interacts with PIF3 in a light-dependent manner, to regulate transcription of a number of genes with light responsive elements (Martinez-Garcia, Huq, and Quail, 2000; Monte et al., 2004; Terzaghi and Cashmore, 1995). Moreover, extensive yeast two-hybrid screens confirmed that phytochrome kinase substrate 1 (PKS1; Fankhauser et al., 1999) and nucleoside diphosphate kinase 2 (NDPK2; Choi et al., 1999) are involved in direct physical interactions with some phytochrome isoforms. To date, numerous downstream signal transduction components have been identified (Kim et al., 2003; Quail, 2000; Quail, 2002; Ryu et al., 2005; Shen et al., 2007), suggesting the existence of a transcriptional cascade that follows R/FR light perception by phytochromes.

1.4 Physiological Responses Regulated by Phytochromes

Phytochromes perceive changes in R and FR light to modulate multiple physiological responses, from seed germination and seedling establishment through onset of reproductive development. Based on responses of seedlings to R and FR light, several classes of phytochrome responses have been characterized. Regulation of antagonistic and complementary functions by phytochrome family members has resulted through gene duplication and divergence (Mathews, 2010). The light-labile phyA molecule is the most abundant phytochrome in etiolated seedlings (Clough and Vierstra, 1997) and is the sensor for irreversible, very low fluence responses (VLFR) including absorption of FR light (Furuya and Schäfer, 1996). Notably, in R light, nuclear-localized phyA has a role

in irradiance-dependent photoprotection (Franklin, Allen, and Whitelam, 2007). Despite a wealth of data obtained through biochemical localization assays and injection of signaling intermediates (i.e. cyclicGMP, calmodulin and calcium; Nagy and Schafer, 2002), functions mediated by phytochromes remaining in the cytosol are poorly understood. However, for cytosolic phyA, a number of physiological functions have been reported (Rösler, Klein, and Zeidler, 2007). phyB through phyE comprise the light-stable phytochrome molecules and phyB is predominantly responsible for the perception of R light and functions as a classic R/FR light reversible molecular switch regulating low fluence responses (LFR; Furuya and Schäfer, 1996). Light-stable phytochromes collectively regulate end-of-day FR response and the shade-avoidance response in adult plants (Azari et al., 2010). Irreversible high irradiance responses (HIR) are also regulated by phytochromes (Smith, 1995) with phyA mediating FR-HIR (Jiao, Lau, and Deng, 2007) and light-stable phytochromes mediating R-HIR (Azari et al., 2010).

The isolation of individual null mutants in all five phytochromes of Arabidopsis and construction of higher-order mutants has enabled thorough examination of responses regulated by phytochromes at seedling stage (Franklin et al., 2003; Franklin and Quail, 2010; Sullivan and Deng, 2003). Through transgenic approaches, molecular mechanisms underlying spatially localized pools of phytochromes in regulating distinct phytochrome-dependent responses have been elucidated (Endo et al., 2007; Endo and Nagatani, 2008; Endo et al., 2005; Montgomery, 2009; Warnasooriya and Montgomery, 2009). However, cell autonomous and cell non-autonomous signaling mediated by phytochromes during short-term physiological responses and long-term adaptive responses await further experimentation.

1.5 Tissue- and Organ-Specific Phytochrome Responses

As phytochrome-mediated light responses are often localized to specific plant tissues or organs (Goosey, Palecanda, and Sharrock, 1997), the distribution of phytochromes at many developmental stages has been analyzed through multiple techniques, each having varying levels of sensitivities in detecting phytochromes *in vivo* or *in vitro* (Nagatani, 1997). Moreover, sites of light perception and sites of light action or sites displaying the physiological response do not always overlap in the plant, highlighting the significance of inter-cellular communication in plant growth and development (Bou-Torrent, Roig-Villanova, and Martinez-Garcia, 2008). Transmission of perceived light signals between tissues or organs that would result in growth and developmental changes at a site, distinct from the cells or tissue that received the light stimulus has been observed *in planta* and at the physiological level, the roles for spatial-specific phytochrome pools have been determined (Montgomery, 2008).

Early physiological studies aimed at studying cell non-autonomous responses have utilized microbeam irradiation of plants or irradiation of detached plant parts to photoactivate phytochromes at a particular site and assay for a measurable phytochrome-dependent phenotypic change at a distant site (De Greef and Caubergs, 1972a; De Greef and Caubergs, 1972b; Mandoli and Briggs, 1982b). For example, in dark-grown bean seedlings, perception of light by leaves and the embryonic axis is required for leaf expansion (De Greef and Caubergs, 1972a). The onset of the transition from dark-grown to light-grown state (also known as de-etiolation) is marked by an increase in respiration. Cell layers in the epidermis and hypodermis of the epicotylar ribs displayed the highest ATP breakdown (De Greef and Caubergs, 1972b) suggesting the presence of epidermal

cell layer responses in dark-grown bean seedlings. The perception of light in cotyledons is responsible for the inhibition of hypocotyl elongation and apical hook opening through intercellular signaling (Black and Shuttleworth, 1974; Caubergs and De Greef, 1975), as well as the pattern and level of accumulation of anthocyanins (Nick et al., 1993).

The most well-studied cell non-autonomous phytochrome response is the photoperiodic induction of flowering in photoperiod-sensitive plant species. In these plants, floral initiation involves perception of light signals in the leaves and the subsequent transport of a photo-induced stimulus from the leaves to the shoot apex through the phloem (Parcy, 2005; Zeevaart, 2006). Through photoreceptor mutant analyses, it is known that phyA and cryptochrome 2 (cry2) are involved in perceiving long-day photoperiods and thus control flowering (Franklin and Quail, 2010). Although promoter-fusion studies indicate that these photoreceptors are ubiquitously expressed throughout the seedlings (Tóth et al., 2001), a wealth of prior studies has confirmed that light perception in leaves is associated with the photoperiodic induction of flowering (Zeevaart, 2006). In dark-grown oat seedlings, photoperception within the mesocotyl mediates its own development. In contrast to the coleoptilar node and tip where phytochromes are most abundant, the sites above and below the coleoptilar node regulate promotion of coleoptile elongation through light piping (Mandoli and Briggs, 1982a). Thus, the sites of photoperception may or may not coincide with the sites of highest phytochrome abundance.

Studies with microbeam irradiation focused on phytochrome responses at a distant site and *cab::luciferase* reporter gene expression experiments have shown luciferase activity in non-irradiated tissues distant from the few irradiated cells in dark-grown

Arabidopsis cotyledons (Bischoff et al., 1997). Results from these studies validate the presence of cell- and tissue-specific phytochrome signaling pathways that regulate distinct aspects of light-dependent growth and development through intercellular and/or interorgan coordination. However, conclusive evidence from many of these early physiological studies that utilized excised plant organs and microbeam irradiation, were confounded due to light piping and light scattering (Mandoli and Briggs, 1982b).

1.6 Probing Spatial-specific Responses via Targeted Chromophore Reduction

The isolation of various mutants in *Arabidopsis* enabled phenomenal progress in light signaling research and the elucidation of the functional roles of phytochromes. Extensive analyses of individual and multiple apophytochrome mutants have uncovered the existence of unique and overlapping photoregulatory roles among the five types of phytochromes (Franklin and Whitelam, 2004). Chromophore biosynthetic mutants, *hy1* and *hy2*, exhibit multiple phytochrome-deficient phenotypes throughout their life cycle due to an absence of all five phytochromes (Hudson, 2000); their study has contributed to our understanding of photoregulatory functions at a global level. However, mutations in a number of genes that encode for phytochrome-interacting proteins have resulted in distinct phenotypes in different tissues within the seedling (Neff, Fankhauser, and Chory, 2000). Therefore, each localized pool of phytochromes may control only a subset of light-mediated responses *in planta*. Definitive information on how these localized pools of phytochromes mediate distinct aspects of plant growth and development is currently limited.

A molecular tool that can render all five types of phytochromes non-functional is essential for probing tissue- and organ-specific phytochrome responses. One tool currently utilized is the expression of a gene encoding a rat kidney enzyme, biliverdin IXα reductase (BVR, Figure 1.3). BVR converts biliverdin IXα, a precursor of phytochrome-chromophore biosynthesis, into bilirubin and metabolizes the chromophore, phytochromobilin to phytochromorubin (Figure 1.3; Terry, Wahleithner, and Lagarias, 1993). The end products of the BVR enzyme cannot covalently assemble with apophytochromes (Terry, Wahleithner, and Lagarias, 1993). Constitutive expression of *BVR* in Arabidopsis has led to the perturbation of many light-dependent phytochrome-mediated responses (Lagarias et al., 1997; Montgomery et al., 1999). Moreover, depending on the subcellular localization of reduced levels of the phytochrome chromophore through *BVR* expression, light-dependent, as well as light-independent phenotypes have been observed in Arabidopsis and Tobacco (*Nicotiana tabacum* cv Maryland Mammoth; Montgomery et al., 2001; Montgomery et al., 1999). Such BVR-dependent phenotypes are very similar to responses displayed by an Arabidopsis phytochrome chromophore-deficient mutant, *hy1* (Montgomery et al., 1999) and indicate loss of photosensory activities of multiple phytochromes. Thus, expression of *BVR* is responsible for altered phytochrome-mediated responses due to reduction of holophytochrome levels (Lagarias et al., 1997).

Transgenic approaches such as over-expression, ectopic expression and mis-expression of transgenes, are useful for the analysis of gene function (Rutherford et al., 2005; Warnasooriya and Montgomery, in press). With tissue- and organ-specific promoters, the expression of *BVR* can be restricted to a distinct subset of cells, tissues or

organs. Spatial-specific regulation of transgene expression has been successfully utilized in many studies that were aimed at further understanding the photoreceptor functions during the life cycle of Arabidopsis (Warnasooriya and Montgomery, in press). One such example is transgenic Arabidopsis lines in which the cry2–GFP fusion was expressed under the control of mesophyll-specific, vascular bundle-specific and epidermal-specific promoters in a *cry2*-deficient mutant background. Only cry2-GFP accumulation or expression in vascular bundles was able to rescue the late flowering phenotype of the *cry2* mutant suggesting that the site of cry2 photoperception that regulates flowering is the vascular bundles (Endo et al., 2007).

Studies with stable transgenic lines displaying mesophyll-specific and meristem-specific phytochrome chromophore deficiencies have revealed that localized pools of phytochromes can regulate distinct physiological responses and established the efficacy of targeted *BVR* expression as a novel molecular technique to investigate sites of light perception (Warnasooriya and Montgomery, 2009). A current limitation is the availability of cloned and characterized promoters that can direct the gene expression in a targeted manner. The limited number of well-characterized promoters and corresponding expression patterns restricts the cell types and developmental processes that can be targeted (Warnasooriya and Montgomery, in press).

A two-component, enhancer-trap mis-expression system based on the yeast GAL4 transcription factor has been used successfully to study regulatory mechanisms during embryonic development in Drosophila (Brand and Perrimon, 1993), root development in Arabidopsis (Laplaze et al., 2005), and improving salinity tolerance in rice (Plett et al., 2010). The bipartite enhancer-trap strategy results in transactivation of the expression of

a gene under control of the Upstream Activation Sequence (UAS) element by a transcriptional activator (Laplaze et al., 2005). A more stringent regulatory system based on promoter/enhancer trap activation can be achieved with transcription factors with sequence-specific DNA-binding activities that are not normally found in plants (Moore et al., 1998). Transgenic enhancer trap lines are T-DNA insertion lines with diverse expression patterns of the yeast transcription factor, GAL4, whose expression depends on the presence of native genomic enhancer sequences. The GAL4- responsive *mGFP5* gene marks the expression pattern mediated by genomic enhancers in green fluorescence (Haseloff, 1999; Laplaze et al., 2005). Two-component transactivation systems overcome the limited availability of cloned and characterized promoters by using native genomic enhancers within a host genome (Wu et al., 2003) and circumvent the necessity to maintain and genotype multiple stable transgenic lines, which is laborious and labor intensive (Warnasooriya and Montgomery, in press). Another advantage of GAL4/UAS two-component enhancer trap system is that distinct expression patterns can be achieved in a localized manner, which makes it an effective tool to determine sites of physiological process such as photoperception that have been shown to have spatial-specific aspects. Use of the Cauliflower mosaic virus (CaMV) 35S minimal promoter-based enhancer-trap system to express *PHYB-GFP* in a phytochrome B (*phyB*) mutant of Arabidopsis revealed that *PHYB-GFP* expression in the mesophyll but not in vascular bundles suppresses the expression of a key flowering regulator, *FLOWERING LOCUS T* (*FT*) in vascular bundles of cotyledons (Endo et al., 2005). This finding indicates that a novel inter-tissue signaling mechanism occurs between mesophyll and vascular bundles making it a critical step in the regulation of flowering by phyB (Endo et al., 2005).

Probing spatial-specific phytochrome responses necessitates reduction of holophytochromes in a selective manner. Enhancer trap-based two-component strategy requires two transgenic parents: the enhancer trap and the UAS-BVR. Genetic crosses between the UAS-BVR parent and a range of GAL4-enhancer trap parents will result in progeny with diverse expression patterns of the *BVR* gene. The sites of *mGFP5* expression should be identical to the sites of *BVR* expression in the progeny. Selective mis-expression of *BVR* through an enhancer trap system will result in site-specific reduction of chromophore availability, inducing local phytochrome-deficiencies within the plant and the functions of localized phytochrome pools can be probed to characterize the sites of photoperception. Comparative analyses of such progeny will expand our current understanding of phytochrome-regulated tissue- and organ-specific responses and possibly gain insight into molecular bases of novel inter-tissue and/or inter-organ signaling mechanisms mediated by phytochromes *in planta.*

1.7 Summary

Plants are sessile organisms solely dependent on light for photosynthesis and thus need to have photosensory mechanisms to adapt to sub-optimal light conditions in the surrounding environment. Photoreceptors render plants the capacity to detect and respond to frequent fluctuations in many components of light. Among the very well characterized plant photosensory systems, phytochromes regulate a vast number of growth and developmental processes in Arabidopsis. Unparalleled progress has been made in determining the physiological roles and dissecting the phytochrome-signaling cascade. Despite the wealth of experimental findings on tissue- and organ-specific responses at

physiological and molecular level, definitive molecular evidence about sites of photoperception, cellular signaling mechanisms of specific pools of phytochromes is yet limited. The identification of the molecular bases of tissue- and organ-specific phytochrome responses and their downstream molecular effectors will broaden our current understanding of the complex signal transduction network in Arabidopsis. Molecular evidence on mechanisms by which phytochromes or different phytochrome isoforms regulate responses at distinct sites in the plant will aid in fine-tuned manipulation of agronomically desirable physiological responses in important crop species.

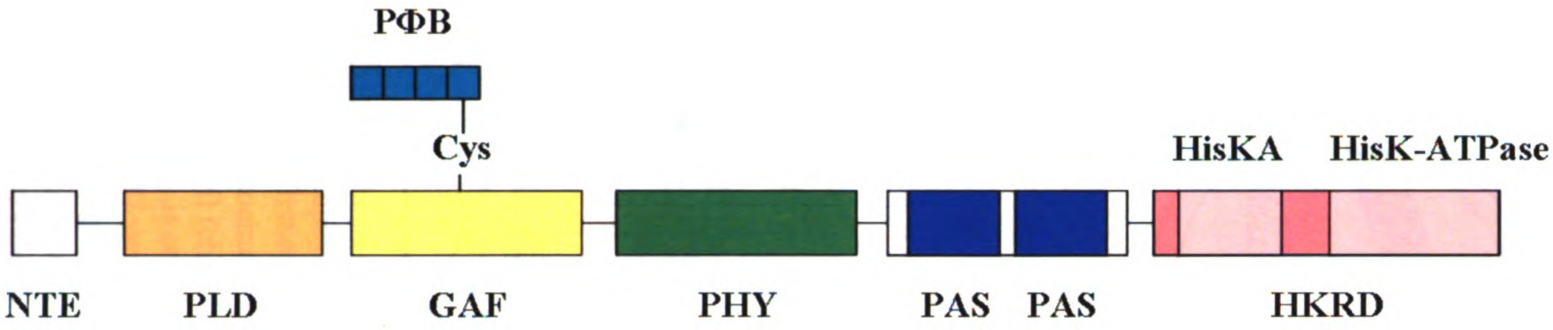

Figure 1.1 Conserved domain structure of phytochrome in plants.
NTE, plant-specific amino-terminal extension; PLD, PAS-like domain; GAF, cGMP phosphodiesterase/adenyl cyclase/FhlA domain distantly related to PAS; PϕB, the phytochrome chromophore, phytochromobilin, attaches to a conserved cysteine (Cys) residue within the GAF domain; PHY, a domain distantly related to PAS and specific to phytochromes; PAS, Per–Arnt–Sim 2 domain for dimerization; HKRD, histidine kinase-related domain lacking a phosphoacceptor His residue and motifs characteristic of histidine kinases; HisKA, histidine kinase A domain-related; HisK-ATPase, histidine kinase ATPase superfamily domain. Figure was adapted from Sharrock, 2008.

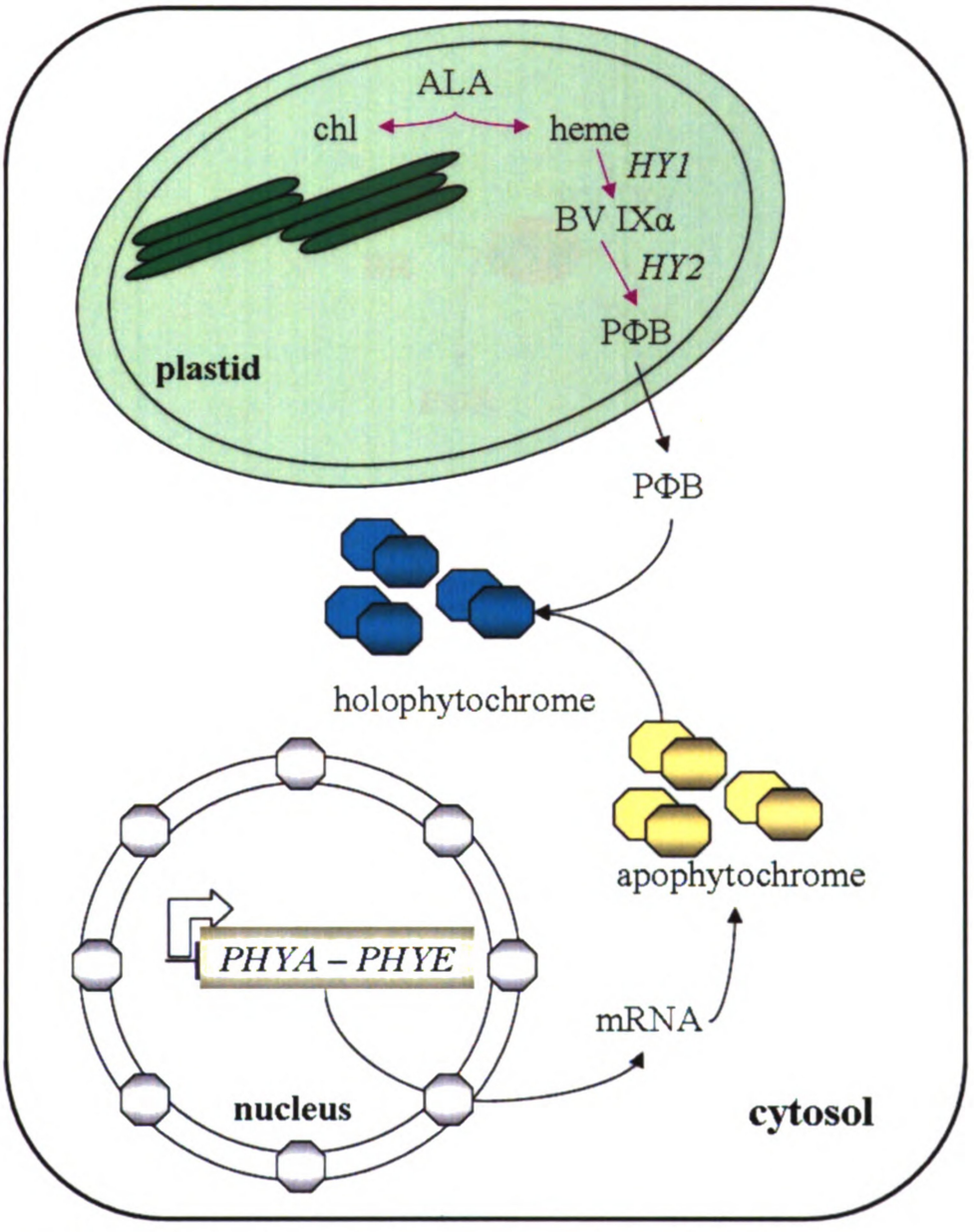

Figure 1.2 Biosynthesis of holophytochrome in Arabidopsis.
Biosynthesis of holophytochrome involves the plastid and nucleus. 5-aminolevulinic acid (ALA) is the first committed precursor of tetrapyrrole biosynthesis. Phytochrome chromophore (phytochromoblin, PΦB) biosynthesis is plastid localized and branches off from chlorophyll (chl) biosynthesis. Heme is the first committed precursor of PΦB biosynthesis. Heme is converted to biliverdin IXα (BV) by a heme oxygenase encoded by the *HY1* gene. BV is reduced to PΦB by a phytochromobilin reductase encoded by the *HY2* gene. PΦB is transported to the cytosol and undergoes autocatalytic assembly with apophytochrome molecules, encoded by nuclear *PHYA-PHYE* genes, to generate photoactive holophytochrome molecules.

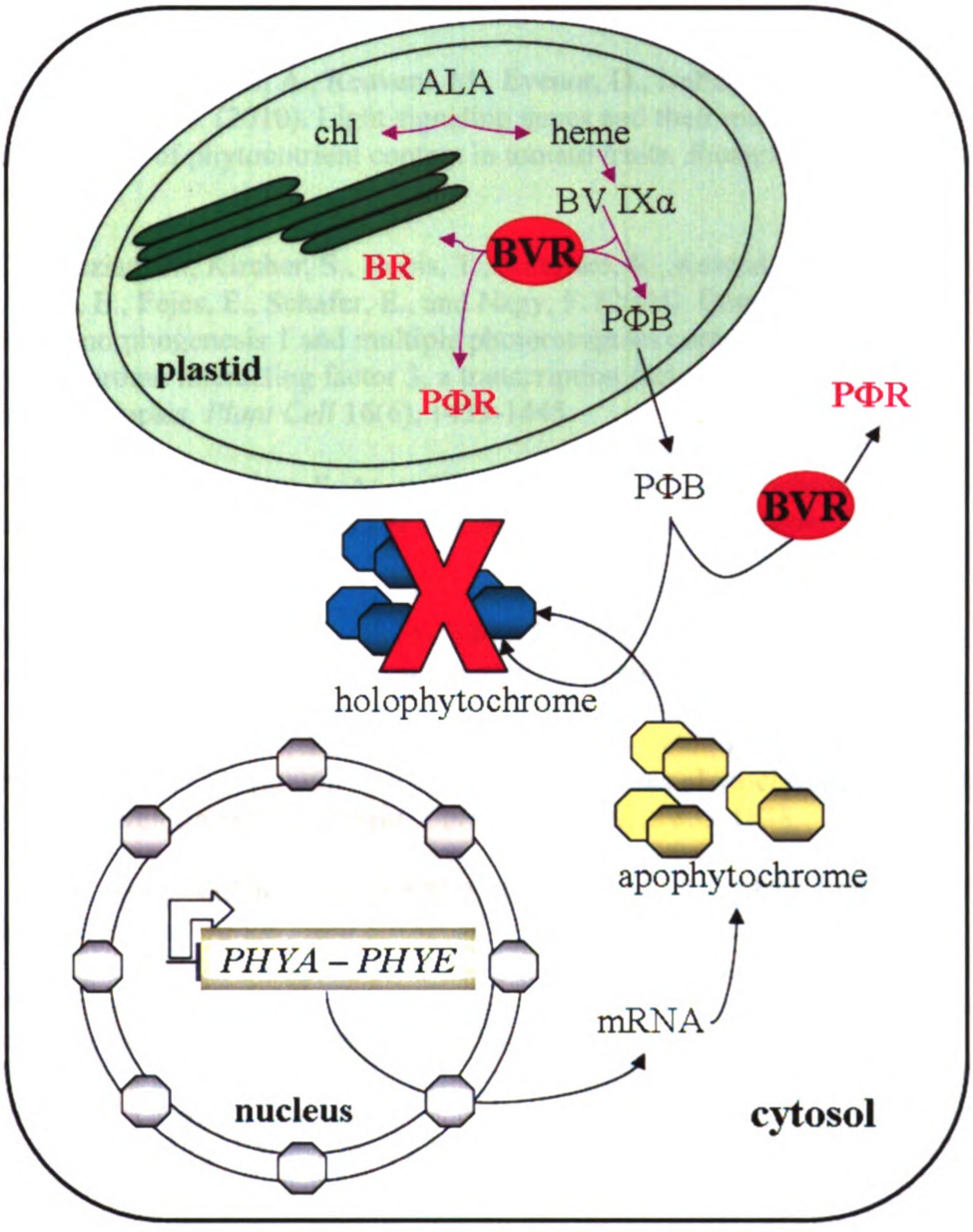

Figure 1.3 Inactivation of holophytochrome through expression of *BVR*. Plastid-targeted biliverdin reductase (BVR) converts a precursor of the phytochromobilin chromophore (PΦB), biliverdin IXα (BV), into bilirubin (BR) or PΦB into phytochromorubin (PΦR). *BVR* expressed in the cytosol metabolizes PΦB into PΦR. Metabolic inactivation of phytochromobilin biosynthesis leads to reduction of holophytochromes in transgenic Arabidopsis seedlings.

1.8 References

Azari, R., Tadmor, Y., Meir, A., Reuveni, M., Evenor, D., Nahon, S., Shlomo, H., Chen, L., and Levin, I. (2010). Light signaling genes and their manipulation towards modulation of phytonutrient content in tomato fruits. *Biotechnol Adv* **28**(1), 108-118.

Bauer, D., Viczian, A., Kircher, S., Nobis, T., Nitschke, R., Kunkel, T., Panigrahi, K. C., Adam, E., Fejes, E., Schafer, E., and Nagy, F. (2004). Constitutive photomorphogenesis 1 and multiple photoreceptors control degradation of phytochrome interacting factor 3, a transcription factor required for light signaling in Arabidopsis. *Plant Cell* **16**(6), 1433-1445.

Bischoff, F., Millar, A. J., Kay, S. A., and Furuya, M. (1997). Phytochrome-induced intercellular signalling activates cab::luciferase gene expression. *The Plant Journal* **12**(4), 839-849.

Black, M., and Shuttleworth, J. E. (1974). The role of the cotyledons in the photocontrol of hypocotyl extension in *Cucumis sativus* L. *Planta* **117**(1), 57-66.

Blumenstein, A., Vienken, K., Tasler, R., Purschwitz, J., Veith, D., Frankenberg-Dinkel, N., and Fischer, R. (2005). The *Aspergillus nidulans* phytochrome FphA represses sexual development in red light. *Curr Biol* **15**(20), 1833-1838.

Bou-Torrent, J., Roig-Villanova, I., and Martinez-Garcia, J. F. (2008). Light signaling: back to space. *Trends Plant Sci* **13**(3), 108-114.

Brand, A. H., and Perrimon, N. (1993). Targeted gene expression as a means of altering cell fates and generating dominant phenotypes. *Development* **118**(2), 401-415.

Brandt, S., von Stetten, D., Gunther, M., Hildebrandt, P., and Frankenberg-Dinkel, N. (2008). The fungal phytochrome FphA from *Aspergillus nidulans*. *J Biol Chem* **283**(50), 34605-34614.

Caubergs, R., and De Greef, J. A. (1975). Studies on hook-opening in *Phaseolus vulgaris* L. by selective R/FR pretreatments of embryonic axis and primary leaves. *Photochem. Photobiol.* **22**(3-4), 139-144.

Chen, M., Chory, J., and Fankhauser, C. (2004). Light signal transduction in higher plants. *Annu Rev Genet* **38**, 87-117.

Choi, G., Yi, H., Lee, J., Kwon, Y. K., Soh, M. S., Shin, B., Luka, Z., Hahn, T. R., and Song, P. S. (1999). Phytochrome signalling is mediated through nucleoside diphosphate kinase 2. *Nature* **401**(6753), 610-613.

Chory, J., Chatterjee, M., Cook, R. K., Elich, T., Fankhauser, C., Li, J., Nagpal, P., Neff, M., Pepper, A., Poole, D., Reed, J., and Vitart, V. (1996). From seed germination to flowering, light controls plant development via the pigment phytochrome. *Proc Natl Acad Sci U S A* **93**(22), 12066-12071.

Clack, T., Shokry, A., Moffet, M., Liu, P., Faul, M., and Sharrock, R. A. (2009). Obligate heterodimerization of Arabidopsis phytochromes C and E and interaction with the PIF3 basic helix-loop-helix transcription factor. *Plant Cell* **21**(3), 786-799.

Clough, R. C., and Vierstra, R. D. (1997). Phytochrome degradation. *Plant, Cell & Environment* **20**(6), 713-721.

Davis, S. J., Vener, A. V., and Vierstra, R. D. (1999). Bacteriophytochromes: phytochrome-like photoreceptors from nonphotosynthetic eubacteria. *Science* **286**(5449), 2517-2520.

De Greef, J. A., and Caubergs, R. (1972a). Interorgan correlations and phytochrome: hypocotyl hook opening. *Arch. Int. Physiol. Biochim.* **80**(5), 959-960.

De Greef, J. A., and Caubergs, R. (1972b). Interorgan correlations and phytochrome: leaf expansion. *Arch. Int. Physiol. Biochim.* **80**(5), 961-962.

Emborg, T. J., Walker, J. M., Noh, B., and Vierstra, R. D. (2006). Multiple heme oxygenase family members contribute to the biosynthesis of the phytochrome chromophore in Arabidopsis. *Plant Physiol* **140**(3), 856-868.

Endo, M., Mochizuki, N., Suzuki, T., and Nagatani, A. (2007). CRYPTOCHROME2 in vascular bundles regulates flowering in Arabidopsis. *Plant Cell* **19**(1), 84-93.

Endo, M., and Nagatani, A. (2008). Flowering regulation by tissue specific functions of photoreceptors. *Plant Signal Behav* **3**(1), 47-48.

Endo, M., Nakamura, S., Araki, T., Mochizuki, N., and Nagatani, A. (2005). Phytochrome B in the mesophyll delays flowering by suppressing FLOWERING LOCUS T expression in Arabidopsis vascular bundles. *Plant Cell* **17**(7), 1941-1952.

Fankhauser, C., and Staiger, D. (2002). Photoreceptors in *Arabidopsis thaliana*: light perception, signal transduction and entrainment of the endogenous clock. *Planta* **216**(1), 1-16.

Fankhauser, C., Yeh, K. C., Lagarias, J. C., Zhang, H., Elich, T. D., and Chory, J. (1999). PKS1, a substrate phosphorylated by phytochrome that modulates light signaling in Arabidopsis. *Science* **284**(5419), 1539-1541.

Fodor, S. P., Lagarias, J. C., and Mathies, R. A. (1990). Resonance Raman analysis of the Pr and Pfr forms of phytochrome. *Biochemistry* **29**(50), 11141-11146.

Franklin, K. A., Allen, T., and Whitelam, G. C. (2007). Phytochrome A is an irradiance-dependent red light sensor. *Plant J* **50**(1), 108-117.

Franklin, K. A., Praekelt, U., Stoddart, W. M., Billingham, O. E., Halliday, K. J., and Whitelam, G. C. (2003). Phytochromes B, D, and E act redundantly to control multiple physiological responses in Arabidopsis. *Plant Physiol* **131**(3), 1340-1346.

Franklin, K. A., and Quail, P. H. (2010). Phytochrome functions in Arabidopsis development. *J Exp Bot* **61**(1), 11-24.

Franklin, K. A., and Whitelam, G. C. (2004). Light signals, phytochromes and cross-talk with other environmental cues. *J Exp Bot* **55**(395), 271-276.

Furuya, M., and Schäfer, E. (1996). Photoperception and signalling of induction reactions by different phytochromes. *Trends Plant Sci* **1**(9), 301-307.

Garcia-Dominguez, M., Muro-Pastor, M. I., Reyes, J. C., and Florencio, F. J. (2000). Light-dependent regulation of cyanobacterial phytochrome expression. *J Bacteriol* **182**(1), 38-44.

Goosey, L., Palecanda, L., and Sharrock, R. A. (1997). Differential patterns of expression of the Arabidopsis PHYB, PHYD, and PHYE phytochrome genes. *Plant Physiol* **115**(3), 959-969.

Haseloff, J. (1999). GFP variants for multispectral imaging of living cells. *Methods Cell Biol* **58**, 139-151.

Hiltbrunner, A., Tscheuschler, A., Viczian, A., Kunkel, T., Kircher, S., and Schafer, E. (2006). FHY1 and FHL act together to mediate nuclear accumulation of the phytochrome A photoreceptor. *Plant Cell Physiol* **47**(8), 1023-1034.

Hudson, M. E. (2000). The genetics of phytochrome signalling in Arabidopsis. *Semin Cell Dev Biol* **11**(6), 475-483.

Hughes, J. (2010). Phytochrome three-dimensional structures and functions. *Biochem Soc Trans* **38**(2), 710-716.

Idnurm, A., and Heitman, J. (2005). Photosensing Fungi: Phytochrome in the spotlight. *Current Biology* **15**(20), R829-R832.

Jiang, Z., Swem, L. R., Rushing, B. G., Devanathan, S., Tollin, G., and Bauer, C. E. (1999). Bacterial photoreceptor with similarity to photoactive yellow protein and plant phytochromes. *Science* **285**(5426), 406-409.

Jiao, Y., Lau, O. S., and Deng, X. W. (2007). Light-regulated transcriptional networks in higher plants. *Nat Rev Genet* **8**(3), 217-230.

Karniol, B., Wagner, J. R., Walker, J. M., and Vierstra, R. D. (2005). Phylogenetic analysis of the phytochrome superfamily reveals distinct microbial subfamilies of photoreceptors. *Biochem J* **392**(Pt 1), 103-116.

Kehoe, D. M., and Grossman, A. R. (1996). Similarity of a chromatic adaptation sensor to phytochrome and ethylene receptors. *Science* **273**(5280), 1409-1412.

Kehoe, D. M., and Gutu, A. (2006). Responding to color: the regulation of complementary chromatic adaptation. *Annu Rev Plant Biol* **57**, 127-150.

Kim, J.-I., Bhoo, S.-H., Han, Y.-J., Zarate, X., Furuya, M., and Song, P.-S. (2006). The PAS2 domain is required for dimerization of phytochrome A. *Journal of Photochemistry and Photobiology A: Chemistry* **178**(2-3), 115-121.

Kim, J., Yi, H., Choi, G., Shin, B., Song, P. S., and Choi, G. (2003). Functional characterization of phytochrome interacting factor 3 in phytochrome-mediated light signal transduction. *Plant Cell* **15**(10), 2399-2407.

Kircher, S., Kozma-Bognar, L., Kim, L., Adam, E., Harter, K., Schafer, E., and Nagy, F. (1999). Light quality-dependent nuclear import of the plant photoreceptors phytochrome A and B. *Plant Cell* **11**(8), 1445-1456.

Kneip, C., Hildebrandt, P., Schlamann, W., Braslavsky, S. E., Mark, F., and Schaffner, K. (1999). Protonation state and structural changes of the tetrapyrrole chromophore during the Pr --> Pfr phototransformation of phytochrome: a resonance Raman spectroscopic study. *Biochemistry* **38**(46), 15185-15192.

Kohchi, T., Mukougawa, K., Frankenberg, N., Masuda, M., Yokota, A., and Lagarias, J. C. (2001). The Arabidopsis HY2 gene encodes phytochromobilin synthase, a ferredoxin-dependent biliverdin reductase. *Plant Cell* **13**(2), 425-436.

Lagarias, D. M., Crepeau, M. W., Maines, M. D., and Lagarias, J. C. (1997). Regulation of photomorphogenesis by expression of mammalian biliverdin reductase in transgenic Arabidopsis plants. *Plant Cell* **9**(5), 675-688.

Lagarias, J. C., and Rapoport, H. (1980). Chromopeptides from phytochrome. The structure and linkage of the PR form of the phytochrome chromophore. *Journal of the American Chemical Society* **102**(14), 4821-4828.

Laplaze, L., Parizot, B., Baker, A., Ricaud, L., Martiniere, A., Auguy, F., Franche, C., Nussaume, L., Bogusz, D., and Haseloff, J. (2005). GAL4-GFP enhancer trap lines for genetic manipulation of lateral root development in *Arabidopsis thaliana*. *J Exp Bot* **56**(419), 2433-2442.

Mandoli, D. F., and Briggs, W. R. (1982a). Optical properties of etiolated plant tissues. *Proc Natl Acad Sci U S A* **79**(9), 2902-2906.

Mandoli, D. F., and Briggs, W. R. (1982b). The photoperceptive sites and the function of tissue light-piping in photomorphogenesis of etiolated oat seedlings. *Plant, Cell & Environment* **5**(2), 137-145.

Martinez-Garcia, J. F., Huq, E., and Quail, P. H. (2000). Direct targeting of light signals to a promoter element-bound transcription factor. *Science* **288**(5467), 859-863.

Mathews, S. (2006). Phytochrome-mediated development in land plants: red light sensing evolves to meet the challenges of changing light environments. *Mol Ecol* **15**(12), 3483-3503.

Mathews, S. (2010). Evolutionary studies illuminate the structural-functional model of plant phytochromes. *Plant Cell* **22**(1), 4-16.

Mathews, S., Lavin, M., and Sharrock, R. A. (1995). Evolution of the phytochrome gene family and its utility for phylogenetic analyses of Angiosperms. *Annals of the Missouri Botanical Garden* **82**(2), 296-321.

Mathews, S., and Sharrock, R. A. (1997). Phytochrome gene diversity. *Plant, Cell & Environment* **20**(6), 666-671.

Monte, E., Al-Sady, B., Leivar, P., and Quail, P. H. (2007). Out of the dark: how the PIFs are unmasking a dual temporal mechanism of phytochrome signalling. *J Exp Bot* **58**(12), 3125-3133.

Monte, E., Tepperman, J. M., Al-Sady, B., Kaczorowski, K. A., Alonso, J. M., Ecker, J. R., Li, X., Zhang, Y., and Quail, P. H. (2004). The phytochrome-interacting transcription factor, PIF3, acts early, selectively, and positively in light-induced chloroplast development. *Proc Natl Acad Sci U S A* **101**(46), 16091-16098.

Montgomery, B. L. (2007). Sensing the light: photoreceptive systems and signal transduction in cyanobacteria. *Mol Microbiol* **64**(1), 16-27.

Montgomery, B. L. (2008). Right place, right time: Spatiotemporal light regulation of plant growth and development. *Plant Signal Behav* **3**(12), 1053-1060.

Montgomery, B. L. (2009). Spatial-specific phytochrome responses during de-etiolation in *Arabidopsis thaliana*. *Plant Signal Behav* **4**(1), 47-49.

Montgomery, B. L., Franklin, K. A., Terry, M. J., Thomas, B., Jackson, S. D., Crepeau, M. W., and Lagarias, J. C. (2001). Biliverdin reductase-induced phytochrome chromophore deficiency in transgenic tobacco. *Plant Physiol* **125**(1), 266-277.

Montgomery, B. L., and Lagarias, J. C. (2002). Phytochrome ancestry: sensors of bilins and light. *Trends Plant Sci* **7**(8), 357-366.

Montgomery, B. L., Yeh, K. C., Crepeau, M. W., and Lagarias, J. C. (1999). Modification of distinct aspects of photomorphogenesis via targeted expression of mammalian biliverdin reductase in transgenic Arabidopsis plants. *Plant Physiol* **121**(2), 629-639.

Moore, I., Galweiler, L., Grosskopf, D., Schell, J., and Palme, K. (1998). A transcription activation system for regulated gene expression in transgenic plants. *Proc Natl Acad Sci U S A* **95**(1), 376-381.

Nagatani, A. (1997). Spatial distribution of phytochromes. *Journal of Plant Research* **110**(1), 123-130.

Nagatani, A. (2004). Light-regulated nuclear localization of phytochromes. *Curr Opin Plant Biol* **7**(6), 708-711.

Nagy, F., and Schafer, E. (2002). Phytochromes control photomorphogenesis by differentially regulated, interacting signaling pathways in higher plants. *Annu Rev Plant Biol* **53**, 329-355.

Neff, M. M., Fankhauser, C., and Chory, J. (2000). Light: an indicator of time and place. *Genes Dev* **14**(3), 257-271.

Nick, P., Ehmann, B., Furuya, M., and Schafer, E. (1993). Cell communication, stochastic cell responses, and anthocyanin pattern in Mustard cotyledons. *Plant Cell* **5**(5), 541-552.

Parcy, F. (2005). Flowering: a time for integration. *Int J Dev Biol* **49**(5-6), 585-593.

Plett, D., Safwat, G., Gilliham, M., Skrumsager Moller, I., Roy, S., Shirley, N., Jacobs, A., Johnson, A., and Tester, M. (2010). Improved salinity tolerance of rice through cell type-specific expression of AtHKT1;1. *PLoS One* **5**(9), e12571.

Purschwitz, J., Muller, S., Kastner, C., Schoser, M., Haas, H., Espeso, E. A., Atoui, A., Calvo, A. M., and Fischer, R. (2008). Functional and physical interaction of blue- and red-light sensors in Aspergillus nidulans. *Curr Biol* **18**(4), 255-259.

Quail, P. H. (1994). Photosensory perception and signal transduction in plants. *Curr Opin Genet Dev* **4**(5), 652-661.

Quail, P. H. (2000). Phytochrome-interacting factors. *Semin Cell Dev Biol* **11**(6), 457-466.

Quail, P. H. (2002). Phytochrome photosensory signalling networks. *Nat Rev Mol Cell Biol* **3**(2), 85-93.

Rockwell, N. C., and Lagarias, J. C. (2010). A brief history of phytochromes. *Chemphyschem* **11**(6), 1172-1180.

Rösler, J., Klein, I., and Zeidler, M. (2007). Arabidopsis fhl/fhy1 double mutant reveals a distinct cytoplasmic action of phytochrome A. *Proc Natl Acad Sci U S A* **104**(25), 10737-10742.

Rudiger, W., Thummler, F., Cmiel, E., and Schneider, S. (1983). Chromophore structure of the physiologically active form Pfr of phytochrome. *Proc Natl Acad Sci U S A* **80**(20), 6244-6248.

Rutherford, S., Brandizzi, F., Townley, H., Craft, J., Wang, Y., Jepson, I., Martinez, A., and Moore, I. (2005). Improved transcriptional activators and their use in mis-expression traps in Arabidopsis. *Plant J* **43**(5), 769-788.

Ryu, J. S., Kim, J. I., Kunkel, T., Kim, B. C., Cho, D. S., Hong, S. H., Kim, S. H., Fernandez, A. P., Kim, Y., Alonso, J. M., Ecker, J. R., Nagy, F., Lim, P. O., Song, P. S., Schafer, E., and Nam, H. G. (2005). Phytochrome-specific type 5 phosphatase controls light signal flux by enhancing phytochrome stability and affinity for a signal transducer. *Cell* **120**(3), 395-406.

Schepens, I., Duek, P., and Fankhauser, C. (2004). Phytochrome-mediated light signalling in Arabidopsis. *Curr Opin Plant Biol* **7**(5), 564-569.

Sharrock, R. A., and Clack, T. (2004). Heterodimerization of type II phytochromes in Arabidopsis. *Proc Natl Acad Sci U S A* **101**(31), 11500-11505.

Shen, Y., Khanna, R., Carle, C. M., and Quail, P. H. (2007). Phytochrome induces rapid PIF5 phosphorylation and degradation in response to red-light activation. *Plant Physiol* **145**(3), 1043-1051.

Smith, H. (1995). Physiological and ecological function within the phytochrome family. *Ann Rev of Plant Physiol Plant Molec Biol* **46**(1), 289-315.

Smith, H. (2000). Phytochromes and light signal perception by plants-an emerging synthesis. *Nature* **407**(6804), 585-591.

Sullivan, J. A., and Deng, X. W. (2003). From seed to seed: the role of photoreceptors in Arabidopsis development. *Dev Biol* **260**(2), 289-297.

Takano, M., Inagaki, N., Xie, X., Yuzurihara, N., Hihara, F., Ishizuka, T., Yano, M., Nishimura, M., Miyao, A., Hirochika, H., and Shinomura, T. (2005). Distinct and cooperative functions of phytochromes A, B, and C in the control of deetiolation and flowering in rice. *Plant Cell* **17**(12), 3311-3325.

Terry, M. J., Wahleithner, J. A., and Lagarias, J. C. (1993). Biosynthesis of the plant photoreceptor phytochrome. *Arch Biochem Biophys* **306**(1), 1-15.

Terzaghi, W. B., and Cashmore, A. R. (1995). Photomorphogenesis. Seeing the light in plant development. *Curr Biol* **5**(5), 466-468.

Tóth, R., Kevei, E., Hall, A., Millar, A. J., Nagy, F., and Kozma-Bognar, L. (2001). Circadian clock-regulated expression of phytochrome and cryptochrome genes in Arabidopsis. *Plant Physiol* **127**(4), 1607-1616.

Ulijasz, A. T., Cornilescu, G., Cornilescu, C. C., Zhang, J., Rivera, M., Markley, J. L., and Vierstra, R. D. (2010). Structural basis for the photoconversion of a phytochrome to the activated Pfr form. *Nature* **463**(7278), 250-254.

Ulm, R., and Nagy, F. (2005). Signalling and gene regulation in response to ultraviolet light. *Curr Opin Plant Biol* **8**(5), 477-482.

Vierstra, R. D., and Davis, S. J. (2000). Bacteriophytochromes: new tools for understanding phytochrome signal transduction. *Semin Cell Dev Biol* **11**(6), 511-521.

Warnasooriya, S. N., and Montgomery, B. L. (2009). Detection of spatial-specific phytochrome responses using targeted expression of biliverdin reductase in Arabidopsis. *Plant Physiol* **149**(1), 424-433.

Warnasooriya, S. N., and Montgomery, B. L. (in press). Using Transgenic Modulation of Protein Accumulation to Probe Protein Signaling Networks in *Arabidopsis thaliana,* Plant Biotechnology and Transgenic Research, Bentham Science Publishers, Oak Park, IL.

Wilde, A., Churin, Y., Schubert, H., and Borner, T. (1997). Disruption of a Synechocystis sp. PCC 6803 gene with partial similarity to phytochrome genes alters growth under changing light qualities. *FEBS Lett* **406**(1-2), 89-92.

Wu, C., Li, X., Yuan, W., Chen, G., Kilian, A., Li, J., Xu, C., Li, X., Zhou, D. X., Wang, S., and Zhang, Q. (2003). Development of enhancer trap lines for functional analysis of the rice genome. *Plant J* **35**(3), 418-427.

Yamaguchi, R., Nakamura, M., Mochizuki, N., Kay, S. A., and Nagatani, A. (1999). Light-dependent translocation of a phytochrome B-GFP fusion protein to the nucleus in transgenic Arabidopsis. *J Cell Biol* **145**(3), 437-445.

Yeh, K. C., Wu, S. H., Murphy, J. T., and Lagarias, J. C. (1997). A cyanobacterial phytochrome two-component light sensory system. *Science* **277**(5331), 1505-1508.

Zeevaart, J. A. (2006). Florigen coming of age after 70 years. *Plant Cell* **18**(8), 1783-1789.

Chapter 2 Regulation of Far-red Light-Mediated High Irradiance Responses by Spatial-specific Phytochromes

Some of the work included in chapter 2 was published in the journal, Plant Physiology.

Warnasooriya SN and Montgomery BL, (2009), Detection of Spatial-Specific Phytochrome Responses Using Targeted Expression of Biliverdin Reductase in Arabidopsis, Plant Physiology, 149(1), 424-433.

Some of the work in chapter 2 is from a manuscript submitted to the journal, Plant, Cell and Physiology.

Warnasooriya SN, Porter KJ and Montgomery BL, Tissue- and Isoform-Specific Phytochrome Regulation of Light-Dependent Anthocyanin Accumulation in *Arabidopsis thaliana* (submitted).

2.1 Overview

Phytochromes, in response to R and FR light, regulate numerous and distinct aspects of light-mediated growth and development (Chen, Chory, and Fankhauser, 2004; Franklin and Quail, 2010; Mathews, 2006). The regulation of these physiological responses encompasses complex intra- as well as, inter-cellular signaling cascades (Montgomery, 2008). A number of studies have confirmed that phytochromes mediate cell- and tissue-specific signaling pathways in controlling discrete aspects of light-dependent growth and development through intercellular and/or inter-organ coordination (Black and Shuttleworth, 1974; Caubergs and De Greef, 1975; De Greef and Caubergs, 1972a; De Greef and Caubergs, 1972b; Mandoli and Briggs, 1982; Nick et al., 1993).

Expression of distinct fractions of the Arabidopsis genome in different organs or tissue types in response to developmental and environmental cues results in spatial-specific responses. Discrete spatial-specific light responses are likely to be impacted by several factors. Light sensitivity of cells or organs is influenced by their physiological differences; i.e. pigmentation due to photosynthetic activity, and metabolic status can affect light sensitivity of a particular tissue (Bou-Torrent, Roig-Villanova, and Martinez-Garcia, 2008). Although spatial expression analyses have concluded that phytochromes are found in all tissues analyzed, even in roots, (Clack, Mathews, and Sharrock, 1994; Nagatani, 1997; Tóth et al., 2001) and thus, are R- and FR-sensitive, in a given tissue or organ, phytochromes and interacting partners downstream of R/FR light perception might not be uniformly distributed (Bou-Torrent, Roig-Villanova, and Martinez-Garcia, 2008). In fact, several concerted efforts related to tissue- and organ-specific expression profiling have confirmed that each organ or tissue type has a well defined genome expression

pattern (Jiao, Lau, and Deng, 2007; Jiao et al., 2005; Ma et al., 2005) and spatial-specific involvement of signaling cascades in different organs and cell types in response to divergent light effects. Thus, most spatial-specific expression patterns of early targets of phytochrome signaling likely define the cellular mechanisms of localized pools of phytochromes that eventually result in different, even opposing, intercellular and/or organ-specific phytochrome responses to the same light stimulus (Bou-Torrent, Roig-Villanova, and Martinez-Garcia, 2008).

2.1.1 Phytochrome-dependent High Irradiance Responses

Plants are exposed to prolonged periods of high intensity light irradiation in natural environments. HIRs are characterized as physiological responses that require relatively high photon fluence rates over a long duration with strong irradiance dependence and a lack of photoreversibility (Caubergs and De Greef, 1975; Deng and Quail, 1999; Neff, Fankhauser, and Chory, 2000). HIRs that have been examined extensively are light-mediated inhibition of hypocotyl elongation and anthocyanin production *in planta* (De Greef and Caubergs, 1972a; De Greef and Caubergs, 1972b). B-, R- and FR-mediated HIRs were first identified through the analysis of action spectra for anthocyanin formation under prolonged irradiation in cabbage and turnip (De Greef and Caubergs, 1972a) and Mohr (1972) later speculated that HIRs with action spectra having a peak in the FR light region were FR-HIR, and the possible involvement of phytochrome in the regulation of FR-HIR. Recently, Shinomura, Uchida, and Furuya, (2000) reported that a transitory signal generated during photoconversion from Pfr to Pr form of

phytochrome is required for FR-HIR in contrast to the more stable phyB-produced signal in R-HIR (Ahmad and Cashmore, 1997; Caubergs and De Greef, 1975).

Typical HIRs include inhibition of seed germination, hypocotyl elongation, and opening of the apical hook, expansion of the cotyledons, accumulation of anthocyanin and a FR-light preconditioned block of greening during seedling development (Neff, Fankhauser, and Chory, 2000). Germination and growth of Arabidopsis seedlings in continuous FR light (FRc) can induce partial photomorphogenesis without the accumulation of chlorophyll. Under these conditions, although seedlings are chlorophyll deficient, hypocotyl elongation is inhibited and the cotyledons are expanded (Whitelam et al., 1993). phyA and phyB have recognized roles in mediating HIR of light-dependent inhibition of hypocotyl elongation in Arabidopsis under FR and R light, respectively (Quail et al., 1995).

2.1.2 Light Perception by Phytochrome A

phyA is unique among the other phytochrome family members due to a number of characteristics in its stability and light perception. In contrast to light-stable phyB-phyE, phyA is light-labile and is responsible for the VLFR and FR-HIR (Nagy and Schafer, 2002; Sharrock and Clack, 2002; Wang and Deng, 2003). phyA is relatively stable in its Pr form and is rapidly degraded upon conversion to the Pfr form (Clough and Vierstra, 1997). Since phyA accumulates to high levels in etiolated seedlings, the primary function of phyA is to promote seed germination during early stages of de-etiolation (Mohr, 1972). However, phyA that exists in de-etiolated tissues is known to regulate numerous responses in the life cycle of light-grown seedlings, namely, inhibition of stem elongation

growth during shade avoidance (Yanovsky, Casal, and Whitelam, 1995), light input to the endogenous clock (Johnson et al., 1994), inhibition of internode elongation (Devlin, Patel, and Whitelam, 1998) and regulation of leaf expansion (Franklin et al., 2003). The observation that inhibition of hypocotyl elongation or anthocyanin accumulation can be partially reversed if the B light pulses are followed by saturating FR-light pulses suggested that phytochromes are involved in B light perception (Casal and Boccalandro, 1995; Mancinelli, Rossi, and Moroni, 1991). Indeed, in later studies, phyA has been shown to have a role in regulating responses under B illumination, i.e. chloroplast gene expression during leaf development, hypocotyl inhibition and anthocyanin accumulation (Chun, Kawakami, and Christopher, 2001; Duek and Fankhauser, 2003; Neff and Chory, 1998; Poppe et al., 1998; Whitelam et al., 1993; Yadav et al., 2005).

Analysis of monogenic and high order mutants in apophytochrome genes has revealed distinct functional roles for phyA during de-etiolation of Arabidopsis seedlings in FR light. *phyA* mutants have long hypocotyls and closed cotyledons as opposed to short hypocotyls and expanded cotyledons in WT seedlings under FR light (Nagatani, Reed, and Chory, 1993; Parks and Quail, 1993; Whitelam et al., 1993). These studies confirmed that phyA is an FR sensor and regulates seedling de-etiolation. Single mutants of Arabidopsis deficient in phyB-phyE resembled WT plants in FRc (Aukerman et al., 1997; Reed et al., 1994) and thus confirm that phyA solely mediates VLFR and FR-HIR (Wang and Deng, 2003) in FR light. Until recently, phyA was thought to be neither necessary nor sufficient for R light perception (Quail et al., 1995) although several studies with *phyAphyB* double mutant and *phyB* mutant in R light (< 50 μmol m^{-2} s^{-1}) indicated that phyA might potentially have a role in regulating hypocotyl inhibition, hook

opening and expansion of cotyledons (Neff and Chory, 1998; Reed et al., 1994). Franklin, Allen, and Whitelam, (2007) reported that phyA is able to regulate de-etiolation and possesses increased stability, as nuclear phyA is subject to irradiance-dependent photoprotection under high intensity R light (> 160 μmol m^{-2} s^{-1}). Results from this study revealed the significance of nuclear phyA being an irradiance-dependent R light sensor as plants are exposed to high intensities of light in natural environments.

2.1.3 Phytochrome A and Downstream Components in Signaling

phyA-mediated signaling, based on light-dependent nuclear transport and differential stability, involves compartmentalization, transcriptional regulation and differential degradation (Hiltbrunner et al., 2006; Rösler, Klein, and Zeidler, 2007; Wang and Deng, 2003; Yang et al., 2009; Yanovsky et al., 2002). Since phyA is solely responsible for regulating responses in FR light conditions (Nagatani, Reed, and Chory, 1993; Parks and Quail, 1993; Whitelam et al., 1993), the approach for identifying the downstream candidates of phyA signaling has been to assess for the disruption of phytochrome-mediated responses in FR in mutants. Based on elongated hypocotyls and unexpanded cotyledons under FR light, more than 15 mutants have been isolated and characterized that encode signal transduction components in the phyA-mediated signaling cascade (Wang and Deng, 2003; Yang et al., 2009). Many of the signal transduction components appear to be transcription factors with which nuclear-localized phyA interacts to mediate discrete responses (Ballesteros et al., 2001; Duek and Fankhauser, 2003; Fairchild, Schumaker, and Quail, 2000; Ni, Tepperman, and Quail, 1998; Rösler, Klein, and Zeidler, 2007). Moreover, since VLFRs saturate upon activation of phyA with

short pulses of very low fluence R or FR light, while HIRs require sustained activation of phyA with higher fluences of FR light, VLFR- and HIR-mediated signaling can be dissected genetically at certain loci that function downstream of phyA in the signaling pathway (Luccioni et al., 2002; Yanovsky, Casal, and Luppi, 1997; Yanovsky, Whitelam, and Casal, 2000). This suggests that signaling downstream of light perception by phyA may branch out into two individual cascades, depending on the mode in which phyA is activated.

Distinct physiological roles have been attributed to nuclear-localized phyA. FHL- and FHY-regulated nuclear transport of phyA allows interaction of phyA with transcription factors (Hiltbrunner et al., 2006; Hiltbrunner et al., 2005). In fact, phyA has been identified to interact with LAF1 and HFR in regulating inhibition of hypocotyl elongation under FR light (Yang et al., 2009). Recently, an analysis of the *fhl/fhy1* double mutant has shown that cytoplasmic phyA is able to regulate R light-enhanced phototropism, abrogation of gravitropism, and inhibition of hypocotyl elongation in B light (Rösler, Klein, and Zeidler, 2007). This raises the possibility that nuclear- and cytoplasmic-localized pools of phyA may engage different downstream interacting partners to regulate discrete physiological responses. Moreover, the analysis of gene expression profiles in roots, hypocotyls and cotyledons of Arabidopsis seedlings (Ma et al., 2005) has indicated that the expression patterns of *PHYA*, *PHYB*, several *PIF*s and a number of early targets of phytochrome signaling action during both de-etiolation and shade avoidance response (i.e. *ATHB2*, *ATHB4*, *HAT2*, *PAR1*, *PIL1*, *RIP*; Roig-Villanova et al., 2006) vary in response to light in the three organs. Thus, upon light perception by nuclear- or cytoplasmic-localized phyA, the transcriptional network might immediately

diverge in a cell- and organ-specific manner, thereby increasing the complexity of phyA-mediated signaling. Although, a significant number of downstream molecular effectors have been identified in the phyA signaling pathway, identification of target genes involved in spatial-specific phyA-mediated signaling requires further analysis.

2.1.4 Outlook

Although much progress has been made in understanding spatial-specific light perception by phytochromes and the subsequent downstream signaling network, definitive molecular evidence about distinct sites of phytochrome photoperception and cellular mechanisms of pools of phytochromes in regulating tissue- and organ-specific phytochrome responses in Arabidopsis is limited. The importance of regulation of such spatial-specific responses is beginning to be recognized, however, much work remains to be accomplished to identify these responses and elucidate them fully at the molecular level (Bou-Torrent, Roig-Villanova, and Martinez-Garcia, 2008; Montgomery, 2008). Knowledge of spatial-specific phytochrome responses to the changing light environment and their underlying molecular bases will provide groundwork for dissecting the complex intercellular and inter-organ molecular processes underlying R- and FR-dependent plant growth and development. The knowledge base generated at the molecular level will help to modify light responses in specific tissues or organs, reducing the detrimental and pleiotropic effects observed when phytochrome action is manipulated in the whole plant.

A molecular tool that is being currently utilized for phytochrome inactivation is the expression of a gene encoding a rat kidney enzyme, biliverdin IXα reductase (*BVR*). Constitutive expression of *BVR* in Arabidopsis has led to the perturbation of many light-

dependent phytochrome-mediated responses (Lagarias et al., 1997; Montgomery et al., 1999). Such BVR-dependent phenotypes are very similar to responses displayed by an Arabidopsis phytochrome chromophore-deficient mutant, *hy1* (Montgomery et al., 1999) and indicate a loss of photosensory activities of multiple phytochromes. In this chapter, two tissue-specific promoters (i.e. CAB3 and MERI5) were utilized to drive the expression of the *BVR* in mesophyll cells and shoot meristamatic tissues, respectively. Studies with stable transgenic lines displaying mesophyll- and meristem-specific phytochrome chromophore deficiencies revealed that localized pools of phytochromes can regulate distinct physiological responses and established the efficacy of targeted *BVR* expression as a novel molecular technique to investigate sites of light perception (Warnasooriya and Montgomery, 2009).

2.2 Materials and Methods

2.2.1 Photomorphogenesis of Transgenic Lines with Targeted Chromophore Inactivation in FRc

Seeds of No-0 WT, 35S::pBVR3, CAB3::pBVR2, Col-0 WT and *phyA* (SALK_014575; Ruckle, DeMarco, and Larkin, 2007) were sterilized with 35 % (v/v) commercial bleach and 0.025 % (v/v) SDS solution and were rinsed 6 times with ultrapure water (Milli-Q, Millipore, MA) according to the protocol published in (Warnasooriya and Montgomery, 2009). Sterilized seeds were planted in 100- x 25-mm petri dishes on media containing 1X Murashige and Skoog salts (Catalog No. MSP09, Caisson Laboratories, UT), 0.9 % (w/v) Phytablend (Catalog No. PTP01, Caisson Laboratories, UT) with 1 % (w/v) Sucrose (Catalog No. 4072-05, J.T. Baker, NJ), adjusted to pH 5.7 with KOH.

Imbibing seeds were cold-stratified at 4 °C for 3 days in darkness. Plates were transferred to a temperature- and humidity-controlled growth chamber with FRc illumination of 5 μmol m^{-2} s^{-1}. Seedling images were scanned at high resolution to show characteristic phenotypes observed in wild-type and transgenic Arabidopsis seedlings during photomorphogenesis in FR light.

2.2.2 Quantification of Anthocyanin Levels in Transgenic Lines with Targeted Chromophore Inactivation

To determine whether mesophyll- and meristem-localized phytochrome deficiencies distinctly affected sucrose-stimulated anthocyanin accumulation, anthocyanin levels were quantified in 4-d-old seedlings grown under FRc and Bc light. Seeds of No-0 WT, 35S::pBVR3, CAB3::pBVR2, Col-0 WT and *phyA* (SALK_ 014575; Ruckle, DeMarco, and Larkin, 2007) were sterilized and planted as described in section 2.2.1. Sterilized seeds were treated with R pulse (approximately 75 μmol m^{-2} s^{-1}) for 5 min prior to imbibition to synchronize germination. Imbibing seeds were cold-stratified at 4 °C for 3 days in darkness. Plates were transferred to a temperature- and humidity-controlled growth chamber with Bc illumination of 25 μmol m^{-2} s^{-1}, FRc illumination of 5 μmol m^{-2} s^{-1}, or in darkness for 4 days at 22 °C. Anthocyanins were extracted from whole-plant seedlings using 1 % (v/v) HCl (Catalog No. HX0603-13, EMD Chemicals Inc., NJ) in methanol (Catalog No. 9070-03, J.T. Baker, NJ) as described previously (Feinbaum and Ausubel, 1988) with the following modifications. The number and weight of fresh whole-plant seedlings were recorded before transferring the harvested seedlings

into glass vials. Anthocyanins were extracted in 1 % (v/v) HCl in methanol at a ratio of 20 µL/mg of fresh tissue overnight (~ 16 hr) with gentle shaking at 4 °C (adapted from Rabino and Mancinelli, (1986). Chloroform (Catalog No. 9180-01, J.T. Baker, NJ) was added at a ratio of 20 µL/mg of fresh tissue. Chloroform-water partitioning was performed by adding sterile H_2O at 0.4 volume of 1 % HCl in methanol and chloroform volumes, followed by centrifugation at 13,000 rpm at room temperature for 5 min (Denville 260D, NJ; adapted from Kerckhoffs et al., (1997). Anthocyanin content was estimated per seedling by measuring the A_{535} minus the A_{650} of the aqueous phase spectrophotometrically (Montgomery et al., 1999). Two-tailed, unpaired Student's t-test was performed to compare anthocyanin contents relative cognate WT seedlings.

2.2.3 Gene Expression Analysis

To identify candidate downstream target genes in regulating FR-dependent hypocotyl development, gene expression analysis was performed as follows. Seeds of No-0 WT, 35S::pBVR3 and CAB3::pBVR2 were sterilized as described in section 2.2.1. Seeds were planted in 150-x 15-mm petri dishes on media prepared according to section 2.2.1. To synchronize germination, plates with seeds were exposed to R light of 75 µmol m^{-2} s^{-1} for 5 min and imbibing seeds were cold-stratified at 4 °C in darkness for 3 days. 7-d-old whole seedlings were quickly (< 1 min) harvested and immediately frozen in liquid nitrogen inside the FR chamber. Total RNA was isolated using RNeasy® Plant Minikit (Catalog No. 16419, Qiagen, CA) according to manufacturer's instructions. After assessing the quality of isolated RNA on the Agilent 2100 Bioanalyzer (Agilent

Technologies, Inc., CA), 500 ng of total RNA were subjected to the synthesis of amplified RNA (aRNA) using the MessageAmp™ Premier RNA Amplification Kit (Catalog No. 4385821, Applied Biosystems/Ambion, TX) according to manufacturer's instructions with the following modifications. For i*n vitro* transcription reaction, samples were incubated for 8 hrs at 40 °C. Binding of aRNA to magnetic beads following addition of 100 % ethanol was carried out for 5 min with gentle shaking. To capture the magnetic beads-aRNA complex, the U bottom plate was held on the magnetic stand for ~ 6 min. aRNA was eluted off of magnetic beads through vigorous shaking for ~ 7 min. The quality of biotin-labeled aRNA was determined on the Agilent 2100 Bioanalyzer (Agilent Technologies, Inc., CA). 11-12 µg of labeled aRNA were submitted to the Research Technology Support Facility at Michigan State University for hybridization with the GeneChip® Arabidopsis ATH1 Genome Array (Catalog No. 900385, Affymetrix, Inc., CA) and acquisition of scanned probe arrays. Each labeled aRNA was hybridized to an individual ATH1 Genome Array and the microarray analysis was conducted with three independent RNA extractions per sample. The expression data were subjected to per chip normalization (shift to the 75th percentile) with baseline transformation to the median of all samples using GeneSpring GX 10.0 (Agilent Technologies Inc., CA). The data were then filtered on flags (present or marginal in at least 1 out of the 9 samples). Analysis of variance on log-transformed expression values was carried out by applying the Benjamini and Hochberg multiple testing correction with a p-value cut off of 0.05 across the three groups (No-0 WT, 35S::pBVR3 and CAB3::pBVR2) to control the false discovery rate. An expression filter of fold change

greater or equal to 2.0 was applied for 35S::pBVR3 and CAB3::pBVR2 samples against the No-0 WT sample. Expression data of CAB3::pBVR2 was compared against 35S::pBVR3 to identify genes with changes in gene expression that are unique to hypocotyl development observed in CAB3::pBVR2 in FR light. Based on the differential expression pattern observed in CAB3::pBVR2 relative to 35S::pBVR3, three genes were selected to prioritize initial analysis: *At1g26220*, *At4g02290* and *At1g52410*. The expression of *At1g26220*, *At4g02290* and *At1g52410* genes were analyzed using publicly available gene expression data. Mean-normalized $\log_2$ values from AtGenExpress and BAR Heatmapper *Plus* (http://www.bar.utoronto.ca) were used to generate heat maps for *At1g26220*, *At4g02290* and *At1g52410* genes.

2.2.4 Validation of *At1g26220*, *At4g02290* and *At1g52410* Expression in Transgenic Lines with Targeted Chromophore Inactivation by RT-PCR

To confirm the respective fold-reduction in the expression levels of *At1g26220*, *At4g02290* and *At1g52410* observed in CAB3::pBVR2 through microarray analysis, total RNA isolated from No-0 WT, 35S::pBVR3 and CAB3::pBVR2 in section 2.2.3 was used in RT-PCR. The quantity of RNA for each sample was analyzed by spectrometry (NanoDrop1000, Thermo Scientific, MA). Oligo$(dT)_{15}$ primed-first-strand cDNA was synthesized from 1 μg of total RNA using a Reverse Transcription System (Catalog No. A3500, Promega, WI) according to manufacturer's instructions with the following modifications: RT reactions were incubated at 42 °C for 1 hr followed by 95 °C for 5 min and 4 °C for 5 min. cDNA was stored at -20 °C overnight before PCR amplification. First-strand cDNA synthesis reactions were diluted 1:16 with nuclease-free water. PCR

was conducted with GoTaqGreen (Catalog No. M7123, Promega, WI) and 4 µl of the diluted cDNA product was used as template in a 25 µl reaction. The gene-specific oligonucleotides for *At1g26220* and *At1g52410* were designed based on the full length cDNA sequence: for *At1g26220*- forward 5'- AGGCACAATCTCCACTCCTCCAGC-3' and reverse 5'- CGGGTCAGAGACGAACCCAAGCG-3', for *At1g52410*- forward 5'- GACAATAACGAAGAAGAACACGCTGC -3' and reverse 5'- AATGAGAATCTGACCGAAATCTTTACG -3'. The gene-specific oligonucleotides for *At4g02290* were designed using a free online database, *AtRTPrimer* (Han and Kim, 2006); forward 5'- TCTTCTTCCTCCTCCTATGCCCTCA -3' and reverse 5'- TGCAAAAACACTGATGGCTCGTTT -3'. PCR amplification was carried out with gene-specific oligonucleotides at 10 µM. The following thermal cycling conditions were used for the PCR amplification: for *At1g26220*, (1) 1 cycle of denaturation at 94 °C for 2 min, (2) 27 cycles of denaturation at 94 °C for 30 s, annealing at 56 °C for 45 s, extension at 72 °C for 38 s and (3) final extension at 72 °C for 5 min with a hold at 4 °C. For *At4g02290*, (1) 1 cycle of denaturation at 94 °C for 2 min, (2) 28 cycles of denaturation at 94 °C for 30 s, annealing at 56 °C for 45 s, extension at 72 °C for 50 s and (3) final extension at 72 °C for 5 min with a hold at 4 °C. For *At1g52410*, (1) 1 cycle of denaturation at 94 °C for 2 min, (2) 27 cycles of denaturation at 94 °C for 30 s, annealing at 56 °C for 45 s, extension at 72 °C for 1 min 10 s and (3) final extension at 72 °C for 5 min with a hold at 4 °C. Expression of *UBC21* (*At5g25760*) was analyzed as an internal control by including *UBC21*-specific primers, forward 5'-

CCTTACGAAGGCGGTGTTTTTCAG-3' and reverse 5'-

CGGCGAGGCGTGTATACATTTG-3' at 10 μM in the same reaction. A 7 μL aliquot of the PCR product was visualized by electrophoresis for 1 hr 30 min at 85V on a 1.5 % agarose gel containing ethidium bromide at 0.02 μg/mL (Catalog No. 15585-011, Invitrogen, CA). Ultraviolet images were obtained using the Gel Doc system (Bio-Rad Laboratories, Inc., CA) at subsaturation settings.

2.2.5 Confirmation of T-DNA Insertion Mutants

SALK_062388, SALK_101567 and SALK_151393 mutants with a T-DNA insertion in an exon of *At1g26220*, *At4g02290* and *At1g52410* respectively, were selected from the Salk T-DNA insertion mutant collection (Alonso et al., 2003) and were genotyped by PCR. Seeds of Col-0 WT and homozygous SALK_062388, SALK_101567 and SALK_151393 mutants were sterilized, planted and subjected to cold stratification as described in section 2.2.1. Plates were transferred to a temperature- and humidity-controlled growth chamber with FRc illumination of 5 μmol m^{-2} s^{-1} for 7 days at 22 °C. Total RNA was isolated from 7-d-old whole seedlings using RNeasy® Plant Minikit (Catalog No. 16419, Qiagen, CA) including on-column DNase treatment (Catalog No. 79254, Qiagen, CA) according to manufacturer's instructions. The quantification of RNA, synthesis of cDNA and analysis of transcript accumulation in Col-0 WT and homozygous SALK_062388 (for *At1g26220*), SALK_101567 (for *At4g02290*) and SALK_151393 (for *At1g52410*) mutants were performed as described in section 2.2.4 with the following modifications: for *At4g02290* and *At1g52410*, annealing temperature

was 55 °C. Number of amplification cycles in the PCR step was 31 for *At4g02290* and *At1g52410*. A 7 µL aliquot of the PCR product was visualized by electrophoresis for 1 hr at 90V on a 1.5 % agarose gel containing ethidium bromide at 0.02 µg/mL (Catalog No. 15585-011, Invitrogen, CA). Ultraviolet images were obtained using the Gel Doc system (Bio-Rad Laboratories, Inc., CA) at subsaturation settings.

2.2.6 Hypocotyl Inhibition Assay

To determine whether the T-DNA insertion mutants in candidate genes selected based on microarray analysis display impaired hypocotyl development in FRc, seeds of homozygous SALK_062388, SALK_101567 and SALK_151393 were sterilized and planted as described in section 2.2.1. Imbibing seeds were cold-stratified at 4 °C for 3 days in darkness. Plates were transferred to a humidity-controlled chamber with FRc illumination of 5 µmol m^{-2} s^{-1} or in darkness for 7 days at 22 °C. Seedlings were scanned and plant images were used to quantify hypocotyl lengths using ImageJ software (NIH). The hypocotyl inhibition assay was repeated 3 times. Percentage dark length and standard deviations of percentage dark length were calculated according to the following equations. Two-tailed, unpaired Student's t-test was performed to compare the percentage dark length of hypocotyls relative to Col-0 WT seedlings.

$$\text{Percentage dark length, \%} = \frac{\text{Length of hypocotyl in Bc, Rc or FRc (X)}}{\text{Length of hypocotyl in dark (Y)}} * 100\%$$

Standard Deviations (with ratio: % = X/Y * 100%):

$$SD = \sqrt{\left(\frac{SDX}{avgX}\right)^2 + \left(\frac{SDY}{avgY}\right)^2}$$

Where: SD is standard deviation

avg is mean hypocotyl length

X is length of hypocotyl in Bc, Rc or FRc

Y is length of hypocotyl in dark

2.3 Results and Discussion

Previously, in Arabidopsis, constitutive expression of *BVR* was shown to result in phytochrome inactivation and has led to perturbation of distinct light-mediated growth and developmental processes. For an example, 35S::pBVR lines displayed elongated hypocotyls under all light conditions tested due to inactivation of phytochromes (Lagarias et al., 1997; Montgomery et al., 1999). Targeted expression of *BVR* using tissue-specific promoters was utilized in this chapter as a molecular tool to investigate the sites of photoperception responsible for regulating discrete responses, and to identify their candidate molecular effectors in FR-mediated photomorphogenesis in Arabidopsis.

2.3.1 Mesophyll-specific Phytochromes Have Distinct Regulatory Roles in Far-red Light

Selective expression of plastid-targeted *BVR* under the control of CAB3 and MERI5 promoters affected leaf morphology and hypocotyl growth in comparison to No-0 WT under FRc conditions. Notably, CAB3::pBVR2 transgenic line with mesophyll-

specific inactivation of phytochromes exhibited closed cotyledons as opposed to open cotyledons in No-0 WT, 35S::pBVR3 and MERI5::pBVR1 (Figure 2.1). A similar phenotype with closed cotyledons was observed in the null *phyA* mutant relative to Col-0WT (Figure 2.1). The phenotype of MERI5::pBVR1 with meristem-specific phytochrome inactivation was identical to the No-0 WT (Figure 2.1). Furthermore, cotyledons of No-0 WT, 35S::pBVR3 and MERI5::pBVR remained yellow even after approximately 1.5 h of exposure to ambient white light during imaging, whereas in CAB3::pBVR2 line, exposure to white light resulted in enhanced greening. Color change in cotyledons of CAB3::pBVR2 line from yellow to green under white light following growth in FR light indicates that this line is defective in the FR block-to-greening response. Defective FR block-to-greening has been observed in *phyA* and *hfr1* mutants previously (Barnes et al., 1996; Fairchild, Schumaker, and Quail, 2000; Yanovsky et al., 2002). The growth of Arabidopsis seedlings in FRc can induce partial photomorphogenesis without the accumulation of chlorophyll and is characterized by inhibition of hypocotyl elongation and open cotyledons (Whitelam et al., 1993). These responses attribute to classic FR-HIR and thus the CAB3::pBVR2 line is impaired in aspects of FR-HIR. Barnes et al., (1996) reported that FR block-to-greening is regulated by phyA. Similarity of impaired FR-HIR between the *phyA* mutant and CAB3::pBVR2 line implies a potential role for mesophyll-specific phyA in the regulation of cotyledon opening and FR block-to-greening under FR light.

A distinct hypocotyl phenotype was obvious in the CAB3::pBVR2 line relative to No-0 WT, 35S::pBVR3 and MERI5::pBVR1 lines (Figure 2.1). The CAB3::pBVR2 line displayed elongated hypocotyls relative to No-0 WT under FRc. Although an elongated

hypocotyl phenotype was observed in the 35S::pBVR3 line relative to No-0 WT, this phenotype was not as severe as what was observed for the CAB::pBVR2 line (Figure 2.1). In contrast to the elongated hypocotyls of 35S::pBVR3 and CAB3::pBVR2 lines, the MERI5::pBVR1 line displayed wild-type hypocotyl growth inhibition (Figure 2.1). The expression of *BVR* in CAB3::pBVR lines is regulated both spatially and by light, whereas in MERI5::pBVR lines, *BVR* expression is regulated spatially. The analysis of fluence-rate dependence of hypocotyl inhibition response for *BVR* expressing transgenic lines 35S::pBVR3, CAB3::pBVR and MERI5::pBVR showed that hypocotyl inhibition was affected distinctively in CAB3::pBVR under FRc illumination.

Comparison of hypocotyl lengths of CAB3::pBVR lines and the 35S::pBVR3 line under FRc indicated that CAB3::pBVR lines were as impaired as 35S::pBVR3 line in response to FRc (Figure 4E, Warnasooriya and Montgomery, 2009). However, MERI5::pBVR lines responded similarly to No-0 WT seedlings (Figure 4F, Warnasooriya and Montgomery, 2009). The observation that the hypocotyl inhibition response of CAB3::pBVR lines was as deficient as 35S::pBVR3 line implies that mesophyll-localized phytochromes are involved in regulating hypocotyl inhibition under FRc illumination. phyA has been recognized as the predominant phytochrome isoform responsible for the FR-dependent inhibition of hypocotyl elongation (Nagatani, Reed, and Chory, 1993; Parks and Quail, 1993; Whitelam et al., 1993). Although (Tóth et al., 2001) showed that both *PHYA* and *PHYC* are expressed at high level in Arabidopsis cotyledons under FRc conditions, a clear role for phyC has not been recognized in FR-mediated inhibition of hypocotyl elongation (Balasubramanian et al., 2006; Monte et al., 2003). Thus, elongated hypocotyls in CAB3::pBVR lines under FRc illumination are a result of

phytochrome deficiency in mesophyll tissues and mesophyll-localized phyA is likely responsible for initiating a signaling cascade in regulating FR-mediated inhibition of hypocotyl elongation. The recognized role for mesophyll-localized phyA in this study corroborates with previous reports indicating that cotyledons are the site of a phytochrome-induced signal that controls hypocotyl growth inhibition (Black and Shuttleworth, 1974) and that cotyledon-localized FR perception is able to impact gene expression in the hypocotyl (Tanaka et al., 2002).

Although CAB3::pBVR lines appeared to be as deficient as the 35S::pBVR3 line in hypocotyl inhibition, close comparison of percentage dark lengths of CAB3::pBVR lines indicate that their hypocotyls were longer under increasing fluences of FR light than those of the 35S::pBVR3 line (Figure 4E, Warnasooriya and Montgomery, 2009). Percentage dark lengths close to 100 % observed for 35S::pBVR3 line suggest that hypocotyls of these lines in FRc were nearly identical in length to dark-grown controls (Figure 4E, Warnasooriya and Montgomery, 2009). This observation suggests that 35S::pBVR3 line was blind to FRc illumination. However, under these conditions, CAB3::pBVR lines are able to perceive FR light and induce hypocotyl elongation. Induction of hypocotyl elongation by FR light leads to an increase in percentage dark lengths (> 100 %) for CAB3::pBVR lines and the hypocotyl elongation response showed further increase in a fluence rate-dependent manner (Figure 4E, Warnasooriya and Montgomery, 2009).

Fluence rate-dependent increase in hypocotyl length in CAB3::pBVR lines suggested that CAB3::pBVR lines are able to perceive FR light and induce hypocotyl elongation. As BVR accumulation occurs only in mesophyll tissues of CAB3::pBVR

lines (thus only mesophyll-localized phytochrome inactivation), the photoactive phyA present in the hypocotyls likely mediate FR-dependent hypocotyl growth through hypocotyl-localized phytochrome signaling. The analysis of publicly available gene expression data using the eFP browser (http://bbc.botany.utoronto.ca/efp/development) indicated that expression of *CAB3* is relatively similar in Rc, FRc, Bc, or Wc light. Thus, the phenotypic differences observed for CAB3::pBVR lines relative to No-0 WT, 35S::pBVR3 and MERI5::pBVR lines under FRc illumination indeed reflect distinct regulatory roles of phytochromes, and the possibility that such phenotypic differences resulted from varying levels of *BVR* expression was ruled out (Warnasooriya and Montgomery, 2009).

2.3.2 Phytochrome A is Involved in Regulating Anthocyanin Accumulation in FRc and Bc

A regulatory role of phytochromes in the induction of sucrose-stimulated anthocyanin accumulation has been reported through comparative analyses of constitutive *BVR* expressing transgenic lines (Montgomery et al., 2001; Montgomery et al., 1999) and through the analysis of *pif3* mutants and *PIF3* over-expresser lines (Kim et al., 2003; Shin, Park, and Choi, 2007). To determine the effects of localized phytochrome inactivation on sucrose-stimulated anthocyanin accumulation and to gain insight into the roles of localized pools of phytochromes in FRc, sucrose-stimulated anthocyanin accumulation levels were compared in FRc-grown and dark-grown representative CAB3::pBVR2, 35S::pBVR3 and No-0 WT plants. Anthocyanin accumulation was barely detectable in dark-grown seedlings and no significant differences in the levels

were obvious between any of the lines (Figure 2.2). In FRc, the levels of accumulated anthocyanins were lower in both of the *BVR* expressing transgenic lines relative to No-0 WT (Figure 2.2). However, in comparison to No-0 WT, the reduction observed for 35S::pBVR3 was not significant ($p=0.0597$). Notably, CAB3::pBVR2 line showed a highly significant reduction in anthocyanin levels relative to No-0 WT ($p>0.0001$) and a similar reduction was observed for the *phyA* mutant, relative to Col-0 WT ($p>0.0001$). This observation suggested that the CAB3::pBVR2 line and the *phyA* mutant are completely deficient in the FR-HIR of sucrose-stimulated anthocyanin accumulation and thus, mesophyll-localized phyA is involved in the regulation of FR-HIR of inducing sucrose-stimulated anthocyanin accumulation (Warnasooriya and Montgomery, 2009).

Previous reports confirm that phyA has a significant role in the induction of anthocyanin accumulation under B illumination (Duek and Fankhauser, 2003; Neff and Chory, 1998; Poppe et al., 1998; Weller et al., 2001). Anthocyanin levels were quantified in a representative *BVR*-expressing transgenic line, CAB3::pBVR2, to determine whether mesophyll-localized phytochrome inactivation leads to a reduction of sucrose-stimulated anthocyanin accumulation under Bc illumination as observed under FRc illumination. In the presence of sucrose, anthocyanins were visible in the No-0 WT under B light (Figure 2.3). The CAB3::pBVR2 line showed reduced levels of anthocyanins compared to No-0 WT in Bc (Figure 2.4). Phytochromes in mesophyll tissues are responsible primarily for the induction of anthocyanins under Bc as the 35S::pBVR3 and CAB3::pBVR2 lines, which exhibited elongated hypocotyls under Bc (Figure 1A and 1B, Montgomery, 2009) displayed comparable level of reduction in anthocyanin accumulation relative to No-0 WT. In comparison to the levels observed for No-0 WT, 35S::pBVR3 and

CAB3::pBVR2 lines accumulated only ~ 41 % and 39 % of No-0 WT level of anthocyanins, respectively (Figure 2.4). However, under FRc illumination, CAB3::pBVR2 and 35S::pBVR3 accumulated 1.8 % and 67 % of the No-0 WT level of anthocyanins, respectively (Figure 2.2). In contrast to the drastic reduction in anthocyanin accumulation observed in the CAB3::pBVR2 line relative to the 35S::pBVR3 line under FRc illumination, a similar degree of reduction in anthocyanin levels in these two transgenic lines in B illumination may be indicative of the possible roles of functional cryptochromes in regulating sucrose-stimulated anthocyanin accumulation under Bc light as reported previously (Ahmad, Lin, and Cashmore, 1995; Lin, Ahmad, and Cashmore, 1996; Mancinelli, 1985; Mancinelli, Rossi, and Moroni, 1991). Moreover, the higher amount of BVR accumulation in cotyledons of CAB3::pBVR3 relative to cotyledons of 35S::pBVR3 is also related to the observed differences in anthocyanin levels in FRc and Bc. Although *BVR* is expressed constitutively in the 35S::pBVR3 line and in mesophyll tissues of the CAB3::pBVR3 line, tissue-specific expression of *BVR* within the cotyledons of the two transgenic lines could differ slightly. Such differences could have distinct functional importance on the amount of phytochrome inactivated in the cotyledons of CAB3::pBVR2 and 35S::pBVR3 under FRc vs. Bc light.

Similar to the function of mesophyll-localized phytochromes under FRc (Warnasooriya and Montgomery, 2009), mesophyll-localized phyA is primarily responsible for the phytochrome-dependent induction of anthocyanin accumulation in Bc (Figure 2.4). Under Bc illumination, the levels of anthocyanins in CAB3::pBVR2 and the *phyA* mutant were reduced to comparable levels relative to their cognate WT parent, i.e., CAB3::pBVR2 accumulates ~ 39 % of the level of anthocyanins accumulated in No-0

WT, whereas the *phyA* mutant accumulates ~ 46% of the Col-0 WT level of anthocyanins. Notably, a *phyB* mutant accumulates at least as much anthocyanin as the Col-0 WT under Bc (Figure 2.4).

Light- and/or sucrose-inducible anthocyanins in most species accumulate in vacuolar space of cells in photosynthetic tissues, i.e. palisade and spongy mesophyll (Gould and Quinn, 1998; Lee and Collins, 2001) and in epidermal cells (Kubo et al., 1999). The comparative analysis of anthocyanin accumulation in the CAB3::pBVR2 line vs. the 35S::pBVR3 and the *phyA* mutant line indicates that phyA in the mesophyll tissues is responsible for the mesophyll-specific induction of anthocyanin accumulation, and may impact inter-tissue anthocyanin accumulation in the epidermis, under Bc, as well as, under FRc illumination.

2.3.3 Mesophyll-localized Phytochrome Inactivation Leads to Distinct Gene Expression Patterns

Comparison of phenotypes between FRc-grown CAB3::pBVR2 and 35S::pBVR3 lines indicated that the CAB3::pBVR2 line was impaired in a number of FR-HIR, i.e. hypocotyl inhibition, cotyledon expansion, FR block-to-greening and sucrose-induced anthocyanin accumulation (Warnasooriya and Montgomery, 2009). Moreover, a unique fluence-rate dependent hypocotyl elongation response mediated by hypocotyl-localized phyA was also apparent in the CAB3::pBVR2 line lacking mesophyll-localized phyA (Warnasooriya and Montgomery, 2009). To identify and characterize genes regulating spatial-specific FR-HIR mediated by phyA, a comparative microarray-based gene expression profiling of FRc-grown No-0 WT, 35S::pBVR3 and CAB3::pBVR2 whole

seedlings was performed. As 7-d-old seedlings of 35S::pBVR3 and CAB3::pBVR2 were phenotypically different in FRc, through comparative gene expression profiling, the aim was to obtain potential insight into the molecular basis of FR-HIR in Arabidopsis.

To identify candidate genes regulating FR-HIR based on the differential gene expression between CAB3::pBVR2 line vs. 35S::pBVR3 line, an expression filter of fold change greater or equal to 2.0 was applied for these two lines against the No-0 WT sample. The comparison of differentially expressed genes in CAB3::pBVR2 vs. 35S::pBVR3, 35S::pBVR3 vs. No-0 WT and CAB3::pBVR2 vs. No-0 WT revealed that 180 genes are shared among the three groups (Figure 2.5). Relative to No-0 WT, 348 genes are differentially expressed commonly in the CAB3::pBVR2 and 35S::pBVR3 lines, whereas 17 genes and 1115 genes show unique differential expression in the 35S::pBVR3 and CAB3::pBVR2 lines relative to No-0 WT, respectively (Figure 2.5). The phenotypic differences between No-0 WT and CAB3::pBVR2 as evident in Figure 2.1, may be a result of differential expression patterns of the 1115 genes enriched in CAB3::pBVR2 relative to No-0 WT. The comparison of CAB3::pBVR2 vs. 35S::pBVR3 and 35S::pBVR3 vs. No-0 WT showed only 3 genes in common that were differentially expressed. These 3 genes are known to encode a transporter-related protein involved in ion transport, an F-box family protein and a nodulin MtN21 family protein (The Arabidopsis Information Resource, TAIR). Although 518 genes are differentially expressed in common between CAB3::pBVR2 vs. No-0 WT and CAB3::pBVR2 vs. 35S::pBVR3, only 11 genes were shown to have unique differential expression in CAB3::pBVR2 vs. 35S::pBVR3 (Figure 2.5). Based on the information from functional categorization of gene ontology annotations, the entity list of 11 genes with unique

differential expression in CAB3::pBVR2 vs. 35S::pBVR3 did not include genes with recognized implications in FR-HIR (Table 2.1). Thus, to narrow down the list of candidate genes, the gene entity list obtained from comparison of CAB3::pBVR2 and 35S::pBVR3 was utilized. From the 712 differentially expressed genes between CAB3::pBVR2 and 35S::pBVR2, ~ 30 genes were selected based on the fold change observed in CAB3::pBVR2 and on information available from functional categorization of gene ontology annotations, TAIR and tissue- and light-dependent gene expression patterns from publicly available gene expression data (AtGenExpress, http://www.weigelworld.org/resources/microarray/AtGenExpress). To prioritize the initial analysis of candidate genes that could be involved in hypocotyl development under FRc, 3 genes were selected based on the fold-change observed in CAB3::pBVR2 vs. 35S::pBVR3: *At1g26220* (probe ID, 245877_at), *At4g02290* (probe ID, 255517_at) and *At1g52410* (probe ID, 59609_at). *At1g26220*, *At4g02290* and *At1g52410* genes are known to encode a GCN5-related N-acetyltransferase (GNAT) family protein, a glycosyl hydrolase family 9 protein and a caldesmon-related protein with a novel calcium-binding repeat sequence, respectively (TAIR). Fold-change in gene expression for *At1g26220*, *At4g02290* and *At1g52410* in CAB3::pBVR3 relative to 35S::pBVR3 was - 2.03, + 5.55 and + 6.27, respectively.

The validation of microarray data by RT-PCR analysis of transcript accumulation of candidate genes, *At1g26220*, *At4g02290* and *At1g52410* in FRc-grown No-0 WT, 35S::pBVR3 and CAB3::pBVR2 indicated that transcript accumulation of *At1g26220* was down-regulated, whereas, transcript accumulation of *At4g02290* and *At1g52410* was up-regulated in the CAB3::pBVR2 line relative to No-0 WT and 35S::pBVR3 line

(Figure 2.6). Thus, the analysis of transcript accumulation by RT-PCR validated the fold-change in gene expression levels in the CAB3::pBVR2 line as evident through microarray analysis for the 3 candidate genes selected for further analysis. Tissue- and light-specific gene expression analysis of *At1g26220*, *At4g02290* and *At1g52410* using publicly available gene expression data (AtGenExpress, http://www.weigelworld.org/resources/microarray/AtGenExpress) revealed unique expression patterns in light vs. dark and in cotyledons and/or hypocotyls in young wild-type Arabidopsis seedlings.

The expression of *At1g26220* was induced under longer duration of exposure to W, B, and R light conditions relative to darkness, whereas exposure to shorter or longer duration of FR light did not change the expression level (Figure 2.7). However, validation of *At1g26220* expression in No-0 WT, 35S::pBVR3 and CAB3::pBVR2 by RT-PCR indicated that accumulation of *At1g26220* transcript expression was higher in No-0 WT (Figure 2.6). As FR light is of lower energy wavelength, exposure of No-0 WT for a prolonged time period (~ 7d) could result in up-regulation of *At1g26220* and down-regulation of this gene in 35S::pBVR3 and CAB3::pBVR2 due to phytochrome inactivation under FRc.

At4g02290 showed distinct patterns of gene expression in dark vs. short and long duration of exposure to different light conditions. In general, the expression of *At4g02290* was up-regulated in dark relative to light and longer duration of darkness, further increased its expression (Figure 2.7). Exposure to shorter duration of B, R and FR illumination led to up-regulation of *At4g02290*; however, longer duration of B, R and FR illumination was able to down-regulate its expression (Figure 2.7). Distinct expression

patterns of *At4g02290* dependent on the presence of light and its duration, especially in FR light and the reduction of its transcript in No-0 WT could implicate a possible role in phenotypic difference observed for CAB3::pBVR2 in FRc. Although expression of *At1g52410* was constant in darkness and under different light conditions, tissue-specific expression analysis showed distinct patterns.

The expression of *At1g52410* was clearly up-regulated in the hypocotyl, shoot apex and rosettes of vegetative wild-type seedlings (Figure 2.8). Although transcript accumulation of *At1g52410* was barely detectable in No-0 WT (Figure 2.6), its distinct expression in the hypocotyl makes it a good candidate for further analysis. The expression of *At1g26220* was up-regulated in spatially-discrete patterns, especially in cotyledons, leaves, vegetative rosettes and green tissues of wild-type seedlings (Figure 2.8). Microarray results and analysis of transcript accumulation by RT-PCR for this gene in No-0 WT also indicated higher expression/transcript accumulation relative to CAB3::pBVR2 with mesophyll-specific phytochrome inactivation. This observation implies that *At1g26220* expression is reduced upon mesophyll-specific inactivation of phytochromes and a putative role in mesophyll-localized phytochrome signaling. Despite the very low transcript accumulation in No-0 WT (Figure 2.6), clear up-regulation was observed for *At4g02290* in the hypocotyls of wild-type seedlings relative to other tissues (Figure 2.8). No-0 WT seedlings have functional mesophyll- and hypocotyl-localized phytochromes and the CAB3::pBVR2 line has functional hypocotyl-localized phytochromes, but lacks functional mesophyll-localized phytochromes. Since microarray analysis and validation of *At4g02290* transcript accumulation by RT-PCR were performed with RNA extracted from FRc-grown whole seedlings, elongated hypocotyls

of the CAB3::pBVR2 line may have contributed a larger proportion of RNA to the total RNA pool (due to more abundant transcripts from hypocotyl-specific *At4g02290* expression in the CAB3::pBVR2 line) and thus are indicative of increased expression of *At4g02290* in the CAB3::pBVR2 line relative to No-0 WT. The hypocotyl-specific increased expression as apparent in the Heatmap (Figure 2.8) and the up-regulation of *At4g02290* in the CAB3::pBVR2 line lacking mesophyll-localized phytochromes implicate a putative role of *At4g02290* in hypocotyl-localized phytochrome signaling.

2.3.4 GCN5- and Caldesmon-related Proteins are Implicated in the Regulation of Hypocotyl Development under FRc

To determine whether candidate genes have functional roles in phytochrome-regulated hypocotyl development in FRc, T-DNA insertion mutants having T-DNA insertions in an exon of *At1g26220*, *At4g02290* and *At1g52410* (Figure 2.9 A, 2.10 A and 2.11 A) were obtained from the Salk T-DNA insertion mutant collection (Alonso et al., 2003). RT-PCR analysis of transcript accumulation of *At1g26220* and *At4g02290* in confirmed homozygous T-DNA insertion mutants indicated that respective transcripts were absent in SALK_062388 (Figure 2.9 B) and SALK_101567 (Figure 2.10 B), respectively, and that these lines were null mutants. However, a T-DNA insertion mutant for *At1g52410*, SALK_151393, displayed a very low level of transcript accumulation and was similar to that of Col-0 WT (Figure 2.11 B). As the T-DNA insertion in SALK_151393 is in the last exon and the primers for RT-PCR analysis were designed to anneal to a region upstream of the T-DNA insertion site, SALK_151393 may accumulate a truncated transcript and lack a functional protein corresponding to *At1g52410*.

Comparative analysis of FRc-grown CAB3::pBVR2 and 35S::pBVR3 indicated that CAB3::pBVR2 has elongated hypocotyls relative to No-0 WT and 35S::pBVR3 and was indicative of hypocotyl-localized phytochrome signaling resulting in hypocotyl elongation in the absence of mesophyll-localized phytochrome action on hypocotyl inhibition (Figure 2.1; as discussed in section 2.3.1). To assess whether the selected candidate genes were involved in hypocotyl development under FRc, hypocotyl inhibition response was quantified as a percentage dark length in FRc-grown 7-d-old homozygous T-DNA insertion mutants, SALK_062388, SALK_101567 and SALK_151393 (Figure 2.12). The SALK_062388 line displayed elongated hypocotyls relative to hypocotyls of Col-0 WT and the increase in length was significant ($p=0.0002$). The increase in the percentage dark length for SALK_062388 was ~ 11 % greater than the percentage dark length of Col-0 WT. A significant increase in the hypocotyl length in SALK_101567 relative to Col-0 WT was not apparent ($p=0.2881$) under FRc (Figure 2.12). However, a marginally significant increase in the hypocotyl length for SALK_151393 relative to Col-0 WT ($p=0.0375$) was observed under FRc. The increase in the percentage dark length for SALK_151393 was ~ 2 % of Col-0 WT percentage dark length (Figure 2.12).

Based on the comparative microarray-based gene expression profiling and validation by RT-PCR analysis, the expression of *At1g26220* was down-regulated in the CAB3::pBVR2 line in FRc. As the T-DNA insertion in an exon of *At1g26220* eliminated the accumulation of its transcript (Figure 2.9 B) in the SALK_062388, the increase in hypocotyl length observed for SALK_062388 relative to Col-0 WT is a result of the lack of the GNAT family protein encoded by *At1g26220* and implicates that in the wild-type

Arabidopsis plants, the GNAT family protein has a regulatory role in hypocotyl inhibition in FRc. Although a short hypocotyl phenotype in a T-DNA disruption mutant of the Arabidopsis *GCN5*, *gcn5-1* under Wc light has been reported (Vlachonasios, Thomashow, and Triezenberg, 2003), any reports on roles of the GNAT family protein encoded by *At1g26220* under FRc condition has not emerged. However, the observation that a mutation of *GCN5* in the *gcn5-1* mutant, leads to shorter hypocotyls in Wc conditions does indicate that a GNAT family protein encoded by a homolog of *At1g26220* as having a putative role in hypocotyl development in Arabidopsis. As a number of molecular effectors are involved in the regulation of hypocotyl development, the contribution of each candidate gene to the overall phenotype can be minor and thus a ~ 11 % increase in hypocotyl length observed for SALK_062388 is reflective of *At1g26220* being a candidate gene in the regulation of hypocotyl development in Arabidopsis under FRc.

The analysis of the hypocotyl inhibition response of SALK_151393 indicated that the increase in the percentage dark length was ~ 2 % of Col-0 WT percentage dark length. As the microarray analysis indicated that *At1g52410* expression was up-regulated by 6.27 X in the CAB3::pBVR2 relative to 35S::pBVR3, a decrease in hypocotyl length was anticipated for SALK_151393 in the absence of the *At1g52410* transcript. However, RT-PCR analysis of SALK_151393 showed very low *At1g52410* transcript accumulation that was similar to the level in Col-0 WT (Figure 2.11 B). The ~ 2 % increase in the percentage dark length relative to Col-0 WT may be indicative of possible residual activity of the caldesmon-related protein encoded by *At1g52410*. Previous reports indicate that *At1g52410* encodes TSA1 (TSK-associating protein 1) that interacts with a

protein complex, TSK/MGO3/BRU, a key factor in cell division control and plant morphogenesis (Suzuki et al., 2005; Yamada et al., 2008) and could have implications in FR-dependent morphogenesis in Arabidopsis.

2.3.5 Summary

Comparative phenotypic analysis of CAB3::pBVR2 and 35S::pBVR3 under FRc and Bc illumination revealed that spatially-distinct pools of phytochromes are able to perceive light and regulate discrete aspects of photomorphogenesis through inter-tissue and inter-organ signaling pathways. The comparison of hypocotyl inhibition responses of 35S::pBVR3 and CAB3::pBVR2 across increasing fluences of FRc illumination showed that mesophyll-localized phyA regulates FR-mediated hypocotyl inhibition. However, in the absence of mesophyll-localized phyA, the functional phyA in hypocotyls is able to mediate cell elongation through hypocotyl-localized phytochrome signaling resulting in FR-dependent hypocotyl elongation. The observation that this growth promotive response, i.e. hypocotyl elongation, is only present in the absence of mesophyll-localized phyA suggests that the inhibitory activity by mesophyll-localized phyA on the hypocotyl is more pronounced relative to the elongation response exerted by hypocotyl-localized phyA. The dissection of growth inhibitory and stimulatory effects of spatial-specific pools of phytochromes indicates that de-etiolation involves coordination between distinct pools of phytochromes. Thus, targeted *BVR* expression has essentially disrupted an inter-tissue signaling between mesophyll tissues and hypocotyl in the CAB3::pBVR2 line allowing the identification of distinct functions mediated by localized pools of phytochromes. Moreover, additional regulatory roles for mesophyll-localized phyA such

as cotyledon opening and FR block-to-greening that are classic FR-HIR could be identified. The similar levels of anthocyanin accumulation under FRc in the CAB3::pBVR2 line and the *phyA* mutant that is completely deficient in the FR-HIR implied that sucrose-stimulated anthocyanin accumulation is regulated by mesophyll-localized phyA specifically and its possible contribution to induction of anthocyanin accumulation under Bc. Comparative microarray-based gene expression profiling of FRc-grown No-0 WT, 35S::pBVR3 and CAB3::pBVR2 whole seedlings allowed initial selection of candidate genes that have significant changes in gene expression levels between CAB3::pBVR2 and 35S::pBVR3. The initial analysis of hypocotyl inhibition responses of T-DNA insertion mutants in *At1g26220* (encodes a GNAT family protein), *At4g02290* (encodes a glycosyl hydrolase family 9 protein) and *At1g52410* (encodes a caldesmon-related protein with a novel calcium-binding repeat sequence) under FRc identified a GNAT family protein and a caldesmon-related protein as candidate signaling intermediates in regulating FR-mediated hypocotyl development by phyA in Arabidopsis.

2.4 Future Perspectives

Comparative microarray-based gene expression profiling of FRc-grown No-0 WT, 35S::pBVR3 and CAB3::pBVR2 whole seedlings revealed that distinct gene expression patterns are observed for CAB3::pBVR2 relative to 35S::pBVR3 and the implications of such gene expression patterns likely represent the molecular and cellular bases of phenotypic differences between the two transgenic lines. Thus, differentially expressed genes in the CAB3::pBVR2 vs. 35S::pBVR3 may have functional roles in hypocotyl inhibition regulated by mesophyll-specific phyA and hypocotyl elongation

regulated by hypocotyl-specific phyA under FRc and/or characteristic FR-HIRs, i.e. cotyledon expansion and FR-block-to-greening regulated by phyA. Although a number of signaling intermediates have been identified in the phyA-specific signaling pathway in FR light (as discussed in section 2.1.3), a comprehensive understanding of the sites of photoperception and the molecular and cellular mechanisms of spatial-specific phyA-mediated responses is yet limited. Therefore, the comparative microarray-based gene expression profiling of CAB3::pBVR3 relative to 35S::pBVR3 aids in the initial analyses and selection of candidate signaling intermediates involved in mesophyll- and hypocotyl-specific phyA signaling underlying the fine-tuning of FR-HIRs in Arabidopsis.

As evident by microarray analysis and subsequent validation by RT-PCR, the expression of *At1g26220* was down-regulated in CAB3::pBVR2 with mesophyll-specific phytochrome inactivation relative to 35S::pBVR3 with constitutive phytochrome inactivation (Figure 2.6). If *At1g26220* has a putative role in regulating hypocotyl inhibition under FR light, a mutant in the *At1g26220* is expected to display more elongated hypocotyls relative to WT seedlings in FR light. The observation that SALK_062388 (a T-DNA insertion mutant in *At1g26220*) had an ~ 11 % increase in percentage dark length relative to Col-0 WT implicates a role of *At1g26220* in regulating hypocotyl inhibition mediated by mesophyll-localized phyA. To rule out the possibility of positional effects of T-DNA insertion on the observed hypocotyl elongation in SALK_062388, the assessment of additional mutant alleles of *At1g26220* for hypocotyl inhibition response under FRc is required. SALK_150736 and SALK_022035 from the Salk T-DNA insertion mutant collection (Alonso et al., 2003) contain a T-DNA insertion in exons of *At1g26220*. If SALK_150736 and SALK_022035 also display a similar

degree of hypocotyl elongation relative to Col-0 WT as SALK_062388, this result would suggest that the *At1g26220* gene has a role in inhibition of hypocotyl elongation in FR light. However, the complementation of T-DNA insertion mutants in the *At1g26220* gene that display elongated hypocotyls under FR light, with a WT copy of *At1g26220* under the regulatory control of the native promoter and subsequent restoration of WT phenotype in the complemented transgenic lines, will confirm that the *At1g26220* gene encoding a GNAT family protein as a signaling intermediate of the FR-dependent inhibition of hypocotyl elongation regulated by mesophyll-specific phyA.

Using microarray analysis and validation by RT-PCR, the expression of *At1g52410* was determined to be up-regulated in CAB3::pBVR2 relative to 35S::pBVR3 (Figure 2.6). Thus, if *At1g52410* has a regulatory role in hypocotyl inhibition under FR light, a mutant in the *At1g52410* may be expected to display hypocotyls of reduced length relative to WT seedlings. However, a marginally significant increase in the hypocotyl length of SALK_151393 relative to Col-0 WT was apparent ($p=0.0375$) under FRc and the increase in the percentage dark length for SALK_151393 was ~ 2 % of Col-0 WT percentage dark length. Moreover, the analysis of transcript accumulation of *At1g52410* by RT-PCR revealed similar levels of transcript accumulation in Col-0 WT, as well as in SALK_151393 (Figure 2.11 B) indicating that SALK_151393 is not a true null mutant. Thus, the analysis of hypocotyl inhibition response in additional T-DNA insertion mutant alleles of *At1g52410*, such as SALK_001102 and GK-299G09-015515 from the Salk T-DNA insertion mutant collection (Alonso et al., 2003) having a T-DNA insertion in the promoter and in an exon, respectively, under FR light can provide additional insight into the involvement of *At1g52410* as a regulator of phyA-mediated hypocotyl inhibition in

FR light. The complementation of T-DNA insertion mutants (with a WT copy of *At1g52410* under the regulatory control of the native promoter) and restoration of WT hypocotyl inhibition response in the complemented lines under FR light will confirm that the caldesmon-related protein encoded by *At1g52410* as a signaling intermediate of inhibition of hypocotyl elongation regulated by mesophyll-specific phyA under FR light.

The phenotypic similarity of CAB3::pBVR2 line and *phyA* null mutant with respect to cotyledon greening induced by white light following growth in FR light, closed cotyledons and elongated hypocotyls indicated that both lines are defective in a number of FR-HIRs (Warnasooriya and Montgomery, 2009). Defective FR block-to-greening has also been observed in *hfr1* mutants previously (Fairchild, Schumaker, and Quail, 2000). *HFR1* is known to encode a phyA-specific signaling intermediate (Duek and Fankhauser, 2003; Fairchild, Schumaker, and Quail, 2000; Jang et al., 2005; Kim et al., 2002). Although FRc is able to inhibit hypocotyl elongation in *hfr1* mutants, the inhibition is significantly impaired in the *hfr1* mutants in moderate (5 μmol m^{-2} s^{-1}) and strong (42 μmol m^{-2} s^{-1}) FRc light (Fairchild, Schumaker, and Quail, 2000). This phenotype contrasts with the complete blindness to FRc of the *phyA* mutant (Barnes et al., 1996; Fairchild, Schumaker, and Quail, 2000; Yanovsky et al., 2002; Yanovsky, Whitelam, and Casal, 2000). Moreover, *hfr1* mutants displayed cotyledons separation in contrast to phyA null mutants (Fairchild, Schumaker, and Quail, 2000). Due to the similarity of phenotypes among CAB3::pBVR3, *phyA* and *hfr1* mutants with respect to hypocotyl inhibition and FR block-to-greening induced by white light following growth in 5 μmol m^{-2} s^{-1} FR light, the analysis of expression of *At1g26220* and *At1g52410* in

CAB3::pBVR3, *phyA* and *hfr1* mutants by qRT-PCR under FRc would reveal the gene expression patterns of putative candidate genes. The similarity of expression levels for *At1g26220* and *At1g52410* among CAB3::pBVR3, *phyA* and *hfr1* mutants will further substantiate the involvement of a GNAT family protein and a caldesmon-related protein as signaling intermediates in regulating phyA-mediated hypocotyl development in Arabidopsis seedlings under FR light.

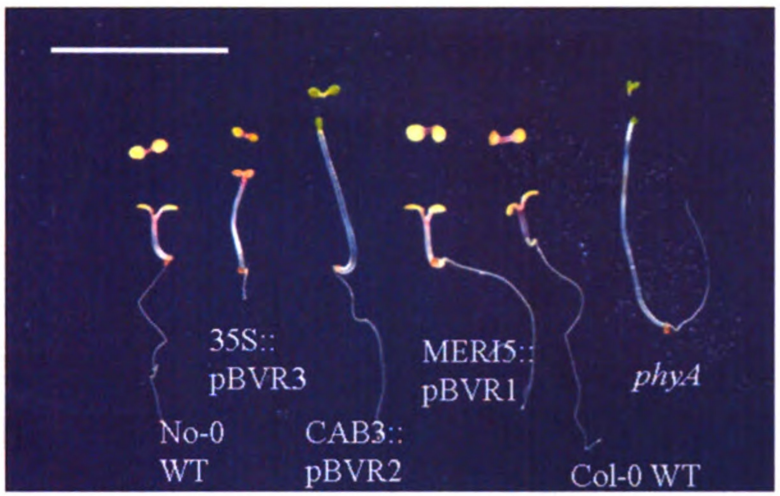

Figure 2.1 Photomorphogenesis of FRc-grown wild-type and transgenic BVR plants.
No-0 wild-type (No-0 WT), 35S::pBVR3, CAB3::pBVR2, MERI5::pBVR1, Col-0 wild-type (Col-0 WT) and *phyA* (SALK_014575) were grown at 20 °C on Phytablend medium containing 1 % Suc for 7 d under FRc illumination of 5 µmol m^{-2} s^{-1}. Above each seedling, cotyledons are shown that were separated and arranged to display the full cotyledon surface area. Scale bar represents 1 cm.

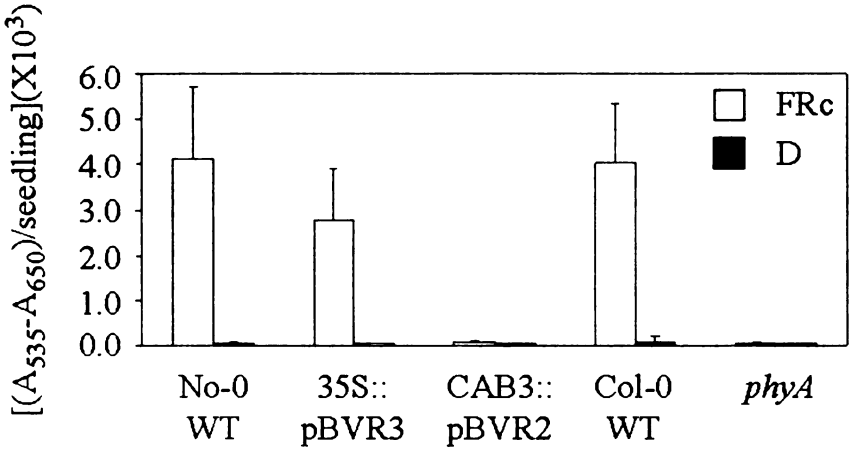

Figure 2.2 Anthocyanin content of wild-type and transgenic BVR seedlings. No-0 wild-type (No-0 WT), 35S::pBVR3, CAB3::pBVR2, Columbia wild-type (Col-0 WT), and *phyA* (SALK_014575) were grown at 20 °C on Phytablend medium containing 1 % Suc for 4 d under FRc illumination of 5 µmol m^{-2} s^{-1}. White bars (FRc) and black bars (dark) represent the mean (±SD) of three independent measurements.

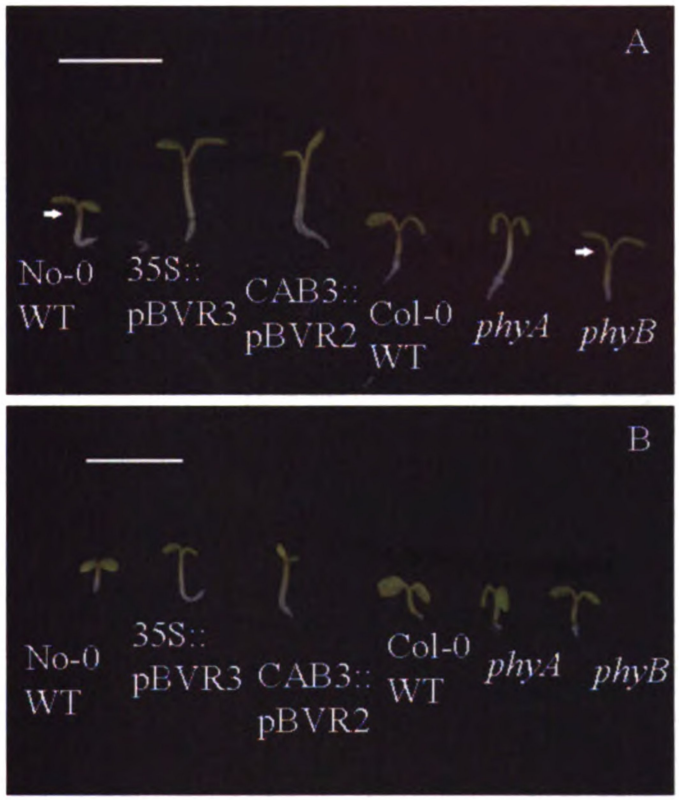

Figure 2.3 Development of wild-type, transgenic BVR and *phy* mutant seedlings under continuous blue light.

No-0 WT, 35S::pBVR3, CAB3::pBVR2, Col-0 WT, *phyA* (SALK_014575), and *phyB* (SALK_022035) seedlings were grown at 22 °C on Phytablend medium with or without 1% sucrose for ~ 4 d under Bc illumination of 25 μmol m^{-2} s^{-1}. (A) Image of seedlings grown on 1% sucrose. Arrows indicate visible anthocyanin. Scale bar represents 1 cm. (B) Image of seedlings grown in the absence of sucrose. Scale bar represents 1 cm.

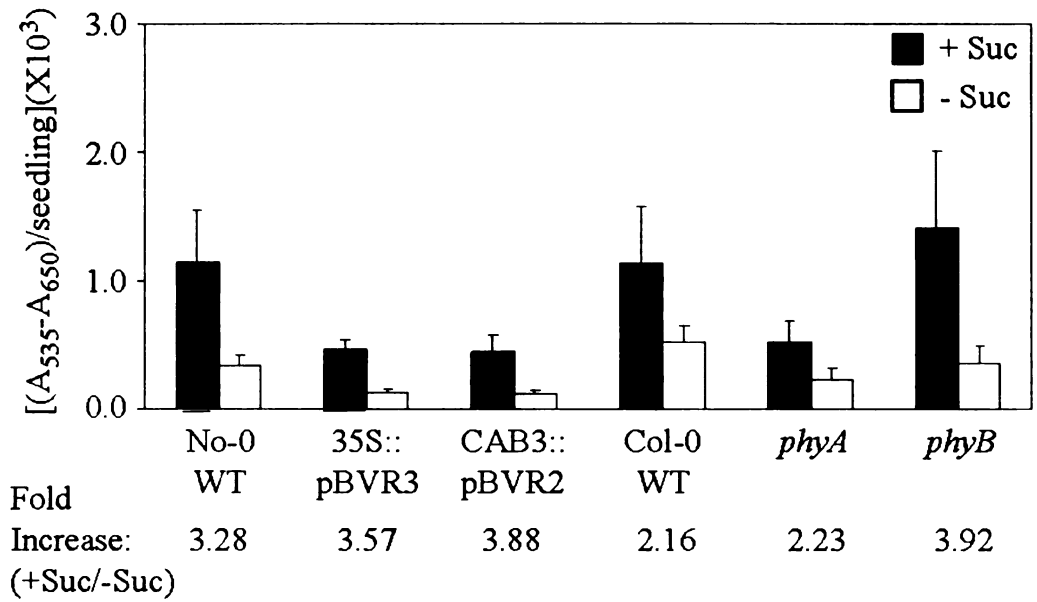

Figure 2.4 Anthocyanin content of wild-type and transgenic BVR seedlings. No-0 wild-type (No-0 WT), 35S::pBVR3, CAB3::pBVR2, Columbia wild-type (Col-0 WT), *phyA* (SALK_014575) and *phyB* (SALK_022035) were grown at 22 °C on Phytablend medium containing 1 % Sucrose or 0 % Sucrose for 4 d under Bc illumination of 25 µmol m^{-2} s^{-1}. Bars, black bars (1 % sucrose) and white bars (no sucrose) represent the mean (±SD) of three independent measurements.

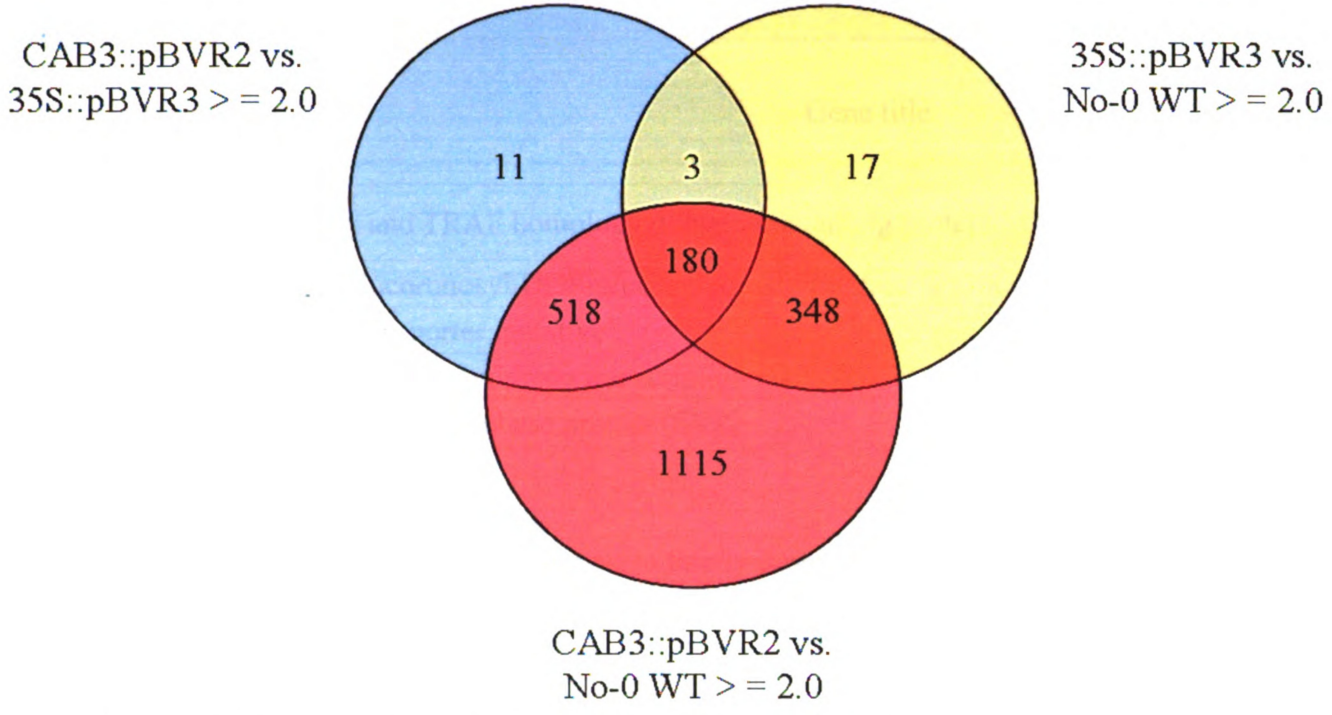

Figure 2.5 Differential expression patterns in 35S::pBVR3 and CAB3::pBVR2.
A 3-way comparison of all differentially-expressed genes (DEGs) in 35S::pBVR3 and CAB3::pBVR2 is shown. To construct the Venn diagram, 3 gene lists were obtained through GeneSpring GX 10.0 (Agilent Technologies Inc., CA) by comparing 35S::pBVR3 and CAB3::pBVR2 each against No-0 WT and CAB3::pBVR2 against 35S::pBVR3 following an expression filter of fold change greater or equal to 2.0 was applied. 7 possible overlap/uniqueness sectors indicated that 17 and 1115 genes were unique to 35S::pBVR3 and CAB3::pBVR2 relative to No-0 WT, respectively. 11 genes were unique to CAB3::pBVR2 relative to 35S::pBVR3.

Table 1 List of genes with unique differential expression in CAB3::pBVR2 vs. 35S::pBVR3

Gene	Fold-change in CAB3::pBVR2 vs. 35S::pBVR3	Gene title
At2g32880	+2.15	meprin and TRAF homology domain-containing protein/MATH domain-containing protein
At2g16890	-2.04	UDP-glucoronosyl/UDP-glucosyl transferase family protein
At1g77210	+2.50	sugar transporter, putative
At2g28550	-2.04	AP2 domain-containing transcription factor RAP2.7 (RAP2.7)
At2g22540	+2.17	short vegetative phase protein (SVP)
At3g15440	+2.94	expressed protein
At3g21870	+2.09	cyclin family protein
At5g05270	-2.91	chalcone-flavanone isomerase family protein
At5g25810	-2.02	AP2 domain-containing transcription factor TINY (TINY)
At4g14030 *At4g14040*	+2.04	selenium-binding protein, putative
At2g40880	+2.03	cysteine protease inhibitor, putative / cystatin, putative (FL3-27)

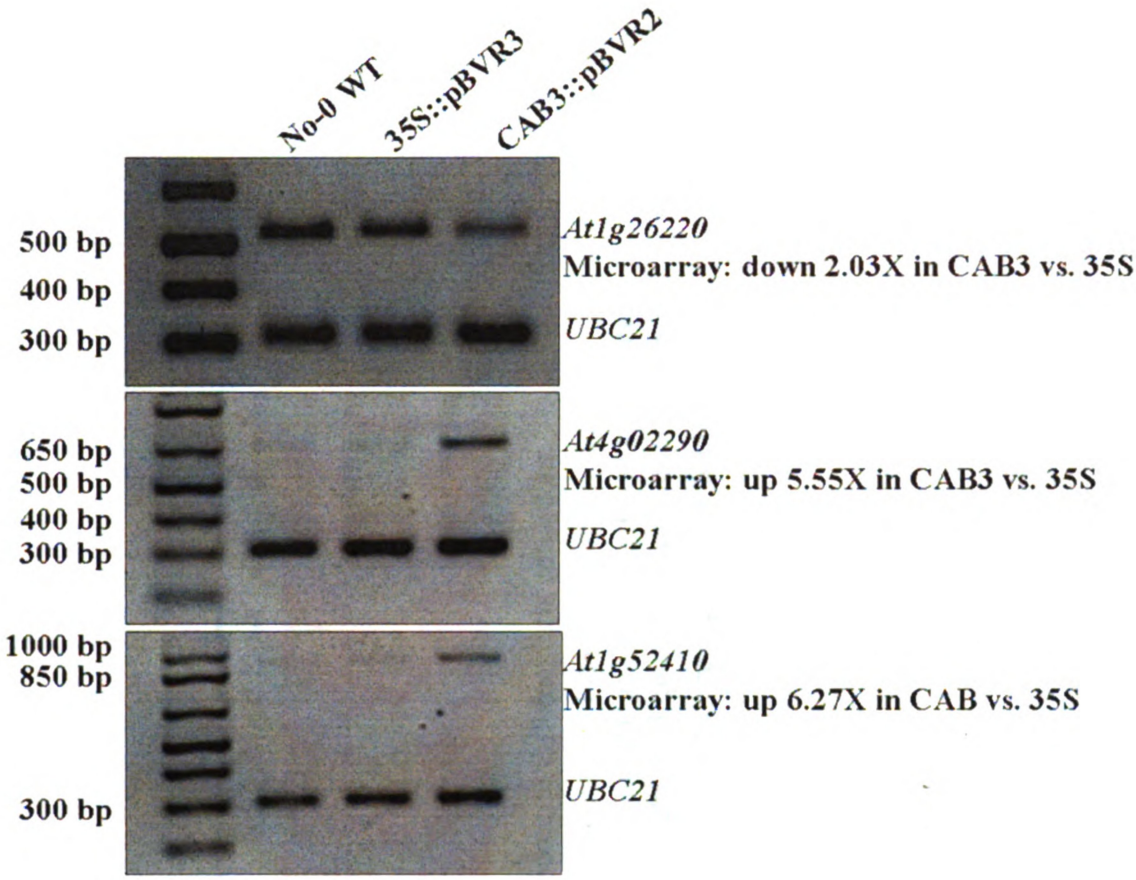

Figure 2.6 Validation of microarray analysis for *At1g26220*, *At4g02290* and *At1g52410* through analysis of transcript accumulation.
Transcript accumulation for *At1g26220*, *At4g02290* and *At1g52410* in No-0 WT, 35S::pBVR3 and CAB3::pBVR2 was analyzed by RT-PCR and corroborated the expression levels for individual genes as noted in the microarray analysis. The expression of the *UBC21* (*At5g25760*) transcript was analyzed as an internal control. A representative biological replicate is shown.

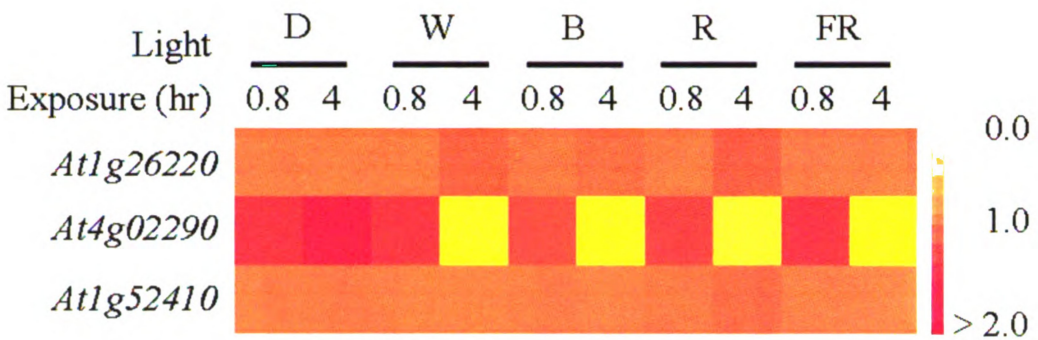

Figure 2.7 Expression profiles in response to different light conditions. Heatmap was constructed using mean-normalized $\log_2$ values obtained from AtGenExpress for *At1g26220*, *At4g02290* and At1g52410 in darkness (D), white (W), blue (B), red (R) and far-red (FR) light conditions after exposure for 0.8 hr and 4 hr. Mean normalized $\log_2$ values are color-coded (red and yellow for relatively higher or lower expression, respectively) as indicated in the scale bar. The lowest and highest $\log_2$ signal value is 0.0 and 1.5, respectively.

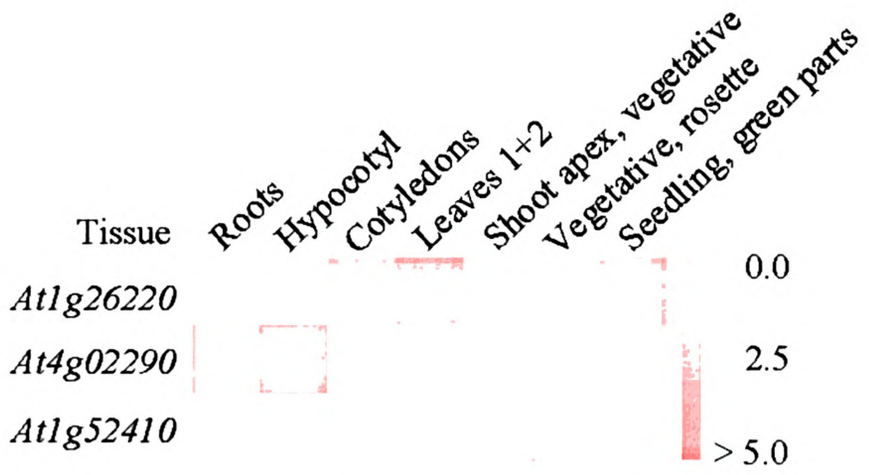

Figure 2.8 Expression profiles in different tissues of Arabidopsis seedlings. Heatmap was constructed using mean-normalized $\log_2$ values obtained from AtGenExpress for *At1g26220*, *At4g02290* and *At1g52410* in different tissues of 7-d-old Arabidopsis seedlings. Mean normalized $\log_2$ values are color-coded (red and yellow for relatively higher or lower expression, respectively) as indicated in the scale bar. The lowest and highest $\log_2$ signal value is 0.0 and 6.9, respectively.

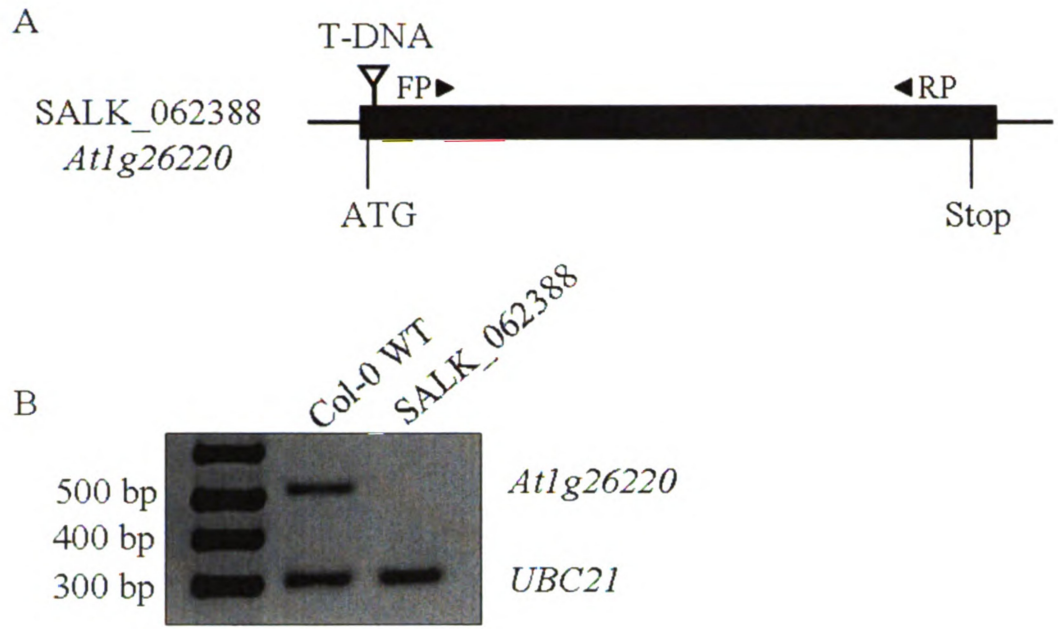

Figure 2.9 Site of T-DNA insertion and transcript accumulation in SALK_062388. (A) Site of T-DNA insertion in SALK_062388. Arrow heads indicate locations of gene-specific oligonucleotide annealing used in RT-PCR analysis. FP, forward primer and RP, reverse primer. (B) Transcript accumulation for *At1g26220* gene in Col-0 WT and SALK_062388.

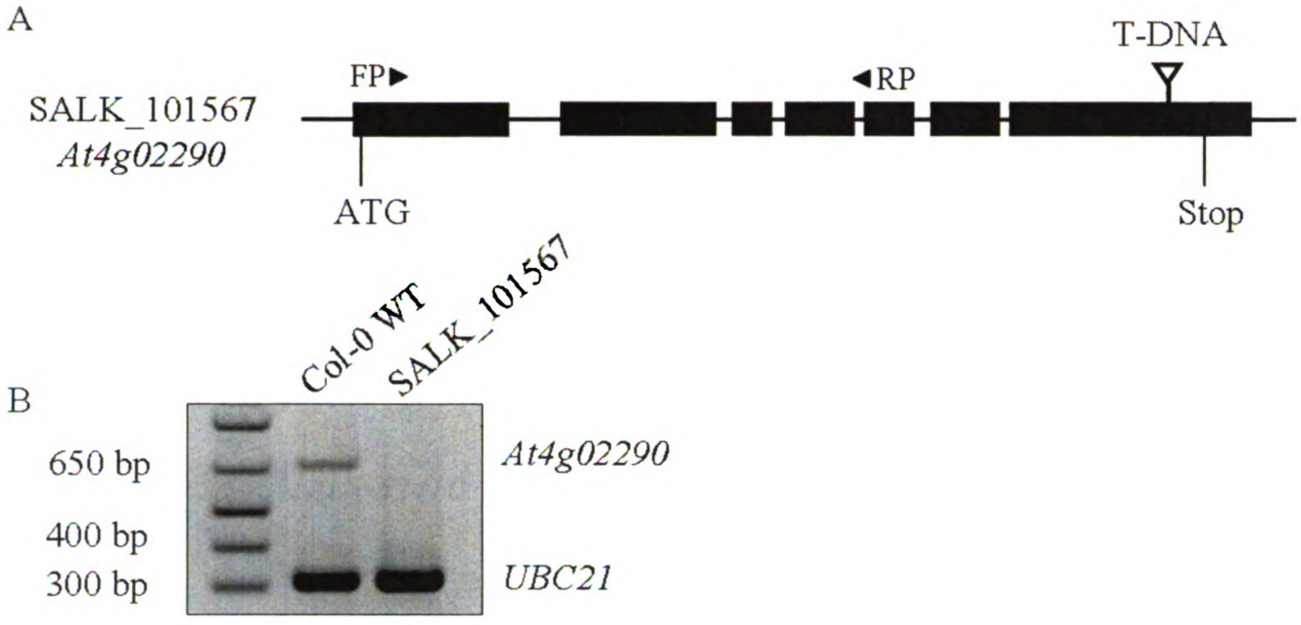

Figure 2.10 Site of T-DNA insertion and transcript accumulation in SALK_101567. (A) Site of T-DNA insertion in SALK_101567. Arrow heads indicate locations of gene-specific oligonucleotide annealing used in RT-PCR analysis. FP, forward primer and RP, reverse primer. (B) Transcript accumulation for *At4g02290* gene in Col-0 WT and SALK_101567.

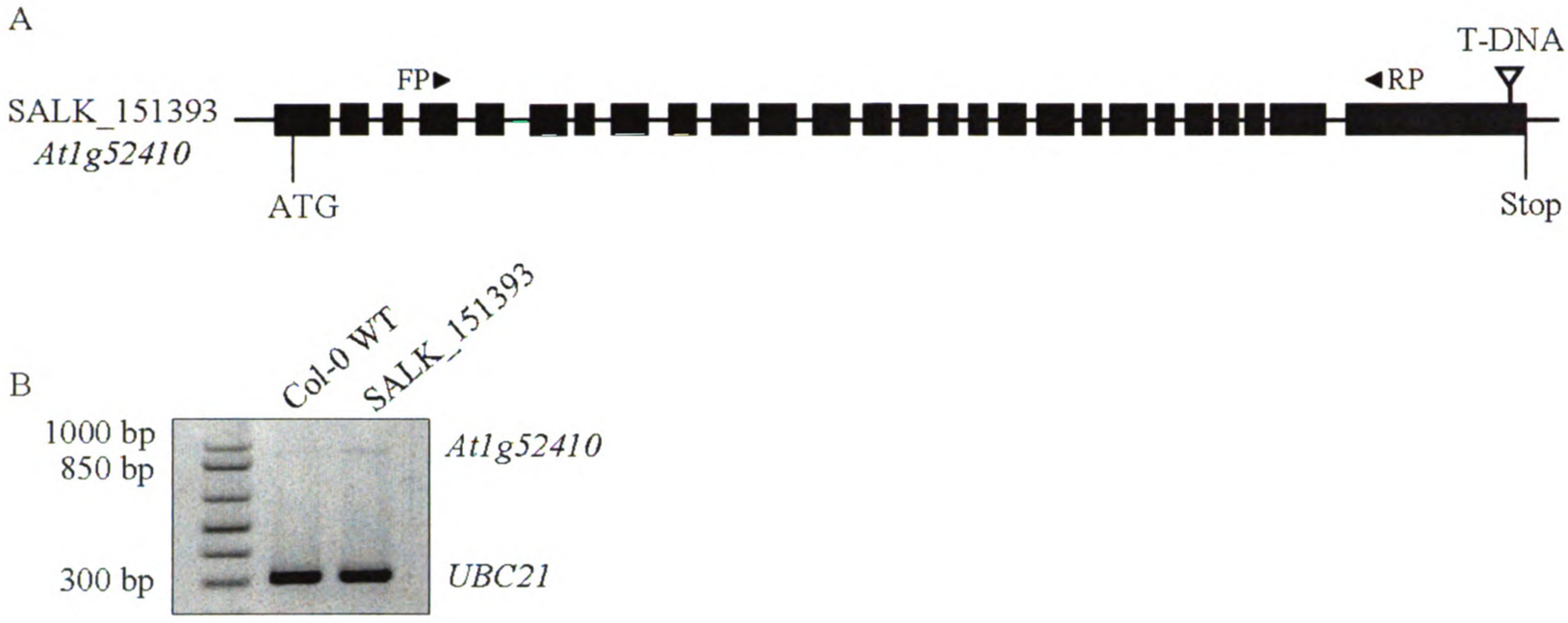

Figure 2.11 Site of T-DNA insertion and transcript accumulation in SALK_151393.
(A) Site of T-DNA insertion in SALK_151393. Arrow heads indicate locations of gene-specific oligonucleotide annealing used in RT-PCR analysis. FP, forward primer and RP, reverse primer.
(B) Transcript accumulation for *At1g52410* gene in Col-0 WT and SALK_151393.

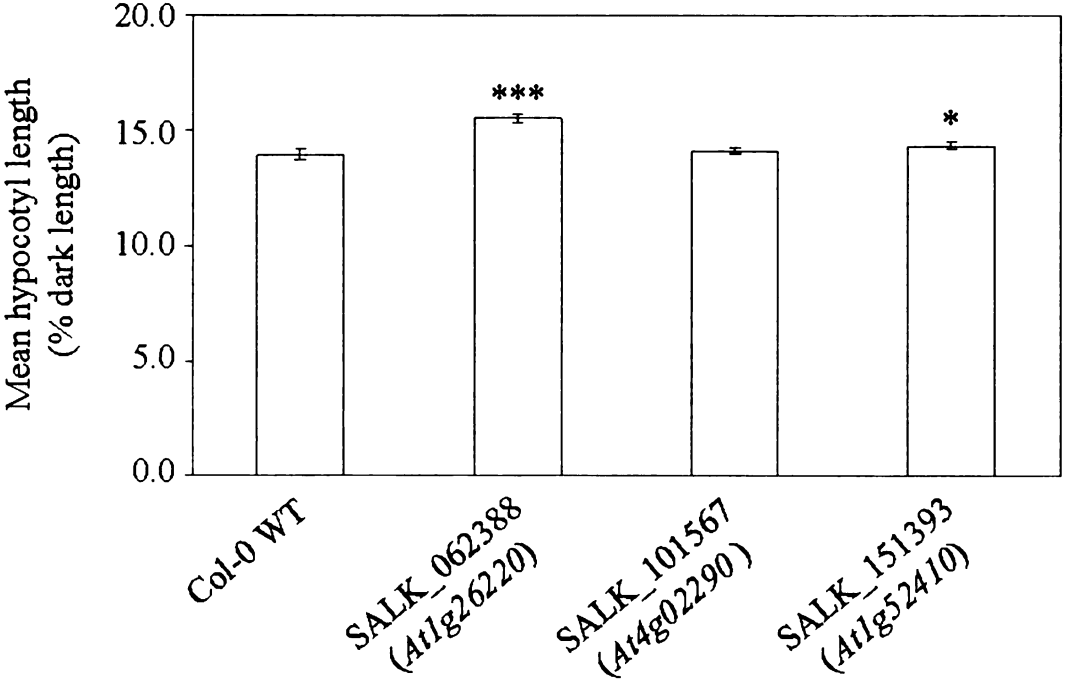

Figure 2.12 Mean hypocotyl length of T-DNA insertion mutants.
Col-0 wild-type (Col-0 WT), SALK_062388, SALK_101567 and SALK_151393 were grown at 22 °C on Phytablend medium containing 1 % Suc for 7d under FRc illumination of 10 µmol m^{-2} s^{-1} or darkness. Mean hypocotyl lengths of seedlings from three independent measurements as a % of dark length are shown. Unpaired, two-tailed Student's t test, *** $p < 0.0005$, * $p < 0.05$.

2.6 References

Ahmad, M., and Cashmore, A. R. (1997). The blue-light receptor cryptochrome 1 shows functional dependence on phytochrome A or phytochrome B in *Arabidopsis thaliana*. *Plant J* **11**(3), 421-427.

Ahmad, M., Lin, C., and Cashmore, A. R. (1995). Mutations throughout an Arabidopsis blue-light photoreceptor impair blue-light-responsive anthocyanin accumulation and inhibition of hypocotyl elongation. *Plant J* **8**(5), 653-658.

Alonso, J. M., Stepanova, A. N., Leisse, T. J., Kim, C. J., Chen, H., Shinn, P., Stevenson, D. K., Zimmerman, J., Barajas, P., Cheuk, R., Gadrinab, C., Heller, C., Jeske, A., Koesema, E., Meyers, C. C., Parker, H., Prednis, L., Ansari, Y., Choy, N., Deen, H., Geralt, M., Hazari, N., Hom, E., Karnes, M., Mulholland, C., Ndubaku, R., Schmidt, I., Guzman, P., Aguilar-Henonin, L., Schmid, M., Weigel, D., Carter, D. E., Marchand, T., Risseeuw, E., Brogden, D., Zeko, A., Crosby, W. L., Berry, C. C., and Ecker, J. R. (2003). Genome-wide insertional mutagenesis of *Arabidopsis thaliana*. *Science* **301**(5633), 653-657.

Aukerman, M. J., Hirschfeld, M., Wester, L., Weaver, M., Clack, T., Amasino, R. M., and Sharrock, R. A. (1997). A deletion in the PHYD gene of the Arabidopsis Wassilewskija ecotype defines a role for phytochrome D in red/far-red light sensing. *Plant Cell* **9**(8), 1317-1326.

Balasubramanian, S., Sureshkumar, S., Agrawal, M., Michael, T. P., Wessinger, C., Maloof, J. N., Clark, R., Warthmann, N., Chory, J., and Weigel, D. (2006). The PHYTOCHROME C photoreceptor gene mediates natural variation in flowering and growth responses of *Arabidopsis thaliana*. *Nat Genet* **38**(6), 711-715.

Ballesteros, M. L., Bolle, C., Lois, L. M., Moore, J. M., Vielle-Calzada, J. P., Grossniklaus, U., and Chua, N. H. (2001). LAF1, a MYB transcription activator for phytochrome A signaling. *Genes Dev* **15**(19), 2613-2625.

Barnes, S. A., Nishizawa, N. K., Quaggio, R. B., Whitelam, G. C., and Chua, N. H. (1996). Far-red light blocks greening of Arabidopsis seedlings via a phytochrome A-mediated change in plastid development. *Plant Cell* **8**(4), 601-615.

Black, M., and Shuttleworth, J. E. (1974). The role of the cotyledons in the photocontrol of hypocotyl extension in *Cucumis sativus* L. *Planta* **117**(1), 57-66.

Bou-Torrent, J., Roig-Villanova, I., and Martinez-Garcia, J. F. (2008). Light signaling: back to space. *Trends Plant Sci* **13**(3), 108-114.

Casal, J. J., and Boccalandro, H. (1995). Co-action between phytochrome B and HY4 in *Arabidopsis thaliana*. *Planta* **197**(2), 213-218.

Caubergs, R., and De Greef, J. A. (1975). Studies on hook-opening in *Phaseolus vulgaris* L. by selective R/FR pretreatments of embryonic axis and primary leaves. *Photochem. Photobiol.* **22**(3-4), 139-144.

Chen, M., Chory, J., and Fankhauser, C. (2004). Light signal transduction in higher plants. *Annu Rev Genet* **38**, 87-117.

Chun, L., Kawakami, A., and Christopher, D. A. (2001). Phytochrome A mediates blue light and UV-A-dependent chloroplast gene transcription in green leaves. *Plant Physiol* **125**(4), 1957-1966.

Clack, T., Mathews, S., and Sharrock, R. A. (1994). The phytochrome apoprotein family in Arabidopsis is encoded by five genes: the sequences and expression of PHYD and PHYE. *Plant Mol Biol* **25**(3), 413-427.

Clough, R. C., and Vierstra, R. D. (1997). Phytochrome degradation. *Plant, Cell & Environment* **20**(6), 713-721.

De Greef, J. A., and Caubergs, R. (1972a). Interorgan correlations and phytochrome: hypocotyl hook opening. *Arch. Int. Physiol. Biochim.* **80**(5), 959-960.

De Greef, J. A., and Caubergs, R. (1972b). Interorgan correlations and phytochrome: leaf expansion. *Arch. Int. Physiol. Biochim.* **80**(5), 961-962.

Deng, X. W., and Quail, P. H. (1999). Signalling in light-controlled development. *Semin Cell Dev Biol* **10**(2), 121-129.

Devlin, P. F., Patel, S. R., and Whitelam, G. C. (1998). Phytochrome E Influences Internode Elongation and Flowering Time in Arabidopsis. *Plant Cell* **10**(9), 1479-1488.

Duek, P. D., and Fankhauser, C. (2003). HFR1, a putative bHLH transcription factor, mediates both phytochrome A and cryptochrome signalling. *Plant J* **34**(6), 827-836.

Fairchild, C. D., Schumaker, M. A., and Quail, P. H. (2000). HFR1 encodes an atypical bHLH protein that acts in phytochrome A signal transduction. *Genes Dev* **14**(18), 2377-2391.

Feinbaum, R. L., and Ausubel, F. M. (1988). Transcriptional regulation of the *Arabidopsis thaliana* chalcone synthase gene. *Mol Cell Biol* **8**(5), 1985-1992.

Franklin, K. A., Allen, T., and Whitelam, G. C. (2007). Phytochrome A is an irradiance-dependent red light sensor. *Plant J* **50**(1), 108-117.

Franklin, K. A., Praekelt, U., Stoddart, W. M., Billingham, O. E., Halliday, K. J., and Whitelam, G. C. (2003). Phytochromes B, D, and E act redundantly to control multiple physiological responses in Arabidopsis. *Plant Physiol* **131**(3), 1340-1346.

Franklin, K. A., and Quail, P. H. (2010). Phytochrome functions in Arabidopsis development. *J Exp Bot* **61**(1), 11-24.

Gould, K. S., and Quinn, B. D. (1998). Do anthocyanins protect leaves of New Zealand native species from UV-B? *N. Z. J. Bot.* **37**, 175–178.

Han, S., and Kim, D. (2006). AtRTPrimer: database for Arabidopsis genome-wide homogeneous and specific RT-PCR primer-pairs. *BMC Bioinformatics* **7**, 179.

Hiltbrunner, A., Tscheuschler, A., Viczian, A., Kunkel, T., Kircher, S., and Schafer, E. (2006). FHY1 and FHL act together to mediate nuclear accumulation of the phytochrome A photoreceptor. *Plant Cell Physiol* **47**(8), 1023-1034.

Hiltbrunner, A., Viczian, A., Bury, E., Tscheuschler, A., Kircher, S., Toth, R., Honsberger, A., Nagy, F., Fankhauser, C., and Schafer, E. (2005). Nuclear accumulation of the phytochrome A photoreceptor requires FHY1. *Curr Biol* **15**(23), 2125-2130.

Jang, I. C., Yang, J. Y., Seo, H. S., and Chua, N. H. (2005). HFR1 is targeted by COP1 E3 ligase for post-translational proteolysis during phytochrome A signaling. *Genes Dev* **19**(5), 593-602.

Jiao, Y., Lau, O. S., and Deng, X. W. (2007). Light-regulated transcriptional networks in higher plants. *Nat Rev Genet* **8**(3), 217-230.

Jiao, Y., Ma, L., Strickland, E., and Deng, X. W. (2005). Conservation and divergence of light-regulated genome expression patterns during seedling development in rice and Arabidopsis. *Plant Cell* **17**(12), 3239-3256.

Johnson, E., Bradley, M., Harberd, N. P., and Whitelam, G. C. (1994). Photoresponses of Light-Grown phyA Mutants of Arabidopsis (Phytochrome A Is Required for the Perception of Daylength Extensions). *Plant Physiol* **105**(1), 141-149.

Kerckhoffs, L. H. J., Schreuder, M. E. L., Tuinen, A. V., Koornneef, M., and Kendrick, R. E. (1997). Phytochrome Control of Anthocyanin Biosynthesis in Tomato Seedlings: Analysis Using Photomorphogenic Mutants. *Photochemistry and Photobiology* **65**(2), 374-381.

Kim, J., Yi, H., Choi, G., Shin, B., Song, P. S., and Choi, G. (2003). Functional characterization of phytochrome interacting factor 3 in phytochrome-mediated light signal transduction. *Plant Cell* **15**(10), 2399-2407.

Kim, Y. M., Woo, J. C., Song, P. S., and Soh, M. S. (2002). HFR1, a phytochrome A-signalling component, acts in a separate pathway from HY5, downstream of COP1 in *Arabidopsis thaliana*. *Plant J* **30**(6), 711-719.

Kubo, H., Peeters, A. J., Aarts, M. G., Pereira, A., and Koornneef, M. (1999). ANTHOCYANINLESS2, a homeobox gene affecting anthocyanin distribution and root development in Arabidopsis. *Plant Cell* **11**(7), 1217-1226.

Lagarias, D. M., Crepeau, M. W., Maines, M. D., and Lagarias, J. C. (1997). Regulation of photomorphogenesis by expression of mammalian biliverdin reductase in transgenic Arabidopsis plants. *Plant Cell* **9**(5), 675-688.

Lee, D. W., and Collins, T. M. (2001). Phylogenetic and ontogenetic influences on the distribution of anthocyanins and betacyanins in leaves of tropical plants. *Int. J. Plant Sci.* **162**(5), 1141-1153.

Lin, C., Ahmad, M., and Cashmore, A. R. (1996). Arabidopsis cryptochrome 1 is a soluble protein mediating blue light-dependent regulation of plant growth and development. *Plant J* **10**(5), 893-902.

Luccioni, L. G., Oliverio, K. A., Yanovsky, M. J., Boccalandro, H. E., and Casal, J. J. (2002). Brassinosteroid Mutants Uncover Fine Tuning of Phytochrome Signaling. *Plant Physiol.* **128**(1), 173-181.

Ma, L., Sun, N., Liu, X., Jiao, Y., Zhao, H., and Deng, X. W. (2005). Organ-specific expression of Arabidopsis genome during development. *Plant Physiol* **138**(1), 80-91.

Mancinelli, A. (1985). Light-dependent anthocyanin synthesis: A model system for the study of plant photomorphogenesis. *The Botanical Review* **51**(1), 107-157.

Mancinelli, A. L., Rossi, F., and Moroni, A. (1991). Cryptochrome, phytochrome, and anthocyanin production. *Plant Physiol* **96**(4), 1079-1085.

Mandoli, D. F., and Briggs, W. R. (1982). The photoperceptive sites and the function of tissue light-piping in photomorphogenesis of etiolated oat seedlings. *Plant, Cell & Environment* **5**(2), 137-145.

Mathews, S. (2006). Phytochrome-mediated development in land plants: red light sensing evolves to meet the challenges of changing light environments. *Mol Ecol* **15**(12), 3483-3503.

Mohr, H. (1972). Lectures on Photomorphogenesis. Springer-Verlag, Berlin, New York.

Monte, E., Alonso, J. M., Ecker, J. R., Zhang, Y., Li, X., Young, J., Austin-Phillips, S., and Quail, P. H. (2003). Isolation and characterization of phyC mutants in Arabidopsis reveals complex crosstalk between phytochrome signaling pathways. *Plant Cell* **15**(9), 1962-1980.

Montgomery, B. L. (2008). Right place, right time: Spatiotemporal light regulation of plant growth and development. *Plant Signal Behav* **3**(12), 1053-1060.

Montgomery, B. L. (2009). Spatial-specific phytochrome responses during de-etiolation in *Arabidopsis thaliana*. *Plant Signal Behav* **4**(1), 47-49.

Montgomery, B. L., Franklin, K. A., Terry, M. J., Thomas, B., Jackson, S. D., Crepeau, M. W., and Lagarias, J. C. (2001). Biliverdin reductase-induced phytochrome chromophore deficiency in transgenic tobacco. *Plant Physiol* **125**(1), 266-277.

Montgomery, B. L., Yeh, K. C., Crepeau, M. W., and Lagarias, J. C. (1999). Modification of distinct aspects of photomorphogenesis via targeted expression of mammalian biliverdin reductase in transgenic Arabidopsis plants. *Plant Physiol* **121**(2), 629-639.

Nagatani, A. (1997). Spatial distribution of phytochromes. *Journal of Plant Research* **110**(1), 123-130.

Nagatani, A., Reed, J. W., and Chory, J. (1993). Isolation and Initial Characterization of Arabidopsis Mutants That Are Deficient in Phytochrome A. *Plant Physiol* **102**(1), 269-277.

Nagy, F., and Schafer, E. (2002). Phytochromes control photomorphogenesis by differentially regulated, interacting signaling pathways in higher plants. *Annu Rev Plant Biol* **53**, 329-355.

Neff, M. M., and Chory, J. (1998). Genetic interactions between phytochrome A, phytochrome B, and cryptochrome 1 during Arabidopsis development. *Plant Physiol* **118**(1), 27-35.

Neff, M. M., Fankhauser, C., and Chory, J. (2000). Light: an indicator of time and place. *Genes Dev* **14**(3), 257-271.

Ni, M., Tepperman, J. M., and Quail, P. H. (1998). PIF3, a phytochrome-interacting factor necessary for normal photoinduced signal transduction, is a novel basic helix-loop-helix protein. *Cell* **95**(5), 657-667.

Nick, P., Ehmann, B., Furuya, M., and Schafer, E. (1993). Cell Communication, Stochastic Cell Responses, and Anthocyanin Pattern in Mustard Cotyledons. *Plant Cell* **5**(5), 541-552.

Parks, B. M., and Quail, P. H. (1993). hy8, a New Class of Arabidopsis Long Hypocotyl Mutants Deficient in Functional Phytochrome A. *Plant Cell* **5**(1), 39-48.

Poppe, C., Sweere, U., Drumm-Herrel, H., and Schafer, E. (1998). The blue light receptor cryptochrome 1 can act independently of phytochrome A and B in *Arabidopsis thaliana*. *Plant J* **16**(4), 465-471.

Quail, P. H., Boylan, M. T., Parks, B. M., Short, T. W., Xu, Y., and Wagner, D. (1995). Phytochromes: photosensory perception and signal transduction. *Science* **268**(5211), 675-680.

Rabino, I., and Mancinelli, A. L. (1986). Light, Temperature, and Anthocyanin Production. *Plant Physiol* **81**(3), 922-924.

Reed, J. W., Nagatani, A., Elich, T. D., Fagan, M., and Chory, J. (1994). Phytochrome A and Phytochrome B Have Overlapping but Distinct Functions in Arabidopsis Development. *Plant Physiol* **104**(4), 1139-1149.

Roig-Villanova, I., Bou, J., Sorin, C., Devlin, P. F., and Martinez-Garcia, J. F. (2006). Identification of primary target genes of phytochrome signaling. Early transcriptional control during shade avoidance responses in Arabidopsis. *Plant Physiol* **141**(1), 85-96.

Rösler, J., Klein, I., and Zeidler, M. (2007). Arabidopsis fhl/fhy1 double mutant reveals a distinct cytoplasmic action of phytochrome A. *Proc Natl Acad Sci U S A* **104**(25), 10737-10742.

Ruckle, M. E., DeMarco, S. M., and Larkin, R. M. (2007). Plastid signals remodel light signaling networks and are essential for efficient chloroplast biogenesis in Arabidopsis. *Plant Cell* **19**(12), 3944-3960.

Sharrock, R. A., and Clack, T. (2002). Patterns of expression and normalized levels of the five Arabidopsis phytochromes. *Plant Physiol* **130**(1), 442-456.

Shin, J., Park, E., and Choi, G. (2007). PIF3 regulates anthocyanin biosynthesis in an HY5-dependent manner with both factors directly binding anthocyanin biosynthetic gene promoters in Arabidopsis. *Plant J* **49**(6), 981-994.

Shinomura, T., Uchida, K., and Furuya, M. (2000). Elementary processes of photoperception by phytochrome A for high-irradiance response of hypocotyl elongation in Arabidopsis. *Plant Physiol* **122**(1), 147-156.

Suzuki, T., Nakajima, S., Morikami, A., and Nakamura, K. (2005). An Arabidopsis protein with a novel calcium-binding repeat sequence interacts with TONSOKU/MGOUN3/BRUSHY1 involved in meristem maintenance. *Plant Cell Physiol* **46**(9), 1452-1461.

Tanaka, S., Nakamura, S., Mochizuki, N., and Nagatani, A. (2002). Phytochrome in cotyledons regulates the expression of genes in the hypocotyl through auxin-dependent and -independent pathways. *Plant Cell Physiol* **43**(10), 1171-1181.

Tóth, R., Kevei, E., Hall, A., Millar, A. J., Nagy, F., and Kozma-Bognar, L. (2001). Circadian clock-regulated expression of phytochrome and cryptochrome genes in Arabidopsis. *Plant Physiol* **127**(4), 1607-1616.

Vlachonasios, K. E., Thomashow, M. F., and Triezenberg, S. J. (2003). Disruption mutations of ADA2b and GCN5 transcriptional adaptor genes dramatically affect Arabidopsis growth, development, and gene expression. *Plant Cell* **15**(3), 626-638.

Wang, H., and Deng, X. W. (2003). Dissecting the phytochrome A-dependent signaling network in higher plants. *Trends Plant Sci* **8**(4), 172-178.

Warnasooriya, S. N., and Montgomery, B. L. (2009). Detection of spatial-specific phytochrome responses using targeted expression of biliverdin reductase in Arabidopsis. *Plant Physiol* **149**(1), 424-433.

Weller, J. L., Beauchamp, N., Kerckhoffs, L. H., Platten, J. D., and Reid, J. B. (2001). Interaction of phytochromes A and B in the control of de-etiolation and flowering in pea. *Plant J* **26**(3), 283-294.

Whitelam, G. C., Johnson, E., Peng, J., Carol, P., Anderson, M. L., Cowl, J. S., and Harberd, N. P. (1993). Phytochrome A null mutants of Arabidopsis display a wild-type phenotype in white light. *Plant Cell* **5**(7), 757-768.

Yadav, V., Mallappa, C., Gangappa, S. N., Bhatia, S., and Chattopadhyay, S. (2005). A basic helix-loop-helix transcription factor in Arabidopsis, MYC2, acts as a repressor of blue light-mediated photomorphogenic growth. *Plant Cell* **17**(7), 1953-1966.

Yamada, K., Nagano, A. J., Nishina, M., Hara-Nishimura, I., and Nishimura, M. (2008). NAI2 is an endoplasmic reticulum body component that enables ER body formation in *Arabidopsis thaliana*. *Plant Cell* **20**(9), 2529-2540.

Yang, S. W., Jang, I. C., Henriques, R., and Chua, N. H. (2009). FAR-RED ELONGATED HYPOCOTYL1 and FHY1-LIKE associate with the Arabidopsis transcription factors LAF1 and HFR1 to transmit phytochrome A signals for inhibition of hypocotyl elongation. *Plant Cell* **21**(5), 1341-1359.

Yanovsky, M. J., Casal, J. J., and Luppi, J. P. (1997). The VLF loci, polymorphic between ecotypes Landsberg erecta and Columbia, dissect two branches of phytochrome A signal transduction that correspond to very-low-fluence and high-irradiance responses. *Plant J* **12**(3), 659-667.

Yanovsky, M. J., Casal, J. J., and Whitelam, G. C. (1995). Phytochrome A, phytochrome B and HY4 are involved in hypocotyl growth responses to natural radiation in Arabidopsis: weak de-etiolation of the phyA mutant under dense canopies. *Plant, Cell & Environment* **18**(7), 788-794.

Yanovsky, M. J., Luppi, J. P., Kirchbauer, D., Ogorodnikova, O. B., Sineshchekov, V. A., Adam, E., Kircher, S., Staneloni, R. J., Schafer, E., Nagy, F., and Casal, J. J. (2002). Missense mutation in the PAS2 domain of phytochrome A impairs subnuclear localization and a subset of responses. *Plant Cell* **14**(7), 1591-1603.

Yanovsky, M. J., Whitelam, G. C., and Casal, J. J. (2000). fhy3-1 retains inductive responses of phytochrome A. *Plant Physiol* **123**(1), 235-242.

Chapter 3 Phytochrome-mediated Light-dependent Anthocyanin Accumulation in Red Light

Some of the work included in chapter 3 was published in the journal, Plant Physiology. **Warnasooriya SN** and Montgomery BL, (2009), Detection of Spatial-Specific Phytochrome Responses Using Targeted Expression of Biliverdin Reductase in Arabidopsis, Plant Physiology, 149(1), 424-433.

Most of the work in chapter 3 is from a manuscript submitted to the journal, Plant, Cell and Physiology.

Warnasooriya SN, Porter KJ and Montgomery BL, Tissue- and Isoform-Specific Phytochrome Regulation of Light-Dependent Anthocyanin Accumulation in *Arabidopsis thaliana* (submitted).

3.1 Overview

Exogenous and endogenous stimuli can lead to biosynthesis and accumulation of flavonoid compounds: flavones, flavonols, isoflavonoids and anthocyanins and among them anthocyanins are the most abundant in plants (Shi and Xie, 2010). The accumulation of flavonoid compounds is highly regulated in response to environmental stimuli such as light, temperature, and nutrient availability (Feinbaum and Ausubel, 1988). Among the external stimuli, light is one of the most important environmental stimuli regulating the expression of flavonoid structural genes (Mol et al., 1996). Metabolites, hormones, and the developmental stage of the tissues are among the endogenous stimuli that regulate anthocyanin biosynthesis and deposition (Mol et al., 1996)

Synthesis and deposition of anthocyanins in different tissues within the plant can exert specific functions. Light-induced anthocyanin biosynthesis and accumulation in the epidermis is thought to have evolved for protection of plants against excess or damaging solar radiation (Drumm-Herrel and Mohr, 1985). Additionally, anthocyanins are important antioxidant molecules and aid in protecting plants from damage by active oxygen species (Nagata et al., 2003). Biosynthesis and accumulation of pigments is one of main aspects of photomorphogenesis in Arabidopsis seedlings upon emergence into the light environment. Photomorphogenesis is regulated by the action of at least two major classes of photoreceptors: phytochromes in R and FR illumination (Mancinelli, 1985) and cryptochromes in UV-A and B illumination (Ahmad, Lin, and Cashmore, 1995). A small nuclear gene family of five members, *PHYA – PHYE*, has been identified in Arabidopsis (Fankhauser and Staiger, 2002; Quail, 1994) and each gene encodes a

phytochrome apoprotein that covalently attaches to a single linear tetrapyrrole chromophore, phytochromobilin (PΦB; Terry, Wahleithner, and Lagarias, 1993). phyA is the phytochrome primarily responsible for FR-dependent growth responses (Nagatani, Reed, and Chory, 1993; Whitelam et al., 1993) and has an additional role in regulating photoresponses under B illumination (Chun, Kawakami, and Christopher, 2001; Duek and Fankhauser, 2003; Neff and Chory, 1998; Whitelam et al., 1993; Yadav et al., 2005). phyB through phyE contribute to the regulation of growth and development, primarily in response to R illumination (Aukerman et al., 1997; Franklin et al., 2003; Monte et al., 2003; Nagatani, Reed, and Chory, 1993; Reed et al., 1993). Anthocyanin biosynthesis and accumulation is one of the characteristic aspects of the photomorphogenesis process and differential expression of anthocyanin structural genes, as well as their regulatory genes is important for mediating anthocyanin biosynthesis. Despite major advances in understanding light-regulated anthocyanin synthesis, information on the involvement of phytochromes in complex signaling cascades to mediate anthocyanin synthesis and deposition is limited. Thus, investigating light-dependent anthocyanin biosynthesis and accumulation is a useful undertaking to gain insight into the photoregulation of pigmentation, as well as to define the discrete and overlapping roles of phytochrome isoforms under different light conditions.

3.1.1 Anthocyanin Biosynthesis and Accumulation

Flavonoids are aromatic secondary metabolites with numerous biological functions (Agati and Tattini, 2010; Lepiniec et al., 2006). However, flavonoid compounds are largely nonessential for plant viability (Nesi et al., 2000). In plants, the

main flavonoid compounds are flavones, flavonols, isoflavonoids and anthocyanins; however, Arabidopsis cannot produce isoflavonoids due to lack of chalcone reductase and isoflavone synthase (Aoki, Akashi, and Ayabe, 2000). The anthocyanin biosynthetic pathway is characterized by two groups of co-regulated structural genes: early biosynthetic genes, i.e., *CHS*, *CHI*, *F3H*, and *FLS*, and the late biosynthetic genes, i.e., *DFR* and *LDOX*, during seedling development (Kubasek et al., 1992). Many of the early and late biosynthetic genes are induced by sucrose and to a lesser degree by other sugars (Gollop et al., 2002; Martin, Oswald, and Graham, 2002; Solfanelli et al., 2006). The expression of early and late biosynthetic genes is highly regulated by the products of multiple regulatory genes and tissue-specific expression of biosynthetic genes and anthocyanin deposition are correlated (Procissi et al., 1997).

The mostly nonessential nature of anthocyanins for plant viability has made the generation of mutants in this biosynthetic pathway feasible and has facilitated the genetic and molecular dissection of the pathway. Isolation and characterization of mutants and functional genomics approaches have identified a number of such regulatory gene families. Regulatory proteins can directly or indirectly regulate the biosynthesis and/or accumulation of anthocyanins. A majority of these regulatory proteins belongs to two of the largest families of regulatory proteins in plants: the MYB and bHLH families (Lepiniec et al., 2006) in addition to WD40, WRKY, WIP, Homeodomain, and bMADS families (Shi and Xie, 2010). The biosynthesis and accumulation of anthocyanins in response to light mainly occur due to transcriptional regulation of genes in the biosynthetic pathway (Martin and Gerats, 1993; Taylor and Briggs, 1990). For example, under high-intensity light conditions, accumulation of anthocyanins is induced in the

leaves and stems of Arabidopsis seedlings and coincides with an increase in chalcone synthase (CHS) activity, which is partly related to an increased rate of *CHS* transcription (Feinbaum and Ausubel, 1988). Differential regulation of transcription factors involved in biosynthesis adds another regulatory level to fine-tune anthocyanin deposition. Regulatory genes that are required for mediating anthocyanin biosynthesis can be expressed constitutively, e.g. *TTG1*, or can be induced by light (Cominelli et al., 2008). Two such examples of light-induced genes are *PIF3* (Phytochrome-Interacting Factor 3, a member of the bHLH family) and *HY5* (Long Hypocotyl 5, a member of the bZIP factors). In R and FR light conditions, PIF3 (Kim et al., 2003) and HY5 (Ang and Deng, 1994; Somers et al., 1991) play a positive role in regulating anthocyanin biosynthesis. Sequence analysis indicated that the promoters of all anthocyanin biosynthetic genes, in addition to the G-box elements, have multiple ACGT-containing elements and E-box elements, which are common to light-regulated genes (Shin, Park, and Choi, 2007). PIF3 and HY5 regulate anthocyanin biosynthesis by directly binding only to G-boxes and ACGT-containing sequence elements, respectively, within the promoters of anthocyanin biosynthetic genes and collaboratively regulate phyA-mediated anthocyanin biosynthesis (Shin, Park, and Choi, 2007). Moreover, PIF3-dependent regulation occurs by activation of the transcription of anthocyanin biosynthetic genes in a HY5-dependent manner (Shin, Park, and Choi, 2007).

Reports have also shown that anthocyanin biosynthesis in Arabidopsis can be induced by different abiotic and biotic factors and induction in biosynthesis is characterized by notable changes in the transcripts of biosynthetic, as well as regulatory genes. An R2R3-MYB factor, PAP1 (also called *AtMYB75*; *At1g56650*) is an essential

regulatory protein of anthocyanin biosynthesis in Arabidopsis (Rowan et al., 2009; Shi and Xie, 2010). In wild-type Arabidopsis seedlings, *PAP1* expression is induced by light (Cominelli et al., 2008; Lea et al., 2007; Lillo, Lea, and Ruoff, 2008; Solfanelli et al., 2006; Teng et al., 2005). PAP1 stimulates light induction of anthocyanin biosynthesis in seedlings (Cominelli et al., 2008; Stracke et al., 2007) by regulating anthocyanin biosynthetic genes (Gonzalez et al., 2008). Expression of *PAP1* is also induced by sucrose (Solfanelli et al., 2006; Teng et al., 2005). Interestingly, sucrose-induced accumulation of anthocyanin is marked by either induction or increase in the expression of *PAP1* (Lea et al., 2007; Rowan et al., 2009; Teng et al., 2005). Furthermore, *PAP1* expression and induction of anthocyanin biosynthesis by sucrose levels is positively correlated (Lillo, Lea, and Ruoff, 2008; Solfanelli et al., 2006; Teng et al., 2005). Notably, *PAP1* expression is induced after 6 hrs of exposure to R light (Cominelli et al., 2008), indicating a possible role of phytochromes in the *PAP1*-regulated anthocyanin accumulation. While PIF3, HY5 and PAP1 have a positive regulatory role, some of the MYB and bHLH regulatory proteins act as repressors of anthocyanin accumulation in Arabidopsis (Dubos et al., 2008; Matsui, Umemura, and Ohme-Takagi, 2008; Yadav et al., 2005; Zhu et al., 2009).

Anthocyanin biosynthesis is indeed subjected to environmental and developmental regulation and induction of biosynthesis and/or accumulation by abiotic and biotic stress factors requires proper coordination of synthesis and deposition in a spatial-, as well as a temporal-specific manner. Deposition of anthocyanins correlates with the transcript accumulation of corresponding early and late biosynthetic genes. The regulation of structural genes at the transcriptional level by regulatory proteins with

inductive and suppressive roles comprises a complex regulatory network of gene expression with positive and negative roles to fine-tune the biosynthesis, accumulation and deposition of anthocyanins in discrete tissues at a defined developmental stage in the life cycle of Arabidopsis.

3.1.2 Spatial-specific Accumulation of Anthocyanins

Accumulation of anthocyanins occurs in specific tissues at discrete developmental stages and is strictly regulated (Tonelli et al., 1994). Among the environmental factors that regulate this process are light, temperature, nutrients, and stress (Rabino and Mancinelli, 1986). Developmental information from such cues is transduced through complex signaling cascades to numerous genes that affect the synthesis, amount and distribution of anthocyanins within seedlings and adult plants.

During de-etiolation, even though anthocyanin biosynthesis is limited to the outer cell layers of young seedlings, its accumulation predominantly occurs in the sub-epidermal layer of the hypocotyl and lower epidermis of the cotyledons (Huub, Kerckhoffs, and Kendrick, 1997). By contrast, in adult plants, anthocyanins are synthesized mainly in the outer cell layers of young developing leaves and the amount of anthocyanins is diluted as the leaf matures (Kerckhoffs et al., 1992). Differential spatial-specific accumulation in young seedlings and adult plants suggests that anthocyanin deposition is developmentally regulated. In tomato, the anthocyanin responses occurring in the de-etiolation process display strong tissue specificity in the hypocotyls, restricted to a single layer of subepidermal cells (Neuhaus et al., 1993).

Tissue-specific expression of certain regulatory genes is able to fine-tune the expression of structural genes, which in turn mediates anthocyanin accumulation in distinct tissues. In maize, regulatory genes that control transcription of structural genes of the anthocyanin biosynthetic pathway exert spatial and temporal regulation of anthocyanin accumulation in numerous tissues (Procissi et al., 1997). Light-inducible tissue-specific activation of *myb* class genes regulates the spatial-specific anthocyanin biosynthesis at different developmental stages in maize seeds. For example, an ACGT-containing sequence element, upstream of the transcription start site of *myb* genes, *C1* and *pl*, confers light inducibility (Cone et al., 1993; Kao et al., 1996). RT-PCR analysis of *pl* and *C1* transcripts indicated that expression of these regulatory genes is restricted to the pericarp and aleurone layer, respectively (Procissi et al., 1997). Light-inducible tissue-specific activation of *pl* regulates pigmentation in the pericarp during the early stages of maize seed development, whereas *C1* regulates pigmentation in the aleurone layer during the advanced stages (Procissi et al., 1997). An example of a regulatory protein conferring spatial-specific activation of anthocyanin biosynthetic genes is a bHLH family protein, Transparent TESTA8 (TT8) that modulates the expression of certain genes of the late flavonoid biosynthetic pathway in Arabidopsis siliques (Mehrtens et al., 2005). Therefore, differential expression of structural genes and regulatory genes in discrete tissues play a major role in regulating spatial-specific anthocyanin biosynthesis and accumulation *in planta*.

Transcriptional regulation of anthocyanin biosynthetic genes is subjected to both spatial and temporal regulation through the activities of regulatory proteins. Previously published data support the existence of spatial-, as well as temporal-specific *de novo*

synthesis and/or accumulation of anthocyanins in Arabidopsis and other plant species (Borevitz et al., 2000; Kubo et al., 1999; Nesi et al., 2000). Despite the extensive amount of work reported on the spatial-specific biosynthesis and accumulation of anthocyanins, the mechanisms that control spatial and temporal regulation of anthocyanin accumulation have not yet been fully elucidated in Arabidopsis. Both phytochromes and cryptochromes regulate anthocyanin biosynthesis and accumulation in plants (Ahmad, Lin, and Cashmore, 1995). Phytochromes and cryptochromes that are localized in specific tissues and/or organs are able to mediate distinct light-dependent responses (Endo et al., 2007; Montgomery, 2009; Warnasooriya and Montgomery, 2009). Localized pools of photoreceptors may regulate anthocyanin synthesis and disposition in which they perceive light or can mediate at distant sites from the site of photoperception. This phenomenon suggests that complex signaling mechanisms exist between perception of light and anthocyanin accumulation in specific tissues within plants. Whether the spatial-specific accumulation of photoreceptors contributes to the synthesis and deposition of anthocyanins in discrete tissues or organs and the functions of different phytochrome isoforms in regulating anthocyanin accumulation under different fluences of R/FR light are yet to be analyzed.

3.1.3 Functions of Phytochromes in Spatial-specific Anthocyanin Accumulation

Light-dependent anthocyanin biosynthesis in seedlings displays characteristics of typical phytochrome-mediated HIR (Mancinelli, 1985). Analysis of photoreceptor mutants has enabled understanding of specific physiological functions mediated by phytochrome isoforms in phytochrome-dependent anthocyanin deposition under different

light conditions. In FR light, the HIR of anthocyanin accumulation was completely absent in a *phyA* mutant, whereas a *phyB* mutant displayed no significant reduction (Kunkel et al., 1996). Therefore, in FR light, phyA is solely responsible for anthocyanin accumulation (Kunkel et al., 1996). It was also reported that phyA has a significant role in the induction of anthocyanin accumulation in B (Duek and Fankhauser, 2003; Neff and Chory, 1998). Under R illumination, a *phyB* mutant had only a slight reduction in anthocyanin levels compared to WT or a *phyA* mutant. This observation suggests that, phyA or other phytochromes, but not phyB, play a significant role in R illumination (Kunkel et al., 1996). In contrast to the evidence for the role of phyA in R illumination in regulating anthocyanin synthesis, phyB1 of tomato is responsible for a significant proportion of anthocyanin biosynthesis in R (Kerckhoffs et al., 1997). A reduction of anthocyanin levels reported for a *phyD* mutant in the Wassilewskija (Ws) ecotype under Wc, was not evident in a *phyD* mutant in the Landsberg *erecta* (L*er*) ecotype, indicating that anthocyanin accumulation is primarily regulated by phyB in the L*er* background (Aukerman et al., 1997). Currently, no reports have been published on the impact of phyC or phyE on anthocyanin accumulation.

Spatially localized pools of phytochromes are known to contribute to the photoregulation of distinct phytochrome-dependent responses (Endo et al., 2007; Endo and Nagatani, 2008; Endo et al., 2005; Montgomery, 2009; Warnasooriya and Montgomery, 2009). In Arabidopsis, exposure to high-intensity light conditions is known to induce accumulation of anthocyanins in the leaves and stems via an increased rate of *CHS* transcription and it is possible that this response is mediated by a photoreceptor (Feinbaum and Ausubel, 1988). Distinct patterns of anthocyanin deposition can be

attributed to the members of the phytochrome family in Arabidopsis and tomato (Kerckhoffs et al., 1997; Warnasooriya and Montgomery, 2009). Based on the fact that both phytochromes and anthocyanins are localized in distinct tissues during different developmental stages of plants, localized pools of phytochromes may have specific physiological functions related to anthocyanin synthesis, accumulation, and/or deposition. In fact, in Arabidopsis, mesophyll-localized phyA is known to regulate FR-dependent induction of anthocyanins and additional mesophyll-localized phytochromes, apart from phyB, have a role in R-induced anthocyanin accumulation (Warnasooriya and Montgomery, 2009). Despite the information available on the spatial- and temporal-specific regulation of phytochrome activity in mediating anthocyanin synthesis and deposition, conclusive reports on whether a particular localized pool of phytochromes can regulate intra- and/or inter-tissue accumulation of anthocyanins under R light have not yet been published.

3.1.4 Outlook

Prior investigations into phytochrome-dependent regulation of anthocyanin accumulation revealed that mesophyll-specific phyA regulates FR-mediated induction of anthocyanin accumulation (Warnasooriya and Montgomery, 2009). The objective of this chapter is to utilize targeted phytochrome inactivation to further analyze the sites of photoperception and gain insight into the roles of phytochrome isoforms in sucrose-stimulated, light-dependent anthocyanin accumulation under Rc conditions. Transgenic Arabidopsis lines with tissue-specific chromophore deficiencies are probed under Rc for phenotypic perturbations. In contrast to the role of mesophyll-localized phyA in

regulating FR-mediated induction of anthocyanin accumulation, under Rc, additional mesophyll-localized phytochromes, in addition to phyB, mediate R-induced anthocyanin accumulation. Given the prior investigations into the functions of phyA and phyB in Arabidopsis and tomato in light-inducible anthocyanin accumulation, the analysis of apophytochrome mutants revealed novel roles for phytochrome isoforms in Rc conditions: phyA, B, C and, D essentially regulate the induction of anthocyanin accumulation, whereas phyE imposes suppression on anthocyanin accumulation in Arabidopsis.

3.2 Materials and Methods

3.2.1 Quantification of Anthocyanin Levels in Transgenic Lines with Targeted Chromophore Inactivation

Seeds of No-0 WT, 35S::pBVR3, CAB3::pBVR2, Col-0 WT and *phyB* (SALK_ 022035; Ruckle, DeMarco, and Larkin, 2007) were sterilized and planted as described in section 2.2.1, and were subjected to treatment with R pulse (approximately 75 μmol m^{-2} s^{-1}) for 5 min prior to imbibition. Imbibing seeds were cold-stratified at 4 °C for 3 days in darkness. Plates were transferred to a temperature- and humidity-controlled growth chamber with Rc illumination of 50 μmol m^{-2} s^{-1} or in darkness for 4 days at 20 °C. Anthocyanins were extracted from whole-plant seedlings and quantified as described in section 2.2.2.

3.2.2 Confirmation of Apophytochrome Mutants

To gain insight into the differential roles of phytochrome isoforms in Rc conditions, apophytochrome mutants, each with a T-DNA insertion in an exon of the respective genes were selected from the Salk T-DNA insertion mutant collection (Alonso et al., 2003). Seeds of Col-0 WT, *phyA* (SALK_014575; (Ruckle, DeMarco, and Larkin, 2007), *phyB* (SALK_ 022035; (Ruckle, DeMarco, and Larkin, 2007), *phyC* (SALK_007004), *phyD* (SALK_027336) and *phyE* (SALK_092529) were sterilized as described in section 2.2.1. Sterilized seeds were treated with R pulse (approximately 75 μmol m^{-2} s^{-1}) for 5 min prior to imbibition. Imbibing seeds were cold-stratified at 4 °C for 3 days in darkness. Plates were transferred to a temperature- and humidity-controlled growth chamber with Rc illumination of 50 μmol m^{-2} s^{-1} for 4 days at 22 °C. 4-d-old whole seedlings were quickly (< 1 min) harvested and immediately frozen in liquid nitrogen inside the R light chamber. Using RNeasy® Plant Minikit (Catalog No. 16419, Qiagen, CA) including on-column DNase treatment (Catalog No. 79254, Qiagen, CA), total RNA was isolated according to manufacturer's instructions. The quantity of RNA was analyzed by spectrometry (NanoDrop1000, Thermo Scientific, MA). $Oligo(dT)_{15}$ primed-first-strand cDNA was synthesized from 1 μg of total RNA using a Reverse Transcription System (Catalog No. A3500, Promega, WI) according to manufacturer's instructions with the modifications as described in section 2.2.4. cDNA was stored at -20 °C overnight before PCR amplification. First-strand cDNA synthesis reactions were diluted 1:16 with nuclease-free water. PCR was conducted with GoTaqGreen (Catalog No. M7123, Promega, WI) and 4 μl of the diluted cDNA product was used as template in

a 25 µl reaction. The gene-specific oligonucleotides for respective genes were designed using a free online database, *AtRTPrimer* (Han and Kim, 2006); *PHYA (At1g09570)*– forward 5'-AAGGAGAATGCACCCAAGGTCATC-3' and reverse 5'-CACCTTCAATCCGCGTAAACTTGTC-3', *PHYB (At2g18790)*– forward 5'-TCGAGGGAAAGGTTATTGGGGCTTT-3' and reverse 5'-GGAACATGTCTCGGACTAGCTCTGG-3', *PHYD (At4g16250)*– forward 5'-GATCGCAAAGGGGAATTCATTCAGG-3' and reverse 5'-TTCCATGGGTGCATAACGGACA-3'and *PHYE (At4g18130)*– forward 5'-GCTTACGGGATGGTCAAAACACGA-3' and reverse 5'-GGCGACTTCAACCCTTAGTTGTGAG-3'. The gene-specific oligonucleotides for *PHYC (At5g35840)* were designed based on the full length cDNA sequence: *PHYC*– forward 5'-CCCTCAACAAATTGGCATATCTCCGCC-3' and reverse 5'-AGATCCTCAGGCAGTCCTGGTGC-3'. PCR amplification was carried out with gene-specific oligonucleotides at 10 µM. The following thermal cycling conditions were used for the PCR amplification: (1) 1 cycle of denaturation at 94 °C for 2 min, (2) 30 cycles of denaturation at 94 °C for 30 s, annealing for 45 s (for *PHYA*, *PHYB* and *PHYE* at 60 °C, for *PHYC* at 61 °C and *PHYD* at 59 °C), extension at 72 °C for 38 s and (3) final extension at 72 °C for 5 min with a hold at 4 °C. Expression of *UBC21* (*At5g25760*) was analyzed as an internal control by including *UBC21*-specific primers, forward 5'-CCTTACGAAGGCGGTGTTTTTCAG-3' and reverse 5'-

CGGCGAGGCGTGTATACATTTG-3') at 10 μM in the same reaction. To rule out the possibility of dependency of transcript accumulation on the number of PCR cycles, amplification with respective gene-specific oligonucleotides was repeated at 45 cycles. A 10 μL aliquot of the PCR product was visualized by electrophoresis for 2 h at 80V on a 1.5% agarose gel containing ethidium bromide at 0.02 μg/mL (Catalog No. 15585-011, Invitrogen, CA). Ultraviolet images were obtained using the Gel Doc system (Bio-Rad Laboratories, Inc., CA) at subsaturation settings.

3.2.3 Quantification of Anthocyanin Levels in Apophytochrome Mutants

Levels of anthocyanins were quantified in apophytochrome mutants that were confirmed to be null in section 3.2.2 according to the protocol described in section 2.2.2, to gain further insight into the roles of individual phytochrome isoforms in the regulation of light-dependent anthocyanin accumulation in Arabidopsis.

3.2.4 Expression Levels of Anthocyanin Marker Genes

Two *MYB* genes, *MYB75/PAP1* and *MYB90/PAP2* are known to regulate anthocyanin biosynthesis, but only *MYB75/PAP1* is required for sucrose-induced anthocyanin accumulation (Borevitz et al., 2000). According to (Teng et al., 2005), *MYB75/PAP1* gene is an important quantitative trait locus (QTL) for sugar-induced anthocyanin induction in Arabidopsis. *DFR* is a late biosynthetic gene and specific for the anthocyanin branch of the flavonoid biosynthetic pathway (Kubasek et al., 1992). An active DFR enzyme is essential for anthocyanin biosynthesis and *MYB75/PAP1* is required for sucrose-stimulated *DFR* expression (Teng et al., 2005). Among the types of

sugars that can induce *MYB75/PAP1* and *DFR*, sucrose appears to be the most effective trigger for both, however, the structural genes upstream of *DFR* display lower induction by sucrose and can also be induced, to a slight degree, by other sugars (Solfanelli et al., 2006; Teng et al., 2005). Due to the requirement of *MYB75/PAP1* and *DFR* for sucrose-induced anthocyanin accumulation in Arabidopsis, *MYB75/PAP1* and *DFR* were selected as anthocyanin marker genes for transcript analysis by RT-PCR.

The levels of *MYB75/PAP1* and *DFR* transcript accumulation in the presence or absence of sucrose was analyzed by RT-PCR to determine if the changes observed in the levels of anthocyanin accumulation in apophytochrome mutants are reflected at the transcript level of selected anthocyanin marker genes. Seeds of Col-0 WT and apophytochrome mutants (*phyA*, *phyB*, *phyC*, *phyD* and *phyE*) were sterilized and planted as described in section 2.2.1. Sterilized seeds were treated with R light pulse (approximately 75 μmol m^{-2} s^{-1}) for 5 min prior to imbibition. Imbibing seeds were cold-stratified at 4 °C for 3 days in darkness. Plates were transferred to a temperature- and humidity-controlled growth chamber with Rc illumination of 50 μmol m^{-2} s^{-1} for 4 days at 22 °C. Extraction and quantification of total RNA were performed as described in section 3.2.2. cDNA was synthesized from 1 μg of total RNA using Reverse Transcription System (Catalog No. A3500, Promega, WI) according to manufacturer's instructions with the modifications as described in section 2.2.4. First-strand cDNA synthesis reactions were diluted 1:16 with nuclease-free water. PCR was conducted with GoTaqGreen (Catalog No. M7123, Promega, WI) and 4 μl of the diluted cDNA product was used as template in a 25 μl reaction. PCR amplification was carried out with the following gene-specific oligonucleotides at 10 μM: *MYB75/PAP1*– forward 5'-

GCTCTGATGAAGTCGATCTTC-3' and reverse 5'- CTACCTCTTGGCTTTCCTCT-3', *DFR1* – forward 5'- GGTTTCATCGGTTCATGGCT-3' and reverse 5'-GGTTTCATCGGTTCATGGCT-3' based on Teng et al., (2005) and Cominelli et al., (2008), respectively. The following thermal cycling conditions were used for the PCR amplification. For *MYB75/PAP1* (1) 1 cycle of denaturation at 94 °C for 2 min, (2) 40 cycles of denaturation at 94 °C for 30 s, annealing at 56.5 °C for 45 s, extension at 72 °C for 3 min and (3) final extension at 72 °C for 10 min with a hold at 4 °C (Teng et al., 2005). For *DFR1*, (1) 1 cycle of denaturation at 94 °C for 3 min, (2) 30 cycles of denaturation at 94 °C for 30 s, annealing at 57 °C for 35 s, extension at 72 °C for 45 s and (3) final extension at 72 °C for 5 min with a hold at 4 °C. Expression of *At5g25760* (*UBC21*) was analyzed as an internal control by including *UBC21*-specific primers as described in section 3.2.2. A 7-µL aliquot of the PCR product was visualized by electrophoresis for 2 h at 80V on a 1.5% agarose gel containing ethidium bromide. Ultraviolet images were obtained using the Gel Doc system (Bio-Rad Laboratories, Inc., CA) at subsaturation settings. Levels of transcript accumulation were quantified using Quantity One®, Version 4.6.3, Bio-Rad Laboratories, Inc., CA).

3.2.5 Complementation of *phyE* Mutant

To test if the phenotype with respect to increased levels of anthocyanin in the *phyE* null mutant can be restored to WT levels, the *phyE* null mutant was complemented with a construct containing a transgene encoding C-terminal myc epitope-tagged phyE driven by the *PHYE* native promoter. pBI-P$_{PHYE}$:phyE-myc$_6$ (*PHYE-m6* hereafter) plant

transformation construct was obtained from Robert A. Sharrock (Clack et al., 2009). The *PHYE-m6* construct was initially introduced into the GV3101pM90 strain of *Agrobacterium tumefaciens* by electroporation (Weigel and Glazebrook, 2006). Transformants were selected on YEP medium containing kanamycin (50 µg/mL; Catalog No. K-4378, Sigma, MO), gentamycin (50 µg/mL; Catalog No. 61-098-RF, Cellgro®, Mediatech, Inc.,VA) and rifampicin (20 µg/mL; Catalog No. R8883, Sigma, MO). Arabidopsis (*Arabidopsis thaliana*) *phyE* mutant (SALK_092529) in the Col-0 WT background was transformed with GV3101 (*PHYE-m6*) using standard Agrobacterium-mediated floral dip transformation (Clough and Bent, 1998). Kanamycin selection of transformants was performed in 150- x 15-mm petri dishes containing 1X Murashige and Skoog salts (Catalog No. MSP09, Caisson Laboratories, UT), 0.6 % (w/v) Phytablend (Catalog No. PTP01, Caisson Laboratories, UT), 1 % (w/v) Sucrose (Catalog No. 4072-05, J.T. Baker, NJ) with kanamycin (Catalog No. K-4378, Sigma, MO) at 50 µg/mL. T1 transgenic seedlings were selected through a rapid selection protocol previously described for identifying transformed Arabidopsis seedlings following floral dip transformation (Harrison et al., 2006). Since the *phyE* mutant (SALK_092529) turned pale green/yellow on media containing kanamycin under Wc, indicating that the kanamycin resistance gene is co-suppressed in the *phyE* mutant background, segregation analysis on complemented *phyE* mutants was performed as described above for selection of primary transformants. T2 seedlings segregated for kanamycin resistance in a 3:1 ratio, which is consistent with the resistance being determined by a single insertion. Based on kanamycin resistance, T3 seedlings that were homozygous for a single T-DNA insertion

were selected to obtain seeds for further analyses on complemented *phyE* mutants (*PHYE-m6/phyE-1* and *PHYE-m6/phyE-11*).

3.2.6 Arabidopsis Seedling Extracts

Seeds of Col-0 WT, complemented *phyE* mutants (*PHYE-m6/phyE-1* and *PHYE-m6/phyE-11*), and *phyE* mutant were sterilized, planted and subjected to cold stratification as described in section 2.2.1. Plates were kept in a humidity-controlled chamber with Rc illumination of 50 μmol m^{-2} s^{-1} for 10 days at 22 °C. Whole-seedling tissues were quickly harvested (< 1 min), weighed and transferred to individual 15 mL sterile tubes. After immediately freezing in liquid nitrogen, tissues were crushed to a powder using a microgrinder. Crude Arabidopsis extracts were prepared according to a protocol adapted from Lagarias et al., (1997); whole-seedling tissues were immediately homogenized in plant extraction buffer: 50 mM Tris-HCl, pH 8.0 (Catalog No. 15568-025, Invitrogen, CA), 100 mM NaCl (Catalog No. 24740-011, GIBCO®, Invitrogen Co., NY), 1 mM EDTA (Catalog No. 15575-038, GIBCO®, Invitrogen Co., NY), 1 mM EGTA (Catalog No. E3889, Sigma, MO), 143 mM 2-mercaptoethanol (Catalog No. M3148, Sigma, MO), 1 mM phenylmethanesulfonyl fluoride (Catalog No. P7626, Sigma, MO), 1 % dimethylsulfoxide (Catalog No. 9224-01, J. T. Baker, NJ), 1X protease inhibitors (Catalog No. 11-836-170-001, Roche, IN), 5 % glycerol (Catalog No. 15514-011, Invitrogen, CA), the latter five components were added just before use. For homogenization, plant extraction buffer was added at a ratio of 3 volumes/fresh weight (mg). The crude homogenates in 15 mL tubes were centrifuged at 4750 rpm for 2 min at

4 °C (Allegra® X-15R Centrifuge, Beckman Coulter, CA) to pellet debris and partially clarified supernatants were transferred to microcentrifuge tubes on ice followed by centrifugation at 13,000 rpm for 15 min at 4 °C (Sorvall® Fresco, Heraeus, NC). Aliquots of clarified supernatants were stored at -80 °C for immunoblot analysis as described in section 3.2.7.

3.2.7 Expression of *PHYE-m6* in Complemented *phyE* Mutant

Total soluble proteins extracted from 10-day-old whole-seedlings were quantified as reported (Warnasooriya and Montgomery, 2009). Protein (~ 60 µg) was separated by SDS-PAGE and subsequent immunoblot analyses were performed as described (Montgomery et al., 1999) using rabbit anti-myc (1:2000; Catalog No. 2278, Cell Signaling, MA). Secondary antibody incubation was performed with goat anti-rabbit IgG (H+L) conjugated to horseradish peroxidase (HRP; 1:4000, Catalog No. 7074, Cell Signaling, MA). Antibody signal (chemiluminescence) was detected using SuperSignal® West Dura Extended Duration substrate (Catalog No. 34075, Thermo Fisher Scientific Inc., IL) on Molecular Imager® VersaDoc™ MP 4000 System (Bio-Rad Laboratories Inc., CA).

3.2.8 Quantification of Anthocyanin Levels in Complemented *phyE* Mutant

Seeds of Col-0 WT, complemented *phyE* mutants (*PHYE-m6/phyE-1* and *PHYE-m6/phyE-11*), and *phyE* mutant were sterilized, planted and subjected to cold stratification as described in section 2.2.1. Plates were kept in a humidity-controlled

chamber with Rc illumination of 50 μmol m^{-2} s^{-1} for 4 days at 22 °C. Levels of anthocyanins were quantified according to the protocol described in section 2.2.2. Two-tailed, unpaired Student's t-test was performed to compare the anthocyanin content relative to Col-0 WT and *phyE* mutant seedlings.

3.3 Results and Discussion

As previously reported, constitutive expression of *BVR* inhibits sucrose-stimulated anthocyanin synthesis in transgenic Arabidopsis plants (Montgomery et al., 2001; Montgomery et al., 1999) and suggests a regulatory role of phytochromes in anthocyanin biosynthesis. Recent analysis of transgenic lines displaying mesophyll-localized phytochrome deficiencies indicated that mesophyll-localized phyA regulates FR-mediated induction of anthocyanin accumulation (Warnasooriya and Montgomery, 2009). Analyses of the *phyA* mutant and CAB3::pBVR lines suggested that phyA in the mesophyll is solely responsible for the regulation of anthocyanin accumulation, as anthocyanin levels in CAB3::pBVR lines and the *phyA* mutant were similar (Warnasooriya and Montgomery, 2009). The objective of this chapter was to utilize targeted expression of *BVR* using tissue-specific promoters to limit the BVR activity to a particular tissue. This novel experimental approach was utilized to investigate the sites of photoperception for phytochrome-dependent anthocyanin accumulation in transgenic Arabidopsis plants.

3.3.1 Spatial-specific Phytochromes Regulate Anthocyanin Accumulation in Rc

Accumulation of anthocyanins occurs in specific tissues at discrete developmental

stages (Tonelli et al., 1994) and a transient developmental peak in flavonoid accumulation occurs when young seedlings are ~ 4-days-old (Kubasek et al., 1992). Therefore, in Arabidopsis, to investigate the impact of monochromatic Rc illumination and determine the roles of localized pools of phytochromes on sucrose-induced accumulation of anthocyanins in seedlings, anthocyanin levels were quantified in 4-d-old representative 35S::pBVR3, CAB3::pBVR2 and null *phyB* T-DNA insertion mutant (Ruckle, DeMarco, and Larkin, 2007) and the cognate wild-type plants.

Anthocyanin accumulation in Rc light was low for all lines compared to their cognate WT plants in the presence, as well as in the absence of sucrose (Figure 3.1). However, in the 35S::pBVR3 line, the anthocyanin levels were not significantly reduced compared to No-0 WT ($p=0.6253$), while the CAB3::pBVR2 line displayed significant reduction compared to No-0 WT ($p<0.0001$, Figure 3.1). This observation suggests that in Rc illumination, inactivation of phytochromes in mesophyll tissues has a more pronounced effect on anthocyanin accumulation at whole-seedling level than the constitutive inactivation of phytochromes. More pronounced effect on anthocyanin accumulation upon mesophyll-localized phytochrome inactivation as compared to constitutive inactivation could also arise due to the differences in the levels of *BVR* expression in cotyledons and tissue specificity of cotyledon tissues vs. mesophyll tissues between 35S::pBVR3 and CAB3::pBVR2 lines. Higher level of *BVR* expression in the cotyledons of CAB3::pBVR2 compared to the level in the cotyledons of 35S::pBVR3 could lead to a drastic reduction of phytochromes within cotyledons causing CAB3::pBVR2 line to have a lesser amount of anthocyanins than all of the other lines, including the *phyB* mutant compared to its wild-type parent, Col-0 WT (Figure 3.1). The

phyB mutant displays a significant reduction in the levels of anthocyanin compared to Col-0 WT in Rc illumination ($p=0.0383$) indicating that phyB has a role in the induction of anthocyanin accumulation in Rc as previously reported (Kunkel et al., 1996) . The response of CAB3::pBVR2 compared to No-0 WT is different from that observed for the *phyB* null mutant (in comparison to Col-0 WT) and hence suggests that phyA and/or light-stable phytochrome isoforms other than phyB have a role in inducing anthocyanin accumulation under Rc illumination.

Anthocyanins are actively sequestered into cell vacuoles for ergastic storage and in most species, they accumulate predominantly in leaf mesophyll (Gould et al., 2000) and epidermal cells (Kubo et al., 1999). Analysis of light- and/or sucrose-inducible anthocyanin accumulation in CAB3::pBVR lines suggests that mesophyll-localized phytochromes are responsible for the induction of anthocyanins in mesophyll tissues in Arabidopsis, and may impact inter-tissue anthocyanin accumulation in the epidermis under Rc.

3.3.2 Phytochrome Family Members Have Differential Roles in Anthocyanin Accumulation in Rc

According to previously published results, phyB is primarily responsive to R wavelengths (Reed et al., 1993). phyA was also recognized to play a significant regulatory role with respect to anthocyanin accumulation in R based on the observation that a *phyA* mutant had a notable reduction in anthocyanin levels compared to WT in contrast to a slight reduction in *phyB* mutant (Kunkel et al., 1996). However, phyB1 of tomato is responsible for a significant proportion of anthocyanin biosynthesis in R

(Kerckhoffs et al., 1997). These observations suggest that phytochrome family members may have differential roles in mediating the anthocyanin accumulation response. To determine which phytochrome isoform(s) may be involved in the regulation of anthocyanin levels in Rc, that anthocyanin levels were quantified in 4-d-old Rc-grown seedlings of apophytochrome mutants. Single apophytochrome mutants obtained from the Salk T-DNA insertion mutant collection were assessed for the absence of respective transcript accumulation by RT-PCR analysis. In the selected T-DNA insertion mutants, the T-DNA was inserted in the exon region of each apophytochrome gene (Figure 3.2). No respective transcript was detected by RT-PCR in apophytochrome mutants and this confirmed that T-DNA insertion mutants were null (Figure 3.3). Levels of anthocyanin accumulation were quantified in the confirmed null mutants under Rc illumination following a 4-d growth period and this analysis revealed that the *phyA, phyB, phyC* and *phyD* mutants displayed lower accumulation of anthocyanins than Col-0 WT (Figure 3.4 C). As previously published, the total levels of anthocyanins are lower for Col-0 WT in Rc than Wc (Neff and Chory, 1998; Warnasooriya and Montgomery, 2009). In the presence of sucrose, anthocyanin levels in the *phyA*, *phyB*, *phyC* and *phyD* mutants were ~ 76 %, 52 % 66 % and 86 % respectively, relative to Col-0 WT, indicating that the levels measured in these mutants were further reduced under Rc. The reduction in the anthocyanin levels for the *phyB* and *phyC* mutants in comparison to Col-0 WT were significant ($p=0.0004$ and $p=0.0079$, respectively). Although the levels in the *phyA* and *phyD* mutant were lower with respect to Col-0 WT, levels for the *phyA* mutant were not quite significantly different ($p=0.0559$) and the *phyD* mutant was not significantly different ($p=0.3238$). However, compared to Col-0 WT, the *phyE* mutant accumulated

significantly more anthocyanins (p=0.0022, Figure 3.4 C). In the *phyE* mutant, levels were ~ 67 % higher than Col-0 WT in the presence of sucrose and anthocyanins were clearly visible at the junction of hypocotyls and cotyledons (Figure 3.4 A). Elevated levels of anthocyanin accumulation is a characteristic of a hyperphotomorphogenic phenotype as previously observed in a transgenic line overexpressing a mutant form of HY5 (HY5-ΔN77) in Wc, Bc, Rc and FRc (Ang et al., 1998). The analysis of anthocyanin accumulation levels in apophytochrome mutants indicated that phyA, phyB, phyC, and phyD contribute to the light-dependent, sucrose-stimulated accumulation of anthocyanins, whereas phyE has a role in repressing anthocyanin synthesis and/or accumulation under Rc. The lowest levels of anthocyanin accumulation in the *phyB* mutant suggest that, in Rc, phyB is having a major quantitative role in the induction of anthocyanins. Under Rc, in the absence of sucrose, anthocyanin levels for the *phyC* and *phyD* mutants were less compared to Col-0 WT and were not quite significant (p=0.4468, p=0.2336, respectively, Figure 3.4 C). However, the reduction observed in the *phyB* mutant was extremely significant (p<0.0001) compared to WT and confirms that phyB indeed has a major role in sucrose-stimulated anthocyanin accumulation in Rc. Notably, the *phyA* and *phyE* mutants accumulate more anthocyanins (~ 29 %, ~79 %, respectively) in the absence of sucrose compared to WT. This increase in anthocyanin levels was quite significant in the *phyA* mutant (p=0.0086) and extremely significant in the *phyE* mutant (p<0.0001) with respect to Col-0 WT.

Anthocyanin levels were compared in apophytochrome mutants with respect to 1 % sucrose vs. 0 % sucrose to determine if a specific member of the phytochrome family could have a role in sucrose-induction of anthocyanin accumulation. Col-0 WT and all

apophytochrome mutants accumulated lower levels of anthocyanins in the absence of sucrose. The fold increase with respect to 1 % sucrose vs. 0 % sucrose was 2.0 for Col-0 WT and 1.8 for the *phyB, phyD* and *phyE* mutants (Figure 3.4C). Anthocyanins were visible only in the *phyE* mutant regardless of the presence or absence of sucrose (Figure 3.4 A and B). The anthocyanin levels with respect to 1 % sucrose vs. 0 % sucrose was quite significant in the Col-0 WT and *phyE* mutant ($p=0.0004$, $p=0.0002$, respectively) and was extremely significant in both the *phyB* and *phyD* mutants ($p<0.0001$). The fold increase for the *phyA* and *phyC* mutants was 1.2 and 1.4, respectively (Figure 3.4 C) and the difference in anthocyanin levels with respect to 1 % sucrose vs. 0 % sucrose was significant for the *phyC* mutant ($p=0.0111$), but not significant for the *phyA* mutant ($p=0.2474$). In the *phyA* mutant, the accumulation of similar levels of anthocyanins regardless of the presence or absence of sucrose in the medium may imply a lack of sucrose stimulation and thus suggest a possible requirement of phyA for sucrose-induction of anthocyanin accumulation in Rc. An apparent difference in the fold increase of anthocyanins was not observed in the *phyE* mutant compared to Col-0 WT with respect to 1 % sucrose vs. 0 % sucrose. This observation may indicate that suppression of phyE on anthocyanin accumulation is independent of the presence of sucrose in the medium.

To confirm that a lack of phyE is responsible for the altered anthocyanin levels observed in the *phyE* mutant line and thus phyE is a true suppressor of anthocyanin accumulation in Arabidopsis, the phyE mutant was complemented with a C-terminal myc-tagged *PHYE* construct, i.e., Pro_{PHYE}:*PHYE-m6*. Based on kanamycin resistance, T3 seedlings that were homozygous for a single transgene insertion were selected to

obtain seeds for further analyses. In T3 seedlings for two independent complemented transgenic lines, i.e., *PHYE-m6/phyE-1* and *PHYE-m6/phyE-11*, a reduction of anthocyanin levels in seedlings grown under Rc was observed (Figure 3.5). The degree of complementation correlated well with levels of myc-tagged phyE protein accumulating in the complemented transgenic lines (Figure 3.6). The observation of reduction in anthocyanin levels was noticeably true for complemented transgenic lines grown under Rc in the presence of sucrose. Complemented line *PHYE-m6/phyE-11*, which had a greater accumulation of myc-tagged phyE protein than line *PHYE-m6/phyE-1*, exhibited a greater reduction of anthocyanin accumulation in the presence of sucrose, i.e. ~72.5 % of that of the *phyE* parent, than did *PHYE-m6/phyE-1*, which exhibited ~82.5 % of the level of anthocyanins measured for *phyE* (Figure 3.5). The reductions observed for sucrose-dependent anthocyanin accumulation for the complemented *PHYE-m6/phyE-1* and *PHYE-m6/phyE-11* lines relative to the *phyE* mutant were significant, i.e., $p=0.0001$ and $p<0.0001$, respectively, as compared to the ~58 % level of anthocyanin accumulation observed for Col-0 WT relative to the *phyE* mutant ($p<0.0001$).

Based on analyses of transgenic plants with mesophyll-specific phytochrome deficiency and subsequent analysis of single *phy* mutants in all five of the apophytochrome genes, all phytochrome family members were shown to contribute to the light-dependent, sucrose-stimulated accumulation of anthocyanins, but with divergent regulatory roles. Notably, phyE is unique in its role of suppressing anthocyanin synthesis and/or accumulation under Rc, whereas other members of the phytochrome family stimulate anthocyanin accumulation under these conditions. These results are of particular interest as, to date, few repressors of anthocyanin biosynthesis have been

reported. A bHLH transcription factor, AtMYC2/JIN1 is a repressor of anthocyanin biosynthesis since the anthocyanin levels in the *atmyc2-3* mutant are higher in FR (Yadav et al., 2005; Zhu et al., 2009). Zhu et al., (2009) reported that a single-repeat R3 MYB transcription factor like CPC (CAPRICE) is a negative regulator of anthocyanin biosynthesis and confers suppression by competing with R2R3-MYB proteins- i.e., MYB75/PAP1 and MYB90/PAP2. Increased levels of anthocyanin accumulation has been observed in the loss of function of a mutant of *AtMYBL2* (*mybl2*) and the suppression of anthocyanin accumulation by AtMYBL2 occurs through negative regulation of the expression of structural and regulatory genes of anthocyanin biosynthesis in Arabidopsis seedlings (Dubos et al., 2008; Matsui, Umemura, and Ohme-Takagi, 2008).

3.3.3 Anthocyanin Marker Genes are Differentially Expressed in Rc

According to previously published data, *MYB75/PAP1* is essential (Borevitz et al., 2000) and an important QTL for sucrose-induced anthocyanin accumulation in Arabidopsis (Teng et al., 2005). *DFR* is specific for the anthocyanin branch of the flavonoid biosynthetic pathway (Kubasek et al., 1992) and an active DFR enzyme is essential for anthocyanin biosynthesis (Teng et al., 2005). Sucrose appears to be the most effective trigger in inducing anthocyanin accumulation for both *MYB75/PAP1* and *DFR* (Solfanelli et al., 2006; Teng et al., 2005) and *MYB75/PAP1* is required for sucrose-stimulated *DFR* expression (Teng et al., 2005). Thus, *MYB75/PAP1* and *DFR* were ideal candidates to determine if the differential accumulation of anthocyanins observed in apophytochrome mutants correlates with steady-state accumulation of *MYB75/PAP1* and

DFR transcripts in the presence/absence of sucrose in 4-d-old Rc-grown apophytochrome mutants.

The analysis of steady-state levels of transcript accumulation for *MYB75/PAP1* in apophytochrome mutants indicated that Col-0 WT, *phyA*, *phyD* and *phyE* mutants accumulate similar levels of *MYB75/PAP1* transcript in the absence as well as, in the presence of 1 % sucrose (Figure 3.7 A, B and 3.8 A). The *phyC* mutant accumulates a higher level of transcript on 1 % sucrose compared to 0 % sucrose (Figure 3.7 A and B). Quantification or relative transcript accumulation for the *phyC* mutant on 0 % vs. 1 % also indicated that in the presence of sucrose, the level of relative transcript accumulation for *MYB75/PAP1* was higher. Notably, the level of relative transcript accumulation for *MYB75/PAP1* was higher in the *phyB* mutant compared to rest of the lines (Figure 3.7 A, B and Figure 3.8 A) and the sucrose-induced transcript accumulation was the highest for *phyB* mutant (Figure 3.7 A and B). The *phyB* mutant displayed significantly higher levels of transcript accumulation for *MYB75/PAP1* compared to Col-0 WT on 1 % sucrose ($p=0.0007$, Figure 3.7 A, B and Figure 3.8 A). In the *phyB* mutant, on 0 % vs. 1 % sucrose, the relative transcript accumulation level for *MYB75/PAP1* was significantly higher in the presence of sucrose ($p=0.0422$, Figure 3.7 A, B and Figure 3.8 A). This observation implies that the *phyB* mutant is responsive to sucrose in the medium. It was previously observed that *MYB75/PAP1* transcript accumulates rapidly within 6 h under R light with an intensity of 125 µmol m^{-2} s^{-1} indicating that *MYB75/PAP1* transcript is light induced (Cominelli et al., 2008). According to Teng et al., (2005), the expression of *MYB75/PAP1* is induced by a sucrose-induced signaling pathway and as a consequence, the anthocyanin biosynthetic pathway is activated. Despite the expression of

MYB75/PAP1 being a QTL for sucrose-induced anthocyanin accumulation in Arabidopsis as previously described (Teng et al., 2005), compared to Col-0 WT, the levels of anthocyanins and relative transcript accumulation for *MYB75/PAP1* in the *phyB* mutant were inversely correlated. Hence, the anthocyanin levels and *MYB75/PAP1* expression can not be correlated for the phyB mutant. This observation implies that sucrose-stimulated, light-dependent anthocyanin accumulation in Rc requires a functional phyB, whereas induction of *MYB75/PAP1* expression under Rc does not. In the *phyB* mutant, the remaining type II phytochromes are able to perceive R light and induce *MYB75/PAP1* expression. However, after sucrose and R light trigger the *MYB75/PAP1* expression, the positive regulatory role of *MYB75/PAP1* on the late anthocyanin biosynthetic genes leading to an induction of anthocyanin biosynthesis possibly require functional phyB under Rc. Although phyB through phyE are primarily responsive to R light (Aukerman et al., 1997; Monte et al., 2003; Reed et al., 1993) and phyB is the predominant type II phytochrome regulating R-HIR and LFR (Nagy and Schafer, 2002; Quail, 2002), functional phyC, phyD and phyE family members in the *phyB* mutant possibly perceive R light resulting in an induction of sucrose-stimulated *MYB75/PAP1* expression under Rc. phyA may not contribute in this regard as it is only known to be an irradiance-dependent light sensor at very high fluences of R light of > 160 μmol m^{-2} s^{-1} (Franklin, Allen, and Whitelam, 2007). The significantly higher levels of transcript accumulation for *MYB75/PAP1* compared to Col-0 WT on 0 % vs. 1 % sucrose could also reflect a possible feedback regulatory role of anthocyanin levels on *MYB75/PAP1* transcript accumulation where Arabidopsis seedlings are responding to low anthocyanin

levels by trying to up-regulate biosynthesis through induction of *MYB75/PAP1* transcript accumulation.

Analysis of transcript accumulation for *DFR* in single apophytochrome mutants indicated that *DFR* expression is higher in Col-0 WT and all of the single apophytochrome mutants in the presence of sucrose compared to barely detectable levels of *DFR* transcript accumulation in the respective lines on 0 % sucrose (Figure 3.7 C and D) and confirms that *DFR* expression is subjected to sucrose-dependent up-regulation as previously published (Solfanelli et al., 2006). The level of *DFR* transcript accumulation observed in the *phyA* mutant was more or less similar to the level observed for Col-0 WT on 1 % sucrose (Figure 3.8 B) and possibly coincides with the similar levels of anthocyanins in the *phyA* mutant compared to Col-0 WT ($p=0.0559$, Figure 3.4 C). Quantification based on densitometry indicated that compared to Col-0 WT, the *phyB* mutant displayed similar levels of *DFR* transcript accumulation in the presence of sucrose. Compared to Col-0 WT, even though, the *phyE* mutant accumulated significantly higher level of anthocyanins on 0 % and 1 % sucrose ($p<0.0001$ and $p=0.0022$ respectively, Figure 3.4 C), the level of *DFR* transcript accumulation was not reflective of this observation (Figure 3.7 C). On 0 % vs. 1 % sucrose, the *phyB* mutant showed significantly higher levels of *DFR* transcript accumulation ($p= 0.0491$, Figure 3.7 C, D and Figure 3.8 B). Despite the specificity of *DFR* gene for anthocyanin biosynthesis within the flavonoid biosynthetic pathway (Kubasek et al., 1992), the difference in the level of accumulated *DFR* transcript may not correlate with the amount of anthocyanin levels when multiple signaling pathways, i.e. phytochrome and sucrose, are involved in determining the overall level of anthocyanin accumulation.

3.3.4 Summary

The quantification of anthocyanin levels in transgenic *BVR*-expressing lines with mesophyll-specific phytochrome inactivation indicates that mesophyll-localized phytochromes regulate sucrose-stimulated accumulation of anthocyanins under Rc. The analysis of anthocyanin levels in single apophytochrome mutants suggests that all phytochrome isoforms contribute to the regulation of anthocyanin accumulation under R light. In this regard, disparate activities of different phytochrome family members on the accumulation of anthocyanins were identified, with phyE functioning as a suppressor and the remaining phytochromes acting as promoters of anthocyanin accumulation under Rc illumination. However, the suppression of phyE on anthocyanin accumulation response appears to be independent of sucrose. By contrast, in other studies, phyB and phyD were shown to negatively impact phyA-mediated seed germination in FR (Hennig et al., 2001; Hennig et al., 2002), however, phyE promotes phyA-mediated germination under FR (Hennig et al., 2002). Thus, fine-tuning of distinct aspects of photomorphogenesis by opposing activities of individual phytochrome isoforms is not limited to the observation of the impact of phytochrome family members on anthocyanin accumulation under Rc. Among the phytochrome isoforms, phyB has the greatest quantitative role in the induction of anthocyanins under Rc (Figure 3.4 C). Although phyA has previously been implicated in the R-dependent regulation of anthocyanin (Kunkel et al., 1996), the levels of anthocyanin accumulation in the *phyA* mutant in this study additionally suggest that phyA has a distinct role in regulating the responsiveness to sucrose under Rc in Arabidopsis seedlings (Figure 3.4 C). Notably, a prior report for a *phyD* mutant in the L*er* background reported lower levels of anthocyanin under white light (Aukerman *et al.*,

1997), although levels were on average lower in the *phyD* mutant under Rc, a significant reduction in anthocyanin levels relative to the Col-0 WT parent in the absence of phyD was not apparent (Figure 3.4 C). No prior reports have been evident for phyC and phyE in the regulation of anthocyanin, but results obtained through quantification of anthocyanin levels for both mutants and the complementation of the *phyE* mutant suggest that phyC and phyE proteins have significant, but divergent roles in regulating anthocyanin levels under Rc. phyC is involved in the induction of anthocyanins, whereas phyE exhibits a distinctive, novel role in the suppression of anthocyanin accumulation under Rc (Figure 3.4 C and Figure 3.5).

The analysis of transcript accumulation levels of anthocyanin marker genes, *MYB75/PAP1* and *DFR* showed sucrose induction in the *phyB* mutant and confirmed sucrose-dependent up-regulation of *DFR* expression as previously published. A correlation between the level of transcript accumulation for *MYB75/PAP1* or *DFR* and the amount of accumulated anthocyanins was not apparent for the apophytochrome mutants and in-depth analysis of genetic as well as biochemical interactions among phytochrome family members would provide more conclusive evidence for the molecular mechanism of regulating sucrose-stimulated anthocyanin biosynthesis and accumulation by phytochromes under Rc.

3.4 Future Perspectives

Probing the biological functions of phytochromes has yielded phenomenal progress through the use of mutants harboring mutations in the genes encoding phytochrome apoproteins, as well as chromophore biosynthetic enzymes. Comparative

phenotypic and photobiological analyses of apophytochrome mutants has aided in studying discrete photoregulatory functions of individual phytochromes and their roles in light-mediated plant growth and developmental processes (Aukerman et al., 1997; Franklin, Larner, and Whitelam, 2005; Franklin and Quail, 2010; Franklin and Whitelam, 2004; Neff, Fankhauser, and Chory, 2000). Chromophore biosynthetic mutants have been used to probe the global effects upon loss of photosensory roles of all phytochromes. For example, *hy1* and *hy2* mutants display multiple phytochrome-deficient phenotypes throughout the life cycle due to the lack of holophytochromes (Hudson, 2000; Terry, 1997). Given the discrete and overlapping functions among the phytochrome family members, the analysis of anthocyanin accumulation response in apophytochrome mutants could overlook the contributions of multiple members on the overall levels of anthocyanins. Additionally, phyA, phyB and phyD form homodimers and, phyB, phyD and phyE are known to exist in all possible heterodimeric combinations (Sharrock and Clack, 2004) whereas phyC and phyE do not homodimerize, but display obligate heterodimerization (Clack et al., 2009). The lack of one partner could cause an imbalance in the amounts of dimerization partners and affect the overall stability of the existing partners (Sharrock and Clack, 2004). Furthermore, a mutation in one of the apophytochrome genes may influence the functions of one or more of the other isoforms and the accumulation of some phytochrome isoforms in light is coordinately regulated, at least in part by the levels of other members of the phytochrome family (Hirschfeld et al., 1998). Thus, heterodimerization and functional inter-dependence of phytochrome family members further increases the complexity in the array of phytochrome functions and the analysis of combinatorial interactions of phytochrome isoforms is pivotal in defining the

steady-state levels, as well as the array of multiple and differentially competent phytochromes (Sharrock and Clack, 2004). Additive and synergistic interactions among the phytochrome family members can be determined through the comparative analysis of higher order mutants (Reed et al., 1993) and such studies have enabled the elucidation of overlapping functions among the five isoforms (Franklin and Quail, 2010). For example, gradually lower levels of anthocyanins accumulate in *phyB*, *phyD,* and *phyBphyD* mutants in Ws background, suggesting that phyB and phyD have an additive contribution and individual contributions of phyB and phyD isoforms are similar in anthocyanin accumulation response (Aukerman et al., 1997). However, in the L*er* ecotype, phyB is highly dominant over phyD in regulating levels of anthocyanin (Aukerman et al., 1997). Currently, information on additive and/or synergistic interactions among the phytochrome family members in regulating anthocyanin biosynthesis and/accumulation remains limited.

The analysis of anthocyanin accumulation in higher order mutants would reveal the additive roles and/or synergistic relationships of phytochrome isoforms in regulating sucrose-dependent anthocyanin accumulation under R. A limitation of comparative analysis of higher order mutants is the dissection of additive or synergistic roles conferred by homodimers and heterodimers. However, in the case of obligate heterodimerizing partners, i.e. phyC and phyE (Clack et al., 2009), based on comparative analysis of anthocyanin accumulation response in the *phyC*, *phyE* and *phyCphyE* mutants, additive or synergistic roles of phyC-phyE heterodimers can be elucidated. The relative expression levels for *MYB75/PAP1* and *DFR* quantified by real-time RT-PCR would indicate whether the varying levels of accumulated anthocyanins correlate with the

expression of anthocyanin marker genes at the molecular level upon loss of multiple phytochrome family members. Through a comprehensive analysis of the anthocyanin accumulation response in high order mutants, the molecular mechanism of phytochrome function can be elucidated.

A wealth of data indicates that phytochrome family members are expressed in a spatial- as well as temporal-specific manner and such localized pools of phytochrome can mediate discrete physiological functions (Bischoff et al., 1997; De Greef and Caubergs, 1972a; De Greef and Caubergs, 1972b; Goosey, Palecanda, and Sharrock, 1997; Montgomery, 2008; Parcy, 2005; Sharrock and Clack, 2002; Zeevaart, 2006). Varying fractions of homodimeric and heterodimeric forms could arise due to differential spatial- and/or temporal-specific expression patterns of *PHY* genes (Sharrock and Clack, 2004). Such physiological consequences could confound conclusions based on comparative phenotypic and photobiological analyses. Therefore, an enhancer trap-driven transactivation of *BVR* expression can be utilized to knock down the five types of phytochromes in a tissue- and/or organ-specific manner to gain insight into phytochrome-mediated inter-tissue signaling cascades underlying spatial-specific anthocyanin accumulation.

Numerous regulatory proteins are involved in the regulation of light-dependent sucrose-stimulated anthocyanin accumulation and are spatially and developmentally regulated. Tissue-specific anthocyanin accumulation is commonly seen in vegetative tissues/organs (Borevitz et al., 2000; Nesi et al., 2000). Anthocyanins accumulate in the vacuolar space of cells in photosynthetic tissues, i.e. palisade and spongy mesophyll (Gould and Quinn, 1998; Lee and Collins, 2001) and epidermal cells (Kubo et al., 1999).

Enhancer trap lines with *GFP* expression patterns that correlate with spatial-specific expression patterns of anthocyanin accumulation (i.e. J1071- vascular/dermal expression throughout the seedling, J1491- dermal expression in shoots and roots, J2093- root cap, epidermis, hypocotyl, apex and stomates, J2662- epidermis in hypocotyl, some expression is seen in cotyledons, (Haseloff, 1999), http://www.plantsci.cam.ac.uk/Haseloff/geneControl/catalogues) can be crossed with UAS-BVR lines to transactivate *BVR* and induce localized phytochrome inactivation at sites that are indicated by *GFP* expression. If cell autonomous signaling is perturbed, localized phytochrome inactivation may lead to a reduction of anthocyanin accumulation at the same site. Previous studies indicate that localized pools of phytochrome can regulate physiological responses at sites away from the site of photoperception (Bischoff et al., 1997; De Greef and Caubergs, 1972a; De Greef and Caubergs, 1972b; Goosey, Palecanda, and Sharrock, 1997; Montgomery, 2008; Parcy, 2005; Zeevaart, 2006). If inter-tissue signaling is involved in phytochrome-mediated anthocyanin accumulation, a reduction in the levels of accumulated anthocyanins may be seen at distant sites away from the site of phytochrome inactivation indicated by *GFP* expression. Changes in the patterns of anthocyanin accumulation in the F3 progeny resulting from the cross between selected enhancer trap parents and UAS-BVR parent can be analyzed through bright field microscopy using cross-sections of fresh tissues. Thus, R/FR photoperception can be correlated with localized pools of phytochrome and anthocyanin accumulation response. Furthermore, molecular bases of cell autonomous and cell non-autonomous phytochrome-mediated signaling of spatial-specific anthocyanin accumulation can be elucidated.

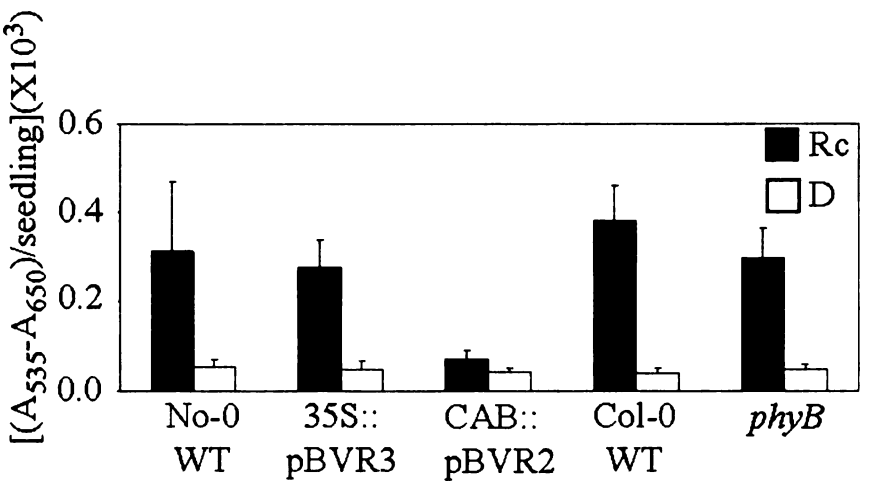

Figure 3.1 Anthocyanin content of wild-type and transgenic BVR seedlings. No-0 wild-type (No-0 WT), 35S::pBVR3, CAB3::pBVR2, Columbia-0 wild-type (Col-0 WT), and *phyB* (SALK_022035) were grown at 20 °C on Phytablend medium containing 1 % Suc for 4d under Rc illumination of 50 μmol m^{-2} s^{-1} or darkness. Black bars (Rc) and white bars (dark) represent the mean (+SD) of three independent measurements.

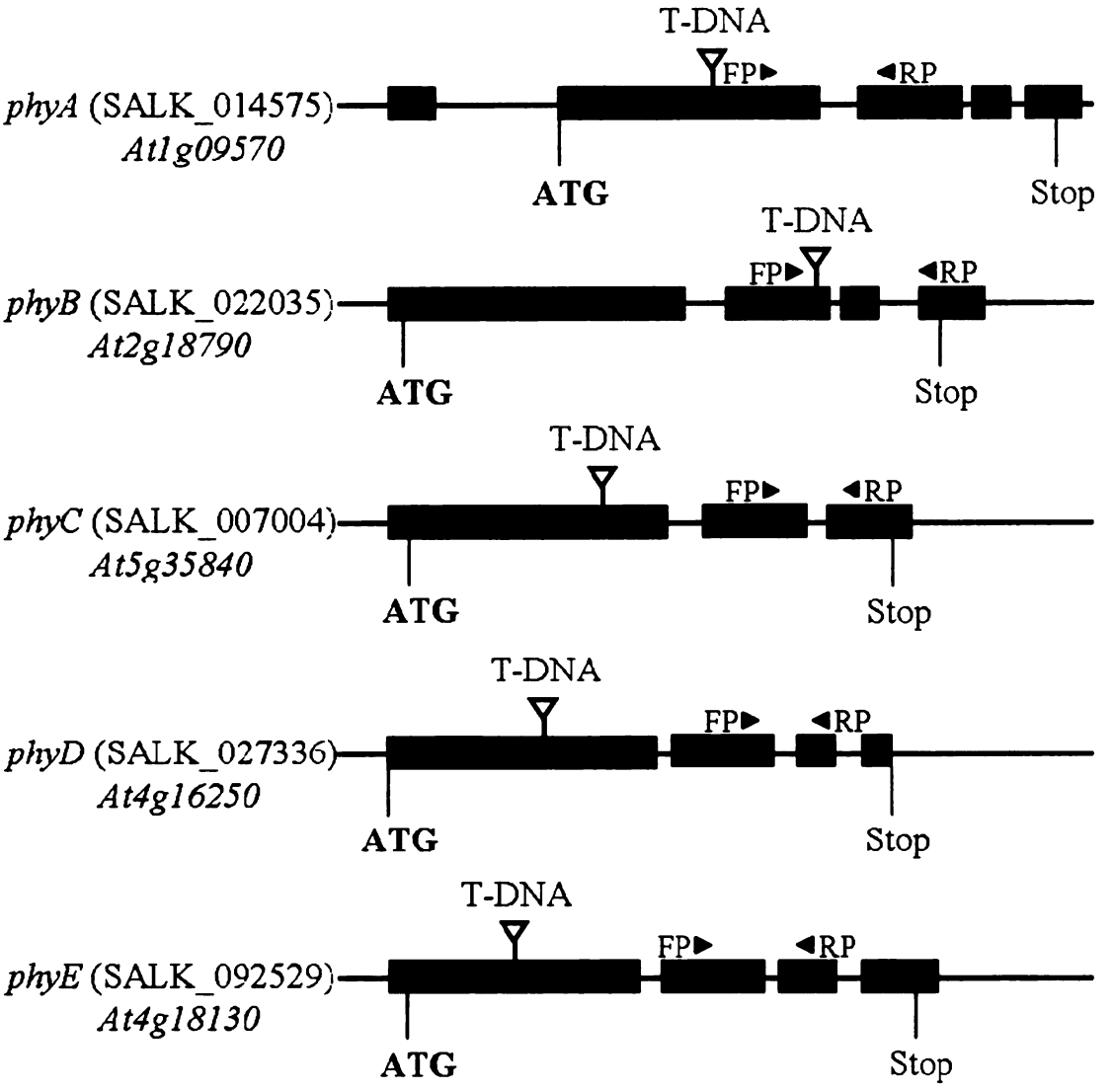

Figure 3.2 Sites of T-DNA insertions in apophytochrome mutants and locations of gene-specific oligonucleotide annealing.
Sites of T-DNA insertions in *phyA* (SALK_014575), *phyB* (SALK_022035), *phyC* (SALK_007004), *phyD* (SALK_027336) and *phyE* (SALK_092529) mutants are shown. Arrow heads indicate locations of gene-specific oligonucleotide annealing used in RT-PCR analysis. FP, forward primer and RP, reverse primer.

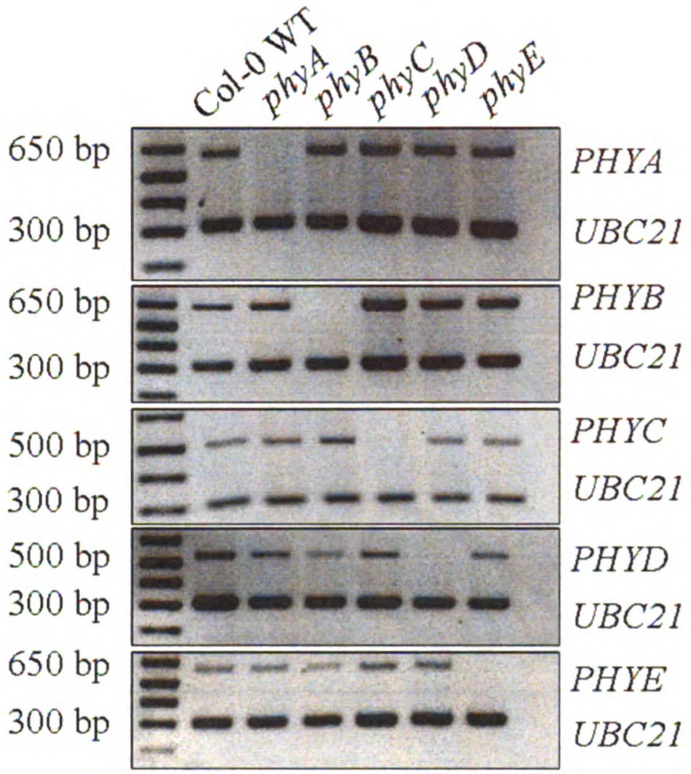

Figure 3.3 Analysis of T-DNA alleles in apophytochrome mutants.
The effects of T-DNA insertions on the expression of *PHYA*, *PHYB*, *PHYC*, *PHYD*, and *PHYE*. RT-PCR to analyze transcript accumulation was performed using primers that span or are downstream of the T-DNA insertion site in the respective genes. RNA was extracted from Columbia-0 (Col-0) wild-type, *phyA* (SALK_014575), *phyB* (SALK_022035), *phyC* (SALK_007004), *phyD* (SALK_ 027336) and *phyE* (SALK_092529) grown at 22 ºC on Phytablend medium containing 1% Suc for 4d under Rc illumination of 50 µmol m^{-2} s^{-1}. The expression of *UBC21 (At5g25760)* transcript was analyzed as an internal control.

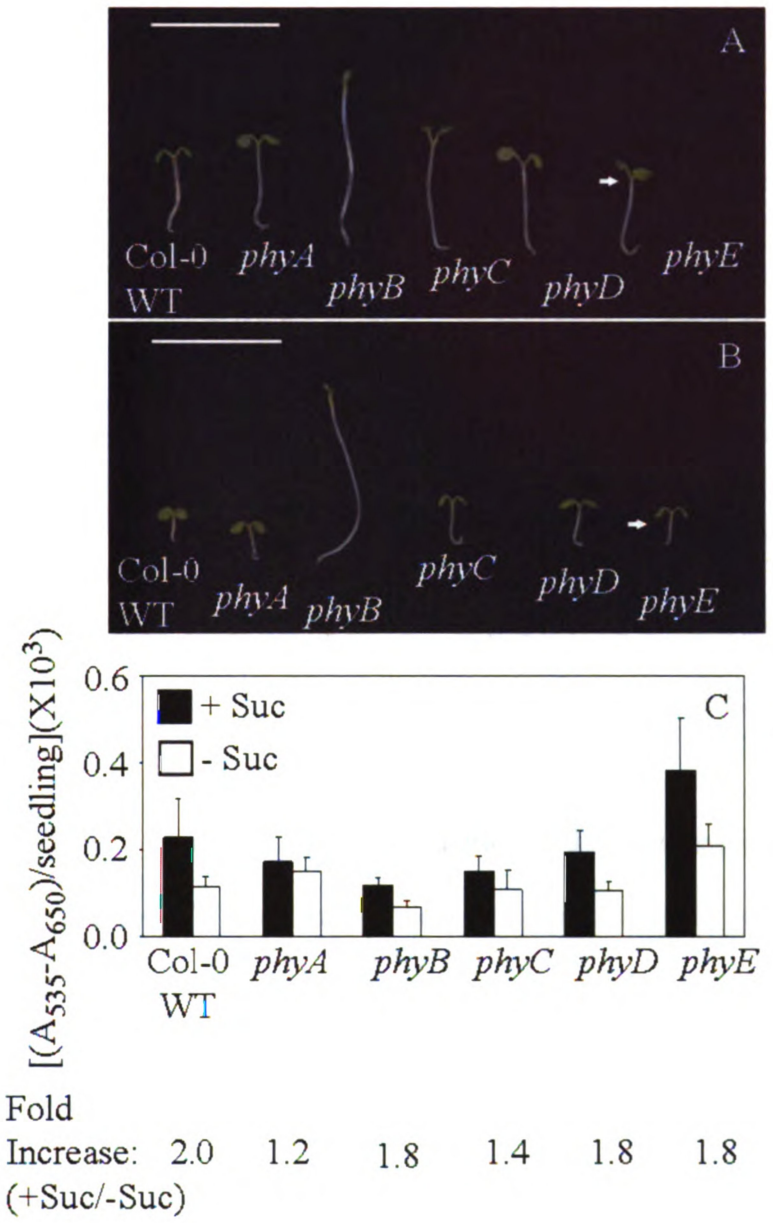

Figure 3.4 Development and sucrose-dependent anthocyanin accumulation of wild-type and apophytochrome mutants.
Columbia-0 wild-type(Col-0 WT), *phyA* (SALK_014575), *phyB* (SALK_022035), *phyC* (SALK_007004), *phyD* (SALK_ 027336) and *phyE* (SALK_092529) were grown at 22 °C on Phytablend medium with or without 1% sucrose for 4d under Rc illumination of 50 µmol m^{-2} s^{-1}. (A) Image of seedlings grown on 1% sucrose. Arrow indicates visible anthocyanin. Scale bar represents 1 cm. (B) Image of seedlings grown in the absence of sucrose. Arrow indicates visible anthocyanin. Scale bar represents 1 cm. (C) Anthocyanin content. Bars, black bars (1% sucrose) and white bars (no sucrose), represent the mean (+SD) of four independent measurements. Fold-increase values for anthocyanin levels determined for seedlings grown on 1% sucrose relative to 0% sucrose are indicated.

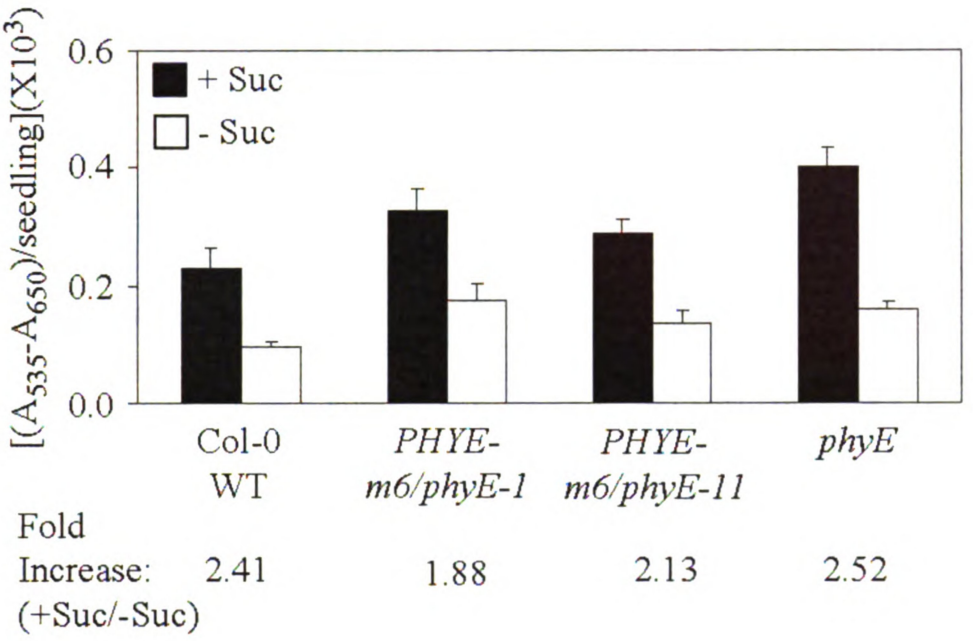

Figure 3.5 Sucrose-dependent anthocyanin accumulation in the complemented *phyE* mutants.
Columbia-0 wild-type(Col-0 WT), two independent complemented *phyE* mutants (*PHYE-m6/phyE-1* and *PHYE-m6/phyE-11)* and *phyE* (SALK_092529) were grown at 22 °C on Phytablend medium with or without 1% sucrose for 4d under Rc illumination of 50 µmol m^{-2} s^{-1}. Bars, black bars (1% sucrose) and white bars (no sucrose), represent the mean (+SD) of three independent measurements. Fold- increase values for anthocyanin levels determined for seedlings grown on 1% sucrose relative to 0% sucrose are indicated.

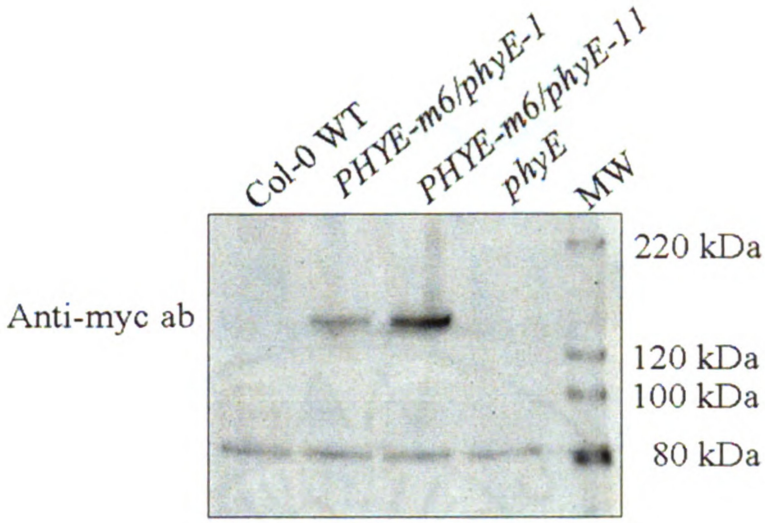

Figure 3.6 Phytochrome protein accumulation in wild-type and the complemented *phyE* mutants.
The *phyE* null mutant was complemented with a transgene containing myc epitope-tagged phyE driven by the *PHYE* native promoter. For immunoblot analysis of expression of *PHYE* in two independent complemented *phyE* mutants (*PHYE-m6/phyE-1* and *PHYE-m6/phyE-11*), transgenic lines were grown at 22 ºC on Phytablend medium with 1 % sucrose for 10d under Rc illumination of 50 µmol m^{-2} s^{-1}. Soluble protein extracts (~ 60 µg) were used for immunoblot analysis with anti-myc antibody. MW, molecular weight marker.

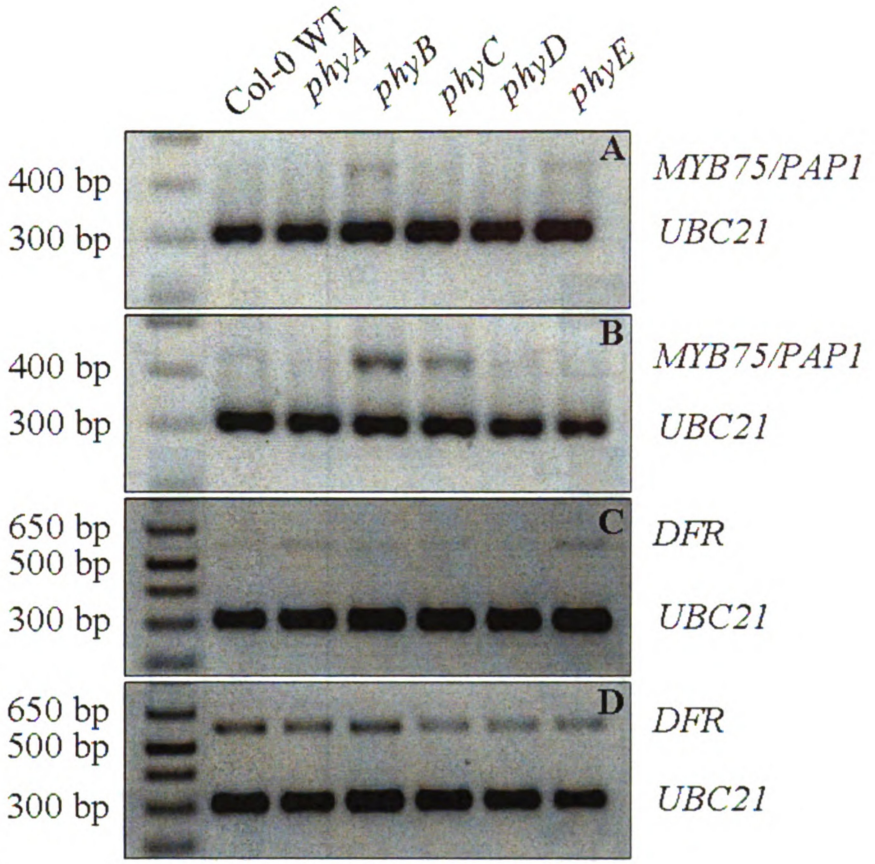

Figure 3.7 Expression of anthocyanin marker genes.
Expression of *MYB75/PAP1 (At1g56650)* and *DFR (At5g42800)* in Columbia-0 (Col-0) wild-type, *phyA* (SALK_014575), *phyB* (SALK_022035), *phyC* (SALK_007004), *phyD* (SALK_ 027336) and *phyE* (SALK_092529) on 0 (A, C) or 1% Suc (B, D). RNA was extracted from 4-d-old seedlings grown at 22 ºC on Phytablend medium containing 0 or 1 % Suc under Rc illumination of 50 µmol m^{-2} s^{-1}. The expression of *UBC21 (At5g25760)* transcript was analyzed as an internal control. A representative biological replicate is shown.

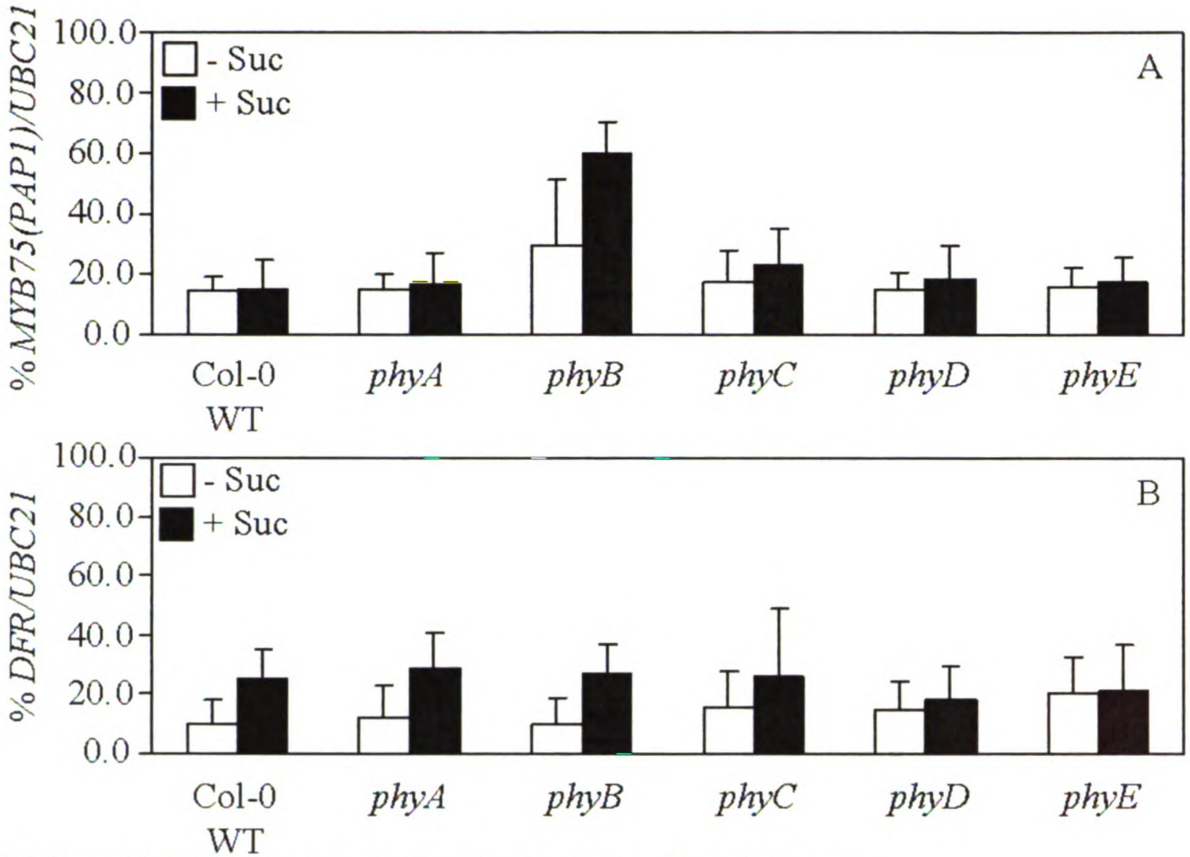

Figure 3.8 Quantification of expression levels of anthocyanin marker genes.
(A) Expression of *MYB75/PAP1 (At1g56650)* and (B) *DFR (At5g42800)* in Columbia-0 wild-type (Col-0 WT), *phyA* (SALK_014575), *phyB* (SALK_022035), *phyC* (SALK_007004), *phyD* (SALK_ 027336) and *phyE* (SALK_092529) on 0 % (white bars) or 1 % Suc (black bars) as a percentage of *UBC21 (At5g25760)* expression. Bars indicate mean expression level (± SD) of 4 biological replicates. RNA was extracted from 4-d-old seedlings grown at 22 ºC on Phytablend medium containing 0 or 1 % Suc under Rc illumination of 50 µmol m^{-2} s^{-1}. Expression levels were quantified based on densitometry using Quantity One®, Version 4. 6. 3, Bio-Rad Laboratories, Inc., CA).

3.5 References

Agati, G., and Tattini, M. (2010). Multiple functional roles of flavonoids in photoprotection. *New Phytol* **186**(4), 786-793.

Ahmad, M., Lin, C., and Cashmore, A. R. (1995). Mutations throughout an Arabidopsis blue-light photoreceptor impair blue-light-responsive anthocyanin accumulation and inhibition of hypocotyl elongation. *Plant J* **8**(5), 653-658.

Alonso, J. M., Stepanova, A. N., Leisse, T. J., Kim, C. J., Chen, H., Shinn, P., Stevenson, D. K., Zimmerman, J., Barajas, P., Cheuk, R., Gadrinab, C., Heller, C., Jeske, A., Koesema, E., Meyers, C. C., Parker, H., Prednis, L., Ansari, Y., Choy, N., Deen, H., Geralt, M., Hazari, N., Hom, E., Karnes, M., Mulholland, C., Ndubaku, R., Schmidt, I., Guzman, P., Aguilar-Henonin, L., Schmid, M., Weigel, D., Carter, D. E., Marchand, T., Risseeuw, E., Brogden, D., Zeko, A., Crosby, W. L., Berry, C. C., and Ecker, J. R. (2003). Genome-wide insertional mutagenesis of *Arabidopsis thaliana*. *Science* **301**(5633), 653-657.

Ang, L. H., Chattopadhyay, S., Wei, N., Oyama, T., Okada, K., Batschauer, A., and Deng, X. W. (1998). Molecular interaction between COP1 and HY5 defines a regulatory switch for light control of Arabidopsis development. *Mol Cell* **1**(2), 213-222.

Ang, L. H., and Deng, X. W. (1994). Regulatory hierarchy of photomorphogenic loci: allele-specific and light-dependent interaction between the HY5 and COP1 loci. *Plant Cell* **6**(5), 613-628.

Aoki, T., Akashi, T., and Ayabe, S.-i. (2000). Flavonoids of Leguminous Plants: Structure, Biological Activity, and Biosynthesis. *Journal of Plant Research* **113**(4), 475-488.

Aukerman, M. J., Hirschfeld, M., Wester, L., Weaver, M., Clack, T., Amasino, R. M., and Sharrock, R. A. (1997). A deletion in the PHYD gene of the Arabidopsis Wassilewskija ecotype defines a role for phytochrome D in red/far-red light sensing. *Plant Cell* **9**(8), 1317-1326.

Bischoff, F., Millar, A. J., Kay, S. A., and Furuya, M. (1997). Phytochrome-induced intercellular signalling activates cab::luciferase gene expression. *The Plant Journal* **12**(4), 839-849.

Borevitz, J. O., Xia, Y., Blount, J., Dixon, R. A., and Lamb, C. (2000). Activation tagging identifies a conserved MYB regulator of phenylpropanoid biosynthesis. *Plant Cell* **12**(12), 2383-2394.

Chun, L., Kawakami, A., and Christopher, D. A. (2001). Phytochrome A mediates blue light and UV-A-dependent chloroplast gene transcription in green leaves. *Plant Physiol* **125**(4), 1957-1966.

Clack, T., Shokry, A., Moffet, M., Liu, P., Faul, M., and Sharrock, R. A. (2009). Obligate heterodimerization of Arabidopsis phytochromes C and E and interaction with the PIF3 basic helix-loop-helix transcription factor. *Plant Cell* **21**(3), 786-799.

Clough, S. J., and Bent, A. F. (1998). Floral dip: a simplified method for Agrobacterium-mediated transformation of *Arabidopsis thaliana*. *Plant J* **16**(6), 735-743.

Cominelli, E., Gusmaroli, G., Allegra, D., Galbiati, M., Wade, H. K., Jenkins, G. I., and Tonelli, C. (2008). Expression analysis of anthocyanin regulatory genes in response to different light qualities in *Arabidopsis thaliana*. *J Plant Physiol* **165**(8), 886-894.

Cone, K. C., Cocciolone, S. M., Moehlenkamp, C. A., Weber, T., Drummond, B. J., Tagliani, L. A., Bowen, B. A., and Perrot, G. H. (1993). Role of the regulatory gene pl in the photocontrol of maize anthocyanin pigmentation. *Plant Cell* **5**(12), 1807-1816.

De Greef, J. A., and Caubergs, R. (1972a). Interorgan correlations and phytochrome: hypocotyl hook opening. *Arch. Int. Physiol. Biochim.* **80**(5), 959-960.

De Greef, J. A., and Caubergs, R. (1972b). Interorgan correlations and phytochrome: leaf expansion. *Arch. Int. Physiol. Biochim.* **80**(5), 961-962.

Drumm-Herrel, H., and Mohr, H. (1985). Photosensitivity of seedlings differing in their potential to synthesize anthocyanin. *Physiologia Plantarum* **64**(1), 60-66.

Dubos, C., Le Gourrierec, J., Baudry, A., Huep, G., Lanet, E., Debeaujon, I., Routaboul, J. M., Alboresi, A., Weisshaar, B., and Lepiniec, L. (2008). MYBL2 is a new regulator of flavonoid biosynthesis in *Arabidopsis thaliana*. *Plant J* **55**(6), 940-53.

Duek, P. D., and Fankhauser, C. (2003). HFR1, a putative bHLH transcription factor, mediates both phytochrome A and cryptochrome signalling. *Plant J* **34**(6), 827-836.

Endo, M., Mochizuki, N., Suzuki, T., and Nagatani, A. (2007). CRYPTOCHROME2 in vascular bundles regulates flowering in Arabidopsis. *Plant Cell* **19**(1), 84-93.

Endo, M., and Nagatani, A. (2008). Flowering regulation by tissue specific functions of photoreceptors. *Plant Signal Behav* **3**(1), 47-48.

Endo, M., Nakamura, S., Araki, T., Mochizuki, N., and Nagatani, A. (2005). Phytochrome B in the mesophyll delays flowering by suppressing FLOWERING LOCUS T expression in Arabidopsis vascular bundles. *Plant Cell* **17**(7), 1941-1952.

Fankhauser, C., and Staiger, D. (2002). Photoreceptors in *Arabidopsis thaliana*: light perception, signal transduction and entrainment of the endogenous clock. *Planta* **216**(1), 1-16.

Feinbaum, R. L., and Ausubel, F. M. (1988). Transcriptional regulation of the *Arabidopsis thaliana* chalcone synthase gene. *Mol Cell Biol* **8**(5), 1985-92.

Franklin, K. A., Allen, T., and Whitelam, G. C. (2007). Phytochrome A is an irradiance-dependent red light sensor. *Plant J* **50**(1), 108-117.

Franklin, K. A., Davis, S. J., Stoddart, W. M., Vierstra, R. D., and Whitelam, G. C. (2003). Mutant analyses define multiple roles for phytochrome C in Arabidopsis photomorphogenesis. *Plant Cell* **15**(9), 1981-1989.

Franklin, K. A., Larner, V. S., and Whitelam, G. C. (2005). The signal transducing photoreceptors of plants. *Int J Dev Biol* **49**(5-6), 653-664.

Franklin, K. A., and Quail, P. H. (2010). Phytochrome functions in Arabidopsis development. *J Exp Bot* **61**(1), 11-24.

Franklin, K. A., and Whitelam, G. C. (2004). Light signals, phytochromes and cross-talk with other environmental cues. *J Exp Bot* **55**(395), 271-276.

Gollop, R., Even, S., Colova-Tsolova, V., and Perl, A. (2002). Expression of the grape dihydroflavonol reductase gene and analysis of its promoter region. *J Exp Bot* **53**(373), 1397-1409.

Gonzalez, A., Zhao, M., Leavitt, J. M., and Lloyd, A. M. (2008). Regulation of the anthocyanin biosynthetic pathway by the TTG1/bHLH/Myb transcriptional complex in Arabidopsis seedlings. *Plant J* **53**(5), 814-827.

Goosey, L., Palecanda, L., and Sharrock, R. A. (1997). Differential patterns of expression of the Arabidopsis PHYB, PHYD, and PHYE phytochrome genes. *Plant Physiol* **115**(3), 959-969.

Gould, K. S., Markham, K. R., Smith, R. H., and Goris, J. J. (2000). Functional role of anthocyanins in the leaves of Quintinia serrata A. Cunn. *J Exp Bot* **51**(347), 1107-1115.

Gould, K. S., and Quinn, B. D. (1998). Do anthocyanins protect leaves of New Zealand native species from UV-B? *N. Z. J. Bot.* **37**, 175–178.

Han, S., and Kim, D. (2006). AtRTPrimer: database for Arabidopsis genome-wide homogeneous and specific RT-PCR primer-pairs. *BMC Bioinformatics* **7,** 179.

Harrison, S. J., Mott, E. K., Parsley, K., Aspinall, S., Gray, J. C., and Cottage, A. (2006). A rapid and robust method of identifying transformed *Arabidopsis thaliana* seedlings following floral dip transformation. *Plant Methods* **2,** 19.

Haseloff, J. (1999). GFP variants for multispectral imaging of living cells. *Methods Cell Biol* **58,** 139-151.

Hennig, L., Poppe, C., Sweere, U., Martin, A., and Schafer, E. (2001). Negative interference of endogenous phytochrome B with phytochrome A function in Arabidopsis. *Plant Physiol* **125**(2), 1036-1044.

Hennig, L., Stoddart, W. M., Dieterle, M., Whitelam, G. C., and Schafer, E. (2002). Phytochrome E controls light-induced germination of Arabidopsis. *Plant Physiol* **128**(1), 194-200.

Hirschfeld, M., Tepperman, J. M., Clack, T., Quail, P. H., and Sharrock, R. A. (1998). Coordination of phytochrome levels in phyB mutants of Arabidopsis as revealed by apoprotein-specific monoclonal antibodies. *Genetics* **149**(2), 523-535.

Hudson, M. E. (2000). The genetics of phytochrome signalling in Arabidopsis. *Semin Cell Dev Biol* **11**(6), 475-483.

Huub, L., Kerckhoffs, J., and Kendrick, R. (1997). Photocontrol of anthocyanin biosynthesis in tomato. *Journal of Plant Research* **110**(1), 141-149.

Kao, C. Y., Cocciolone, S. M., Vasil, I. K., and McCarty, D. R. (1996). Localization and interaction of the cis-acting elements for abscisic acid, VIVIPAROUS1, and light activation of the C1 gene of maize. *Plant Cell* **8**(7), 1171-1179.

Kerckhoffs, L. H. J., Kendrick, R. E., Whitelam, G. C., and Smith, H. (1992). Extension growth and anthocyanin responses of photomorphogenic tomato mutants to changes in the phytochrome: photoequilibrium during the daily photoperiod. *Photochemistry and Photobiology* **56**(5), 611-615.

Kerckhoffs, L. H. J., Schreuder, M. E. L., Tuinen, A. V., Koornneef, M., and Kendrick, R. E. (1997). Phytochrome Control of Anthocyanin Biosynthesis in Tomato Seedlings: Analysis Using Photomorphogenic Mutants. *Photochemistry and Photobiology* **65**(2), 374-381.

Kim, J., Yi, H., Choi, G., Shin, B., Song, P. S., and Choi, G. (2003). Functional characterization of phytochrome interacting factor 3 in phytochrome-mediated light signal transduction. *Plant Cell* **15**(10), 2399-2407.

Kubasek, W. L., Shirley, B. W., McKillop, A., Goodman, H. M., Briggs, W., and Ausubel, F. M. (1992). Regulation of Flavonoid Biosynthetic Genes in Germinating Arabidopsis Seedlings. *Plant Cell* **4**(10), 1229-1236.

Kubo, H., Peeters, A. J., Aarts, M. G., Pereira, A., and Koornneef, M. (1999). ANTHOCYANINLESS2, a homeobox gene affecting anthocyanin distribution and root development in Arabidopsis. *Plant Cell* **11**(7), 1217-1226.

Kunkel, T., Neuhaus, G., Batschauer, A., Chua, N.-H., and Schäfer, E. (1996). Functional analysis of yeast-derived phytochrome A and B phycocyanobilin adducts. *Plant J.* **10**(4), 625-636.

Lagarias, D. M., Crepeau, M. W., Maines, M. D., and Lagarias, J. C. (1997). Regulation of photomorphogenesis by expression of mammalian biliverdin reductase in transgenic Arabidopsis plants. *Plant Cell* **9**(5), 675-688.

Lea, U. S., Slimestad, R., Smedvig, P., and Lillo, C. (2007). Nitrogen deficiency enhances expression of specific MYB and bHLH transcription factors and accumulation of end products in the flavonoid pathway. *Planta* **225**(5), 1245-1253.

Lee, D. W., and Collins, T. M. (2001). Phylogenetic and ontogenetic influences on the distribution of anthocyanins and betacyanins in leaves of tropical plants. *Int. J. Plant Sci.* **162**(5), 1141-1153.

Lepiniec, L., Debeaujon, I., Routaboul, J. M., Baudry, A., Pourcel, L., Nesi, N., and Caboche, M. (2006). Genetics and biochemistry of seed flavonoids. *Annu Rev Plant Biol* **57**, 405-430.

Lillo, C., Lea, U. S., and Ruoff, P. (2008). Nutrient depletion as a key factor for manipulating gene expression and product formation in different branches of the flavonoid pathway. *Plant Cell Environ* **31**(5), 587-601.

Mancinelli, A. (1985). Light-dependent anthocyanin synthesis: A model system for the study of plant photomorphogenesis. *The Botanical Review* **51**(1), 107-157.

Martin, C., and Gerats, T. (1993). Control of Pigment Biosynthesis Genes during Petal Development. *Plant Cell* **5**(10), 1253-1264.

Martin, T., Oswald, O., and Graham, I. A. (2002). Arabidopsis seedling growth, storage lipid mobilization, and photosynthetic gene expression are regulated by carbon:nitrogen availability. *Plant Physiol* **128**(2), 472-481.

Matsui, K., Umemura, Y., and Ohme-Takagi, M. (2008). AtMYBL2, a protein with a single MYB domain, acts as a negative regulator of anthocyanin biosynthesis in Arabidopsis. *Plant J* **55**(6), 954-967.

Mehrtens, F., Kranz, H., Bednarek, P., and Weisshaar, B. (2005). The Arabidopsis transcription factor MYB12 is a flavonol-specific regulator of phenylpropanoid biosynthesis. *Plant Physiol* **138**(2), 1083-1096.

Mol, J., Jenkins, G., Schäfer, E., Weiss, D., and Walbot, V. (1996). Signal perception, transduction, and gene expression involved in anthocyanin biosynthesis. *Critical Reviews in Plant Sciences* **15**(5), 525-557.

Monte, E., Alonso, J. M., Ecker, J. R., Zhang, Y., Li, X., Young, J., Austin-Phillips, S., and Quail, P. H. (2003). Isolation and characterization of phyC mutants in Arabidopsis reveals complex crosstalk between phytochrome signaling pathways. *Plant Cell* **15**(9), 1962-1980.

Montgomery, B. L. (2008). Right place, right time: Spatiotemporal light regulation of plant growth and development. *Plant Signal Behav* **3**(12), 1053-1060.

Montgomery, B. L. (2009). Spatial-specific phytochrome responses during de-etiolation in *Arabidopsis thaliana*. *Plant Signal Behav* **4**(1), 47-49.

Montgomery, B. L., Franklin, K. A., Terry, M. J., Thomas, B., Jackson, S. D., Crepeau, M. W., and Lagarias, J. C. (2001). Biliverdin reductase-induced phytochrome chromophore deficiency in transgenic tobacco. *Plant Physiol* **125**(1), 266-277.

Montgomery, B. L., Yeh, K. C., Crepeau, M. W., and Lagarias, J. C. (1999). Modification of distinct aspects of photomorphogenesis via targeted expression of mammalian biliverdin reductase in transgenic Arabidopsis plants. *Plant Physiol* **121**(2), 629-639.

Nagata, T., Todoriki, S., Masumizu, T., Suda, I., Furuta, S., Du, Z., and Kikuchi, S. (2003). Levels of active oxygen species are controlled by ascorbic acid and anthocyanin in Arabidopsis. *J Agric Food Chem* **51**(10), 2992-2999.

Nagatani, A., Reed, J. W., and Chory, J. (1993). Isolation and Initial Characterization of Arabidopsis Mutants That Are Deficient in Phytochrome A. *Plant Physiol* **102**(1), 269-277.

Nagy, F., and Schafer, E. (2002). Phytochromes control photomorphogenesis by differentially regulated, interacting signaling pathways in higher plants. *Annu Rev Plant Biol* **53**, 329-355.

Neff, M. M., and Chory, J. (1998). Genetic interactions between phytochrome A, phytochrome B, and cryptochrome 1 during Arabidopsis development. *Plant Physiol* **118**(1), 27-35.

Neff, M. M., Fankhauser, C., and Chory, J. (2000). Light: an indicator of time and place. *Genes Dev* **14**(3), 257-721.

Nesi, N., Debeaujon, I., Jond, C., Pelletier, G., Caboche, M., and Lepiniec, L. (2000). The TT8 gene encodes a basic helix-loop-helix domain protein required for expression of DFR and BAN genes in Arabidopsis siliques. *Plant Cell* **12**(10), 1863-1878.

Neuhaus, G., Bowler, C., Kern, R., and Chua, N. H. (1993). Calcium/calmodulin-dependent and -independent phytochrome signal transduction pathways. *Cell* **73**(5), 937-952.

Parcy, F. (2005). Flowering: a time for integration. *Int J Dev Biol* **49**(5-6), 585-93.

Procissi, A., Dolfini, S., Ronchi, A., and Tonelli, C. (1997). Light-Dependent Spatial and Temporal Expression of Pigment Regulatory Genes in Developing Maize Seeds. *Plant Cell* **9**(9), 1547-1557.

Quail, P. H. (1994). Photosensory perception and signal transduction in plants. *Curr Opin Genet Dev* **4**(5), 652-661.

Quail, P. H. (2002). Phytochrome photosensory signalling networks. *Nat Rev Mol Cell Biol* **3**(2), 85-93.

Rabino, I., and Mancinelli, A. L. (1986). Light, Temperature, and Anthocyanin Production. *Plant Physiol* **81**(3), 922-924.

Reed, J. W., Nagpal, P., Poole, D. S., Furuya, M., and Chory, J. (1993). Mutations in the gene for the red/far-red light receptor phytochrome B alter cell elongation and physiological responses throughout Arabidopsis development. *Plant Cell* **5**(2), 147-157.

Rowan, D. D., Cao, M., Lin-Wang, K., Cooney, J. M., Jensen, D. J., Austin, P. T., Hunt, M. B., Norling, C., Hellens, R. P., Schaffer, R. J., and Allan, A. C. (2009). Environmental regulation of leaf colour in red 35S:PAP1 *Arabidopsis thaliana*. *New Phytol* **182**(1), 102-115.

Ruckle, M. E., DeMarco, S. M., and Larkin, R. M. (2007). Plastid signals remodel light signaling networks and are essential for efficient chloroplast biogenesis in Arabidopsis. *Plant Cell* **19**(12), 3944-3960.

Sharrock, R. A., and Clack, T. (2002). Patterns of expression and normalized levels of the five Arabidopsis phytochromes. *Plant Physiol* **130**(1), 442-456.

Sharrock, R. A., and Clack, T. (2004). Heterodimerization of type II phytochromes in Arabidopsis. *Proc Natl Acad Sci U S A* **101**(31), 11500-11505.

Shi, M. Z., and Xie, D. Y. (2010). Features of anthocyanin biosynthesis in pap1-D and wild-type *Arabidopsis thaliana* plants grown in different light intensity and culture media conditions. *Planta* **231**(6), 1385-1400.

Shin, J., Park, E., and Choi, G. (2007). PIF3 regulates anthocyanin biosynthesis in an HY5-dependent manner with both factors directly binding anthocyanin biosynthetic gene promoters in Arabidopsis. *Plant J* **49**(6), 981-994.

Solfanelli, C., Poggi, A., Loreti, E., Alpi, A., and Perata, P. (2006). Sucrose-specific induction of the anthocyanin biosynthetic pathway in Arabidopsis. *Plant Physiol* **140**(2), 637-646.

Somers, D. E., Sharrock, R. A., Tepperman, J. M., and Quail, P. H. (1991). The hy3 long hypocotyl mutant of Arabidopsis is deficient in phytochrome B. *Plant Cell* **3**(12), 1263-1274.

Stracke, R., Ishihara, H., Huep, G., Barsch, A., Mehrtens, F., Niehaus, K., and Weisshaar, B. (2007). Differential regulation of closely related R2R3-MYB transcription factors controls flavonol accumulation in different parts of the *Arabidopsis thaliana* seedling. *The Plant Journal* **50**(4), 660-677.

Taylor, L. P., and Briggs, W. R. (1990). Genetic regulation and photocontrol of anthocyanin accumulation in maize seedlings. *Plant Cell* **2**(2), 115-127.

Teng, S., Keurentjes, J., Bentsink, L., Koornneef, M., and Smeekens, S. (2005). Sucrose-specific induction of anthocyanin biosynthesis in Arabidopsis requires the MYB75/PAP1 gene. *Plant Physiol* **139**(4), 1840-1852.

Terry, M. J. (1997). Phytochrome chromophore-deficient mutants. *Plant, Cell & Environment* **20**(6), 740-745.

Terry, M. J., Wahleithner, J. A., and Lagarias, J. C. (1993). Biosynthesis of the Plant Photoreceptor Phytochrome. *Archives of Biochemistry and Biophysics* **306**(1), 1-15.

Tonelli, C., Dolfini, S., Ronchi, A., Consonni, G., and Gavazzi, G. (1994). Light inducibility and tissue specificity of the *R* gene family in maize. *Genetica* **94**(2), 225-234.

Warnasooriya, S. N., and Montgomery, B. L. (2009). Detection of spatial-specific phytochrome responses using targeted expression of biliverdin reductase in Arabidopsis. *Plant Physiol* **149**(1), 424-433.

Weigel, D., and Glazebrook, J. (2006). Transformation of Agrobacterium Using Electroporation. *Cold Spring Harb Protoc* **2006**(30), pdb.prot4665-.

Whitelam, G. C., Johnson, E., Peng, J., Carol, P., Anderson, M. L., Cowl, J. S., and Harberd, N. P. (1993). Phytochrome A null mutants of Arabidopsis display a wild-type phenotype in white light. *Plant Cell* **5**(7), 757-768.

Yadav, V., Mallappa, C., Gangappa, S. N., Bhatia, S., and Chattopadhyay, S. (2005). A basic helix-loop-helix transcription factor in Arabidopsis, MYC2, acts as a repressor of blue light-mediated photomorphogenic growth. *Plant Cell* **17**(7), 1953-1966.

Zeevaart, J. A. (2006). Florigen coming of age after 70 years. *Plant Cell* **18**(8), 1783-1789.

Zhu, H. F., Fitzsimmons, K., Khandelwal, A., and Kranz, R. G. (2009). CPC, a single-repeat R3 MYB, is a negative regulator of anthocyanin biosynthesis in Arabidopsis. *Mol Plant* **2**(4), 790-802.

Chapter 4 Regulation of Root Development by Phytochromes and Jasmonic Acid

4.1 Overview

Light is the primary energy source for photosynthesis and the most important environmental signal regulating plant growth and development throughout the plant life cycle (Chory et al., 1996; Franklin and Quail, 2010; Franklin and Whitelam, 2004; Neff, Fankhauser, and Chory, 2000; Schepens, Duek, and Fankhauser, 2004). The regulation of physiological responses depends upon complex intracellular, intercellular and inter-organ signaling cascades (Montgomery, 2008). Through inter-tissue and inter-organ signaling, opposing physiological responses in different plant tissues or organs can be regulated by the same light stimulus (Bou-Torrent, Roig-Villanova, and Martinez-Garcia, 2008). Although definitive information on molecular mechanisms of such inter-tissue and inter-organ communication is limited, tissue-specific gene expression analyses suggest that there are distinct subsets of light-mediated genes in discrete tissues in several plant species. In Arabidopsis, in cotyledons, hypocotyls, and roots, less than 1 % of light-regulated genes are common to all three types of tissues (Jiao et al., 2007). Despite the similarity in the mechanism of photoperception and initial signaling in cotyledons and roots in Arabidopsis (Cashmore et al., 1999; Quail, 2002), distinct subsets of light-regulated genes have been identified from cotyledons vs. roots (Jiao, Lau, and Deng, 2007; Ma et al., 2005). In rice, roots appear to have more light-regulated genes than shoots (Jiao, Lau, and Deng, 2007). Root-specific, light-regulated gene expression suggests that perception of light by root-localized photoreceptors has biological importance.

Light penetration has been observed in the upper layers of soil up to several millimeters in natural environments (Mandoli et al., 1990). Phytochromes, as well as

other photoreceptors, are localized in roots and render roots capable of sensing and responding to light (Kiss et al., 2003; Okada and Shimura, 1992; Somers and Quail, 1995). By 'light piping' through the vascular tissue, the light signals perceived above ground can be extended to roots in deeper layers of soil (Mandoli and Briggs, 1982; Mandoli and Briggs, 1984). In the light spectrum, FR light is conducted most efficiently through internal light piping (Sun, Yoda, and Suzuki, 2005; Sun et al., 2003). Thus, light that is perceived from aboveground portions of the plant can travel to the root to regulate root photomorphogenesis (Lauter, 1996). Root-localized phytochromes are able to perceive light directly and impact root growth and development in natural environments. Published data confirm that phytochromes are expressed in roots of Arabidopsis (Tóth et al., 2001) and are known have an important role in root development (Correll and Kiss, 2005; Salisbury et al., 2007). Localization of phytochromes and light-dependent growth responses in roots indicate that light perception by roots is an important component of photomorphogenesis in plants.

4.1.1 Role of Phytochromes in Root Growth and Development

The ability of light to penetrate into the upper soil layers allows germinating seeds and roots in natural environments to perceive light (Mandoli et al., 1990; Tester and Morris, 1987). Perception of light by germinating seeds is critical for detecting the location within the soil stratum. Phytochromes play a major role in ensuring that germination is induced at a specific time that a young seedling is able to reach the soil surface post-germination (Seo et al., 2009). Salisbury et al., (2007) reported that phyA,

phyD and phyE are highly expressed in primary and lateral root tips, whereas phyD is expressed throughout the elongation zone of the primary root.

Detection of light by root-localized phytochromes and transmission of light through internal light piping can impact root growth and development in plants and discrete functions of phytochromes have been identified within the root system of Arabidopsis. Root-localized phytochromes regulate gravitropism in Arabidopsis in response to R light (Correll et al., 2003; Correll and Kiss, 2005). In roots of maize seedlings, both phyA and phyB are involved in regulating light-induced gravitropism (Feldman and Briggs, 1987). In Arabidopsis, phyA and phyB play a key role in R light-induced positive phototropism in roots (Kiss et al., 2003). Phytochrome action in roots is not limited to the tropic responses. Root-localized phytochromes in Arabidopsis, regulate root elongation under R light (Correll et al., 2003; Correll and Kiss, 2005) and phyA and phyB have been shown to control R light-mediated elongation of the primary root (Correll and Kiss, 2005). Phytochromes also mediate the orientation of lateral roots (Kiss et al. 2002) and lateral root production is regulated by stimulatory effects of phyA, phyB and phyE, and inhibitory effect of phyD (Salisbury et al., 2007). The observation that initiation of lateral root growth is regulated by phytochromes in Arabidopsis plants grown on soil indicates that even in a more natural environment roots display phytochrome-dependent development (Salisbury et al., 2007).

Comparison of total amount of root hairs and root hair densities in light vs. dark-grown Arabidopsis seedlings by De Simone, Oka, and Inoue, (2000) indicated that light enhances root hair formation. Notably, under R light, phyA and phyB contribute to root hair development (De Simone, Oka, and Inoue, 2000; Reed et al., 1993) and the

observation that a *hy3* mutant (phytochrome B deficient or *phyB* mutant) exhibited longer root hairs than the wild type suggests that the perception of light by phyB could inhibit root hair elongation (Reed et al., 1993). In fact, expression profiling of Arabidopsis roots using microarrays after 1 hr of exposure to R light indicates that expression of some genes involved in photomorphogenesis and root development is regulated by R light (Molas, Kiss, and Correll, 2006). A role for phytochromes in root hair initiation in lettuce seedlings has been reported and a site within the root itself may be a potential site of light perception for this response (De Simone, Oka, and Inoue, 2000). Not only R light, but also continuous exposure to FR light promotes root growth. In a *phyA* mutant, the lack of stimulation of root growth only under FR light suggests that phyA stimulates root growth in FR light (Kurata and Yamamoto, 1997). However, the observation that white, R or FR light was unable to stimulate root growth in a *phyB* mutant, suggests that phyB is essential for the roots to respond to light (Kurata and Yamamoto, 1997). According to Reed et al., (1993), phyA is the only phytochrome mediating root hair formation under FRc.

In addition to the recognized roles for phytochromes in Arabidopsis, emerging data indicate that phytochromes regulate root development in rice. Shimizu et al., (2009) reported that seminal root growth inhibition in FR light was mediated exclusively by phyA, whereas in R light, both phyA and phyB were functional. Despite the detection of phyA, phyB and phyC in roots immunochemically, phyC appeared to have a minor or no role in growth inhibition of seminal roots in rice (Shimizu et al., 2009). In seminal roots, the photoperceptive site for phytochrome-dependent inhibition appeared to be phytochromes within the roots themselves (Shimizu, Shinomura, and Yamamoto, 2010;

Shimizu et al., 2009). Although reports on functions of phytochromes during regulation of root growth and development are available, biological importance of global loss of phytochromes on root development in Arabidopsis has just begun to be explored. Interactions between hormone and light signaling have been extensively studied in the plant kingdom (Alabadi and Blazquez, 2009; Jaillais and Chory, 2010; Seo et al., 2009). The plant hormone, jasmonic acid (JA), in addition to its recognized role in regulating defense responses, is a regulator of plant growth and development (Browse, 2005). JA inhibits root elongation (Staswick, Su, and Howell, 1992) and a number of reports indicate that phytochrome chromophore deficiency affects JA-mediated root inhibition (Muramoto et al., 1999; Zhai et al., 2007), but the current understanding of interaction of JA and phytochrome signaling in light-regulated root development is limited.

4.1.2 Biology of Jasmonic Acid

JA and related compounds, collectively called jasmonates, are involved in numerous processes related to plant growth, development and survival. Among the physiological processes regulated by jasmonates are defense responses against biotic stresses (i.e. herbivore attack and pathogen infection), reproduction, secondary metabolism and senescence (Avanci et al., 2010; Browse, 2005; Seo et al., 2001; Wasternack, 2007; Wasternack and Hause, 2002). The jasmonates-JA, methyl jasmonate, JA conjugated to leucine and isoleucine and octadecanoid precursors-are produced from α-linolenic acid present on chloroplast membranes (Avanci et al., 2010). Upon biotic or abiotic stress, phospholipases release α-linolenic acid from chloroplast membranes and α-linolenic acid serves as the precursor for JA biosynthesis via the octadecanoid pathway (Mueller et al., 1993) involving three sub-cellular compartments: chloroplasts,

peroxisomes and cytoplasm (Browse, 2009; Mueller et al., 1993; Seo et al., 2001). The enzyme encoded by *JAR1*, belonging to the acyl-adenylate enzyme class, catalyzes the conjugation of JA to the amino acid isoleucine (Ile) and generates jasmonoyl-L-isoleucine (JA-Ile; Guranowski et al., 2007; Staswick and Tiryaki, 2004; Staswick, Tiryaki, and Rowe, 2002; Suza and Staswick, 2008). The observations that *in vitro* synthesized JAR1 protein had the enzymatic activity to conjugate JA to Ile and that JA-Ile was able to inhibit root growth was confirmed by the *jar1* mutant and indicated that JA-Ile is the bioactive form of JA as a signaling molecule (Fonseca et al., 2009; Staswick and Tiryaki, 2004; Thines et al., 2007).

Inhibition of root growth by JA has been widely used to identify mutants impaired in JA-biosynthesis and signaling based on insensitivity to growth inhibition upon exogenous application of JA or JA analogs. A number of key signaling intermediates in the JA signal transduction pathway have been identified in Arabidopsis (Avanci et al., 2010; Browse, 2009; Wasternack, 2007; Wasternack and Hause, 2002). The *COI1* gene was identified in such a screen in the presence of a JA-Ile analog, coronatine (Feys et al., 1994) and the *coi1* mutant was impaired in all known JA responses indicating that the F-box protein COI is essential for JA signaling (Xie et al., 1998). The COI protein was later identified as a receptor for the bioactive form of JA (Fonseca et al., 2009; Thines et al., 2007). Several groups identified that COI1 binds to S-PHASE KINASE-ASSOCIATED PROTEIN1 and CULLIN to form the SCF^{COI1} complex, an E3 ubiquitin ligase that degrades target proteins via the 26S proteosome in response to JA (Devoto et al., 2002; Xu et al., 2002). The COI protein confers target specificity to the SCF^{COI1} complex (Feys et al., 1994; Xie et al., 1998). The target proteins of the SCF^{COI1} complex are

jasmonate ZIM domain (JAZ) proteins that repress transcription of JA-responsive genes by blocking the activity of transcriptional activators (Chini et al., 2007; Thines et al., 2007). Binding of JA-Ile to the SCF^{COI1} complex induces degradation of JAZ repressors via the 26S proteosome and de-represses transcriptional activators allowing transcriptional activation of early response genes by jasmonates (Chini et al., 2007; Thines et al., 2007).

4.1.3 Phytochrome and Jasmonic Acid Signaling

The contribution of jasmonates to regulation of cell expansion, cell division, growth orientation, and tissue and organ formation is known to affect plant morphogenesis (Avanci et al., 2010; Koda, 1997). Extensive overlap exists between the growth and developmental processes regulated by light and plant hormones (Jaillais and Chory, 2010) and plant hormones function to integrate light responses (Bou-Torrent, Roig-Villanova, and Martinez-Garcia, 2008). Although limited, several breakthroughs in understanding the signaling network mediated by phytochromes and JA have been made in recent years.

The initial report on a connection between JA and phytochrome signaling is the identification of a mutant displaying an FR-specific long hypocotyl phenotype in Col-0 WT background and the mutant was found to have a mutation in the *FAR-RED-INSENSITIVE219 (FIN219)* gene, a suppressor of the *constitutive photomorphogenesis1* (*COP1*) mutation (Hsieh et al., 2000). Later, the *fin219* mutation was found to be allelic to the *jar1* mutation (Staswick, Tiryaki, and Rowe, 2002) and *JAR1* encodes a JA-amino synthetase, catalyzing the conjugation of JA to Ile, required for optimal signaling in

jasmonate responses in Arabidopsis (Staswick and Tiryaki, 2004). Both *jar1* and *fin219* mutants display a long hypocotyl phenotype under FRc compared to WT (Chen et al., 2007) suggesting that mutants are impaired in phytochrome-mediated signaling in FR. Another example of a link between JA and phytochrome signaling is *jasmonate insensitive1 (jin1)*, an allele of *MYC2* (Lorenzo et al., 2004) and *ZBF1* (Yadav et al., 2005). In FR light, the patterns of expression of certain gene are altered in the presence of mutations in *ZBF1* gene (Yadav et al., 2005). Moreover, published data indicate that phytochrome chromophore biosynthesis and JA signaling are interconnected. *HY1*, *HO2*, *HO3* and *HO4* genes encode multiple heme oxygenases (Emborg et al., 2006) and *HY1* is expressed in roots of Arabidopsis (Davis et al., 2001; Davis, Kurepa, and Vierstra, 1999; Emborg et al., 2006). Under white light, a *hy1* mutant (*hy1*[21.84N]) displays longer roots compared to the L*er* WT parent (Muramoto et al., 1999). By contrast, Zhai et al., (2007) reported that *hy1* mutants in Col-0 WT background (*hy1-100* and *hy1-101*) have shorter roots and upon JA treatment and *HY1* expression is down-regulated. This observation indicates that JA impacts phytochrome chromophore biosynthesis in Arabidopsis. Significance of interactions between JA and phytochrome signaling in the natural environment was recently discovered through comparative analyses of Arabidopsis plants subjected to insect herbivory after growth in high density or exposure to high FR light (Moreno et al., 2009). Plants which are grown in shade or supplemented with FR light display characteristic shade-avoidance responses (Ballare, 2009; Ballare, Scopel, and Sanchez, 1990). phyB detects changes in the R/FR ratio of light and is able to suppress shade avoidance responses under light with high R/FR ratio (Franklin et al., 2003). Work by Moreno et al., (2009) confirmed that, while phyB induces shade

avoidance responses in plants grown in high density or exposed to high FR light, induction of shade-avoidance responses also leads to a reduction in sensitivity to jasmonates accompanied by suppression of JA-mediated gene expression and defense responses upon insect herbivory. Selective insensitivity to jasmonates may have a role in diverting resources away from defense pathways and channeling towards stem elongation to reach light and maximize photosynthesis. Additionally, selective desensitization to jasmonates can also have implications in avoiding the inhibitory effects of jasmonates on cell growth, which could affect stem elongation, a characteristic response of the shade avoidance response (Yan et al., 2007).

Light perceived in leaves can regulate the development of organs at a distant site through manipulation of hormone signaling (Salisbury et al., 2007). Global organ responses to R and FR light require the integration of cell autonomous responses with intercellular and inter-organ signaling to connect and coordinate them. Phenotypic and photobiological analyses of transgenic lines with targeted phytochrome inactivation will be an attractive tool to expand currently limited understanding of the cellular and molecular nature of signaling cascades involved in regulating phytochrome-dependent root development in Arabidopsis.

4.1.4 Targeted Chromophore Deficiency through Transactivation of Biliverdin Reductase

Constitutive expression of *BVR* in Arabidopsis perturbs many light-dependent phytochrome-mediated responses (Lagarias et al., 1997; Montgomery et al., 1999). Studies with stable transgenic lines displaying mesophyll-specific and meristem-specific

phytochrome chromophore-deficiencies have revealed that localized pools of phytochromes can regulate distinct physiological responses and established the efficacy of targeted *BVR* expression as a novel molecular technique to investigate sites of light perception (Warnasooriya and Montgomery, 2009).

A current limitation is the availability of cloned and characterized promoters that can direct the gene expression in a targeted manner. A two-component, enhancer-trap mis-expression system overcomes the limited availability of cloned and characterized promoters by using native genomic enhancers within a host genome (Wu et al., 2003) and circumvents the necessity to maintain and genotype multiple stable transgenic lines (Warnasooriya and Montgomery, in press). Genetic crosses between the UAS-BVR parent and a range of GAL4-enhancer trap parents will result in progeny with diverse expression patterns of the *BVR* gene and results in distinct *BVR* expression patterns in a localized manner, which makes it an effective tool to determine sites of physiological processes, such as photoperception, that have been shown to have spatial-specific aspects.

4.1.5 Outlook

Numerous studies establish the interactions between JA- and phytochrome-mediated signaling (Ballare, 2009; Ballare, Scopel, and Sanchez, 1990; Chen et al., 2007; Lorenzo et al., 2004; Moreno et al., 2009; Muramoto et al., 1999; Robson et al; 2010; Yadav et al., 2005; Zhai et al., 2007). Even though published work has confirmed the presence and emphasized the importance of the link between the two signaling pathways, information on the possible tradeoffs between phytochromes- and JA-mediated signaling is limited. Moreover, collective functional roles of phytochromes and JA, and possible

sites of phytochrome photoperception during regulation of root elongation in Arabidopsis require further analysis. Muramoto et al., (1999) observed longer roots in a chromophore biosynthetic mutant, *hy1* mutant (*hy1*[21.84N]), compared to the L*er* WT, whereas, Zhai et al., (2007) reported that *hy1* mutants in Col-0 WT background (*hy1-100* and *hy1-101*) have shorter roots upon JA treatment. Thus, the objective of this study is to analyze if root-localized chromophore deficiencies alter light-dependent root morphogenesis and/or sensitivity of roots to JA-mediated root inhibition. A UAS-BVR transgenic line was crossed to the M0062 enhancer trap line displaying root-specific *GFP* expression (Haseloff, 1999). Comparative phenotypic analyses of transgenic lines with constitutive-, mesophyll- and meristem-specific chromophore deficiencies and M0062>>UAS-BVR progeny with root-specific chromophore deficiency indicate that lack of root-localized phytochrome/chromophore affects root development in a light-dependent manner in *A. thaliana*.

4.2 Materials and Methods

4.2.1 Transactivation of *BVR*

Wild type Arabidopsis ecotype C24 plants were transformed with UAS-BVR construct by floral dip as described by (Clough and Bent, 1998). Kanamycin selection of transformants was performed as described in section 3.2.5. T1 transgenic seedlings were selected through a rapid selection protocol for identifying transformed Arabidopsis seedlings following floral dip transformation (Harrison et al., 2006). T3 plants of UAS-BVR1 were crossed with M0062 enhancer trap line (Haseloff, 1999) and F1 progeny were planted on kanamycin for selection. The genotyping of F1 seedlings was performed

by PCR with GoTaqGreen (Catalog No. M7123, Promega, WI). PCR amplification was carried out with the following gene-specific oligonucleotides at 10 μM in a 25 μl reaction: *BVR*– forward 5'–GCTGAGGGACTTGAAGGATCCAC–3' and reverse 5'–CACTTCTTCTGGTGGCAAAGCTTC–3', *GAL4*– forward, 5'–AGTGTCTGAAGAACAACTGGGAG–3'and reverse 5'–CGAGTTTGAGCAGATGTTTACC–3'. Thermal cycling conditions were (1) 1 cycle of denaturation at 95 °C for 2 min, (2) 40 cycles of denaturation at 95 °C for 1 min, annealing for 1 min (for *BVR* at 60 °C and for *GAL4* at 58 °C), extension at 72 °C for 1 min and (3) final extension at 72 °C for 5 min with a hold at 4 °C. A 10-μL aliquot of the PCR product was visualized by electrophoresis for 2 h at 80V on a 0.8% agarose gel containing ethidium bromide (Catalog No. 15585-011, Invitrogen, CA) at 0.02 μg/mL (w/v). Ultraviolet images were obtained using a Gel Doc system (Bio-Rad Laboratories, Inc., CA) at subsaturation settings. F1 seedlings that were positive with both primers sets were transferred to soil to obtain F2 and F3 seeds. The F3 and F4 seeds of UAS-BVR1 x M0062 cross were used for subsequent analyses (M0062>>UAS-BVR).

4.2.2 Whole-mount Immunohistochemistry

Seeds of C24 WT and M0062>>UAS-BVR were sterilized as described in section 2.2.1 and were planted in 100- x 100- x 15-mm square petri dishes on media containing 1X Murashige and Skoog salts (Catalog No. MSP09, Caisson Laboratories, UT), 0.8 % (w/v) Phytablend (Catalog No.PTP01, Caisson Laboratories, UT), 0.05 % (w/v) 4-Morpholineethanesulfonic acid (Catalog No. M3672, Sigma, MO), 1 % (w/v) Sucrose (Catalog No. 4072-05, J.T. Baker, NJ), adjusted to pH 5.7 with KOH. Imbibing seeds

were cold-stratified at 4 °C for 3 days in darkness. Plates were kept vertically in a humidity-controlled chamber with Wc illumination of 100 μmol m^{-2} s^{-1} for 3.5 days at 22 °C. 3.5-d-old seedlings were subjected to whole-mount *in situ* protein localization to visualize proteins in root tips, lateral roots, and embryos, as previously described with limited modifications (Sauer et al., 2006). Seedlings were treated with the paraformaldehyde-based fixative solution (4 % paraformaldehyde, Catalog No. P6148, Sigma, MO in 1X PBS, supplemented with 0.1 % Triton X-100, Catalog No. A3352, Research Products International Corp., IL) for 30 min followed by washing with 1X PBS for 2x10 min and with sterile water for 2x5 min. Fixed seedlings were mounted on Poly-Prep slides (Catalog No. P0425, Sigma, MO) in a droplet of water and were air-dried for 2.5 h at room temperature. Cell walls were digested with 2 % Driselase (Catalog No. D9515, Sigma, MO) in 1X PBS for 30 min at 37 °C. Slides were washed with 1X PBS for 3x10 min. Tissues were permeabilized with 3 % IGEPAL CA-630 (Catalog No. I3021, Sigma, MO) containing 10 % dimethylsulfoxide (Catalog No. 9224-01, J. T. Baker, NJ) for 1 h at room temperature, followed by washing with 1X PBS for 4x10 min. Blocking with 3 % Bovine Serum Albumin Fraction V (Catalog No. 03 116 964 001, Roche Diagnostics, IN) was carried out for 1 h at room temperature. Fixed and permeated seedlings were incubated with rabbit anti-BVR antibody (Catalog No. 56257-100, QED Biosciences Inc., CA) at 1:2000 dilution in 1X PBS or with 1X PBS alone for control samples overnight at 4 °C. Excess primary antibody was removed by washing slides with 1X PBS for 3x10 min. Following incubation with the primary antibody and washing, seedlings were incubated with goat anti-rabbit IgG (H+L) conjugated to Hilyte Plus™ 555 (Catalog No. 61056-Plus555, AnaSpec, CA) at 0.005 mg/mL dilution in 1X PBS for

6 h at 37 °C. To remove excess secondary antibody, slides were washed with 1X PBS for 4x10 min. Drops of antifade mounting medium, Citifluor (Catalog No. 19470, Ted Pella Inc., CA) were placed on treated seedlings and covered with cover slips. Slides were stored overnight in darkness at 4 °C before imaging. Root tips of seedlings were imaged on an inverted Axiovert 200 Zeiss LSM 510 Meta confocal laser scanning microscope (Carl Zeiss MicroImaging, NY) using differential interference contrast (DIC) optics and fluorescence excitation/emission filters. A 20x0.75 Plan Apochromat objective lens was used for imaging. DIC imaging was performed using the 543-nm laser. Fluorescence from the secondary antibody was collected using a 543-nm laser for excitation and a 560 – 615 nm band pass filter for emission. Images were acquired using the LSM FCS Zeiss 510 Meta AIM imaging software (Carl Zeiss MicroImaging, NY).

4.2.3 Arabidopsis Seedling Extracts

Seeds of No-0 WT and 35S::cBVR1 were sterilized as described in section 2.2.1. Imbibing seeds were cold-stratified at 4°C for 3 days in darkness in 1.5 mL microcentrifuge tubes. In Phytatrays (Catalog No. P1552, Sigma, MO), imbibed seeds were planted on NITEX® nylon membrane (Catalog No. 03-100/32, Sefar Filtration Inc., NY) placed on a raft in contact with a liquid medium containing 1X Murashige and Skoog salts (Catalog No. MSP09, Caisson Laboratories, UT) with 1 % (w/v) Sucrose (Catalog No. 4072-05, J.T. Baker, NJ), adjusted to pH 5.7 with KOH. Phytatrays were kept in a humidity-controlled chamber with Wc illumination of 100 $\mu mol\ m^{-2}\ s^{-1}$ for 21 days at 22 °C. Leaf and root tissues were quickly harvested (< 1 min) above and below the nylon membrane, weighed and transferred to separate 15 mL sterile tubes. After

immediately freezing in liquid nitrogen, tissues were crushed to a powder using a microgrinder. Crude Arabidopsis extracts were prepared according to a protocol adapted from (Lagarias et al., 1997), leaf and root tissues were immediately homogenized in plant extraction buffer as described in section 3.2.6, however, for homogenization, plant extraction buffer was added at a ratio of 2 volumes/fresh weight (mg). The crude homogenates were clarified as described in sections 3.2.6. The aliquots of clarified supernatants were stored at -80 °C for immunoblot analysis in section 4.2.4.

4.2.4 Immunoblotting

Total soluble proteins extracted from 21-day-old whole-plants were quantified as reported (Warnasooriya and Montgomery, 2009). For immunoblot analysis to confirm BVR accumulation in shoot and root extracts of 35S::cBVR1, ~ 25 µg of total protein was separated by SDS-PAGE and subsequent immunoblot analyses were performed as described (Montgomery et al., 1999) using rabbit anti-BVR antibody (1:3000; Catalog No. 56257-100, QED Biosciences Inc., CA) and ImmunoPure® goat anti-rabbit IgG (H+L) conjugated to horseradish peroxidase (HRP; 1:5000, Catalog No. 31460, Pierce Biotechnology, Inc., IL) as the secondary antibody. Antibody signal (chemiluminescence) was detected using SuperSignal® West Dura Extended Duration substrate (Catalog No. 34075, Thermo Fisher Scientific Inc., IL) on Molecular Imager® VersaDoc™ MP 4000 System (Bio-Rad Laboratories Inc., CA).

4.2.5 Hypocotyl Inhibition Assays

Seeds of No-0 WT, 35S::cBVR1, C24 WT, and UAS-BVR1>>M0062 were sterilized and planted as described in section 2.2.1. Imbibing seeds were cold-stratified at 4 °C for 3 days in darkness. Plates were kept in a humidity-controlled chamber with Bc or Rc illumination of 30 μmol m^{-2} s^{-1} and 50 μmol m^{-2} s^{-1}, respectively, or in darkness for 7 days at 22 °C. Seedlings were scanned and plant images were used to quantify hypocotyl lengths using ImageJ software (NIH). The hypocotyl inhibition assay was repeated 3 times. Percentage dark length and standard deviations of percentage dark length were calculated according to the equation described in section 2.2.6. Two-tailed, unpaired Student's t-test was performed to compare the percentage dark length of hypocotyls of transgenic lines relative to cognate WT seedlings, except for C24 WT, and UAS-BVR1>>M0062 grown in Rc and FRc, where two-tailed, unpaired Mann-Whitney test U-test was performed to compare the percentage dark length of hypocotyls of UAS-BVR1>>M0062 to that of C24 WT .

4.2.6 Root Inhibition Assays

Seeds of No-0 WT, 35S::pBVR3, 35S::cBVR1, CAB3::pBVR2, MERI5::pBVR1, Col-0 WT, *jar1*, *myc02-05*, C24 WT, M0062>>UAS-BVR, C20 WT, *hy1-1* and *hy2-1*, were sterilized and planted on media prepared as described in section 4.2.2 with or without 20 μM Jasmonic acid (Catalog No. 392707, Sigma, MO). Imbibing seeds were cold-stratified at 4 °C for 3 days in darkness. Plates were kept vertically in a humidity-controlled chamber with Wc illumination of 100μmol m^{-2} s^{-1} for 10 days at 22 °C. Plates were scanned and plant images were used to quantify root lengths using ImageJ software

(NIH). The root elongation assay was repeated 6 times. Two-tailed, unpaired Student's t-test was performed to compare the means of root lengths.

4.2.7 Expression Levels of Jasmonic Acid-inducible Marker Genes

To determine if spatial-specific deficiency of chromophore *in vivo* affects the expression of JA-inducible marker genes, real-time quantitative RT-PCR (qRT-PCR) was performed to quantify the levels of transcripts of a JA biosynthetic gene, *12-OPDA REDUCTASE3 (OPR3; At2g06050*; Zhai et al., 2007), and a JA-inducible marker gene, *vegetative storage protein1* (*VSP1*; *At5g24780*; Zhai et al., 2007). Seeds of No-0 WT, 35S::pBVR3, 35S::cBVR1, CAB3::pBVR2, MERI5::pBVR1, Col-0 WT, *jar1*, *myc02-05*, C24 WT, M0062>>UAS-BVR, C20 WT, *hy1-1* and *hy2-1* were planted in 245- x 245- x 18-mm square petri dishes on media prepared as described in section 4.2.2 with or without 20 μM Jasmonic acid (Catalog No. 392707, Sigma, MO). Imbibing seeds were cold-stratified at 4 °C for 3 days in darkness. Plates were kept vertically in a humidity-controlled chamber with Wc illumination of 100 μmol m^{-2} s^{-1} for 10 days at 22 °C. 10-d-old whole seedlings were quickly (< 1 min) harvested and immediately frozen in liquid nitrogen. Using RNeasy® Plant Minikit (Catalog No. 16419, Qiagen, MD) including on-column DNase treatment (Catalog No. 79254, Qiagen, MD), total RNA was isolated according to manufacturer's instructions. Quantity of the RNA was analyzed by spectrometry (NanoDrop1000, Thermo Scientific, DA). First-strand cDNA synthesis was performed using the Reverse Transcription System (Catalog No. A3500, Promega, WI) with random primers according to the manufacturer's instructions using a 20 μL reaction volume. The incubation times of first-strand cDNA synthesis with total RNA of 0.2 μg

was (1) 10 min at room temperature, (2) 1 h (instead of 15 min) at 42 °C, (3) 5 min at 95 °C and (4) 5 min at 4 °C. The cDNA reaction mixture was diluted forty-fold with Nuclease-Free Water, and 4 µL of the diluted cDNA product was used as template in a 10 µL qPCR reaction using the Applied Biosystems FAST 7500 real-time PCR system in FAST mode with Fast SYBR® Green Master Mix (Applied Biosystems, CA) according to manufacturer's instructions. For transcript analysis, annealing/extension temperature was 60 °C for both the *OPR3* and *VSP1* primer sets. Reactions were performed in triplicate and products were checked by melting curve analysis. The abundance of transcripts was analyzed using the ddCt method based on relative quantitation, normalizing to the reference transcript *UBC21* (*At5g25760*). All qRT-PCR experiments were repeated with three independent biological replicates.

4.3 Results and Discussion

To regulate light-dependent root elongation and certain tropic responses within the Arabidopsis root system, roots themselves appear to be the site of photoperception (Correll et al., 2003; Correll and Kiss, 2005). Elongated roots have been observed in a phytochrome chromophore biosynthetic mutant, *hy1* (*hy1*[21.84N]; having a 13 bp deletion in the *HY1* gene) compared to L*er* WT by Muramoto et al., (1999), in contrast to shorter roots in *hy1* mutants (*hy1-100* and *hy1-101*) in Col-0 WT background as observed by Zhai et al., (2007). Thus, definitive evidence on the impact of phytochrome or phytochromobilin on JA-mediated root inhibition in Arabidopsis has been confounding. Furthermore, published reports indicate that JA and related compounds regulate distinct aspects of plant morphogenesis (Avanci et al., 2010; Koda, 1997) and

JA- and phytochrome-mediated signaling pathways are linked (Ballare, 2009; Ballare, Scopel, and Sanchez, 1990; Chen et al., 2007; Lorenzo et al., 2004; Moreno et al., 2009; Muramoto et al., 1999; Yadav et al., 2005; Zhai et al., 2007). Since FR light is conducted most efficiently through internal light piping (Sun, Yoda, and Suzuki, 2005; Sun et al., 2003) and phytochrome is the only known photoreceptor that is able to absorb R and FR light, at least in Arabidopsis, two novel molecular approaches were employed for targeting phytochrome inactivation to roots and to study the effects of phytochrome inactivation on root development. The sensitivity of roots to JA and JA-mediated root inhibition response in transgenic lines accumulating BVR in discrete tissues were analyzed in this chapter. Comparative phenotypic analyses of transgenic lines with constitutive, mesophyll-, meristem- and root-specific chromophore deficiencies indicate that lack of root-localized phytochrome or phytochrome chromophore affect root development in a light-dependent manner in *A. thaliana*.

4.3.1 Transactivation of *BVR* in M0062>>UAS-BVR

A GAL4-based bipartite enhancer trap approach (Laplaze et al., 2005) was used to generate an Arabidopsis line having phytochrome chromophore deficiency in roots. Through genetic crosses of the enhancer trap line, M0062 with root-specific *GFP* expression, and the UAS-BVR line, a transgenic BVR line, M0062>>UAS-BVR was isolated. Accumulation of BVR protein was confirmed by whole-mount immunohistochemistry on roots of the M0062>>UAS-BVR line (Figure 4.1). In the M0062>>UAS-BVR line, expression of *BVR* leads to root-specific holophytochrome

deficiencies and is used as a tool to study the impact of root-specific phytochrome inactivation on light-dependent root development in Arabidopsis.

4.3.2 Root-localized Phytochrome Inactivation does not Affect Hypocotyl Inhibition Response

The observation that constitutive *BVR*-expressing seedlings had elongated hypocotyls in Rc, FRc and Bc light indicated that lack of phytochromes within the seedlings is responsible for the phenotype (Lagarias et al., 1997). As 'light piping' allows the light signals perceived above ground to affect responses in roots (Mandoli and Briggs, 1982; Mandoli and Briggs, 1984), it is possible that phytochrome inactivation in roots might affect physiological responses in tissues other than roots. To test whether root-localized phytochrome inactivation affects hypocotyl inhibition and rule out residual activity of the BVR enzyme in shoots as would be evident by elongated hypocotyls in B, R and FR light, phytochrome-mediated hypocotyl inhibition response was analyzed in M0062>>UAS-BVR and 35S::cBVR1 under Bc, Rc and FRc.

The 35S::cBVR1 line accumulates BVR protein in shoots and roots (Figure 4.2). The analysis of hypocotyl inhibition response in the 35S::cBVR1 line showed a significant increase in hypocotyl length compared to the No-0 WT parent under Bc, Rc and FRc ($p>0.0001$, Figure 4.3 and Figure 4.4) and as reported by Montgomery et al., (1999). The percentage dark length of M0062>>UAS-BVR compared to C24 WT was not significantly different under the Bc light condition tested ($p=0.7146$, Figure 4.3 and Figure 4.4). However, in Rc and FRc light, the frequency distribution analysis of hypocotyl lengths measured for C24 WT and M0062>>UAS-BVR seedlings showed that

lengths for C24 WT represented a normal distribution, whereas the lengths for M0062>>UAS-BVR seedlings represented a slightly negatively skewed distribution. Thus, two-tailed, unpaired Mann-Whitney test U-test was performed to compare the percentage dark length of hypocotyls of M0062>>UAS-BVR to that of C24 WT. In both Rc and FRc, the percentage dark lengths of M0062>>UAS-BVR compared to C24 WT was not significantly different (Figure 4.4, $p=1.0$ in Rc and FRc). This observation suggests that root-localized phytochromes have no or a minor role in regulating hypocotyl inhibition in Rc, FRc and Bc and residual BVR activity is absent in shoots of M0062>>UAS-BVR.

4.3.3 Phytochrome or Phytochromobilin Affects Root Elongation in Arabidopsis

To more fully understand the regulation of light-dependent root development by phytochromes or phytochromobilin, root elongation responses were analyzed in transgenic Arabidopsis lines with constitutive, mesophyll-, meristem- and root-specific phytochrome inactivation through the expression of *BVR*. Root lengths of cognate WT plants and *BVR*-expressing transgenic lines were quantified in Wc illumination. BVR accumulation in the 35S::pBVR3 and 35S::cBVR1 roots was confirmed by immunoblot analyses (Warnasooriya and Montgomery, 2009 and Figure 4.2). The 35S::pBVR3 and 35S::cBVR1 lines had significantly longer roots relative to No-0 WT ($p<0.0001$, Figure 4.5). The roots of 35S::pBVR3 and 35S::cBVR1 seedlings were ~ 45 % and ~ 90 % longer, respectively, than the roots of No-0 WT seedlings. As previously published, the CAB3::pBVR2 seedlings accumulated BVR in mesophyll tissue, but not in roots and thus leads to mesophyll-specific phytochrome inactivation (Warnasooriya and Montgomery,

2009). The CAB3::pBVR2 seedlings showed ~ 21 % longer roots compared to No-0 WT (p=0.0165, Figure 4.5) and the percentage elongation was not to the same degree as observed in the 35S::pBVR3 and 35S::cBVR1. The root lengths of MERI5::pBVR1 with shoot-apex-specific BVR accumulation (Warnasooriya and Montgomery, 2009) were on average ~ 8 % longer, but not significantly different from No-0 WT (p=0.3424, Figure 4.5).

Zhai et al., (2007) observed shorter roots in the *hy1-101* mutant compared to Col-0 WT. In comparative analysis with *BVR*-expressing transgenic lines, root lengths were quantified in two chromophore biosynthetic mutants, *hy1-1* and *hy2-1*. Relative to the C20 WT, roots of *hy1-1* were ~ 15 % shorter and roots of *hy2-1* were ~ 23 % longer (Figure 4.5). However, compared to the C20 WT, the differences observed in root length for *hy1-1* and *hy2-1* were not statistically significant (p=0.1524 and p=0.0859, respectively). M0062>>UAS-BVR with root-localized phytochrome chromophore deficiencies showed roots ~ 12 % longer in length relative to C24 WT (Figure 4.5), a response that was similar to the root elongation observed for 35S::pBVR3, 35S::cBVR1 and *hy2-1*. A characteristic phytochrome-deficient phenotype of 35S::pBVR3 and 35S::cBVR1 transgenic lines with constitutive phytochrome inactivation is elongation of hypocotyls under R, FR and Bc (Lagarias et al., 1997; Montgomery et al., 1999) and such a phenotype was not observed in the M0062>>UAS-BVR line as described in section 4.3.2 (Figure 4.3 and 4.4). This observation provides additional evidence that M0062>>UAS-BVR lacks root-localized phytochromes and the elongated roots likely represent a specific perturbation of a phytochrome-regulated root inhibition response.

On average, statistically significant increases in root lengths under Wc illumination were observed for transgenic lines with BVR accumulation in roots (i.e. 35S::pBVR3, 35S::cBVR1 and M0062>>UAS-BVR, thus root-localized phytochrome inactivation) with respect to lines lacking BVR accumulation in roots (i.e. No-0 WT, CAB3::pBVR2 and MERI5::pBVR1, Figure 4.5). A similar phenotype was also apparent in the chromophore-deficient mutant, *hy2-1* relative to C20 WT (Figure 4.5). As previously reported, subcellular localization of BVR affects distinct subsets of light-mediated and light-independent processes in Arabidopsis (Montgomery et al., 1999). For example, 35S::pBVR3 with plastid-localized *BVR* expression is intolerant to higher light fluences and displays a fluence-rate-dependent reduction in chlorophyll levels accompanied by an increase in the chlorophyll a/b ratio (Lagarias et al., 1997). This phenotype could be related to changes in plastid metabolism (Franklin et al., 2003) upon BVR activity in plastids and/or due to lack of BV/phytochromobilin that would otherwise play an important regulatory role within the plastid compartment (Montgomery et al., 1999). A response to higher light fluences, as such, was not obvious in 35S::cBVR1 with cytosolic *BVR* expression (Montgomery et al., 1999). Since 35S::cBVR1 and M0062>>UAS-BVR exhibit cytosolic *BVR* expression, increased root lengths observed in these lines compared to their cognate WT plants are expected to be associated with lack of phytochromobilin or phytochromes and likely reflect disruption of the phytochrome-mediated root inhibition response as reported for R light-dependent inhibition of root elongation (Correll and Kiss, 2005).

The presence of longer roots in the CAB3::pBVR2 line relative to No-0 WT may be due to the disruption of phytochrome-mediated signaling between mesophyll- and

root-localized phytochrome pools and implies that mesophyll-localized phytochromes may be involved in long-distance communication to regulate root elongation. This observation corroborates an already demonstrated phenomenon by Salisbury et al., (2007) that light-perception by shoot-localized phytochromes can impact root development in Arabidopsis. The impaired phytochrome-mediated root inhibition in transgenic lines with mesophyll- and root-specific phytochrome inactivation with respect to lines with constitutive phytochrome inactivation suggests that both mesophyll- and root-localized phytochromes distinctly contribute to light-dependent regulation of root development in Arabidopsis.

4.3.4 Root-localized Phytochrome or Phytochromobilin Reduces Jasmonic Acid-mediated Root Inhibition

Zhai et al., (2007) confirmed that phytochromobilin deficiency in the *hy1-101* mutant enhances JA-mediated root inhibition. Inhibition of root elongation is promoted by JA and derivatives of JA (Staswick, Su, and Howell, 1992). By measuring root lengths of *BVR*-expressing transgenic lines, root inhibition responses were quantified in the presence of exogenous methyl JA (MeJA) to determine whether the lack of phytochromobilin impacts JA-mediated root inhibition. Comparative analysis of root lengths indicated that lines with phytochrome inactivation in roots had reduced sensitivity to MeJA. Root lengths of 35S::pBVR3, 35S::cBVR1, *hy1-1* and *hy2-1* were ~ 101 %, ~ 82 %, ~ 73 % and ~ 97 % longer than the root lengths of their cognate WT parents, respectively, and were significantly longer ($p \leq 0.0001$ for all) in the presence of 20 μM of MeJA (Figure 4.6). Root elongation to a similar degree in the presence of MeJA was

also observed in the JA-insensitive mutants, *jar1* and *myc02-5*, with ~ 100 % and ~ 61 % increase respectively, compared to root lengths measured for Col-0 WT (Figure 4.6). In the absence of MeJA, the root lengths of 35S::pBVR3 and 35S::cBVR1 were longer than No-0 WT (Figure 4.5), thus, for more accurate quantitative comparison of sensitivity of roots to MeJA, relative MeJA-sensitivity was calculated. For a particular line, the relative MeJA-sensitivity was the ratio of the root length in the absence of exogenous MeJA to the root length in the presence of 20 μM of MeJA (Table 2). In the absence of MeJA, the 35S::pBVR3 line with plastid-targeted *BVR* expression in roots displayed a 3.45-fold difference in root length relative to 4.75-fold difference in No-0 WT (Table 2). The difference between No-0 WT and 35S::pBVR3 reflects a ~ 27 % reduction in sensitivity to MeJA application (Table 2) and of all the lines tested, JA-insensitive mutants, *jar1* and *myc02-5* displayed the most reduction in JA-sensitivity (~ 66 % and ~ 49 %, respectively) compared to Col-0 WT (Table 2). A 4.95-fold increase was apparent for 35S::cBVR1 with cytosolic BVR accumulation in the absence of MeJA relative to 20 μM of MeJA (Table 2) and suggests that 35S::cBVR1 is as sensitive as No-0 WT to JA-mediated inhibition of root elongation. In the 35S::cBVR1 line, the roots were significantly longer than the roots of No-0 WT on 0 μM as well as 20 μM MeJA. The relative JA-sensitivity in M0062>>UAS-BVR also indicated a reduced response to 20 μM of MeJA. In the absence of MeJA, the fold difference for M0062>>UAS-BVR was 4.46 compared to 4.8 for C24 WT (Table 2). The roots of M0062>>UAS-BVR were significantly longer than the roots of C24 WT ($p=0.0266$) and showed ~ 7 % reduction in sensitivity to MeJA application (Table 2). As noted for 35S::pBVR3 and M0062>>UAS-BVR, chromophore biosynthetic mutants, *hy1-1* and *hy2-1* also exhibited hyposensitivity to MeJA treatment

(Figure 4.6). Reduction in relative JA-sensitivity for *hy1-1* and *hy2-1* was ~ 51 % and ~ 37 % respectively (Table 2) and both lines displayed longer roots compared to C20 WT (Figure 4.6). However, contrasting responses were observed in *hy1-1* and *hy2-1* in the absence of MeJA; roots were shorter in *hy1-1*, but longer in *hy2-1* relative to C20 WT (Figure 4.5). The presence of longer roots in *hy1-1* on MeJA treatment was distinctive from the shorter roots reported for *hy1-101* allele in Col-0 WT background by Zhai et al., (2007). However, the relative JA-sensitivity in *hy1-101* (Zhai et al., 2007) and *hy1-1* appeared to be similar despite the differences in sensitivities of different Arabidopsis ecotypes to treatment with JA (Matthes, Pickett, and Napier, 2008), duration of growth and MeJA concentration.

Transgenic lines with phytochromobilin deficiencies in roots, i.e. 35S::pBVR3 and M0062>>UAS-BVR, relative to other *BVR*-expressing lines displayed the most reduction in sensitivity to MeJA (~ 27 % and ~ 7 %, respectively) and suggests that lack of phytochrome or phytochromobilin in roots impacts light-dependent, JA-mediated root inhibition. The response of *hy1-1* on 0 μM and 20 μM of MeJA was analogous to *jar1* and *myc02*-5 having shorter roots than their cognate WT lines in the absence of MeJA and longer roots upon exogenous application of 20 μM of MeJA. The response of the *hy2-1* mutant resembled closely the responses observed in the 35S::pBVR3 line and M0062>>UAS-BVR, having longer roots relative to cognate WT lines regardless of the absence or the presence of MeJA treatment, but all three lines displayed hyposensitivity to MeJA. The 35S::cBVR1 line was discrete in its relative response to application of MeJA. Even though the 35S::cBVR1 line had longer roots compared to No-0 WT regardless of the absence or presence of MeJA, the line was not impaired in relative

sensitivity to MeJA compared to No-0 WT. Despite their cytosolic *BVR* expression, the contrasting response to MeJA in 35S::cBVR1 and M0062>>UAS-BVR, i.e. 35S::cBVR1 being as sensitive as No-0 WT and M0062>>UAS-BVR being hyposensitive relative to C24 WT, may be due to a perturbation of communication between the shoot and root and/or between phytochrome- and JA-mediated signaling. The differences in the amounts of BVR being accumulated in roots of 35S::cBVR1 and M0062>>UAS-BVR could also account for the disparate responses to MeJA application. A possible reason for the 35S::cBVR1 line to have similar sensitivity to MeJA as No-0 WT and hyposensitivity to MeJA in the 35S::pBVR3 line could be due to indirect effects of changes to plastid metabolism on JA biosynthesis. p*BVR* expression could affect the stability of phytochromobilin synthase (Montgomery et al., 1999) and/or alter plastid heme levels (Lagarias et al., 1997; Montgomery et al., 1999). As targeting of *BVR* expression to plastids could alter plastid metabolism (Franklin et al., 2003; Montgomery et al., 1999) and JA biosynthesis involves chloroplasts/plastids (Mueller et al., 1993), changes to plastid metabolism could impact early steps of JA biosynthesis occurring in the chloroplasts/plastids (Wasternack, 2007). Based on the comparative analysis of relative sensitivities to MeJA in the 35S::pBVR3 line with plastid-localized BVR accumulation and the M0062>>UAS-BVR line with cytosolic BVR accumulation, it is evident that the observed hyposensitivity to MeJA is likely related to a lack of phytochromobilin and/or phytochrome, but not due to indirect consequences of accumulated BVR on plastid metabolism.

4.3.5 Root-localized Phytochrome Deficiencies Impact Expression of Jasmonic Acid-inducible Marker Genes

To determine whether the presence of longer roots in lines with root-localized phytochrome inactivation is correlated with lower endogenous levels of JA and/or whether the hyposensitivity to JA-mediated root inhibition is reflected at gene expression level, the expression of *OPR3* (*At2g06050*) and *VSP1* (*At5g24780*) was analyzed by qRT-PCR. In the absence of MeJA treatment, the expression of *OPR3*, a JA-biosynthetic gene, was low in all the lines tested (Figure 4.7). Expression levels of *OPR3* in 35S::pBVR3 and 35S::cBVR1 with constitutive phytochrome inactivation was ~ 74 % and ~ 66 %, respectively, relative to No-0 WT (Figure 4.7). The expression level of *OPR3* in M0062>>UAS-BVR with root-localized phytochrome inactivation was ~ 90 % compared to its WT, C24. This is only an ~ 10 % reduction in expression as opposed to ~ 26 % and ~ 34 % reduction observed in the 35S::pBVR3 and 35S::cBVR1 lines, respectively. Thus, distinct differences in the levels of *OPR3* expression are obvious for lines with constitutive vs. root-specific phytochrome chromophore deficiency.
~ 22 % and ~ 16 % reduction in *OPR3* expression levels relative to No-0 WT was apparent in the CAB3::pBVR2 and MERI5::pBVR1 lines, respectively, lacking phytochrome inactivation in roots (Figure 4.7). In contrast to what was observed for the 35S::pBVR3 and 35S::cBVR1 lines with constitutive phytochrome inactivation in the absence of MeJA, ~ 10 % and ~ 25 % increase in *OPR3* expression level relative to C20 WT was obvious in *hy1-1* and *hy2-1*, respectively, (Figure 4.7). Previously, an increased level of *OPR3* expression in the absence of MeJA treatment was reported for a different *hy* mutant, *hy1-101*, relative to Col-0 WT by Northern blot analysis (Zhai et al., 2007).

Relative to Col-0 WT, the *jar1* mutant had ~ 13 % increase, whereas *myc02-5* had ~ 15 % decrease in *OPR3* expression level (Figure 4.7). Reductions in *OPR3* expression levels have been reported for JA-insensitive mutants as determined previously by Northern blot analysis (Chung et al., 2008; Koo et al., 2009).

Upon exogenous application of 20 μM of MeJA, the expression of *OPR3* was induced relative to expression levels on 0 μM of MeJA in all the lines, but the degree of induction was clearly variable in comparison to their cognate WT plants. The 35S::pBVR3 and 35S::cBVR1 lines with phytochrome inactivation in roots showed ~ 64 % and ~ 54 % levels of *OPR3* expression, respectively, relative to No-0 WT (Figure 4.7). However, the level of *OPR3* expression for M0062>>UAS-BVR with root-localized phytochrome inactivation was more or less identical to the expression level observed for C24 WT (Figure 4.7). The *OPR3* expression was ~ 62 % in the CAB3::pBVR2 line with mesophyll-specific phytochrome inactivation, whereas the level for the MERI5::pBVR1 line with meristem-specific phytochrome inactivation was ~ 74 % relative to No-0 WT. In the *hy1-1* mutant, the *OPR3* expression was ~ 88 % and by contrast, in the *hy2-1* mutant, it was slightly higher (~ 4 %) than that of No-0 WT (Figure 4.7). An expression level of ~ 82 % and ~ 75 % was observed in the *jar1* and the *myc02-5* mutants, respectively, relative to Col-0 WT (Figure 4.7). Most lines with hyposensitivity to JA-regulated root inhibition displayed lower levels of *OPR3* expression relative to their cognate WT plants, with M0062>>UAS-BVR and *hy2-1* being exceptions. Even though variations in the level of *OPR3* expression were apparent, all phytochrome-deficient lines were responsive to exogenous application of MeJA.

The expression level of JA-inducible marker gene *VSP1* was undetectable or barely detectable in all of the lines in the absence of exogenous MeJA application (Figure 4.8). However, all the lines tested showed robust induction of *VSP1* expression in the presence of MeJA treatment suggesting that *OPR3* and *VSP1* have distinct expression patterns. Lower levels of *VSP1* expression were evident in the 35S::pBVR3, 35S::cBVR1, CAB3::pBVR2, MERI5::pBVR1, *jar1* and *myc02-5* lines with respect to the expression levels in cognate WT plants. The 35S::pBVR3 and 35S::cBVR1 lines showed ~ 58 % and ~ 53 % *VSP1* expression, respectively, comparative to No-0 WT, whereas the CAB3::pBVR2 and MERI5::pBVR1 lines showed ~ 67 % and ~ 69 % *VSP1* expression, respectively. These results suggest distinct differences in *VSP1* expression level for lines with constitutive and tissue-specific phytochrome deficiencies. ~ 50 % increase in *VSP1* expression relative to C24 WT was observed for M0062>>UAS-BVR with root-localized chromophore deficiency and suggests that M0062>>UAS-BVR is responsive to exogenous application of MeJA. Chromophore deficient *hy1-1* and *hy2-1* mutants showed a similar increase, ~ 59 % and ~ 50 %, in *VSP1* expression, respectively, with respect to C20 WT. This observation correlates with a substantial increase in *VSP1* expression in the *hy1-101* mutant relative to Col-0 WT on MeJA application as previously reported by (Zhai et al., 2007). As determined by Northern blot analysis of *VSP1* expression in JA-insensitive mutants in prior studies (Chung et al., 2008; Koo et al., 2009), ~ 48 % and ~ 36 % reductions were evident in *jar1* and *myc02-5*, respectively, compared to their WT, Col-0 (Figure 4.8).

The analysis of expression of JA-inducible marker genes, *OPR3* and *VSP1* by qRT-PCR in *BVR*-expressing transgenic lines indicated that *OPR3* and *VSP1* expression

is generally reduced for lines with constitutive and tissue-specific phytochrome chromophore deficiencies relative to cognate WT plants. *OPR3* expression was detectable on 0 μM, whereas *VSP1* expression was barely detectable. However, all of the lines tested were responsive to MeJA and *VSP1* expression showed robust induction on 20 μM. The 35S::pBVR3 and 35S::cBVR1 lines with constitutive phytochrome chromophore deficiency had reduced levels of *OPR3* and *VSP1* expression relative to No-0 WT. Even though such a reduction was apparent in the CAB3::pBVR2 line with mesophyll-specific chromophore deficiency and in the MERI5::pBVR1 line with meristem-specific chromophore deficiency, the reduction was not as extensive as in the 35S::pBVR3 and 35S::cBVR1 lines. A possible explanation for the reduction of *OPR3* and *VSP1* expression in the CAB3::pBVR2 and MERI5::pBVR1 lines is disruption of inter-tissue phytochrome- and JA-mediated signaling upon mesophyll- and meristem-specific phytochrome deficiencies. The M0062>>UAS-BVR line showed similar *OPR3* expression to that of C24 WT on MeJA, but expression was increased by ~ 50 % for *VSP1* relative to C24 WT on MeJA application. In general, the expression pattern of *OPR3* and *VSP1* observed for M0062>>UAS-BVR is unique from two other lines (i.e. 35S::pBVR3 and 35S::cBVR1) with phytochrome inactivation in roots and may be related to a higher level of BVR accumulation in roots or a distinct phenotype at the molecular level due to root-localized phytochromobilin or phytochrome deficiencies. JA-insensitive mutants, *jar1* and *myc02-5*, both showed reductions in *OPR3* and *VSP1* expression relative to Col-0 WT as previously reported (Chung et al., 2008; Koo et al., 2009). The increase in *OPR3* expression for *hy2-1* and increase in *VSP1* expression for hy1-1 and *hy2-1* correlated with the apparent increase in the expression of the two genes

in the *hy1-101* allele in Col-0 WT background as previously published (Zhai et al., 2007). However, the reduction in *OPR3* expression evident for the *hy1-1* mutant may be a result of ecotypic differences between C20 WT and Col-0 WT.

4.3.6 Summary

Increased root lengths of 35S::cBVR1 and M0062>>UAS-BVR lines with cytosolic *BVR* expression compared to their cognate WT plants are expected to be associated with a lack of phytochromobilin or phytochromes and likely reflect disruption of the phytochrome-mediated root inhibition response. The presence of longer roots in the CAB3::pBVR2 line relative to No-0 WT may be due to the disruption of phytochrome-mediated signaling between mesophyll- and root-localized phytochrome pools and implies that mesophyll-localized phytochromes may be involved in long-distance communication to regulate root elongation. This observation corroborates an already demonstrated phenomenon by Salisbury et al., (2007) that light-perception by shoot-localized phytochromes can impact root development in Arabidopsis. The impaired phytochrome-mediated root inhibition in transgenic lines with mesophyll- and root-specific phytochrome inactivation with respect to lines with constitutive phytochrome inactivation suggests that both mesophyll- and root-localized active phytochromes contribute to light-dependent regulation of root development in Arabidopsis.

Expression analysis of *OPR3* and *VSP1* indicates that the two genes have distinct expression patterns in the lines with chromophore deficiencies. *OPR3* is expressed to detectable levels in the absence of MeJA and is induced in all of the lines on exogenous MeJA application. By contrast, the level of *VSP1* expression was barely detectable in the

absence of MeJA and shows robust induction in all of the lines on exogenous MeJA treatment. The PHYTOCHROME AND FLOWERING TIME1 (PFT1) functions as a subunit of the Mediator complex and negatively regulates phytochrome signaling (Kidd et al., 2009). PFT1 is also required for JA-dependent expression of defense genes in Arabidopsis (Kidd et al., 2009). As JA and phytochrome signaling have antagonistic effects (Zhai et al., 2007), PFT1 also exhibits divergent functions (Kidd et al., 2009) indicating a definitive molecular link between phytochrome and JA-inducible marker genes.

Arabidopsis lines with root-localized BVR accumulation have defects in light-dependent root elongation. Arabidopsis lines with root-localized *BVR* expression, i.e. 35S::pBVR3 and M0062>>UAS-BVR, exhibit hyposensitivity to exogenous application of the JA-derivative, MeJA. These results provide evidence that the root-specific phytochrome chromophore or root-localized phytochromes are vital for photoregulation of root elongation and impact JA sensitivity.

4.4 Future Perspectives

The experimental findings of this chapter and previously published data confirm that JA- and phytochrome mediated signaling is interconnected (Lorenzo et al., 2004; Moreno et al., 2009; Robson et al., 2010; Staswick, Tiryaki, and Rowe, 2002) and the lack of phytochromobilin or phytochromes in roots negatively impacts root inhibition by JA (Zhai et al., 2007). The elongation of roots observed for *BVR*-expressing transgenic lines with phytochrome deficiencies in roots (notably, where *BVR* expression was targeted to the plastids, i.e. 35S::pBVR3) could be due to already lower levels of

endogenous JA in them. The accumulation of BVR in plastids is known to affect plastid metabolism (Franklin et al., 2003) and the involvement of plastids in JA biosynthesis (Wasternack, 2007) could potentially have indirect effects on overall JA levels. In lines with root-localized phytochrome deficiencies, even though the expression level of a JA-biosynthetic gene, *OPR3*, was similar to the level noted for their cognate WT, the lack of phytochromobilin or phytochrome could impact downstream or upstream enzymatic activities relative to OPR3 activity. To determine whether the accumulation of BVR or its end products, i.e. bilirubin and phytochromorubin, has an impact on JA biosynthetic genes leading to changes in JA production, the endogenous JA and JA-Ile levels can be quantified by liquid chromatography-mass spectrometry (LC-MS) before and after mechanical wounding as previously published (Chung et al., 2008; Koo et al., 2009; Li et al., 2005). Furthermore, to develop a mechanistic interpretation of data from LC-MS, the expression levels of several JA-biosynthetic genes, such as *LOX2* (*At3g45140*), *AOS* (*At5g42650*) and *AOC1* (*At3g25760*), as well as JA-inducible marker genes, *Thionin* (*Thi2.1*, *At1g72260*), *JAZ5* (*At1g17380*) and *JAZ7* (*At2g34600*) can be analyzed by qRT-PCR. qRT-PCR analysis of JA-biosynthetic, as well as JA-inducible marker genes, together with LC-MS data will reveal if the endogenous JA levels are markedly different among the lines with chromophore deficiencies relative to WT.

Ecological significance of cross talk between phytochrome and JA signaling was revealed by Moreno et al., (2009). In plants grown in high density or exposed to high FR light, phyB mediates shade avoidance responses accompanied by a reduction in sensitivity to jasmonates. Hyposensitivity to JA is characterized by suppression of JA-mediated gene expression and defense responses upon insect herbivory (Moreno et al.,

2009). As BVR accumulation leads to reduction of phytochromobilin and thus a reduction of the five types of phytochromes (Lagarias et al., 1997; Montgomery et al., 1999), to determine whether the lines with chromophore deficiencies are compromised in resistance to insect herbivory, feeding assays using the generalist *Spodoptera exigua* followed by the analysis of JA-marker gene expression can be performed. Feeding assays with *S. exigua* would represent conditions encountered by plants in a more natural environment and information from the feeding assays could expand the understanding of ecological importance of an antagonistic relationship between phytochrome and JA signaling.

Perception of light by root-localized phytochromes (Correll et al., 2003; Correll and Kiss, 2005) and transmission of perceived light information through internal light piping (Mandoli and Briggs, 1982; Mandoli and Briggs, 1984) can impact growth, development and tropic responses in the Arabidopsis root system. Although phytochromes are known to be expressed in roots and root tips of Arabidopsis (Salisbury et al., 2007; Tóth et al., 2001), information on perception of light by phytochromes localized in different root tissues that regulate root photomorphogenesis is lacking. Enhancer trap lines; J1103, KS074 and Q0171, with *GFP* expression in the root cap and emerging lateral roots, root tip and root cap, respectively (Haseloff, 1999), http://www.plantsci.cam.ac.uk/Haseloff/geneControl/catalogues) can be crossed with UAS-BVR lines to transactivate *BVR* and induce localized phytochrome inactivation at sites that are indicated by *GFP* expression. Comparative phenotypic analysis of F3 progeny would indicate whether phytochromes localized in specific root tissues are involved in light perception. Furthermore, analysis of JA-mediated responses (i.e. root

inhibition), feeding assays and quantification of endogenous JA levels in such F3 progeny lines will provide information on interaction between root-specific phytochrome signaling and JA-mediated signaling.

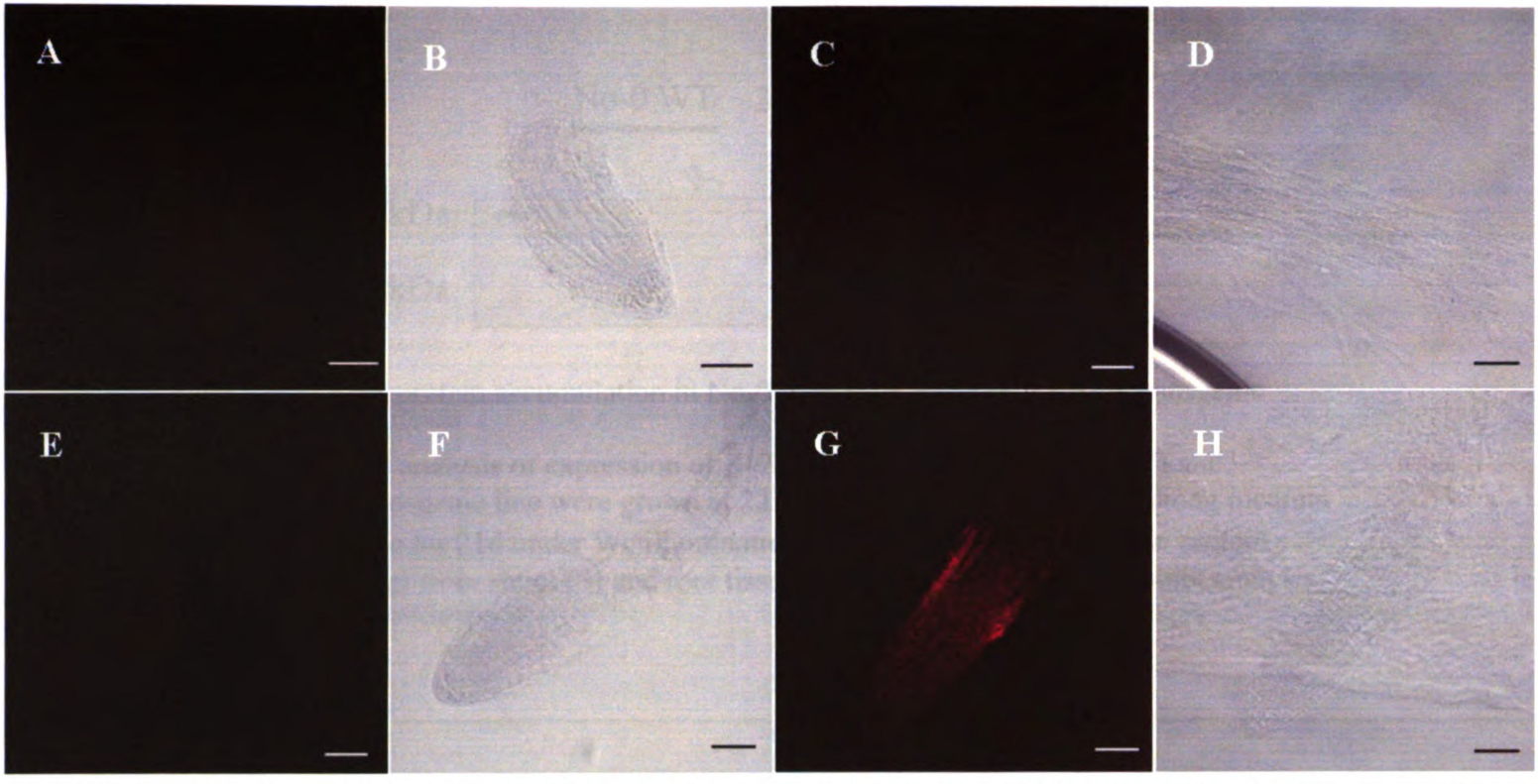

Figure 4.1 Whole-mount immunolocalization of BVR protein accumulation in roots of M0062>>UAS-BVR by Confocal laser scanning microscopy.
A through D: C24 WT, E through H: M0062>>UAS-BVR. (A) Buffer control, C24 WT roots incubated in 1XPBS without the anti-BVR primary antibody. (B) DIC image of A. (C) Negative control, C24 WT roots incubated with the anti-BVR primary antibody. (D) DIC image of C. (E) Buffer control, M0062>>UAS-BVR roots incubated in 1XPBS without the anti-BVR primary antibody. (F) DIC image of E. (G) M0062>>UAS-BVR roots incubated with the anti-BVR primary antibody. (H) DIC image of G. Images were collected on an inverted Axiovert 200 Zeiss LSM 510 Meta confocal laser scanning microscope (Carl Zeiss MicroImaging, Inc., NY) using differential interference contrast (DIC) optics and fluorescence excitation/emission filters using a 543-nm laser for excitation. Each image is a representative slice from a Z-series with 0.5-µm interval size and was captured using a 20x lens objective. Fluorescence images were collected using a 560-615 nm band pass filter. Bars = 50 µm.

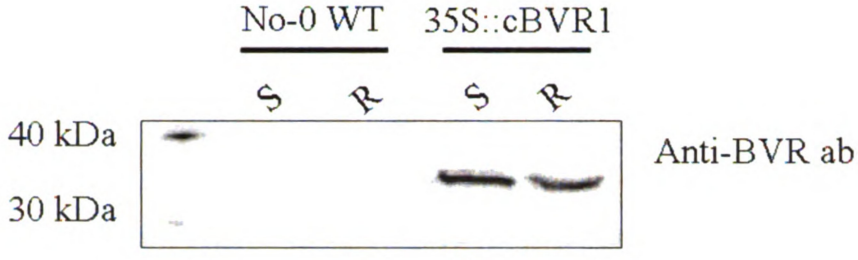

Figure 4.2 BVR protein accumulation in No-0 wild-type and 35S::cBVR1 transgenic seedlings.
For immunoblot analysis of expression of *BVR* in No-0 wild-type (No-0 WT) and 35S::cBVR1 transgenic line were grown at 22 ºC on liquid Murashige and Skoog medium with 1 % sucrose for 21d under Wc illumination of 100 µmol m^{-2} s^{-1}. Soluble protein extracts (~ 25 µg) from shoot (S) and root tissues (R) were used for immunoblot analysis with anti-BVR antibody

Figure 4.3 Photomorphogenesis of wild-type and *BVR*-expressing seedlings.
No-0 wild-type (No-0 WT), 35S::cBVR1, C24 wild-type (C24 WT) and M0062>>UAS-BVR lines were grown on Phytablend medium containing 1 % (w/v) Suc for 7 d at 22 °C under (A) Bc light of 30 μmol m^{-2} s^{-1}, (B) Rc light of 50 μmol m^{-2} s^{-1}, and (C) FRc light of 10 μmol m^{-2} s^{-1}. Bar = 1 cm.

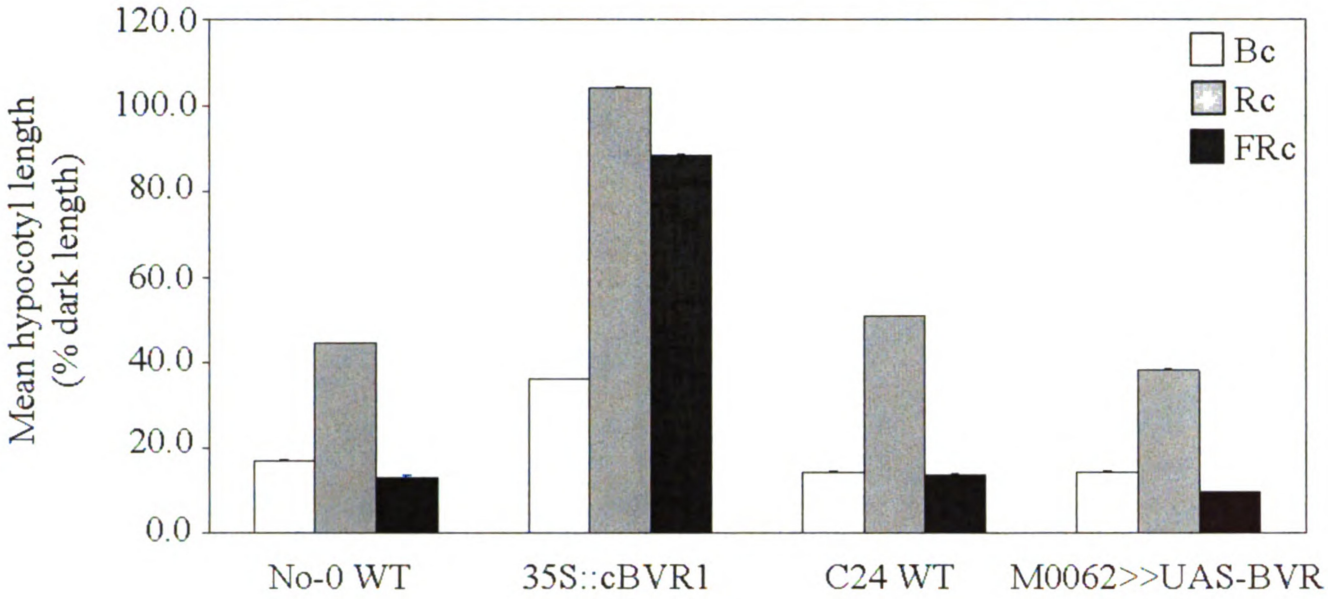

Figure 4.4 Mean hypocotyl lengths of wild-type and *BVR*-expressing seedlings.
No-0 wild-type (No-0 WT), 35S::cBVR1, C24 wild-type (C24 WT) and M0062>>UAS-BVR lines were grown on Phytablend medium containing 1 % (w/v) Suc for 7 d at 22 °C under Bc light of 30 µmol m^{-2} s^{-1} (white bars), Rc light of 50 µmol m^{-2} s^{-1} (gray bars), and FRc light of 10 µmol m^{-2} s^{-1} (black bars). Bars represent means (± SD) of 10 or more hypocotyls measured from 3 independent experiments.

Figure 4.5 Mean root lengths of wild-type, *BVR*-expressing and mutant seedlings. No-0 wild-type (No-0 WT), 35S::pBVR3, 35S::cBVR1,CAB3::pBVR2, MERI5::pBVR1, C24 wild-type (C24 WT), M0062>>UAS-BVR, Col-0 wild-type (Col-0 WT), *jar1*, *myc02-5*, C20 wild-type (C20 WT), *hy1-1* and *hy2-1* lines were grown on Phytablend medium containing 0.8 % Suc for 10 d at 22 °C under Wc light of 100 μmol m^{-2} s^{-1}. Data points represent means (± SD) of 6 or more roots measured from 6 independent experiments. Fold-difference values for root lengths determined for seedlings with respect to cognate wild-types are indicated.

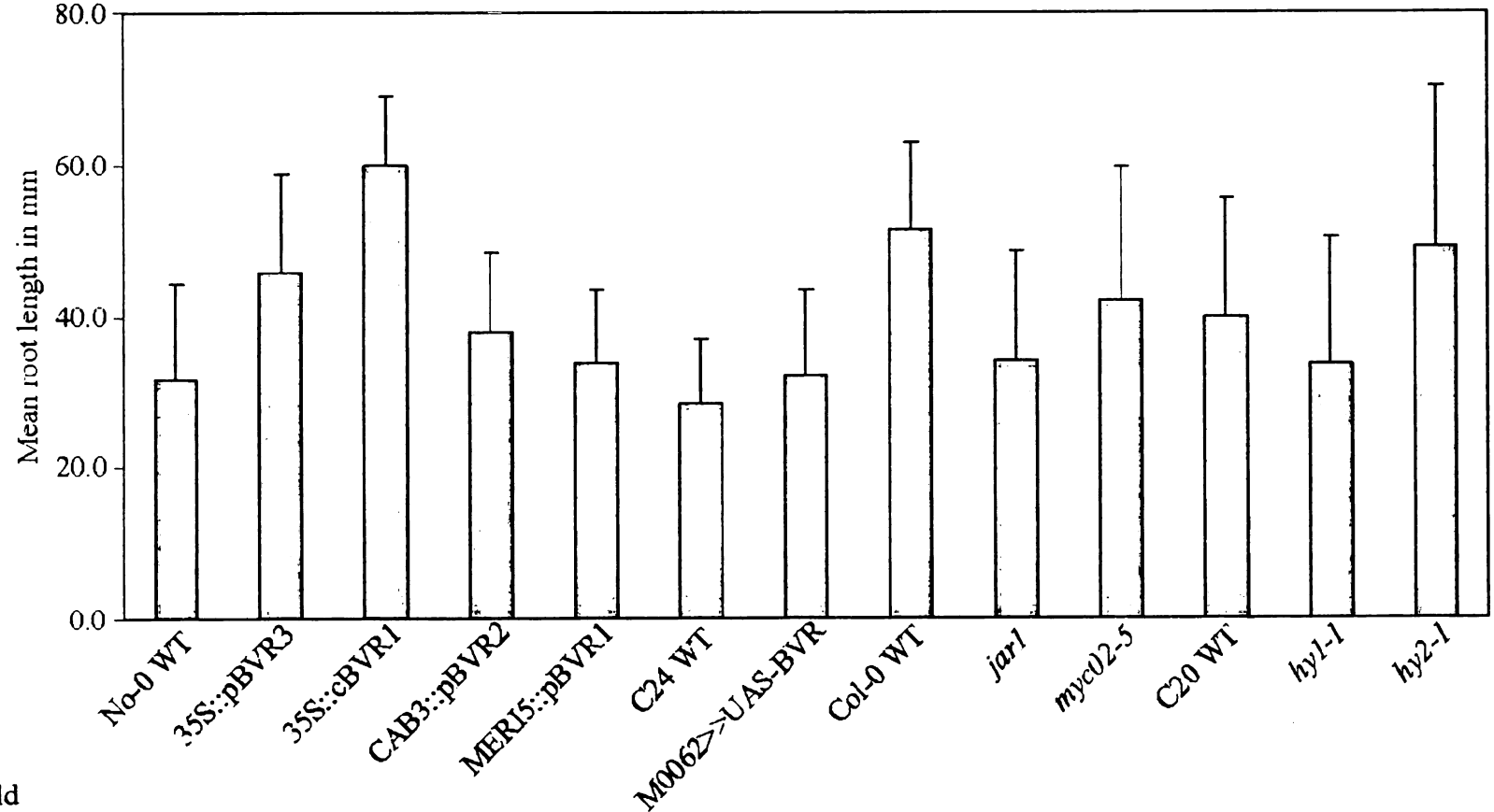

Fold difference: (relative to WT)	1.45	1.90	1.21	1.08		1.12			0.67	0.82		0.85	1.23

Figure 4.6 Mean root lengths of wild-type, *BVR*-expressing and mutant seedlings. No-0 wild-type (No-0 WT), 35S::pBVR3, 35S::cBVR1,CAB3::pBVR2, MERI5::pBVR1, C24 wild-type (C24 WT), M0062>>UAS-BVR, Col-0 wild-type (Col-0 WT), *jar1*, *myc02-5*, C20 wild-type (C20 WT), *hy1-1* and *hy2-1* lines were grown on Phytablend medium containing 0.8 % Suc with 20 μM jasmonic acid for 10 d at 22 °C under Wc light of 100 μmol m^{-2} s^{-1}. Data points represent means of 6 or more roots measured from 6 independent experiments. Fold-difference values for root lengths determined for seedlings with respect to cognate wild-types are indicated.

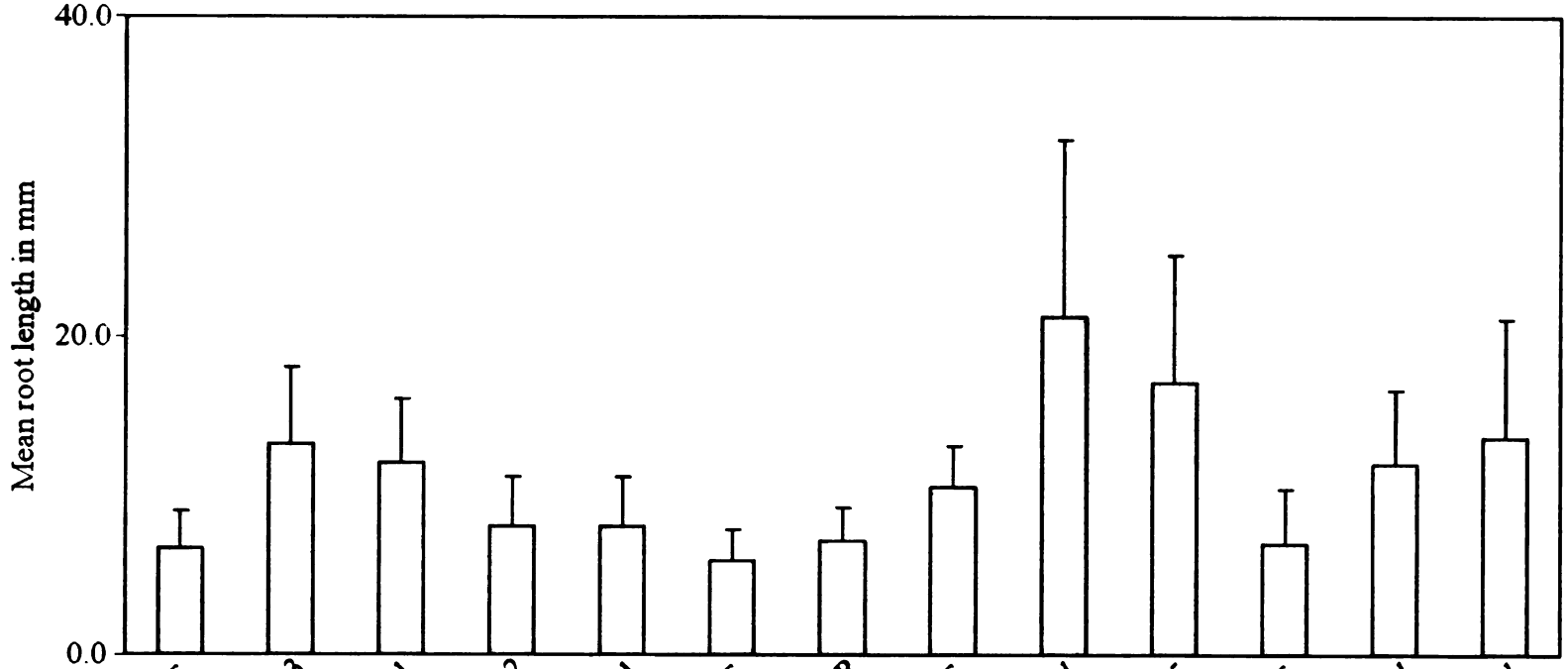

	No-0 WT	35S::pBVR3	35S::cBVR1	CAB3::pBVR2	MERI5::pBVR1	C24 WT	M0062>>UAS-BVR	Col-0 WT	*jar1*	*myc02-5*	C20 WT	*hy1-1*	*hy2-1*
Fold difference: (relative to WT)	2.01	1.82	1.22	1.21		1.21			2.00	1.61		1.73	1.97

Table 2 Fold-difference in root lengths of wild-type, *BVR*-expressing and mutant seedlings.
Fold-difference values for root lengths determined for seedlings on 0 μM JA relative to 20 μM JA are indicated.

Plant line	Fold difference (-JA/+JA) (relative sensitivity to MeJA)
No-0 WT	4.75
35S::pBVR3	3.45
35S::cBVR1	4.95
CAB3::pBVR2	4.74
MERI5::pBVR1	4.23
C24 WT	4.80
M0062>>UAS-BVR	4.46
Col-0 WT	4.85
jar1	1.62
myc02-5	2.48
C20 WT	5.76
hy1-1	2.82
hy2-1	3.60

Figure 4.7 Relative expression levels of *OPR3* in wild-type, *BVR*-expressing and mutant seedlings.
No-0 wild-type (No-0 WT), 35S::pBVR3, 35S::cBVR1,CAB3::pBVR2, MERI5::pBVR1, C24 wild-type (C24 WT), M0062>>UAS-BVR, Col-0 wild-type (Col-0 WT), *jar1*, *myc02-5*, C20 wild-type (C20 WT), *hy1-1* and *hy2-1* lines were grown on Phytablend medium containing 0.8 % Suc with 0 or 20 μM jasmonic acid for 10 d at 22 °C under Wc light of 100 μmol m^{-2} s^{-1}. Expression of *UBC21* (*At5g25760*) was analyzed as a reference. Bars, black bars, -JA and white bars, + $JA_{20\ \mu M}$. Quantification by qRT-PCR was performed with 3 independent experiments.

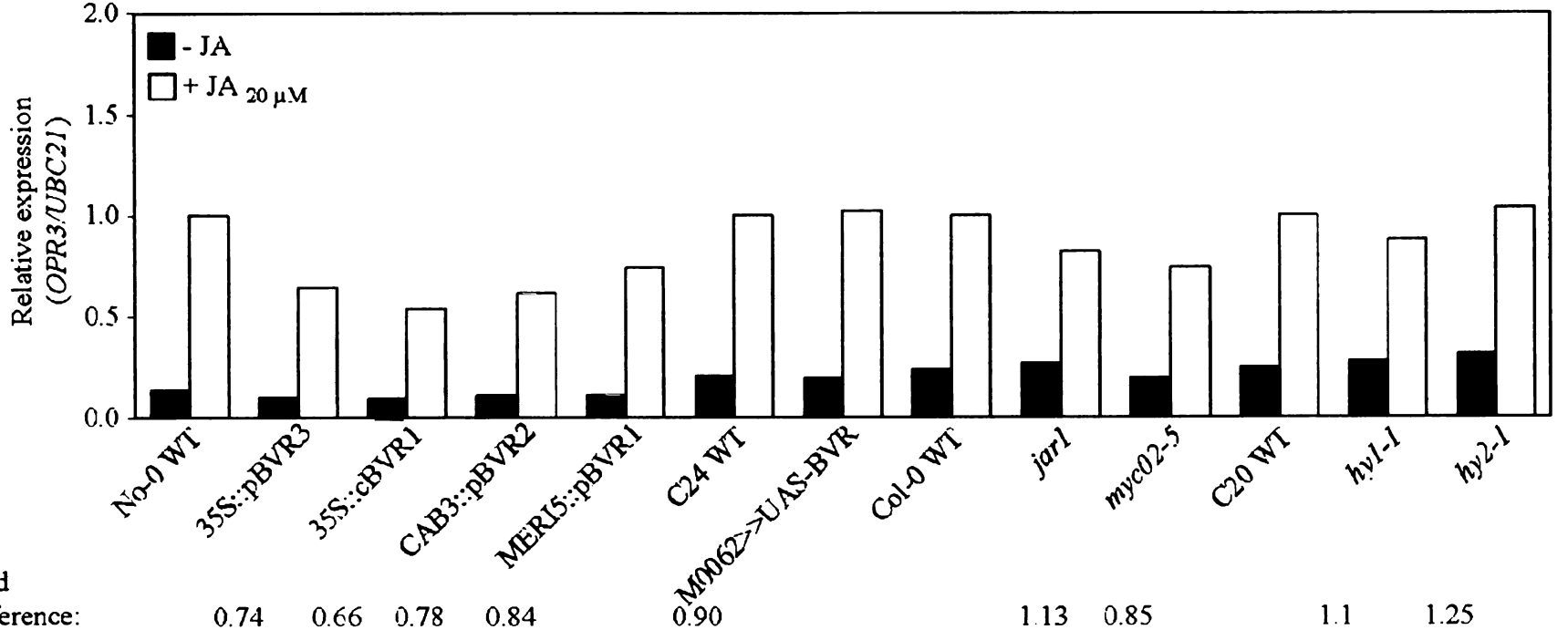

Fold difference: (relative to WT, -JA)	0.74	0.66	0.78	0.84	0.90	1.13	0.85	1.1	1.25
Fold difference: (relative to WT, +JA)	0.64	0.54	0.62	0.74	1.02	0.82	0.75	0.88	1.04

Figure 4.8 Relative expression levels of *VSP1* in wild-type, *BVR*-expressing and mutant seedlings.
No-0 wild-type (No-0 WT), 35S::pBVR3, 35S::cBVR1,CAB3::pBVR2, MERI5::pBVR1, C24 wild-type (C24 WT), M0062>>UAS-BVR, Col-0 wild-type (Col-0 WT), *jar1*, *myc02-5*, C20 wild-type (C20 WT), *hy1-1* and *hy2-1* lines were grown on Phytablend medium containing 0.8 % Suc with 0 or 20 μM jasmonic acid for 10 d at 22 °C under Wc light of 100 μmol m^{-2} s^{-1}. Expression of *UBC21* (*At5g25760*) was analyzed as a reference. Bars, black bars, -JA and white bars, + $JA_{20\ \mu M}$. Quantification by qRT-PCR was performed with 3 independent experiments.

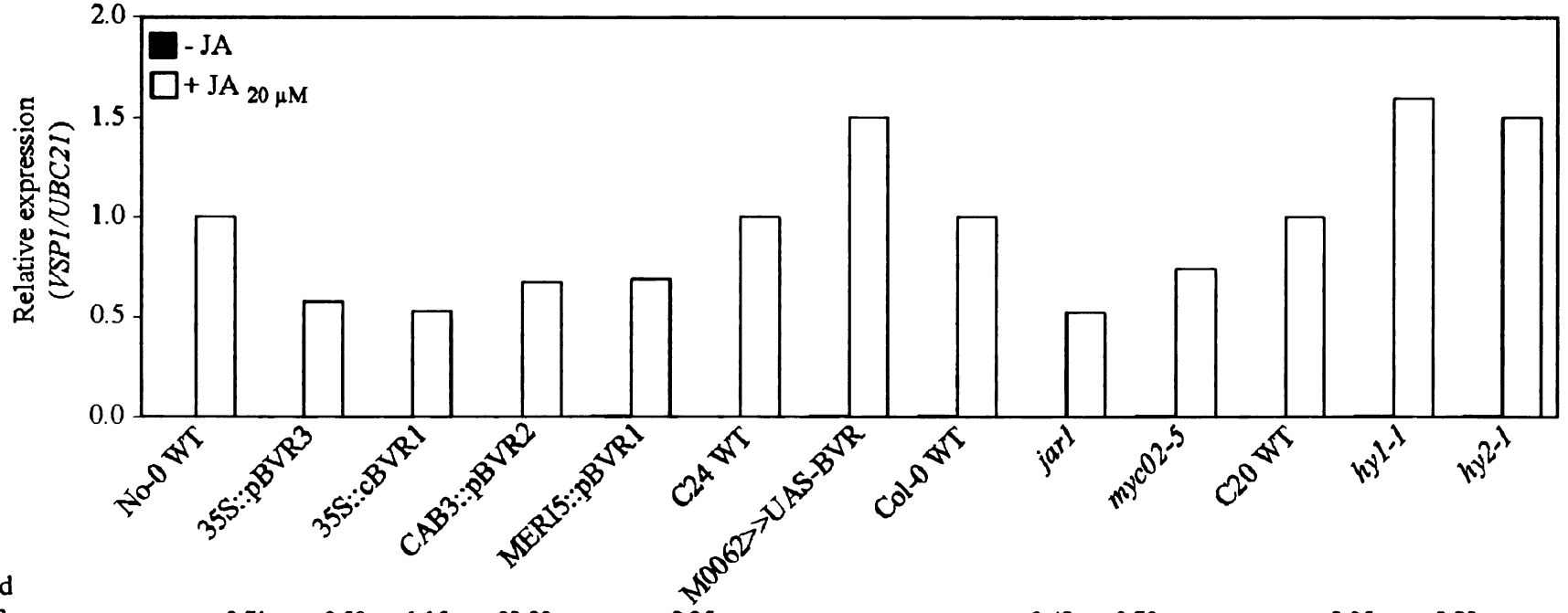

Fold difference: (relative to WT, -JA)	0.71	0.59	1.15	02.20	3.35	0.48	0.79	2.05	2.82
Fold difference: (relative to WT, +JA)	0.58	0.53	0.67	0.69	1.50	0.52	0.74	1.59	1.50

4.5 References

Alabadi, D., and Blazquez, M. A. (2009). Molecular interactions between light and hormone signaling to control plant growth. *Plant Mol Biol* **69**(4), 409-417.

Avanci, N. C., Luche, D. D., Goldman, G. H., and Goldman, M. H. (2010). Jasmonates are phytohormones with multiple functions, including plant defense and reproduction. *Genet Mol Res* **9**(1), 484-505.

Ballare, C. L. (2009). Illuminated behaviour: phytochrome as a key regulator of light foraging and plant anti-herbivore defence. *Plant Cell Environ* **32**(6), 713-725.

Ballare, C. L., Scopel, A. L., and Sanchez, R. A. (1990). Far-red radiation reflected from adjacent leaves: an early signal of competition in plant canopies. *Science* **247**(4940), 329-332.

Bou-Torrent, J., Roig-Villanova, I., and Martinez-Garcia, J. F. (2008). Light signaling: back to space. *Trends Plant Sci* **13**(3), 108-114.

Browse, J. (2005). Jasmonate: an oxylipin signal with many roles in plants. *Vitam Horm* **72**, 431-456.

Browse, J. (2009). Jasmonate passes muster: a receptor and targets for the defense hormone. *Annu Rev Plant Biol* **60**, 183-205.

Cashmore, A. R., Jarillo, J. A., Wu, Y. J., and Liu, D. (1999). Cryptochromes: blue light receptors for plants and animals. *Science* **284**(5415), 760-765.

Chen, I. C., Huang, I. C., Liu, M. J., Wang, Z. G., Chung, S. S., and Hsieh, H. L. (2007). Glutathione S-transferase interacting with far-red insensitive 219 is involved in phytochrome A-mediated signaling in Arabidopsis. *Plant Physiol* **143**(3), 1189-1202.

Chini, A., Fonseca, S., Fernandez, G., Adie, B., Chico, J. M., Lorenzo, O., Garcia-Casado, G., Lopez-Vidriero, I., Lozano, F. M., Ponce, M. R., Micol, J. L., and Solano, R. (2007). The JAZ family of repressors is the missing link in jasmonate signalling. *Nature* **448**(7154), 666-671.

Chory, J., Chatterjee, M., Cook, R. K., Elich, T., Fankhauser, C., Li, J., Nagpal, P., Neff, M., Pepper, A., Poole, D., Reed, J., and Vitart, V. (1996). From seed germination to flowering, light controls plant development via the pigment phytochrome. *Proc Natl Acad Sci U S A* **93**(22), 12066-12071.

Chung, H. S., Koo, A. J., Gao, X., Jayanty, S., Thines, B., Jones, A. D., and Howe, G. A. (2008). Regulation and function of Arabidopsis JASMONATE ZIM-domain genes in response to wounding and herbivory. *Plant Physiol* **146**(3), 952-964.

Clough, S. J., and Bent, A. F. (1998). Floral dip: a simplified method for Agrobacterium-mediated transformation of *Arabidopsis thaliana*. *The Plant Journal* **16,** 735-743.

Correll, M. J., Coveney, K. M., Raines, S. V., Mullen, J. L., Hangarter, R. P., and Kiss, J. Z. (2003). Phytochromes play a role in phototropism and gravitropism in Arabidopsis roots. *Adv Space Res* **31**(10), 2203-2210.

Correll, M. J., and Kiss, J. Z. (2005). The roles of phytochromes in elongation and gravitropism of roots. *Plant Cell Physiol* **46**(2), 317-323.

Davis, S. J., Bhoo, S. H., Durski, A. M., Walker, J. M., and Vierstra, R. D. (2001). The heme-oxygenase family required for phytochrome chromophore biosynthesis is necessary for proper photomorphogenesis in higher plants. *Plant Physiol* **126**(2), 656-669.

Davis, S. J., Kurepa, J., and Vierstra, R. D. (1999). The *Arabidopsis thaliana* HY1 locus, required for phytochrome-chromophore biosynthesis, encodes a protein related to heme oxygenases. *Proc Natl Acad Sci U S A* **96**(11), 6541-6546.

De Simone, S., Oka, Y., and Inoue, Y. (2000). Effect of Light on Root Hair Formation in *Arabidopsis thaliana* Phytochrome-Deficient Mutants. *Journal of Plant Research* **113**(1), 63-69.

Devoto, A., Nieto-Rostro, M., Xie, D., Ellis, C., Harmston, R., Patrick, E., Davis, J., Sherratt, L., Coleman, M., and Turner, J. G. (2002). COI1 links jasmonate signalling and fertility to the SCF ubiquitin-ligase complex in Arabidopsis. *Plant J* **32**(4), 457-466.

Emborg, T. J., Walker, J. M., Noh, B., and Vierstra, R. D. (2006). Multiple heme oxygenase family members contribute to the biosynthesis of the phytochrome chromophore in Arabidopsis. *Plant Physiol* **140**(3), 856-868.

Feldman, L. J., and Briggs, W. R. (1987). Light-regulated gravitropism in seedling roots of maize. *Plant Physiol* **83,** 241-243.

Feys, B., Benedetti, C. E., Penfold, C. N., and Turner, J. G. (1994). Arabidopsis Mutants Selected for Resistance to the Phytotoxin Coronatine Are Male Sterile, Insensitive to Methyl Jasmonate, and Resistant to a Bacterial Pathogen. *Plant Cell* **6**(5), 751-759.

Fonseca, S., Chini, A., Hamberg, M., Adie, B., Porzel, A., Kramell, R., Miersch, O., Wasternack, C., and Solano, R. (2009). (+)-7-iso-Jasmonoyl-L-isoleucine is the endogenous bioactive jasmonate. *Nat Chem Biol* **5**(5), 344-350.

Franklin, K. A., Praekelt, U., Stoddart, W. M., Billingham, O. E., Halliday, K. J., and Whitelam, G. C. (2003). Phytochromes B, D, and E act redundantly to control multiple physiological responses in Arabidopsis. *Plant Physiol* **131**(3), 1340-1346.

Franklin, K. A., and Quail, P. H. (2010). Phytochrome functions in Arabidopsis development. *J Exp Bot* **61**(1), 11-24.

Franklin, K. A., and Whitelam, G. C. (2004). Light signals, phytochromes and cross-talk with other environmental cues. *J Exp Bot* **55**(395), 271-276.

Guranowski, A., Miersch, O., Staswick, P. E., Suza, W., and Wasternack, C. (2007). Substrate specificity and products of side-reactions catalyzed by jasmonate:amino acid synthetase (JAR1). *FEBS Lett* **581**(5), 815-820.

Harrison, S. J., Mott, E. K., Parsley, K., Aspinall, S., Gray, J. C., and Cottage, A. (2006). A rapid and robust method of identifying transformed *Arabidopsis thaliana* seedlings following floral dip transformation. *Plant Methods* **2**, 19.

Haseloff, J. (1999). GFP variants for multispectral imaging of living cells. *Methods Cell Biol* **58**, 139-151.

Hsieh, H. L., Okamoto, H., Wang, M., Ang, L. H., Matsui, M., Goodman, H., and Deng, X. W. (2000). FIN219, an auxin-regulated gene, defines a link between phytochrome A and the downstream regulator COP1 in light control of Arabidopsis development. *Genes Dev* **14**(15), 1958-1970.

Jaillais, Y., and Chory, J. (2010). Unraveling the paradoxes of plant hormone signaling integration. *Nat Struct Mol Biol* **17**(6), 642-645.

Jiao, Y., Lau, O. S., and Deng, X. W. (2007). Light-regulated transcriptional networks in higher plants. *Nat Rev Genet* **8**(3), 217-230.

Kidd, B. N., Edgar, C. I., Kumar, K. K., Aitken, E. A., Schenk, P. M., Manners, J. M., and Kazan, K. (2009). The mediator complex subunit PFT1 is a key regulator of jasmonate-dependent defense in Arabidopsis. *Plant Cell* **21**(8), 2237-2252.

Kiss, J. Z., Mullen, J. L., Correll, M. J., and Hangarter, R. P. (2003). Phytochromes A and B mediate red-light-induced positive phototropism in roots. *Plant Physiol* **131**(3), 1411-1417.

Koda, Y. (1997). Possible involvement of jasmonates in various morphogenic events. *Physiologia Plantarum* **100**(3), 639-646.

Koo, A. J., Gao, X., Jones, A. D., and Howe, G. A. (2009). A rapid wound signal activates the systemic synthesis of bioactive jasmonates in Arabidopsis. *Plant J* **59**(6), 974-986.

Kurata, T., and Yamamoto, K. T. (1997). Light-stimulated root elongation in *Arabidopsis thaliana*. *J. Plant Physiol.* **151** (3), 346-351.

Lagarias, D. M., Crepeau, M. W., Maines, M. D., and Lagarias, J. C. (1997). Regulation of photomorphogenesis by expression of mammalian biliverdin reductase in transgenic Arabidopsis plants. *Plant Cell* **9**(5), 675-688.

Laplaze, L., Parizot, B., Baker, A., Ricaud, L., Martiniere, A., Auguy, F., Franche, C., Nussaume, L., Bogusz, D., and Haseloff, J. (2005). GAL4-GFP enhancer trap lines for genetic manipulation of lateral root development in *Arabidopsis thaliana*. *J Exp Bot* **56**(419), 2433-2442.

Lauter, F. R. (1996). Root-specific expression of the LeRse-1 gene in tomato is induced by exposure of the shoot to light. *Mol Gen Genet* **252**(6), 751-754.

Li, C., Schilmiller, A. L., Liu, G., Lee, G. I., Jayanty, S., Sageman, C., Vrebalov, J., Giovannoni, J. J., Yagi, K., Kobayashi, Y., and Howe, G. A. (2005). Role of beta-oxidation in jasmonate biosynthesis and systemic wound signaling in tomato. *Plant Cell* **17**(3), 971-986.

Lorenzo, O., Chico, J. M., Sanchez-Serrano, J. J., and Solano, R. (2004). JASMONATE-INSENSITIVE1 encodes a MYC transcription factor essential to discriminate between different jasmonate-regulated defense responses in Arabidopsis. *Plant Cell* **16**(7), 1938-5190.

Ma, L., Sun, N., Liu, X., Jiao, Y., Zhao, H., and Deng, X. W. (2005). Organ-specific expression of Arabidopsis genome during development. *Plant Physiol* **138**(1), 80-91.

Mandoli, D. F., and Briggs, W. R. (1982). The photoperceptive sites and the function of tissue light-piping in photomorphogenesis of etiolated oat seedlings. *Plant, Cell & Environment* **5**(2), 137-145.

Mandoli, D. F., and Briggs, W. R. (1984). Fiber-optic plant tissues: Spectral dependence in dark-grown and green tissues. *Photochemistry and Photobiology* **39**(3), 419-424.

Mandoli, D. F., Ford, G. A., Waldron, L. J., Nemson, J. A., and Briggs, W. R. (1990). Some spectral properties of several soil types: implications for photomorphogenesis. *Plant, Cell & Environment* **13**(3), 287-294.

Matthes, M. C., Pickett, J. A., and Napier, J. A. (2008). Natural variation in responsiveness of *Arabidopsis thaliana* to methyl jasmonate is developmentally regulated. *Planta* **228**(6), 1021-1028.

Molas, M. L., Kiss, J. Z., and Correll, M. J. (2006). Gene profiling of the red light signalling pathways in roots. *J Exp Bot* **57**(12), 3217-3229.

Montgomery, B. L. (2008). Right place, right time: Spatiotemporal light regulation of plant growth and development. *Plant Signal Behav* **3**(12), 1053-1060.

Montgomery, B. L., Yeh, K. C., Crepeau, M. W., and Lagarias, J. C. (1999). Modification of distinct aspects of photomorphogenesis via targeted expression of mammalian biliverdin reductase in transgenic Arabidopsis plants. *Plant Physiol* **121**(2), 629-639.

Moreno, J. E., Tao, Y., Chory, J., and Ballare, C. L. (2009). Ecological modulation of plant defense via phytochrome control of jasmonate sensitivity. *Proc Natl Acad Sci U S A* **106**(12), 4935-4940.

Mueller, M. J., Brodschelm, W., Spannagl, E., and Zenk, M. H. (1993). Signaling in the elicitation process is mediated through the octadecanoid pathway leading to jasmonic acid. *Proc Natl Acad Sci U S A* **90**(16), 7490-7494.

Muramoto, T., Kohchi, T., Yokota, A., Hwang, I., and Goodman, H. M. (1999). The Arabidopsis photomorphogenic mutant hy1 is deficient in phytochrome chromophore biosynthesis as a result of a mutation in a plastid heme oxygenase. *Plant Cell* **11**(3), 335-348.

Neff, M. M., Fankhauser, C., and Chory, J. (2000). Light: an indicator of time and place. *Genes Dev* **14**(3), 257-71.

Okada, K., and Shimura, Y. (1992). Mutational analysis of root gravitropism and phototropism of *Arabidopsis thaliana* seedlings. *Functional Plant Biology* **19**(4), 439-448.

Quail, P. H. (2002). Phytochrome photosensory signalling networks. *Nat Rev Mol Cell Biol* **3**(2), 85-93.

Reed, J. W., Nagpal, P., Poole, D. S., Furuya, M., and Chory, J. (1993). Mutations in the gene for the red/far-red light receptor phytochrome B alter cell elongation and physiological responses throughout Arabidopsis development. *Plant Cell* **5**(2), 147-157.

Robson, F., Okamoto, H., Patrick, E., Harris, S. R., Wasternack, C., Brearley, C., and Turner, J. G. (2010). Jasmonate and phytochrome A signaling in Arabidopsis wound and shade responses are integrated through JAZ1 stability. *Plant Cell* **22**(4), 1143-1160.

Salisbury, F. J., Hall, A., Grierson, C. S., and Halliday, K. J. (2007). Phytochrome coordinates Arabidopsis shoot and root development. *Plant J* **50**(3), 429-38.

Sauer, M., Paciorek, T., Benkova, E., and Friml, J. (2006). Immunocytochemical techniques for whole-mount in situ protein localization in plants. *Nat Protoc* **1**(1), 98-103.

Schepens, I., Duek, P., and Fankhauser, C. (2004). Phytochrome-mediated light signalling in Arabidopsis. *Curr Opin Plant Biol* **7**(5), 564-569.

Seo, H. S., Song, J. T., Cheong, J. J., Lee, Y. H., Lee, Y. W., Hwang, I., Lee, J. S., and Choi, Y. D. (2001). Jasmonic acid carboxyl methyltransferase: a key enzyme for jasmonate-regulated plant responses. *Proc Natl Acad Sci U S A* **98**(8), 4788-4793.

Seo, M., Nambara, E., Choi, G., and Yamaguchi, S. (2009). Interaction of light and hormone signals in germinating seeds. *Plant Mol Biol* **69**(4), 463-472.

Shimizu, H., Shinomura, T., and Yamamoto, K. T. (2010). Similarities and differences between phytochrome-mediated growth inhibition of coleoptiles and seminal roots in rice seedlings. *Plant Signal Behav* **5**(2), 134-135.

Shimizu, H., Tanabata, T., Xie, X., Inagaki, N., Takano, M., Shinomura, T., and Yamamoto, K. T. (2009). Phytochrome-mediated growth inhibition of seminal roots in rice seedlings. *Physiol Plant* **137**(3), 289-297.

Somers, D. E., and Quail, P. H. (1995). Phytochrome-Mediated Light Regulation of PHYA- and PHYB-GUS Transgenes in *Arabidopsis thaliana* Seedlings. *Plant Physiol* **107**(2), 523-534.

Staswick, P. E., Su, W., and Howell, S. H. (1992). Methyl jasmonate inhibition of root growth and induction of a leaf protein are decreased in an *Arabidopsis thaliana* mutant. *Proc Natl Acad Sci U S A* **89**(15), 6837-6840.

Staswick, P. E., and Tiryaki, I. (2004). The oxylipin signal jasmonic acid is activated by an enzyme that conjugates it to isoleucine in Arabidopsis. *Plant Cell* **16**(8), 2117-2127.

Staswick, P. E., Tiryaki, I., and Rowe, M. L. (2002). Jasmonate response locus JAR1 and several related Arabidopsis genes encode enzymes of the firefly luciferase superfamily that show activity on jasmonic, salicylic, and indole-3-acetic acids in an assay for adenylation. *Plant Cell* **14**(6), 1405-1415.

Sun, Q., Yoda, K., and Suzuki, H. (2005). Internal axial light conduction in the stems and roots of herbaceous plants. *J Exp Bot* **56**(409), 191-203.

Sun, Q., Yoda, K., Suzuki, M., and Suzuki, H. (2003). Vascular tissue in the stem and roots of woody plants can conduct light. *J Exp Bot* **54**(387), 1627-1635.

Suza, W. P., and Staswick, P. E. (2008). The role of JAR1 in Jasmonoyl-L-isoleucine production during Arabidopsis wound response. *Planta* **227**(6), 1221-1232.

Tester, M., and Morris, C. (1987). The penetration of light through soil. *Plant, Cell & Environment* **10**(4), 281-286.

Thines, B., Katsir, L., Melotto, M., Niu, Y., Mandaokar, A., Liu, G., Nomura, K., He, S. Y., Howe, G. A., and Browse, J. (2007). JAZ repressor proteins are targets of the SCF(COI1) complex during jasmonate signalling. *Nature* **448**(7154), 661-665.

Tóth, R., Kevei, E., Hall, A., Millar, A. J., Nagy, F., and Kozma-Bognar, L. (2001). Circadian clock-regulated expression of phytochrome and cryptochrome genes in Arabidopsis. *Plant Physiol* **127**(4), 1607-1616.

Warnasooriya, S. N., and Montgomery, B. L. (2009). Detection of spatial-specific phytochrome responses using targeted expression of biliverdin reductase in Arabidopsis. *Plant Physiol* **149**(1), 424-343.

Warnasooriya, S. N., and Montgomery, B. L. (in press). Using Transgenic Modulation of Protein Accumulation to Probe Protein Signaling Networks in *Arabidopsis thaliana,* Plant Biotechnology and Transgenic Research, Bentham Science Publishers, Oak Park, IL.

Wasternack, C. (2007). Jasmonates: an update on biosynthesis, signal transduction and action in plant stress response, growth and development. *Ann Bot* **100**(4), 681-697.

Wasternack, C., and Hause, B. (2002). Jasmonates and octadecanoids: signals in plant stress responses and development. *Prog Nucleic Acid Res Mol Biol* **72**, 165-221.

Wu, C., Li, X., Yuan, W., Chen, G., Kilian, A., Li, J., Xu, C., Li, X., Zhou, D. X., Wang, S., and Zhang, Q. (2003). Development of enhancer trap lines for functional analysis of the rice genome. *Plant J* **35**(3), 418-427.

Xie, D. X., Feys, B. F., James, S., Nieto-Rostro, M., and Turner, J. G. (1998). COI1: an Arabidopsis gene required for jasmonate-regulated defense and fertility. *Science* **280**(5366), 1091-1094.

Xu, L., Liu, F., Lechner, E., Genschik, P., Crosby, W. L., Ma, H., Peng, W., Huang, D., and Xie, D. (2002). The SCF(COI1) ubiquitin-ligase complexes are required for jasmonate response in Arabidopsis. *Plant Cell* **14**(8), 1919-1935.

Yadav, V., Mallappa, C., Gangappa, S. N., Bhatia, S., and Chattopadhyay, S. (2005). A basic helix-loop-helix transcription factor in Arabidopsis, MYC2, acts as a repressor of blue light-mediated photomorphogenic growth. *Plant Cell* **17**(7), 1953-1966.

Yan, J., Zhang, C., Gu, M., Bai, Z., Zhang, W., Qi, T., Cheng, Z., Peng, W., Luo, H., Nan, F., Wang, Z., and Xie, D. (2009). The Arabidopsis CORONATINE INSENSITIVE1 protein is a jasmonate receptor. *Plant Cell* **21**(8), 2220-2236.

Yan, Y., Stolz, S., Chetelat, A., Reymond, P., Pagni, M., Dubugnon, L., and Farmer, E. E. (2007). A downstream mediator in the growth repression limb of the jasmonate pathway. *Plant Cell* **19**(8), 2470-2483.

Zhai, Q., Li, C. B., Zheng, W., Wu, X., Zhao, J., Zhou, G., Jiang, H., Sun, J., Lou, Y., and Li, C. (2007). Phytochrome chromophore deficiency leads to overproduction of jasmonic acid and elevated expression of jasmonate-responsive genes in Arabidopsis. *Plant Cell Physiol* **48**(7), 1061-1071.

Appendix

Investigating tissue- and organ-specific phytochrome responses using Fluorescence Activated Cell Sorting (FACS)-assisted cell-type specific expression profiling in *Arabidopsis thaliana*.

Most of the work included in the appendix was published in the Journal of Visualized Experiments.

Warnasooriya SN and Montgomery BL, (2010), Investigating Tissue- and Organ-specific Phytochrome Responses using FACS-assisted Cell-type Specific Expression Profiling in *Arabidopsis thaliana*, Journal of Visualized Experiments, 39. https://www.jove.com/index/details.stp?id=1925, doi: 10.3791/1925

A1 Overview

Phytochromes are the red/far-red light-absorbing photoreceptor class and they mediate unique and overlapping functions in all higher plant systems in which they have been studied (Franklin and Quail, 2010). In the life cycle of Arabidopsis, an array of light responses is regulated by phytochromes and such responses are often localized to specific plant tissues or organs (Montgomery, 2008) and indicate the existence of spatial-specific phytochrome-dependent responses. Even though much progress on the discovery and elucidation of individual and redundant phytochrome functions have been made through mutational analyses, conclusive evidence on discrete photoperceptive sites and the molecular mechanisms of localized pools of phytochromes that mediate spatial-specific phytochrome responses still remain elusive. Based on the hypotheses that specific sites of phytochrome photoperception regulate tissue- and organ-specific aspects of photomorphogenesis, and that localized phytochrome pools engage distinct subsets of downstream target genes in intracellular and/or in cell-to-cell signaling, a biochemical approach to selectively reduce functional phytochromes in a tissue- and organ-specific manner within transgenic plants was developed. The biochemical approach is based on a bipartite enhancer-trap strategy that results in transactivation of the expression of a gene under control of the Upstream Activation Sequence (UAS) element by the transcriptional activator GAL4 (Laplaze et al., 2005). In the UAS-BVR parent, the biliverdin reductase (*BVR*) gene under the control of the UAS is silently maintained in the absence of GAL4-mediated transactivation (Costigan, Warnasooriya and Montgomery, unpublished data). Genetic crosses between a UAS-BVR transgenic line and a GAL4-GFP enhancer trap line (Haseloff, 1999) result in specific expression of the *BVR* gene in cells marked by

GFP expression (Costigan, Warnasooriya and Montgomery, unpublished data). BVR accumulation in Arabidopsis plants results in phytochrome chromophore deficiency at specific locations *in vivo* (Lagarias et al., 1997; Montgomery et al., 1999; Warnasooriya and Montgomery, 2009). Thus, progeny transgenic plants that have been produced through genetic crosses display GAL4-dependent *GFP* expression, as well as activation of the *BVR* gene that leads to biochemical inactivation of phytochrome (Figure A1). Through comparative photobiological and molecular genetic analyses of *BVR* transgenic lines, insight into tissue- and organ-specific phytochrome-mediated responses that are associated with corresponding sites of photoperception can be gained. Putative downstream target genes involved in mediating spatial-specific phytochrome responses can be identified by fluorescence activated cell sorting (FACS) of GFP-positive, enhancer-trap-induced *BVR*-expressing plant protoplasts followed by cell-type-specific gene expression profiling by microarray analysis. FACS-mediated cell-type-specific expression profiling will expand our understanding of sites of light perception, the mechanisms through which various tissues or organs cooperate in light-regulated plant growth and development, and advance the molecular dissection of complex phytochrome-mediated cell-to-cell signaling cascades.

A2 Materials and Methods

A2.1 Generation of J0571>>UAS-BVR

UAS-BVR plants at T3 generation were obtained as described in section 4.2.1. T3 plants of UAS-BVR were crossed with the J0571 enhancer trap line (Figure A1), which exhibits *GFP* expression in cortex/endodermis including initials, with a broad pattern of

expression in hypocotyl and cotyledons (Figure A2; Haseloff, 1999). Selection of F1 seedlings based on kanamycin resistance and PCR screening was performed as described in section 4.2.1. F1 seedlings that were positive in PCR with *BVR*- and *GAL4*-specific primer sets were transferred to soil to obtain F2 seeds and to progress to the F3 generation. F3 seeds of the UAS-BVRXJ0571 cross were used for subsequent analyses (J0571>>UAS-BVR).

A2.2 Plant Growth

Wild-type (C24 WT), parental enhancer trap line (J0571) and confirmed J0571>>UAS-BVR progeny isolated as described in section A2.1, were sown on soil, i.e. ~ 2000 sterilized seeds per line. J1071, which exhibits *GFP* expression in vascular/dermal tissue throughout the seedling (Figure A2), was included as a control to determine the efficiency of FACS where *GFP* expression is observed in limited tissues. C24 WT, J0571, J1071 and J0571>>UAS-BVR plants were grown for 5 weeks on soil under white illumination of 100 μmol m^{-2} s^{-1} at 22 °C and 70 % humidity.

A2.3 Reagent Preparation

TEX buffer was prepared as follows. For 1 liter TEX buffer, the following components: 3.1 g of Gamborg's B5 salts (Catalog No. G5768, Sigma, MO), 0.5 g of 2-(N-morpholino) ethanesulfonic acid (MES; at 2.56 mM, Catalog No. M3671, Sigma, MO), 0.75 g of calcium chloride dihydrate ($CaCl_2.2H_2O$; at 6.75 mM, Catalog No. C2536, Sigma, MO), 0.25 g of ammonium nitrate (NH_4NO_3; at 3.12 mM, Catalog No. ,

A3795, Sigma, MO), 136.9 g of sucrose (at 0.4 M, Catalog No. 4072-05, J.T. Baker, NJ) were weighed and dissolved completely in ~ 900 mL of deionized, distilled water (ddH_2O) and the pH was adjusted to 5.7 with 1 M KOH. Final volume was adjusted to 1 liter and was filter sterilized with a 0.2 μm bottle-top filter connected to a vacuum pump. 10X leaf digestion stock solution was prepared by dissolving 2 % (w/v) Macerozyme R-10 (Catalog No. MSPC 0930, SERVA Electrophoresis GmbH, Crescent Chemical Company, NY), 4 % (w/v) Cellulase "Onozuka" R-10 (Catalog No. PTC 001, SERVA Electrophoresis GmbH, Crescent Chemical Company, NY) in TEX buffer followed by filter sterilization with 0.2 μm filter. 5 mL aliquots were frozen at -80 °C. 1X leaf digestion solution was prepared by adding 45 mL fresh TEX buffer to a 5 mL aliquot of 10X leaf digestion stock solution prior to use.

A2.4 Leaf Protoplast Isolation

Leaf protoplast isolation protocol was adapted from Denecke and Vitale (1995). Green, healthy leaves were collected from 5-week-old plants (~ 250 mL of leaves loosely packed in a beaker) and rinsed 4x with ~ 40 mL ddH_2O, followed by rinsing twice with sterile ddH_2O. Using a #20 scalpel, leaves were cut into thin strips and leaf tissue strips were divided equally into two 50 mL sterile plastic tubes. The 1X leaf digestion solution was prepared as described in section A2.3 and ~ 25 mL of 1X leaf digestion solution per 50 mL tube was added to cover all leaf tissue. Leaf tissue in 1X digestion solution was vacuum infiltrated in open tubes for 1 hr at room temperature using a vacuum desiccator connected to a water pump followed by 3-hr incubation at room temperature on a rocker

with gentle shaking. Capped tubes with leaf tissue in 1X leaf digestion solution were kept wrapped in aluminum foil during this incubation to prevent exposure to light. After 3 hrs, the rocker speed was increased for ~ 2 min to release protoplasts. The crude protoplast suspension was filtered through two layers of sterile cheese cloth to remove debris and the filtrate was collected in a sterile glass beaker. The filtrate was filtered through a sterile 100 μm nylon mesh into a sterile Petri dish. The flow through was collected and transferred to a new sterile 50 mL tube. About 15-20 mL of fresh TEX buffer was used to wash the sterile Petri dish and any protoplasts adhering to the surface were collected. The flow through was centrifuged using a swing bucket rotor at 100xg at 10 °C for 15 min (Acceleration 6, Deceleration 0; Allegra® X-15R Centrifuge, Beckman Coulter, CA). ~ 25 – 30 mL of the liquid (which contains residual and pelleted debris) below the floating protoplast layer, was removed with a sterile 9" glass Pasteur pipette connected to a peristaltic pump (Model 3100, Welch Rietschle Thomas, IL) without disturbing the floating protoplast layer and ~ 10 – 15 mL volume was left in the 50 mL tube. Fresh TEX buffer was added to a final volume of 40 mL while gently resuspending the protoplasts. Centrifugation, removal of liquid below the floating protoplast layer and gentle resuspension of the protoplasts by adding fresh TEX buffer were repeated two times as described above to remove as much cellular debris as possible. The centrifugation time is reduced to 10 min in the first repetition and to 5 min in the final repetition. Floating protoplasts were aspirated with a cut, sterile 1 mL transfer pipette into a new 15 mL tube wrapped in aluminum foil to prevent exposure to light and were kept on ice until sorting. Sorting was performed directly after isolation of leaf protoplasts.

A2.5 Protoplast Sorting by Fluorescence-Activated Cell Sorting (FACS)

Before isolated protoplasts were subject to sorting, protoplasts were examined by Confocal Laser Scanning Microscopy (CLSM) using a 488-nm argon laser for excitation to confirm protoplast integrity, minimal amount of debris (to avoid clogging the FACS sorting nozzle) and the presence of GFP fluorescence in the protoplast pool. Isolated protoplasts were sorted in TEX buffer via FACS (BD FACSVantage SE, BD Biosciences, CA) using a 200-μm nozzle on a macro sort head at event rates between 6,000 and 15,000, with a system pressure of around 3-9 p.s.i. following an adapted protocol (Birnbaum et al., 2005). C24 WT non-GFP protoplasts were used to determine the autofluorescence thresholds. To collect GFP-positive protoplasts in J0571, J1071 and J0571>>UAS-BVR suspensions, protoplasts were sorted using an air-cooled argon laser (Spectra Physics Model 177, Newport Corporation, CA) operated at 100 mw on a 488-nm argon line. GFP fluorescence was detected using a 530/30 band pass filter. For J0571>>UAS-BVR, while GFP-positive protoplasts were being collected, in a separate channel, GFP-negative protoplasts were collected as a negative control for subsequent microarray analyses. Following the collection of GFP-positive protoplasts, sorted protoplast fractions were examined for presence/absence of GFP fluorescence and protoplast integrity by CLSM as described above. Total RNA from sorted protoplast fractions was extracted using RNeasy® Plant Minikit (Catalog No. 16419, Qiagen, CA) including on-column DNase treatment (Catalog No. 79254, Qiagen, CA) according to manufacturer's instructions. The quantity of RNA in the samples for C24 WT (GFP negative), J0571 (GFP positive), J1071 (GFP positive) and J0571>>UAS-BVR (GFP positive) was analyzed by spectrometry (NanoDrop1000, Thermo Scientific, MA).

A3 Results

A significant number of GFP-positive protoplasts were detected in the GFP channel by FACS for J0571, J1071 and J0571>>UAS-BVR samples (Figure A3 and A4). In optimization assays using GFP-enhancer trap lines, J0571 with GFP expression in cortex/endodermis including initials, with a broad pattern of expression in hypocotyl and cotyledons, displayed ~ 17 % to 24 % GFP-positive protoplasts, whereas the line with vascular and dermal expression, J1071, had ~ 1.4 % GFP-positive protoplasts. F3 progeny, J0571>>UAS-BVR, displayed ~ 32 % GFP-positive protoplasts (Table A1). Sorting of 3 x 500 µL (~ 1.5 mL total of protoplast suspension) of J0571 protoplasts for 1 h gave ~ 100,000 GFP-positive protoplasts. Sorting of 3 x 500 µL (~ 1.5 mL total protoplast suspension) of J1071 protoplasts for 1.5 h gave ~ 3,000 GFP-positive protoplasts. Sorting of 3 x 500 µL (~ 1.5 mL total protoplast suspension) of J0571>>UAS-BVR protoplasts for 1.5 h gave ~ 104,000 GFP-positive protoplasts and 109, 000 GFP-negative protoplasts (Table A1). Confocal images indicated a very high yield of protoplasts for both J0571 and J1071 samples before sorting was carried out (Figure A5-C and E), and the sorted fractions contained only bright GFP-fluorescent protoplasts (Figure A5-G and E). The non-GFP protoplasts can also be sorted and collected in a separate channel. For J0571>>UAS-BVR, the protoplasts in non-GFP protoplast fraction displayed only chlorophyll autofluorescence (Figure A6-G). This observation indicates that intact GFP-positive protoplasts can be sorted via FACS and the fractions, which were sorted based on the presence of GFP, do not contain GFP-negative protoplasts. RNA extraction from isolated protoplasts (1 mL) yields RNA of sufficient quantity for detection by fluorospectrometry (Table A2). RNA yields from pre-sorted

C24 wild-type protoplasts or FACS-sorted, GFP-positive protoplast fractions exceeded the minimum 20 ng needed for use in RNA-labeling assays for microarray (Table A2). cDNA can be prepared for hybridization as described in Affymetrix GeneChip® Expression Analysis Technical Manual and then hybridized to GeneChip® Arabidopsis ATH1 Genome Array (Catalog No. 900385, Affymetrix, Inc., CA) for cell-, tissue- or organ-type-specific gene expression profiling.

A4 Discussion

Gene expression profiling through microarrays has revealed that more than 30 % of the genes in Arabidopsis seedlings are light regulated (Ma et al., 2001) and has identified a vast group of genes encoding light signal transduction components involved in the phytochrome signaling cascade (Chen, Chory, and Fankhauser, 2004; Ulm and Nagy, 2005). Such studies suggest that light induces rapid and long-term changes in gene expression. A wealth of data indicate that phytochrome family members are expressed in a spatial- as well as temporal-specific manner and localized pools of phytochrome can mediate discrete physiological functions *in planta* (Bischoff et al., 1997; De Greef and Caubergs, 1972; De Greef and Verbelen, 1972; Parcy, 2005; Goosey, Palecanda, and Sharrock, 1997; Montgomery, 2008; Sharrock and Clack, 2002; Zeevaart, 2006). Each localized pool of phytochromes may control only a subset of distinct developmental and adaptive responses. Moreover, it is likely that downstream signaling components interact with phytochromes in a cell- and tissue-specific manner in mediating discrete physiological responses (Ma et al., 2005; Montgomery, 2008; Neff, Fankhauser, and Chory, 2000). Through comparative analysis of gene expression changes in GAL4-GFP

X UAS-BVR progeny and parental lines, distinct changes in gene expression that result from localized phytochrome deficiencies can be determined. Based on gene expression profiles, genes that encode negative and positive regulators of phytochrome-mediated cell-to-cell signaling can be elucidated. Recent data suggest that several hundred transcripts are induced by protoplasting of plant tissues (Birnbaum et al., 2003). Thus, the ideal negative control for microarray analysis is RNA isolated from non-GFP protoplasts collected during sorting. Transcripts that are induced by protoplasting of plant tissue can be excluded from data analysis using these controls, resulting in the identification of target genes specifically involved in tissue- and organ-specific phytochrome signaling and/or responses. To confirm steady-state changes in expression of genes identified via cell-type-specific expression profiling, qRT-PCR can be carried out on poly (A) RNA isolated from the sorted GFP-positive and GFP-negative protoplasts. Genes whose expression is changed significantly in microarray analyses and confirmed by qRT-PCR are identified as candidate genes involved in discrete phytochrome-mediated intercellular signaling. If T-DNA insertion mutants are already available in the identified candidate genes, they can be analyzed for light-impaired phenotypes in R and FR. By comparing the phenotypes of mutants carrying mutations in candidate genes and known phytochrome mutants to wild type, specific responses in which candidate genes have regulatory roles can be identified. If the mutants with mutations in candidate genes display phytochrome-deficient phenotypes in R and/or FR conditions, this will confirm that the identified downstream target genes are potentially involved in mediating distinct phytochrome-regulated responses.

Figure A1 GAL4 enhancer-trap-based induction of Biliverdin reductase (*BVR*) expression in transgenic *Arabidopsis thaliana* plants.
(A). An individual selected from a library of GAL4-based enhancer trap lines, which contain a GAL4-responsive green fluorescent protein (GFP) marker gene, is crossed with a line containing a GAL4-responsive target gene (*BVR*) to induce expression of the *BVR* gene in GAL4-containing cells marked by GFP fluorescence. Based on a figure from Dr. Jim Haseloff (http://www.plantsci.cam.ac.uk/Haseloff/geneControl/GAL4Frame.html). (B) Production of phytochrome chromophore, phytochromobilin (PΦB) and holophytochrome in parent lines. (C) Left, Reduction of biliverdin IXα (BV IXα) and PΦB by biliverdin reductase (BVR) activity to bilirubin (BR) and phytochromorubin (PΦR), respectively. BVR activity results in depletion of PΦB and leads to a reduction in the production of photoactive holophytochrome. Right, the reaction catalyzed by BVR is shown.

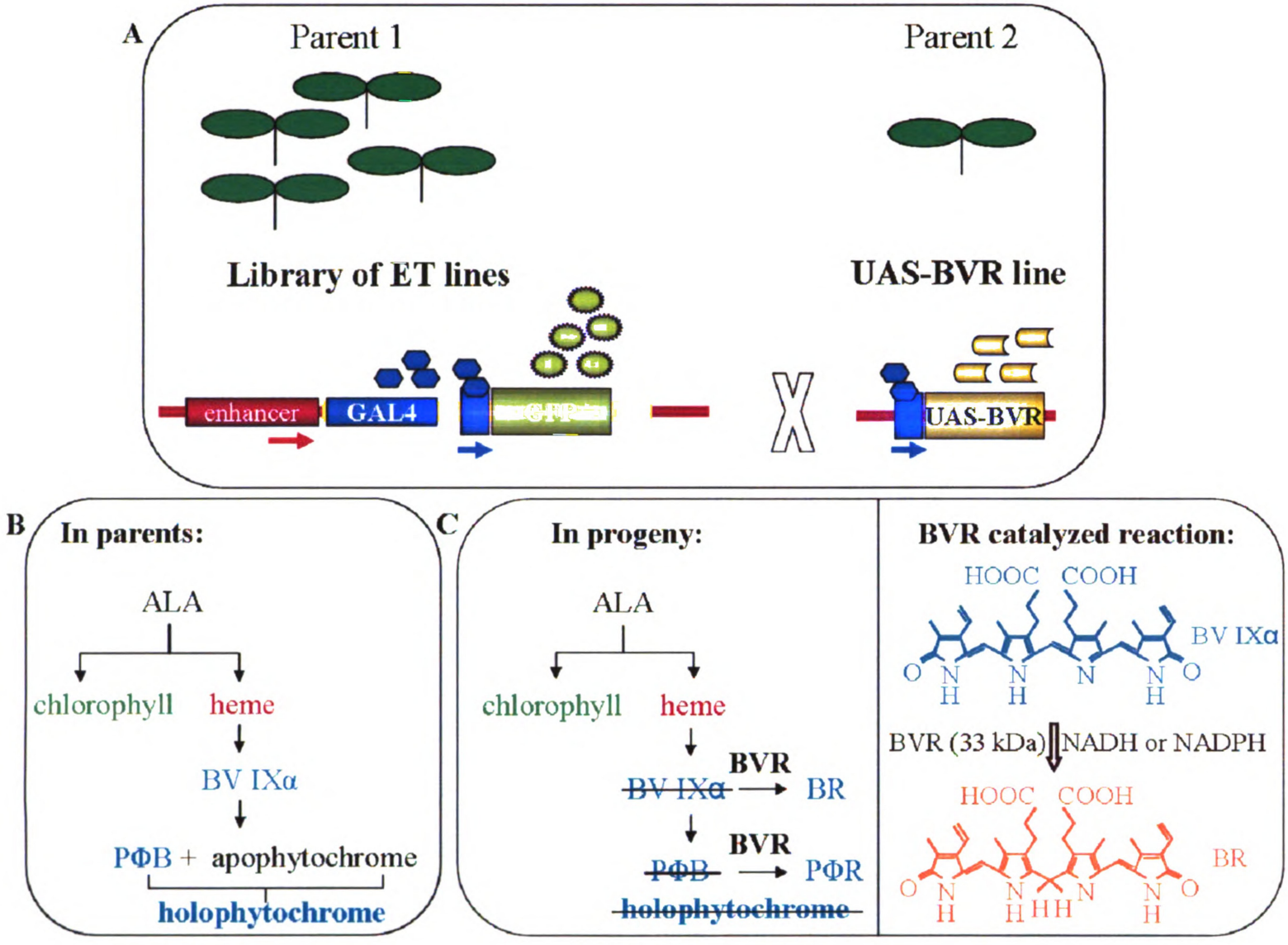
A
Parent 1
Parent 2
Library of ET lines
UAS-BVR line
enhancer
GAL4
UAS-BVR
B
In parents:
ALA
chlorophyll
heme
BV IXα
PΦB + apophytochrome
holophytochrome
C
In progeny:
ALA
chlorophyll
heme
BVR
BV IXα
BR
BVR
PΦB
PΦR
holophytochrome
BVR catalyzed reaction:
HOOC
COOH
BV IXα
BVR (33 kDa)
NADH or NADPH
HOOC
COOH
BR

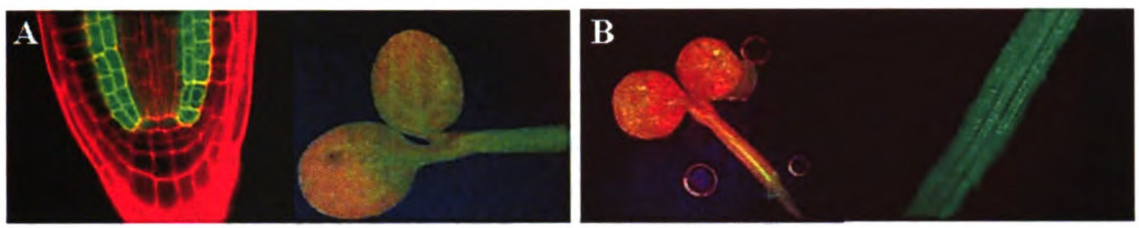

Figure A2 Expression patterns of green fluorescent protein in enhancer trap lines. (A) J0571-cortex/endodermis including initials, with broad pattern of expression in hypocotyl and cotyledons, (B) J1071- vascular/dermal expression throughout the seedling. Images were adapted from http://www.plantsci.cam.ac.uk/Haseloff/geneControl/catalogues/Jlines/index.html

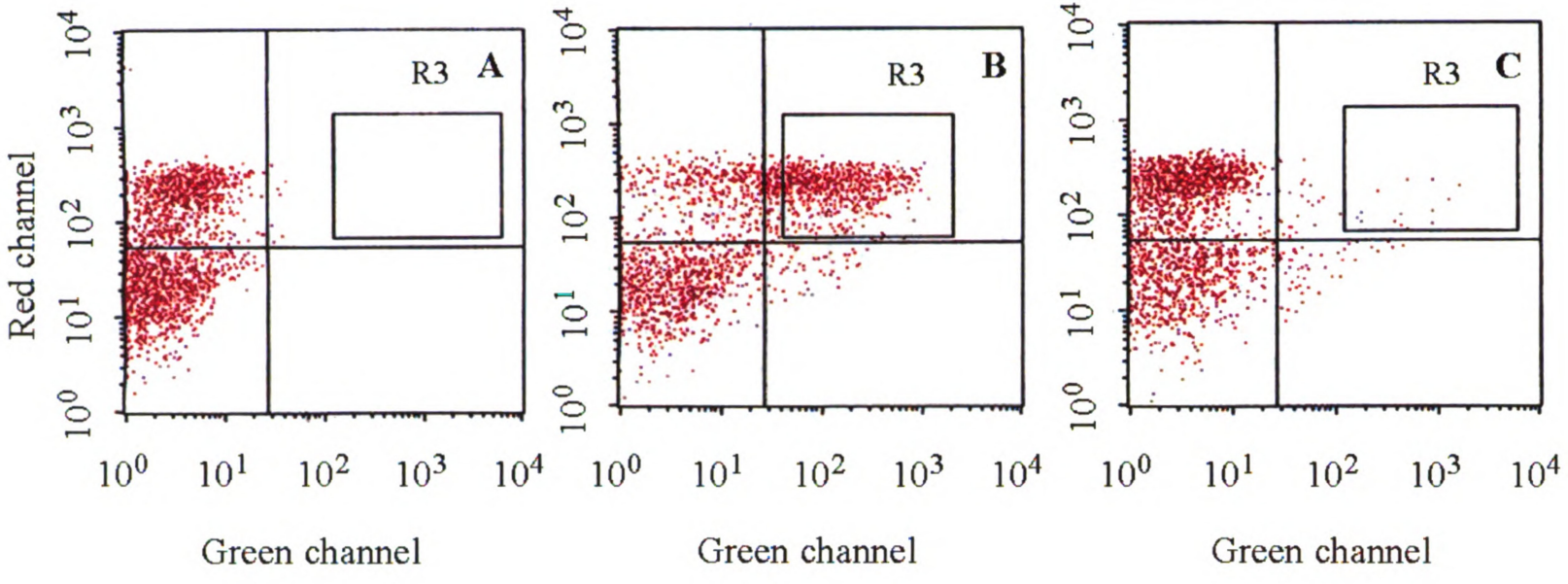

Figure A3 Fluorescence Activated Cell Sorting (FACS) acquisition dot plots.
Comparison of protoplast sorting for (A) C24 wild type, (B) J0571 and (C) J1071. (A) Acquisition dot plot of non-GFP fluorescent C24 wild-type protoplasts excited by a 488-nm argon laser and used to determine autofluorescence threshold. (B) and (C) acquisition dot plots show proportions of protoplasts that are GFP-positive in response to excitation by a 488-nm laser. R3 sorting gates in B and C delimit the GFP-positive targets that were sorted by Fluorescence-Activated Cell Sorter (BD FACSVantage SE, BD Biosciences, CA) and collected. Red channel indicates values for chlorophyll autofluorescence from protoplasts and green channel indicates values for GFP fluorescence.

Table A1 GFP-positive protoplasts before and after Fluorescence Activated Cell Sorting (FACS). Percentage of GFP-positive protoplasts from two enhancer trap lines (J0571 and J1071) and progeny line (J0571 >>UAS-BVR) before sorting and the number of GFP-positive protoplasts collected by running 500 µL of protoplast suspension through the Fluorescence Activated Cell Sorter (BD FACSVantage SE, BD Biosciences).

Enhancer Trap Line/Progeny	% of GFP-positive protoplasts before sorting	Number of sorted GFP protoplasts
J0571	17.18 % ~ 24.06 %	26, 400 ~ 36,000
J1071	~ 1.43 %	1,000 ~ 1,300
J0571>>UAS-BVR	~ 32 %	31,000 ~ 41, 000

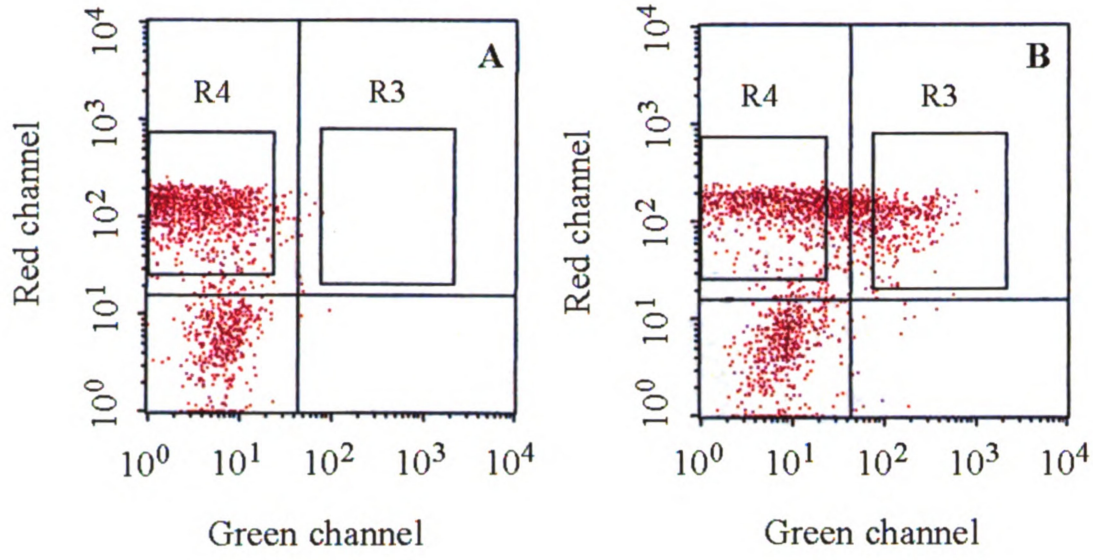

Figure A4 Fluorescence Activated Cell Sorting (FACS) acquisition dot plots.
Comparison of protoplast sorting for (A) C24 wild type and (B) J0571>>UAS-BVR1. (A) Acquisition dot plot of non-GFP fluorescent C24 wild-type protoplasts excited by a 488-nm argon laser and used to determine autofluorescence threshold. (B) Acquisition dot plot shows proportions of protoplasts that are GFP-positive in response to excitation by a 488-nm laser. R3 sorting gates in B delimit the GFP-positive targets that were sorted by Fluorescence-Activated Cell Sorter (BD FACSVantage SE, BD Biosciences, CA) and collected, and R4 sorting gates delimit the chlorophyll-positive, GFP-negative targets collected for negative control. Red channel indicates values for chlorophyll autofluorescence from protoplasts and green channel indicates values for GFP fluorescence.

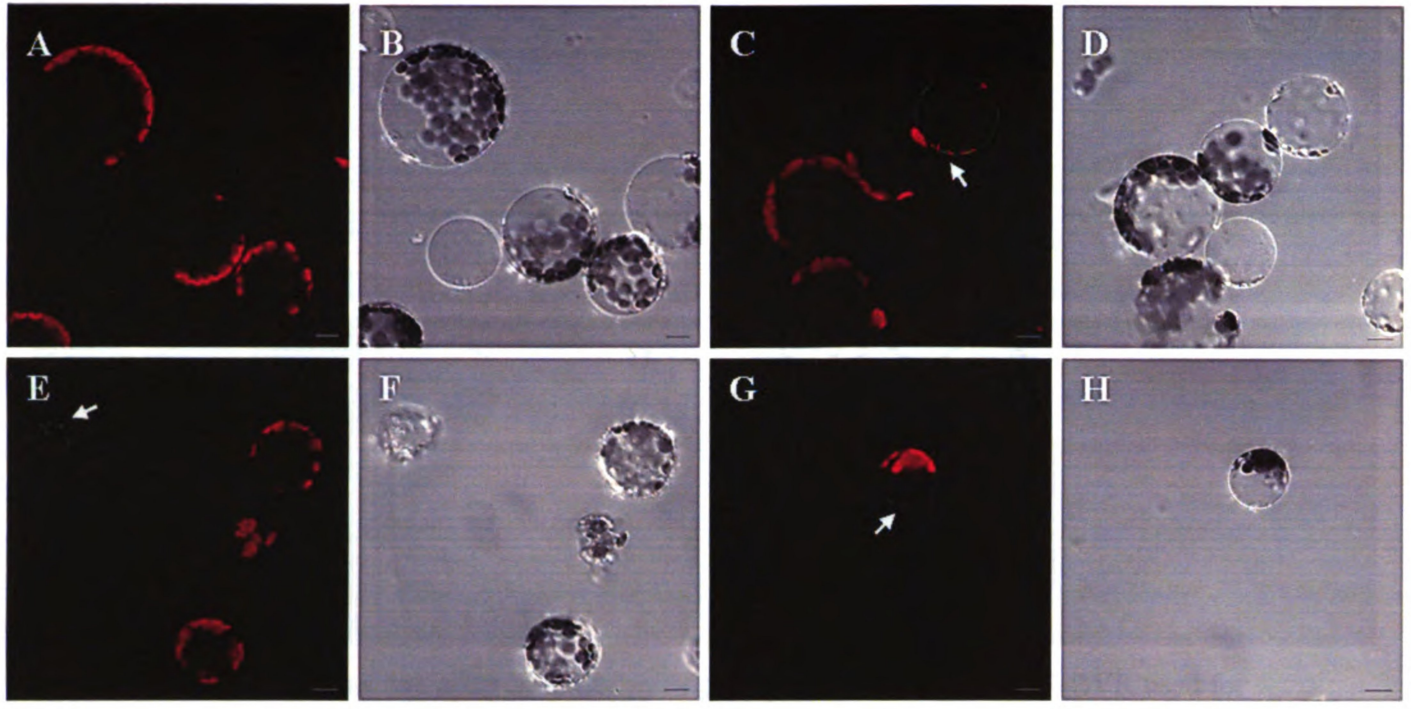

Figure A5 Confocal laser scanning microscopy of plant protoplasts used for fluorescence activated cell sorting.

Confocal laser scanned images of protoplasts from C24 wild type (A, B), J1071 (C, D) and J0571 (E, F, G, H) are shown. Images A, C and E are before sorting and image G is after sorting via Fluorescence-Activated Cell Sorter (FACS). B, D, F and H are DIC images. Images C, E and G are merged images of GFP fluorescence (Band pass filter 505 nm - 575 nm) and autofluorescence (Long pass filter 650 nm). In C, E and G, arrows indicate GFP fluorescence. A through H are average of 4 scans and were captured under 63x oil objective. Bar = 10 µm. Images were collected on an inverted Axiovert 200 Zeiss LSM 510 Meta confocal laser scanning microscope (Carl Zeiss MicroImaging, Inc., NY) using differential interference contrast (DIC) optics and fluorescence excitation/emission filters using a 488-nm laser for excitation.

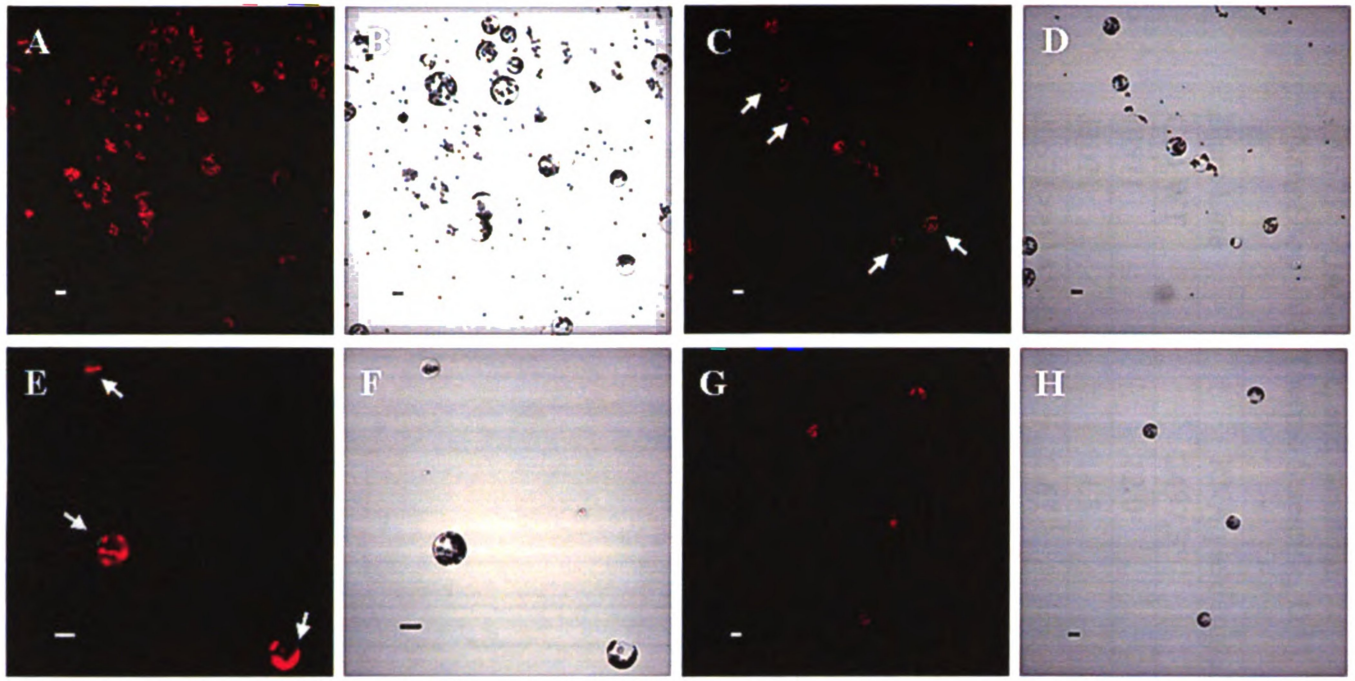

Figure A6 Confocal laser scanning microscopy of protoplasts of J0571>>UAS-BVR used for fluorescence activated cell sorting.
Confocal laser scanned images of protoplasts from C24 wild type (A, B), J0571>>UAS-BVR (C, D), GFP-positive J0571>>UAS-BVR (E, F) and GFP-negative J0571>>UAS-BVR (G, H) are shown. Images A and C are before sorting and images E and G are after sorting via Fluorescence-Activated Cell Sorter (FACS). B, D, F and H are respective DIC images. Images A, C, E and G are merged images of GFP fluorescence (Band pass filter 500 nm-530 nm) and autofluorescence (Band pass filter 649 nm-749 nm). In C and E, arrows indicate GFP fluorescence. A through H are average of 4 scans. A, B, C, D, G and H were captured under 20x objective. E and F were captured under 40x oil objective. Bar = 20 µm. Images were collected on an inverted IX81 Olympus FluoView FV1000 confocal laser scanning microscope (Olympus America, Inc., PA) using differential interference contrast (DIC) optics and fluorescence excitation/emission filters using a 488-nm laser for excitation.

Table A2 Quantification of RNA.
Yield from RNA isolation from protoplasts. RNA was isolated from pre-sorted C24 wild-type or sorted GFP-positive protoplasts from two enhancer trap lines (J0571 and J1071) and progeny line (J0571>>UAS-BVR) and quantified (NanoDrop1000, Thermo Scientific, DA).

Plant Line	RNA yield (ng/μL)
C24 WT	2497.3
J0571	12.0
J1071	14.3
J0571>>UAS-BVR	7.67

A5 References

Birnbaum, K., Jung, J. W., Wang, J. Y., Lambert, G. M., Hirst, J. A., Galbraith, D. W., and Benfey, P. N. (2005). Cell type-specific expression profiling in plants via cell sorting of protoplasts from fluorescent reporter lines. *Nat Methods* **2**(8), 615-619.

Birnbaum, K., Shasha, D. E., Wang, J. Y., Jung, J. W., Lambert, G. M., Galbraith, D. W., and Benfey, P. N. (2003). A gene expression map of the Arabidopsis root. *Science* **302**(5652), 1956-1960.

Bischoff, F., Millar, A.J., Kay, S.A., and Furuya, M. (1997) Phytochrome-induced intercellular signalling activates *cab*::luciferase gene expression, *The Plant Journal* **12**(4), 839-849.

Chen, M., Chory, J., and Fankhauser, C. (2004). Light signal transduction in higher plants. *Annu Rev Genet* **38**, 87-117.

De Greef, J.A., and Caubergs, R. (1972). Interorgan correlations and phytochrome: leaf expansion. *Arch Int Physiol Biochim* **80**, 961-962.

De Greef, J.A., and Verbelen, J.P. (1972). Interorgan correlations and phytochrome: changes in plastid ultrastructure during de-etiolation processes. *Arch Int Physiol Biochim* **80**, 962-963.

Denecke, J., and Vitale, A. (1995). The use of protoplasts to study protein synthesis and transport by the plant endomembrane system. *Methods Cell Biol* **50**, 335-48.

Franklin, K. A., and Quail, P. H. (2010). Phytochrome functions in Arabidopsis development. *J Exp Bot* **61**(1), 11-24.

Goosey, L., Palecanda, L., and Sharrock, R. A. (1997). Differential patterns of expression of the Arabidopsis PHYB, PHYD, and PHYE phytochrome genes. *Plant Physiol* **115**(3), 959-969.

Haseloff, J. (1999). GFP variants for multispectral imaging of living cells. *Methods Cell Biol* **58**, 139-151.

Lagarias, D. M., Crepeau, M. W., Maines, M. D., and Lagarias, J. C. (1997). Regulation of photomorphogenesis by expression of mammalian biliverdin reductase in transgenic Arabidopsis plants. *Plant Cell* **9**(5), 675-688.

Laplaze, L., Parizot, B., Baker, A., Ricaud, L., Martiniere, A., Auguy, F., Franche, C., Nussaume, L., Bogusz, D., and Haseloff, J. (2005). GAL4-GFP enhancer trap lines for genetic manipulation of lateral root development in *Arabidopsis thaliana*. *J Exp Bot* **56**(419), 2433-2442.

Ma, L., Li, J., Qu, L., Hager, J., Chen, Z., Zhao, H., and Deng, X. W. (2001). Light control of Arabidopsis development entails coordinated regulation of genome expression and cellular pathways. *Plant Cell* **13**(12), 2589-2607.

Ma, L., Sun, N., Liu, X., Jiao, Y., Zhao, H., and Deng, X. W. (2005). Organ-specific expression of Arabidopsis genome during development. *Plant Physiol* **138**(1), 80-91.

Montgomery, B. L. (2008). Right place, right time: Spatiotemporal light regulation of plant growth and development. *Plant Signal Behav* **3**(12), 1053-1060.

Montgomery, B. L., Yeh, K. C., Crepeau, M. W., and Lagarias, J. C. (1999). Modification of distinct aspects of photomorphogenesis via targeted expression of mammalian biliverdin reductase in transgenic Arabidopsis plants. *Plant Physiol* **121**(2), 629-639.

Neff, M. M., Fankhauser, C., and Chory, J. (2000). Light: an indicator of time and place. *Genes Dev* **14**(3), 257-271.

Parcy, F. (2005) Flowering: a time for integration. *Int J Dev Biol* **49**, 585-593.

Sharrock, R. A., and Clack, T. (2002). Patterns of expression and normalized levels of the five Arabidopsis phytochromes. *Plant Physiol* **130**(1), 442-456.

Ulm, R., and Nagy, F. (2005). Signalling and gene regulation in response to ultraviolet light. *Curr Opin Plant Biol* **8**(5), 477-482.

Warnasooriya, S. N., and Montgomery, B. L. (2009). Detection of spatial-specific phytochrome responses using targeted expression of biliverdin reductase in Arabidopsis. *Plant Physiol* **149**(1), 424-433.

Zeevaart, J. A. (2006). Florigen coming of age after 70 years. *Plant Cell* **18**(8), 1783-1789.